Palpography

Palpography

Palpografie

Thesis

to obtain the degree of Doctor from the
Erasmus University Rotterdam
by command of the rector magnificus

Prof. dr. S.W.J. Lamberts

and according to the decision of Doctoral Board.

The public defense shall be held on

Friday 10th June 2005 at 11.00 hours

by

Johannes Antonius Schaar

born at Griesbach im Rottal, Germany

Doctoral Comittee

Promotors:	Prof.dr.ir. A.F.W. van der Steen Prof.dr. P.W.J.C. Serruys
Other members:	Prof. dr. P.J. de Feijter Prof. J.E. Muller Prof. dr. Y. Saijo

To my wife, Maximilian and Sophia

and

Dr. Frits

Table of Contents

Part I
Introduction

Chapter 1

Diagnosis of Vulnerable Plaques in the Cardiac Catheterization Laboratory

Based on:

Schaar JA, van der Steen AFW, Arampatzis CA, Kram R, Slager CJ, ten Have AG, van der Poll SW, Gijsen FJ, Wentzel JJ, de Feyter PJ, Serruys PW.
Diagnosis of Vulnerable Plaque in the Cardiac Catheterization Laboratory.
In Saijo Y, van der Steen AFW (Eds): Vascular Ultrasound. 2003 Springer ISBN 4-431-70328-4

and

Schaar JA, Regar E, Arampatzis CA, van der Ven ARA, Slager CJ, Gijsen FJ, Wentzel JJ, de Feyter PJ, van der Steen AFW, Serruys PW.
Diagnosis of Vulnerable Plaque in the Cardiac Catheterization Laboratory.
In Khachigian LM (Ed): High-Risk Atherosclerotic Plaques: Mechanisms, Imaging, Models, and Therapy. 2005 CRC Press ISBN 0-8493-3028-9

Rupture of thin-cap fibroatheromas is the main cause of acute coronary syndrome and myocardial infarction.

Rupture of thin-cap fibroatheromas is the main cause of acute coronary syndrome and myocardial infarction. Identification of this form of vulnerable plaque is therefore essential to enable the development of treatment modalities to stabilize such plaque. Because myocardial infarction and its consequences are so important, we must investigate options to identify those areas that will be responsible for future events. The vulnerable plaque contains certain features that could be diagnosed by various specialized methods. The ideal technique would provide morphological, mechanical and chemical information, however at present, no diagnostic modality providing such all-embracing assessment is available. In this chapter the current available techniques in the cathlab are discussed with special emphasis on angiograms, angioscopy, optical coherence tomography, intravascular ultrasound, palpography, thermography, Raman Spectroscopy, near-infrared spectroscopy and magnetic resonance imaging. All these techniques are still under development and at present, none of them can identify a vulnerable plaque alone or predict its further development. This is related to fundamental methodological insufficiencies that may be resolved in the future. From a clinical point of view, most techniques currently assess only one feature of the vulnerable plaque. Thus the combination of several modalities will be of importance in the future to ensure a high sensitivity and specificity in detecting vulnerable plaque.

A wide variety exists in the stability of coronary atherosclerotic plaques, which will be extensively discussed in chapter 2. A plaque may be stable for years, however abrupt disruption of his structure is the main cause of acute coronary syndrome (Libby 1995).

There are three forms of vulnerable plaques

There are three forms of vulnerable plaques:

A) The thin-cap fibroatheroma

Thin-cap fibroatheroma = TCFA

Pathologic studies of plaque rupture with thrombosis suggest that prior to a thrombotic event, the plaque was an inflamed, thin-cap fibroatheroma (TCFA). TCFA appear in 75% of all cases. The major components of such TCFA are: (i) an atheromatous core, (ii) a thin fibrous cap, with macrophage and lymphocyte infiltration and decreased smooth muscle cell content, (iii) expansive remodelling.

B) Erosion

Pathologic studies have shown that prior to an event the endothelium was injured at the place where a thrombus was formed. This endothelium consists of proteoglycan rich endothelial cells. Erosion occurs in 30% of all cases.

C) Calcified nodule

Pathologic studies of plaques with thrombosis covering a calcified nodule suggest that the plaque appeared to be heavily calcified with a calcified nodule projecting into the lumen prior to 5% of all events.

This chapter will discuss the current development of imaging techniques that have the potential to detect vulnerable plaques. The vulnerable plaque contains certain features that could be diagnosed by various specialized methods. The ideal technique would provide morphological, mechanical and chemical information, however at present, no diagnostic modality providing such all-embracing assessment is available.

The characteristics of vulnerable plaque have been described by numerous reviewers (Falk 1999) (Virmani 2002). It is important to characterize the following features:

1 size of the lipid core (40% of the entire plaque)
2 thickness of the fibrous cap
3 presence of inflammatory cells
4 amount of remodelling and extent of plaque free vessel wall
5 3D morphology

Angiography

The culprit lesion prior to a myocardial infarction has in 48-78% of all cases a stenosis smaller than 50%

Coronary angiography has been so far the gold standard to assess the severity of obstructive lumenal narrowing. Furthermore it serves as a decision tool to direct therapy such as PTCA or CABG. Using coronary angiography we can assess the lumen boundaries, but cannot assess information about plaque burden, plaque delineation and plaque components. The predictive power of occurrence of myocardial infarction is rather low since 70% of acute coronary occlusions are in areas that were previously angiographically normal, and only a minority occur where there was severe stenosis (Little 1988). Other studies have affirmed, that the culprit lesion prior to a myocardial infarction has, in 48-78% of all cases, a stenosis smaller than 50% (Nobuyoshi 1991, Ambrose 1988, Giroud 1992). Coronary angiograms also often fail to identify the culprit lesion of nontransmural myocardial infarction (Kerensky 2002). The majority of ulcerated plaques are not big enough to be detected by angiography, but can be well assessed pathologically (Frink 1994).

The presence of multiple complex plaques is associated with an increased incidence of recurrent acute coronary syndrome.

Furthermore, we have to take into account that the predictive power of angiography is strongly dependent on the time interval between the angiogram and the myocardial infarction, because both time and interim therapy can influence atherosclerosis. In one study, the angiograms were performed between 1 and 77 months before the event and showed that atherosclerosis can be a rapidly progressive process. A recent study evaluated angiograms made one week before acute myocardial infarction showing that signs of thrombosis and rupture were present in a majority of patients (Ojio 2000). During the year after myocardial infarction, the presence of multiple complex plaques is associated with an increased incidence of recurrent acute coronary syndrome (Goldstein 2000).

Thus, patients with silent non-obstructive coronary atherosclerosis harbour vulnerable plaques that cannot be detected by angiograms, but which are associated with adverse clinical outcomes. If a disrupted ulcerated plaque is seen on angiography, the existence of additional rupture prone plaques is to be expected.

Angiography has a low discriminatory power to identify the vulnerable plaque

Angiography therefore, has a low discriminatory power to identify the vulnerable plaque, but does provide information about the entire coronary system and serves as guide for invasive imaging techniques and therapy.

In the future non-invasive luminography and vessel wall assessment may become an integral part of our daily diagnostic procedure (Kim 2001).

Angioscopy

Intracoronary angioscopy offers a direct visualization of the plaque surface and intra-lumenal structures like tears and thrombi. It allows assessment of the color of the plaque and thrombus (Mizuno 1992) with a sensitivity in detecting such structures higher than when compared to angiography (Sherman 1986). Angioscopic plaque rupture and thrombus have been shown to be associated with adverse clinical outcomes in patients with complex lesions (Feld 1996). Furthermore yellow plaques seem to have an increased instability, in comparison between IVUS and angioscopy (Tacano 2001). In patients with myocardial infarction all three coronary arteries are widely diseased and have multiple yellow plaques (Asakura 2001). In a 12-month follow-up study of 157 patients with stable angina, acute coronary syndrome occurred more frequently in patients with yellow plaques than in those with white plaques.

Acute coronary syndromes occur more frequently in patients with yellow plaques

These results indicate that acute coronary syndromes occur more frequently in patients with yellow plaques, which can be imaged with angioscopy, but not angiography (Uchida 1995). However, angioscopy is difficult to perform, invasive and only a limited part of the vessel tree can be investigated. Most importantly, to enable clear visualization of the vessel wall, the vessel has to be occluded and the remaining blood flushed away with saline, thereby potentially inducing ischaemia. Information regarding the degree of plaque extension into the vessel wall is not provided by angioscopy.

IVUS

Intravascular coronary ultrasound (IVUS) provides real-time high-resolution images of the vessel wall and lumen (Bom 1998). The

size of IVUS catheters is between 2.9 to 3.5 French. Depending on the distance from the catheter the axial resolution is about 150 microns, the lateral 300 microns. The images appear real time at a frequency of up to 30 frames/sec. Features of the vessel can be detected based on the echogenicity and the thickness of the material. Small structures can be visualized, however only those sized over 160 microns can be estimated accurately. The normal thickness of the media is about 125-350 mm.

IVUS provides some insight into the composition of coronary plaques. In IVUS images, calcification is characterized by a bright echo signal with distal shadowing which hides plaque components and deeper vessel structures. In comparative studies between histology and IVUS, plaque calcification can be detected with a sensitivity of between 86 and 97% (Di Mario 1992) (Sechtem 1993). The sensitivity to detect micro-calcification ranges around 60% (Friedrich 1994).

IVUS can detected lipid depositions with a specificity of 30%.

In IVUS images lipid depositions are described as echolucent zones and can be detected with a sensitivity of between 78% and 95% and specificity of 30% (Potkin 1990) (Rasheed 1995). This sensitivity is dependent on the amount of lipid and can drop down further if the echo-lucent area is smaller than a quarter of the plaque. Echolucent zones can also be caused by loose tissue and shadowing from calcium, which makes the interpretation of echolucent areas difficult. The sensitivity to differentiate between fibrous and fatty tissue is between 39 and 52% (Hiro 1996).

The detection of vulnerable plaques by IVUS is mainly based on a series of case reports (Ge 1995) (Jeremias 1997). The main focus of these reports is the detection of already ruptured plaques. To evaluate the role of IVUS in detecting plaque rupture, a study was performed of 144 patients with angina. Ruptured plaques were characterized by a cavity (echolucent area within the plaque) and a tear of the thin fibrous cap. They were identified in 31 patients of whom 23 (74%) presented with unstable angina. Plaque rupture was confirmed by injecting contrast medium and seeing filling of the plaque cavity on IVUS. Of the patients without plaque rupture (n = 108), only 19 (18%) had unstable angina. The echolucent area (cavity) to total plaque area ratio was larger in the unstable group than in the stable group. The thickness of the fibrous cap in the un-

stable group was also found to be smaller than in the stable group (Ge 1999).

The problem of these studies is the lack of prospectivity and follow up. Only Yamagishi et al. have performed a prospective study with a follow up period of about two years. Large eccentric plaques containing an echolucent zone by IVUS were found to be at increased risk of instability even though the lumen area was preserved at the time of initial study (Yamagishi 2000).

Intravascular ultrasound assessment of vascular remodelling may help to classify plaques with the highest probability of spontaneous rupture.

It has been demonstrated, that suspected to be vulnerable plaques are associated with positive remodelling. Intravascular ultrasound assessment of vascular remodelling may help to classify plaques with the highest probability of spontaneous rupture (von Birgelen 2001).

A number of groups have investigated the potential of ultrasound radio-frequency signal analysis for tissue characterization (Nair 2001) (Landini 1986) (Wilson 1994) (Jeremias 1999) (Wickline 2000) (Bridal 2000) (Spencer 1997). Many of these studies revealed the potential to identify calcified plaques, but although promising, none has yet produced a technique with sufficient spatial and parametric resolution to identify a lipid pool covered by a thin fibrous cap.

Thermography

Inflammation produces a temperature rise in the affected tissue. Since atherosclerosis is accompanied by inflammation the hypothesis was created that a temperature rise could be measured at the surface of a plaque. As vulnerable plaque is a very active metabolic area, the hypothesis was extended that vulnerable plaques may have an even higher temperature rise.

There was a negative correlation between temperature difference and cap thickness (R^2 = -0.34)

Casscells et al. reported that carotid plaques taken at endarterectomy from 48 patients have temperature heterogeneity (Casscells 1996). The temperature difference between different areas was up to 2.2 °C, and correlated with cell density (R^2= -0.47, p=0.0001). There was a negative correlation between temperature difference and cap thickness (R^2= -0.34, p=0.0001). The same group reported approximately the same in vitro findings in atherosclerotic rabbits

(Casscells 1999). A correlation between temperature rise and macrophage infiltration has also been suggested in an in-vivo rabbit trial (Verheye 2002). Stefanadis et al. performed studies in humans. Patients with stable angina, unstable angina, and acute myocardial infarction were studied. The thermistor of the thermography catheter has a temperature accuracy of 0.05 °C, a time constant of 300 ms, and a spatial resolution of 0.5 mm. The thermistor of the catheter was driven against the vessel wall by the force of blood flow, without the help of a mechanical device like a balloon. Temperature was constant within the arteries of the control subjects, whereas most atherosclerotic plaques showed higher temperatures compared with healthy vessel wall. Temperature differences between atherosclerotic plaque and healthy vessel wall increased progressively from stable angina to patients with acute myocardial infarction with a maximum difference of 1.5 +/- 0.7 °C (Stefanadis 1999). Furthermore patients with a high temperature gradient have a significantly worse outcome than patients with a low gradient (Stefanadis 2001). However, this data has yet to be confirmed prospectively in other centers, and the influence of parameters such as coronary blood flow (Diamantopulos 2003) or catheter design has to be studied in the future.

Optical Coherence Tomography

OCT can provide images with ultrahigh resolution

Optical Coherence Tomography (OCT) can provide images with ultrahigh resolution. The technique measures the intensity of back-reflected light in a similar way as IVUS measures acoustic waves (Huang 1991). It is an invasive technique with a catheter advanced over a 0.014'' wire. With a Michelson interferometer light is split into two signals. One is sent into the tissue and the other to a reference arm with a mirror. Both signals are reflected and cross-correlated by interfering the light beams. To achieve cross correlation at incremental penetration depths in the tissue, the mirror is dynamically translated. The intensity of the interfering signals at a certain mirror position represents backscattering at a corresponding depth. High-resolution images with a resolution ranging from 4-20 mm can be achieved (Boppart 1998) with a penetration depth up to 2 mm. Images can be acquired real time at 15 frames/sec.

Early attempts were made to validate OCT using histology. A lipid pool generates decreased signal areas, and a fibrous plaque produces

a homogenous signal rich lesion (Jang 2000). In vitro comparison of OCT with IVUS demonstrated superior delineation by OCT of structural details like thin caps or tissue proliferation (Brezinski 1997).

Limitations of OCT are the low penetration depth, which hinders studying large vessels, and the light absorbance by blood which currently needs to be overcome by saline infusion or balloon occlusion with associated potential for ischaemia. Special techniques like index matching may improve imaging through blood (Brezinski 2001).

Raman Spectroscopy

Raman spectroscopy is a technique that can characterize the chemical composition by utilizing the Raman effect (Baraga 1992). The Raman effect is created when incident light (wave length 750 - 850 nm) excites molecules in a tissue sample, which backscatter the light while changing wave length. This change in wave length is the Raman effect (van de Poll 2002). The wave length shift and the signal intensity are dependent on the chemical components of the tissue sample. Due to this unique feature, Raman spectroscopy can provide quantitative information about the molecular composition of the sample (Hanlon 2000). The spectra obtained from tissue require post-processing to differentiate between plaque components.

Even in the presence of blood, Raman spectra have been shown to be obtainable in vivo from the aortic arch of sheep (Buschman 2000). In a study using mice that received a high-fat/high-cholesterol diet for 0, 2, 4, or 6 months, Raman spectroscopy showed good correlation between cholesterol accumulation and total serum cholesterol exposure (r approximately 0.87, $P<0.001$). In female mice (n=10) that were assigned to an HFC diet, with or without 0.01% atorvastatin, a strong reduction in cholesterol accumulation (57%) and calcium salts (97%) ($P<0.01$) was demonstrated in the atorvastatin-treated group. Raman spectroscopy can therefore be used to quantitatively study the size and distribution of depositions of cholesterol and calcification (van de Poll 2001).

Limitations of the technique are the limited penetration depth (1 - 1.5 mm), the long acquisition time and the absorbance of the light by blood. Raman spectroscopy gives no geometrical information.

Near-Infrared Spectroscopy

NIR spectroscopy obtains information on the chemical components of the coronary vessel wall.

Near-infrared (NIR) spectroscopy also obtains information on the chemical components of the coronary vessel wall. Molecular vibrational transitions measured in the NIR region (750 - 2500 nm) give qualitative and quantitative results on plaque composition. NIR spectroscopy sensitivity and specificity for the histological features of plaque vulnerability were 90% and 93% for lipid pool, 77% and 93% for thin cap, and 84% and 89% for inflammatory cells (Moreno 2002). A differentiation between vulnerable and non-vulnerable carotid plaques could be achieved ex vivo (Wang 2002). Future studies will address the question whether NIR spectroscopy is feasible in vivo. Problems like acquisition time, blood scattering, influence of pH and temperature must be addressed.

Magnetic Resonance Imaging

High-resolution magnetic resonance imaging (MRI) is a non-invasive modality to characterize atherosclerotic plaques. Combining information from T1 and T2-weighted imaging can permit in vitro identification of the atheromatous core, collageneous cap, calcification, media, adventitia, and perivascular fat (Toussaint 1995). In a small number of patients (n=6) a matching between in vivo and in vitro measurements of carotid arteries was seen (Toussaint 1996). Yuan et al. determined the accuracy of in vivo MRI for measuring the cross-sectional maximum wall area of atherosclerotic carotid arteries in a group of 14 patients undergoing carotid endarterectomy. The authors showed a strong correlation between in vivo and in vitro measurements (Yuan 1998). Although not perfect, it may be possible to identify carotid plaques at high risk for stroke using MRI (Yuan 2001). Images of carotid arteries can be further improved using a coil placed close to the carotid artery at the surface of the neck (Hayes 1996). An in-plane resolution of 0.4 x 0.4 mm and a slice thickness of 3 mm may allow an assessment of fibrous cap thickness and integrity (Hatsukami 2000).

Imaging of coronary arteries with MRI is more difficult than imaging carotid plaques

Imaging of coronary arteries with MRI is more difficult than imaging carotid plaques since cardiac and respiratory motion, the small plaque size, and the location of the coronary arteries can cause acquisition problems. Nevertheless, high resolution MRI of the human coronary wall of angiographically normal and abnormal vessels has been shown to be feasible. In a study by Botnar et al. the coronary wall thickness and wall area were significantly enlarged in patients with coronary artery disease demonstrated by angiography (Botnar 2000). Small plaque structures like fibrous caps cannot yet be assessed using current MR techniques. Thinner slices and higher in plane resolution are needed to better delineate coronary plaques.

ANGUS and Shear Stress

High-resolution reconstruction of 3D coronary lumen and wall morphology is obtained by combining angiography and IVUS (Slager 2000). Briefly a biplane angiogram of a sheath-based IVUS catheter taken at end-diastole allows reconstruction of the 3D pullback trajectory of the catheter. Combining this path with lumen and wall information derived from IVUS images that are successively acquired during catheter pullback at end-diastole gives accurate 3D lumen and wall reconstruction with resolution determined by IVUS. Filling the 3D lumen space with a high resolution 3D mesh allows calculation of the detailed blood velocity profile in the lumen (Thury 2001).

Shear stress influences a variety of biological processes.

For this purpose absolute flow and blood viscosity need to be provided as boundary conditions. From the blood velocity profile local wall shear stress on the endothelium can be accurately derived. Wall shear stress is the frictional force, normalized to surface area that is induced by the blood passing the wall. Although from a mechanical point of view shear stress is of a very small magnitude compared to blood pressure induced tensile stress it has a profound influence on vascular biology (Malek 1999) and explains the localization of atherosclerotic plaque in the presence of systemic risk factors (Asakura 1990). Many of these biological processes also influence the stability of the vulnerable plaque including inflammation, thrombogenicity, vessel remodelling, intimal thickening or regression and smooth muscle cell proliferation. Therefore, the study of this parameter as derived by image-based modelling is of utmost importance.

Concluding remarks

Assessment of atherosclerosis by imaging techniques is essential for in vivo identification of vulnerable plaques. Several invasive and noninvasive imaging techniques are currently in development.

OCT has the advantage of high resolution, thermography measures metabolism and NIR spectroscopy obtains information on chemical components. IVUS is easy to perform and can assess morphology. Shear stress is an important mechanical parameter deeply influencing vascular biology. MRI and CT have the advantage of non-invasive imaging.

Nevertheless all techniques are still under development and at present, none of them can identify a vulnerable plaque alone or predict its further development.

This is related to fundamental methodological insufficiencies that may be resolved in the future. From a clinical point of view, most techniques currently assess only one feature of the vulnerable plaque. Thus the combination of several modalities will be of importance in the future to ensure a high sensitivity and specificity in detecting vulnerable plaque.

Chapter 2

Terminology for High-risk and Vulnerable Coronary Artery Plaques

Based on:

Johannes A. Schaar, James E. Muller, Erling Falk, Renu Virmani, Valentin Fuster, Patrick W. Serruys, Antonio Colombo, Christodoulos Stefanadis, S. Ward Casscells, Pedro R. Moreno, Attilio Maseri, Anton F.W. van der Steen

Terminology for high-risk and vulnerable coronary artery plaques

Report of a Meeting on the Vulnerable Plaque, June 17 and 18, 2003, Santorini, Greec

European Heart Journal (2004) 25, 1077–1082

A group of investigators met for two days in Santorini,Greece, to discuss progress in the field of identification and treatment of high risk/vulnerable atherosclerotic plaques and patients. Many differences in the manner in which terms are being utilized were noted. It was recognized that increased understanding of the pathophysiology of coronary thrombosis and onset of acute coronary syndromes has created the need for agreement on nomenclature.

The participants spent considerable time discussing the topic and reached agreement on their own usage of the terms as described below. It is the hope that this usage might be of value to the larger community of scientists working in this field, and that widespread adoption of a common nomenclature would accelerate progress in the prevention of acute coronary events.

Conceptual terms

Overview

The terms in Fig. 1 are proposed for use on a conceptual basis. The progression from asymptomatic atherosclerosis,to a high-risk/vulnerable plaque, to a thrombosed plaque, and to clinical events is presented. It is of note that the later stages of the progression may be repeated in a relatively short time interval as documented by the high short-term risk of a recurrent event in patients with acute coronary syndromes. This may be caused by rethrombosis of the lesion causing the index event, and/or the simultaneous occurrence of multiple high-risk/vulnerable plaques and/or thrombosed plaques, that have not previously caused symptoms. An acute coronary syndrome may be a clinical marker of widespread (multifocal) disease activity in the coronary arteries, possibly related to inflammation (Maseri 2003) (Asakura 2001) (Goldstein 2002) (Rioufol 2002) (Buffon 2003) (Casscells 2003a) (Krams 2003) (Libby 2002b).

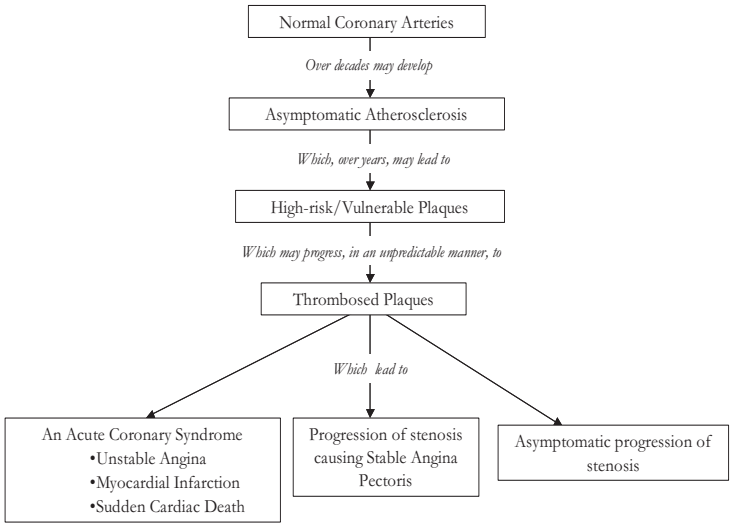

Fig. 1: Development of atherosclerosis and progression to thrombosis and clinical events.

The vulnerable patient

The primary clinical and preventive goal is to identify patients who are vulnerable to acute coronary thrombosis. Such patients are likely to have a high atherosclerotic burden, high-risk/vulnerable plaques, and/or thrombogenic blood (Maseri 2003). Traditional and newly identified risk factors (Pearson 2003) and imaging, both invasive and non-invasive, are likely to be of increasing utility in identifying such patients (Naghavi 2001) (Fayad 2001) (de Feyter 2002) (Sosnovsk 2002) (Arampatzis 2003) (MacNeill 2003). It is well established that patients with the recent onset of an acute coronary syndrome remain at risk of suffering recurrent events in the weeks and months following their initial presentation.

There is an important need to improve diagnostic methods to identify vulnerable patients, and the plaques, which contribute to their increased risk.

High-risk/vulnerable plaques

Studies indicate that there are plaques at increased risk of thrombosis and rapid progression, which often lead to symptomatic disease. It is proposed that the terms “high-risk” or “vulnerable” be used as

synonyms to describe a plaque that is at increased risk of thrombosis and rapid stenosis progression. The term "thrombosis-prone" may also be applied to such plaques.

At the present time, there is no widely accepted diagnostic method to prospectively identify such "highrisk"/"vulnerable" plaques. Until such information is provided, these terms should only be used to describe the concept and function of such plaques, and not their histologic basis.

In addition, the complicated thrombi that occur in non-disrupted predominantly fibrotic and severely stenotic plaques may well be

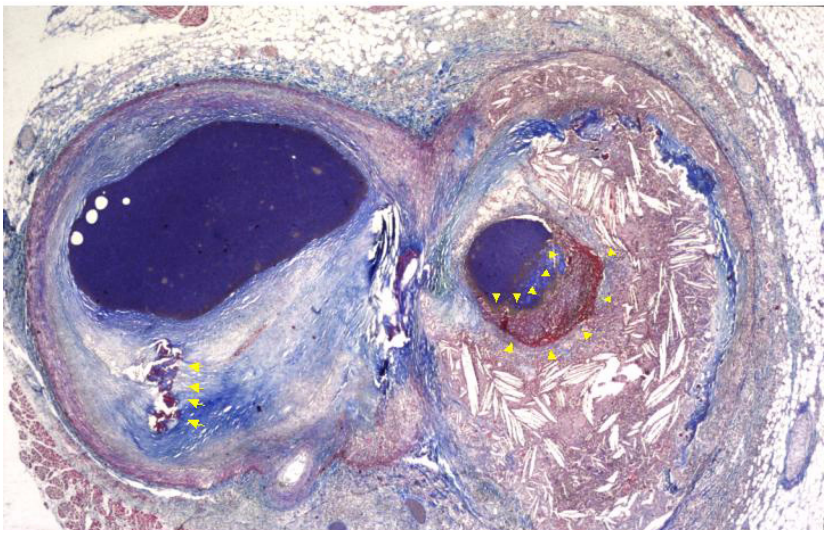

Fig.2a: Ruptured plaque with thrombosis. Cross-section of a coronary artery cut just distal to a bifurcation. The athero-sclerotic plaque to the left (circumflex branch) is fibrotic and partly calcified whereas the plaque to the right (marginal branch) is lipid-rich with a non-occluding thrombus super-imposed.

dependent on a thrombogenic state which can be considered to be a condition of "highrisk blood". Thus, an individual patient can be "highrisk" because of the presence of high-risk/vulnerable plaques and/or high-risk blood and/or an increased conventional risk factor profile (Maseri 2003).

Histologic features of plaques causing coronary artery thrombosis

At present, the most detailed evidence concerning the plaques causing coronary thrombosis and rapid lesion progression, or sympto-

matic disease, is derived from autopsy studies (van der Wal 1994) (Arbustini 1999) (Falk 1999) (Davies 2000) (Virmani 2000). While this evidence is retrospective, the findings have established the nature of the lesions causing most clinical events. Such plaques are called "culprit lesions". In most cases, culprit lesions can be identified by angiography combined with other clinical findings and/or at autopsy.

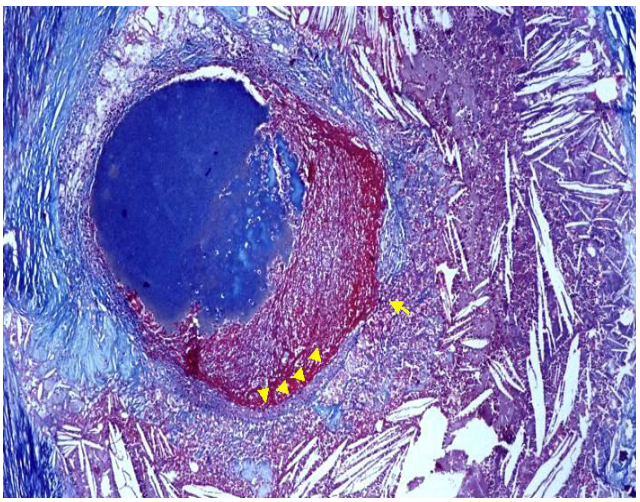

Fig 2b: Higher magnification of the plaque–thrombus interface reveals that the fibrous cap over the lipid-rich core is extremely thin, inflamed and ruptured with a real defect – a gap – in the cap. Both arteries contain contrast medium injected postmortem. Trichrome stain, staining collagen blue and thrombus red.

In the acute coronary syndromes, the culprit lesion is often a plaque complicated by thrombosis extending into the lumen (Falk 1999) (Davies 2000) (Virmani 2000) Libby 2001). Such plaques are termed "thrombosed plaques". In some cases, multiple thrombosed plaques may exist, only one of which is acting as the culprit lesion. A plaque may also develop thrombosis, which remains asymptomatic due to the presence of collaterals, or failure of the thrombus to significantly impede blood flow. However, such sub-clinical thrombosis may contribute to the rapid progression of stenosis

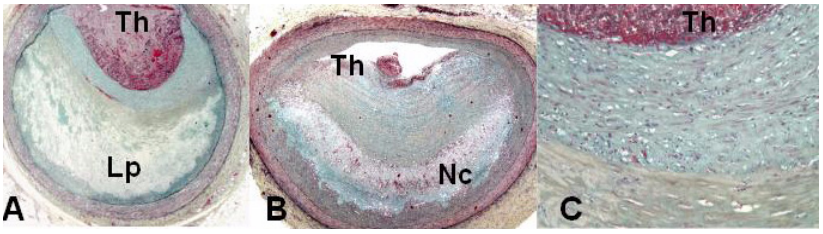

Fig. 3 Eroded plaque with thrombosis. (a,b) Plaque erosion lesions from two different patients showing in (a) a lesion with lipid pool (Lp) and in (b) a necrotic core (Nc) with lumenal thrombi (Th). Note a thick fibrous cap above the necrotic core in (b) and a lack of communication between it and the lumenal. (c) A high power view of the lesion (shown in (a)), note that the lesion is rich in proteoglycan and smooth muscle cells beneath the thrombus.

(Burke 2001) (Mann 1999). In cases of stable angina, the culprit lesion is often a non-thrombosed plaque.

The plaque, including its endothelium, is not the only determinant of thrombosis – the loss of the normal thrombotic–thrombolytic equilibrium in the circulating blood, and local flow conditions are also important contributors to thrombosis.

The following terms are proposed to describe the thrombosed plaques causing the coronary syndromes:

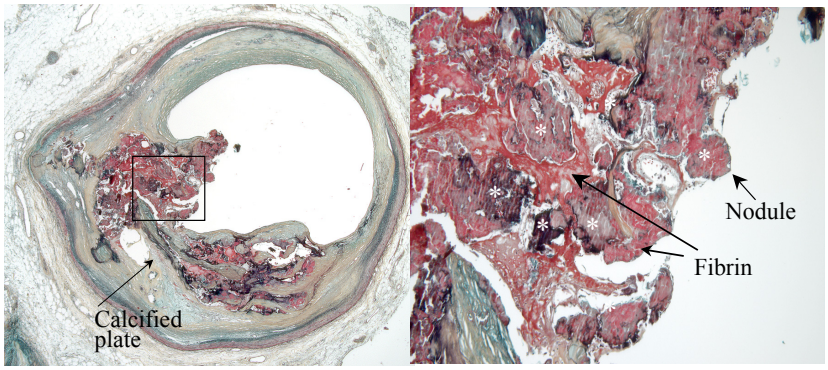

Fig. 4: Calcified nodule. *(left)* Section of the mid right coronary artery showing an eccentric lesion with extensive calcification (calcified plate) and surface calcified nodules with loss of fibrous cap and lumenal fibrin deposition (red). *(right)* High power view of the boxed area in (a) showing calcified nodules (*) intermingled, and on the surface of the nodules fibrin deposition can be observed.

"A ruptured plaque". A plaque with deep injury with a real defect or gap in the fibrous cap that had separated its lipid-rich atheromatous core from the flowing blood, thereby exposing the thrombogenic core of the plaque (Fig. 2a/b). This is the most common cause of coronary thrombosis (Arbustini 1999) (Falk 1999) (Davies 2000).

"An eroded plaque". A plaque with loss and/or dysfunction of the lumenal endothelial cells leading to thrombosis (Fig. 3). There is no structural defect (beyond endothelial injury) or gap in the plaque, which is often rich in smooth muscle cells and proteoglycans (Virmani 2000).

"A plaque with a calcified nodule". A heavily calcified plaque with the loss and/or dysfunction of endothelial cells over a calcified nod-

ule (Fig. 4). This is the least common of the three causes of thrombosis described here (Virmani 2000).

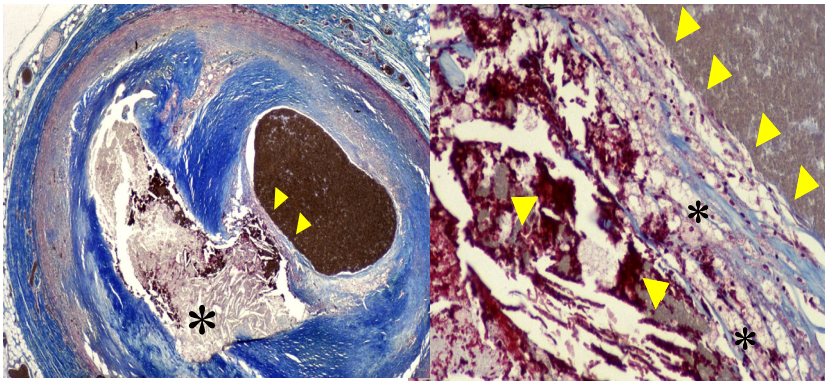

Fig. 5: Inflamed thin-cap fibroatheroma. *(left)* Coronary artery containing a large lipid-rich core that is covered by in thin fibrous cap. The lumen contains contrast medium injected postmortem. *(right)* Higher magnification reveals that the fibrous cap is severely inflamed, containing many macrophage foam cells, and extravasated erythrocytes are seen within the necrotic and avascular core just beneath the cap, indicating that the cap is ruptured nearby. Trichrome stain, rendering lipid colorless, collagen blue, and erythrocytes red.

Prospective identification of a high-risk/vulnerable plaque

There is considerable interest in the identification of plaques prior to the occurrence of thrombosis, since their early detection would lead to trials of novel preventive measures. As described above, it is proposed that such plaques be termed "high-risk", "vulnerable" or "thrombosis-prone" plaques with the three terms used as synonyms.

On the basis of knowledge of the types of plaques identified as causes of thrombosis (ruptured, eroded and calcific nodule plaques), the following types of plaques are suspected to be high-risk/vulnerable plaques:

A plaque prone to rupture

Retrospective pathologic studies of plaque rupture with thrombosis suggest that prior to the event, the plaque was an inflamed, thin-cap fibroatheroma (TCFA)(Fig. 5) (Arbustini 1999) (Falk 1999) (Davies 2000) (Virmani 2000) (Varmana 2002) (Ambrose 1991) (Vallabhajosula 1997).

The major components of such TCFA are:

- A lipid-rich, atheromatous core
- A thin fibrous cap, with
  - macrophage and lymphocyte infiltration
  - decreased smooth muscle cell content
- Expansive remodelling.

A plaque prone to erosion

Retrospective pathologic studies of plaque erosion with thrombosis suggest that, prior to the event, the plaque was often rich in proteoglycans, but, in most cases, lacked a distinguishing structure such as a lipid pool or necrotic core. If a lipid-rich core is present, the fibrous cap is usually thick and rich in smooth muscle cells (Virmani 2000). These plaques are often associated with constrictive remodeling.

A plaque with a calcified nodule

Retrospective pathologic studies of plaques with thrombosis covering a calcified nodule suggest that, prior to the event, the plaque appeared to be heavily calcified with a calcified nodule protruding into the lumen (Virmani 2000).

While such plaques (an inflamed TCFA, a proteoglycan-rich plaque, and a plaque with a calcified nodule) are suspected to be high risk/vulnerable/thrombosis-prone plaques, they cannot be designated as such until prospective studies provide the necessary supporting data. Hence, an inflamed TCFA is best described as a "suspected" high risk/vulnerable plaque, since, while confirmatory data are lacking, its structure definitely resembles that of ruptured plaques.

Novel imaging techniques will provide additional information on vulnerable plaques

Multiple new technologies to improve characterization of plaque in patients are under development (Ambrose 1991) Vallabhajosula 1997) (Huang 2001) (Schmermund 2001) (Jang 2002) (Nair 2002) (Nieman 2003) Moreno 2003) (Schaar 2003a) (Stefanadis 2003) Naghavi 2003) (Casscells 2003b) (Burke 2003). These techniques seek to identify the histologic features, discussed above, of plaques suspected to represent vulnerability, and provide additional information about plaques that has not heretofore been available (data on structure, composition, deformability, pathophysiology, metabolism, temperature, etc.). The novel information will expand the list of features suspected to represent high-risk/vulnerability.

Terms	Definition
Culprit lesion	A lesion in a coronary artery considered, on the basis of angiographic, autopsy or other findings, to be responsible for the clinical event. In unstable angina, myocardial infarction and sudden coronary death, the culprit lesion is often a plaque complicated by thrombosis extending into the lumen.
Eroded plaque	A plaque with loss and/or dysfunction of the lumenal endothelial cells leading to thrombosis. There is usually no additional defect or gap in the plaque, which is often rich in smooth muscle cells and proteoglycans.
High-risk, vulnerable and thrombosis-prone plaque	These terms can be used as synonyms to describe a plaque that is at increased risk of thrombosis (or rethrombosis) and rapid stenosis progression.
Inflamed thin-cap fibroatheroma (TCFA)	An inflamed plaque with a thin cap covering a lipid-rich, necrotic core. An inflamed TCFA is suspected to be a high-risk/vulnerable plaque.
Plaque with a calcified nodule	A heavily calcified plaque with the loss and/or dysfunction of endothelial cells over a calcified nodule, resulting in loss of fibrous cap, that makes the plaque at high-risk/vulnerable. This is the least common of the three types of suspected high-risk/vulnerable plaques.
Ruptured plaque	A plaque with deep injury with a real defect or gap in the fibrous cap that had separated its lipid-rich atheromatous core from the flowing blood, thereby exposing the thrombogenic core of the plaque. This is the most common cause of thrombosis.

Table 1: Definitions

TERMS	DEFINITION
Thrombosed plaque	A plaque with an overlying thrombus extending into the lumen of the vessel. The thrombus may be occlusive or non-occlusive.
Vulnerable patient	A patient at high-risk (vulnerable, prone) to experience a cardiovascular ischemic event due to a high atherosclerotic burden, high-risk/vulnerable plaques, and/or thrombogenic blood.

TABLE 1: DEFINITIONS

Prospective clinical trials are required

All features suspected to represent high-risk/vulnerability require validation in longitudinal, prospective, clinical trials that will document the natural history of plaques with features suspected to make them high-risk and vulnerable. If such trials are positive, it may then be possible to identify a high risk/vulnerable plaque prospectively in an individual patient.

It is also recognized that high-risk/vulnerability may vary over time. The use of systemic markers of inflammation may assist in assessment of the currently unknown time-course of risk. It is hoped that the terminology defined above and summarized in Table 1 will diminish the need for the use of several other terms (plaque disruption, plaque fissuring and unstable plaque) that have been less specifically defined in previous usage.

Treatment

Potential new treatments with systemic, regional, and local approaches have been proposed and also require evaluation in clinical trials (Meier 1997) (Mercado 2003). Improved identification and treatment of high-risk/vulnerable plaques is a goal of great importance since it would result in major decreases in coronary artery disease morbidity and mortality.

Participants in the meeting

The meeting was convened and directed by Drs. Patrick W. Serruys, Antonio Colombo, Christodoulos I. Stefanadis, and Johannes A Schaar.

Drs. Erling Falk, Valentin Fuster, James Muller, and Renu Virmani served on the drafting committee for terminology.

The following participants contributed to the development of, and support the consensus terminology described above:

John A. Ambrose, Nico Bruining, George Dangas, Zahi A. Fayad, Pim J. de Feyter, Enrique P. Gurfinkel, Frank J.H. Gijsen, Antoinette ten Have, Victoria L.M. Herrera, Ik-Kyung Jang, Bob Jones, Dominique P. de Kleijn, Chris L. de Korte, Rob Krams, Richard T. Lee, Lars Lind, Frits Mastik, William McPheat, Gerard Pasterkamp, Sweder W.E. van de Poll, Evelyn Regar, Axel Schmermund, Bernward A. Schoelkens, Jean-Francois Tanguay, Shankar Vallabhajosula, Glenn Van Langenhove, Stefan Verheye, Jolanda J. Wentzel, Robert L. Wilensky, Andrew Zalewski.

Part II
Validation in Vitro

Chapter 3

Effect of Temperature Increase and Freezing on Elastography

Based on:

Johannes A. Schaar, Chris L. de Korte, Frits Mastik, Anton FW van der Steen
Effect of temperature increase and freezing on intravascular elastography
Ultrasonics (2002) 40, 879–881

As an extension of the current intravascular ultrasound (IVUS) technique, intravascular elastography is capable to measure strain using the high frequency rf-ultrasound signal. The radial strain is obtained from cross-correlation analysis of rf-signals recorded at different intravascular pressures (de Korte 1998a). Physiologically applied pressure changes the vascular wall after every heartbeat. The changes are dependent on the composition of the vascular wall (Wada 1997). The structure and the composition of the vessel changes with age, physical activities, components of nutrition, hypertension, diabetes mellitus and many other factors (Schmermund 1999). Since composition of the vessel wall engenders the mechanical properties of a vessel, measurement of this mechanics may influence our understanding of the pathophysiology of the diseases and their treatment. Because atherosclerosis is one of the leading causes of vessel changes and in this respects also a main cause for death, measurement of elasticity in vessels is of major impact.

Arteries were stored at -80 °C, but experiments were performed at room temperature

For validation extensive experiments with coronary and femoral arteries were performed. In vitro experiments demonstrated that different strain values were measured in fibrous, fatty and fibro-fatty tissue indicating the potential of intravascular elastography to distinguish different plaque morphologies (de Korte 2000a). For these experiments artery segments were excised within 24 h after death, measured and after that stored at -80 °C. The arteries were thawed, connected to the experimental setup and experiments were performed at room temperature in a watertank.

Aim of the study was to investigate the influence of temperature on elastography

The aim of the present study was to investigate the influence of storage and measurement temperatures on intravascular elastography. As measurement points were chosen: 23 °C (room temperature), 37 °C (body temperature) and 23 °C after freezing at -80 °C.

Methods

Cross sections were marked with a needle

Atherosclerotic human femoral (n=1), carotid (n=1) and coronary (n=4) artery segments were excised within 24 h post mortem and measured within 3 h after excision. After closing side branches with suture material the arteries were scanned at different positions, with a gap of more than 10 mm. These cross-sections (n =12) were marked with a surgical needle, inserted tangentially in the adventitia, which is clearly visible in the echogram. Inserting the needle into the adventitia doesn't destroy the vascular wall and has no influence on the mechanical properties of the vessel. This surgical needle was inserted till the end of the experiment, to make sure, that the spots of interest were retrieved. The ultrasound experiments were performed in a physiological saline solution in a water tank at room temperature (23 ± 1 ^{o}C).

A water column system, containing a de-gassed physiological saline solution, was connected to the proximal sheath: Intraluminal pressures of 80 and 100 mm Hg were applied. This sheath also was used to insert the IVUS catheter. The arteries were scanned with an InVision 20-MHz IVUS catheter (Jomed Inc., Rancho Cordova, CA). The pressure was monitored with the use of a pressure gauge (DTX/plus, Ohmeda) connected to the distal sheath.

Radio frequency data were sampled at 100 MHz

The catheter was connected to an InVision echo apparatus (Jomed Inc., Rancho Cordova, CA); 512 angles containing 10 s of radio frequency data sampled at 100 MHz were acquired at 30 frames/s. First, an IVUS frame was acquired at 80 mm Hg intravascular pressure. After 10 μs, an IVUS frame was acquired at 100 mmHg to achieve different strain levels of the material. The data were captured using a PC-based acquisition system, connected to the digital interface of an InVision Echo machine. The acquisitions were stored on a CD-ROM for off-line processing.

The resolution of the strain in the radial direction is 200 μm

Elastograms were calculated as described before (de Korte 1999). The local strain was calculated from the gated radio frequency traces and displayed using color code from red for low strain through green for 2% strain and plotted as a complementary image to the IVUS echogram. The resolution of the strain in the radial direction is 200 μm.

After the first recording of an elastogram the saline in the watertank was heated from room temperature to 37 °C. Due to the surrounding saline the vessel temperature also increased to 37 °C. Thirty minutes later the measurements were repeated as described above. Temperature was measured in the water bath by a thermometer (ITI 20-2 B, AoiP Mesures, France).

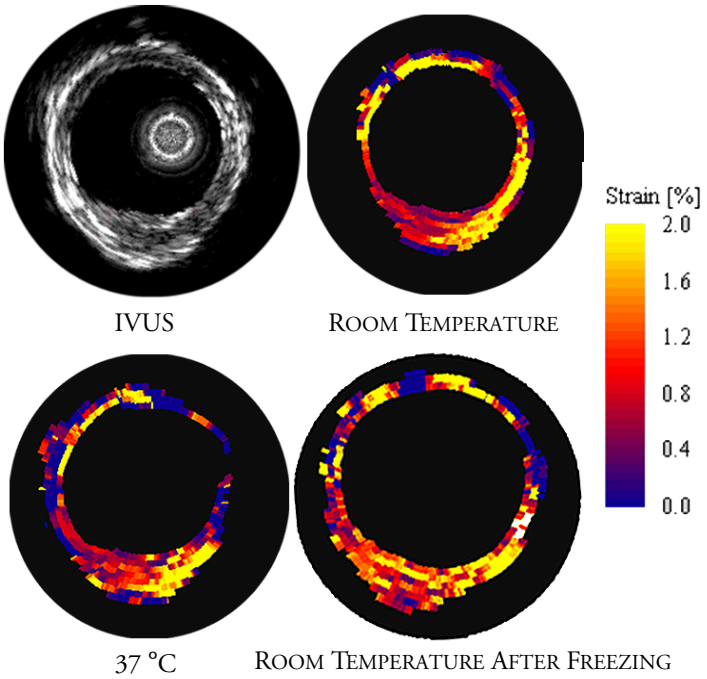

Fig. 1: Intravascular elastograms under influence of different temperatures.

The vessel was disconnected from the sheath and frozen at -80 °C for 12–24 h. The vessels were thawed and the measurements were repeated at the same spot, which was marked by a surgical needle.

The mean strain in the plaques was determined for all acquisitions.

All statistical analysis was performed with the use of SPSS 10.1.4 software. First, the distribution of the average strain was tested for normality using the Shapiro–Wilk test (Altman 1997). These tests revealed that the strain was normally distributed in each group of temperature (p=0.34 for 23 °C, p=0.20 for 37 °C, p=0.35 for 23 °C after freezing).

To test the differences between the groups a paired samples t-test was performed. Values of $p < 0:05$ were considered significant.

Results

In this study, 12 cross-sections were analyzed from six arteries. One measurement in the 37 °C group and in the 23 °C after freezing group failed due to recording problems. In the cross-section the region of interest was defined by the size of the plaque. The mean strain of the region of interest was determined for every temperature group shortly after each other to ensure measurement in identical areas. An IVUS echogram and elastogram of a carotid artery cross-section at different temperatures is presented in Fig. 1. The echogram shows an eccentric plaque between the 6 and 9 o'clock positions.

A qualitative comparison between the elastograms at different temperatures and after freezing reveals that the strain in the plaque looks similar. A slightly increased strain is found in the elastogram of the fresh artery. The white lines indicate the region used for the statistical analysis.

	23 °C	37 °C	23 °C After Freezing
Number of valid measurements	12	11	11
Mean strain in %	0.93	0.91	0.79
Standard error of mean strain in %	0.20	0.21	0.21
Standard deviation mean strain in %	0.68	0.71	0.69

Table 1: Mean Strain and The Influence of Freezing and Different Temperatures

Table 1 shows the frequencies, the mean strain value and the deviation for the different groups. Table 2 presents the results of the of the paired sample t-test. For comparison the 23 °C group, the 37 °C group and the 23 °C group after freezing was chosen. The difference between the groups was not statistically significant.

		Mean strain difference in %	Standard deviation in %	Standard error of mean in %	p
Pair 1	23°C vs. 37°C	0.01	0.15	0.05	0.848
Pair 2	23°C - at 23°C	0.12	0.36	0.11	0.313

Table 2: Mean Strain Differences

Discussion

Imaging the atherosclerotic plaque with IVUS gave important insights into the morphology of atherosclerosis (Kinlay 2001). Elastography can add mechanical information to the current used IVUS pictures and lead into the direction of tissue characterization (de Korte 2000b). Since intravascular elastography may play an important role in the future for characterizing mechanical properties of vascular tissue a proper validation is necessary. One part of this validation process is the accomplishment of in vitro experiments with vessels of human nature. The experimental setup should be on one side convenient to use, on the other side reflect also clinical circumstances.

In this study we examined the influence of different temperatures on the elastograms to be sure, that temperature effects do not harm our experimental setup and curtail the results of the validation process.

We measured vessels in a scenario, which was chosen in previously published studies, where the experiments were performed at room temperature (de Korte 2000c). Fatty tissue has different elastic properties in vivo and in vitro, most likely related to different temperatures. Since the body temperature is approximately at 37 °C, we performed a measurement in a human body like environment at body temperature to establish the original state of the tissue as close as possible and prove the effect of temperature changes. Also of in-

terest was the effect of freezing on mechanical properties since it is convenient to store vessel specimens before an investigation.

There is no statistically difference between different temperature influence on elastograms

There is no statistically difference between 23 and 37 °C. We conclude that future in vitro experiments can be performed at room temperature without affecting strain measurements. Also no influence on strain measurements of freezing was seen. The average strain in the region of interest was not significant different in the measurement after a freezing period. We conclude that specimens can be stored in a -80 °C refrigerator before a experiment, without affecting the mechanical properties. This results lead into the direction of a convenient use of arterial specimens in experimental setups of IVUS elastography.

Chapter 4

Characterizing Vulnerable Plaque Features With Intravascular Elastography

Based on:

Johannes A. Schaar, Chris L. de Korte, Frits Mastik, Chaylendra Strijder; Gerard Pasterkamp, Eric Boersma, Patrick W. Serruys, Anton F.W. van der Steen
Characterizing Vulnerable Plaque Features With Intravascular Elastography
Circulation (2003) 108, 2636-2641

Myocardial infarction, sudden cardiac death, and unstable angina have in common a genesis of coronary thrombosis, which develops as a result of a ruptured vulnerable or an eroded atherosclerotic plaque. As long as atherosclerotic lesions do not rupture and eroded plaques do not induce thrombosis, coronary artery disease may be a clinically silent disease associated with low mortality (Virmani 2001). Whenever plaques start to rupture and thrombogenic material is coming in contact with circulating blood, a situation is created that may lead to acute coronary syndrome associated with high mortality (Falk 1999)

Plaque rupture is related to a fragilization process of the cap over an atheromatous core

Plaque rupture is related to a fragilization process of the cap over an atheromatous core (Loree 1992). This process is triggered by an accumulation of inflammatory cells like macrophages, which produce metalloproteinases (matrix-degrading enzymes) (Libby 1995). To understand the mechanisms of plaque destabilization and guide a pharmacological treatment, it would be of major interest to image the fragile part of the atheromatous plaque and to differentiate between high-risk and low-risk plaques (Muller 1994).

Physiological pressure strains the vascular wall during every heartbeat

As an add-on to intravascular ultrasound (IVUS), intravascular elastography is able to measure strain using cross-correlation analysis of radio frequency ultrasound signals recorded at different intravascular pressures (de Korte 1998a). Physiological pressure strains the vascular wall during every heartbeat (Lendon 1993). The underlying principle is that the strain of the tissue is a function of its mechanical properties. The local strain of the tissue is displayed as an additional image (elastogram) to the IVUS echogram (de Korte 2000c). Preliminary experiments revealed that it is feasible to discriminate between fatty, fatty fibrous, and fibrous material with this technique (de Korte 2000a).

Aim of the study is to evaluated the ability of intravascular elastography to identify vulnerable plaque features

The structure and the composition of the vessel change with age, hypertension, diabetes mellitus, and many other factors (Schmermund 1999). Because composition of the vessel wall affects the mechanical properties of a vessel, the analysis of mechanical behaviour of the vessel wall may enhance our understanding of the pathophysiology of atherosclerotic disease. Furthermore, rupture of plaques may occur in regions with increased mechanical stress (Burleigh 1992).

In this study, we evaluated the ability of intravascular elastography to identify vulnerable plaque features. We tested the hypothesis that a pattern consisting of a high-strain region at the surface adjacent to low-strain regions corresponds to vulnerable plaque in histology. Furthermore, we looked at the relation between vulnerable plaque features and local high strain regions.

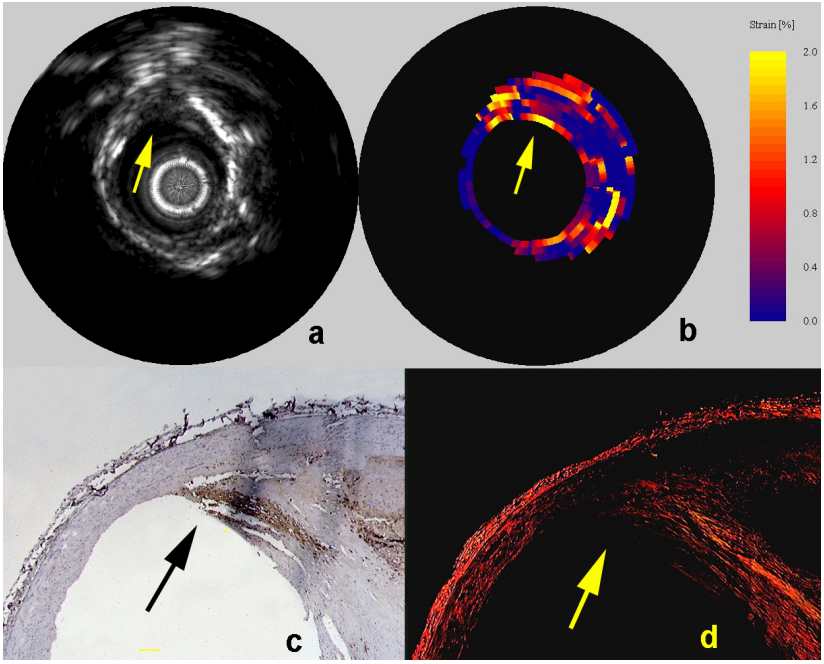

Fig 1: Vulnerable plaque marked in IVUS (a), elastogram (b), macrophage staining (c), and collagen staining (d). In the elastogram, a vulnerable plaque is indicated by a high strain on the surface. In the corresponding histology, a high amount of macrophages (c) is visible with a thin cap (d) and a lipid pool.

Methods

Atherosclerotic human coronary (n=24) artery segments of 23 patients were excised and measured within 24 hours postmortem. All patients (mean age, 65±6 years) died of non-coronary causes, such as
pneumonia (n=9), cancer (n=11), aortic dissection (n=1), and liver

failure (n=2). Fifteen left coronary arteries and 9 right coronary arteries were used. The arteries were mounted between 2 sheaths. Before a defined constant pressure in the artery was achieved, the vessel was pressurized several times to detect leakage caused by even the smallest side branches still left open. After closing the remaining side branches, the vessel was pressurized several times to ensure the absence of leakage. Immediately after the ultrasound, experiments were performed in physiological saline solution in a water tank at room temperature.

A water column system, also containing physiological saline solution, was connected to the proximal sheath. This sheath was used to insert an 20-MHz IVUS catheter (Jomed Inc, Rancho Cordova, CA, USA) connected to an InVision echo apparatus (Jomed Inc, Rancho Cordova, CA, USA).

IVUS frame was acquired at 80 and 100 mmHg

First, an IVUS frame was acquired at 80 mm Hg intravascular pressure. After 10 seconds, another IVUS frame was acquired at 100 mm Hg to obtain the incremental strain of the material. The data were captured using a PC-based acquisition system, connected to the digital interface of the echo machine, and stored on a CD-ROM for off-line processing.

58 cross sections were scanned

Fifty-eight cross sections were scanned with an interval of more than 10 mm to ensure uncorrelated observations. After the elastographic acquisition, the position of the ultrasonic cross sections was marked in the echogram with a clearly visible surgical needle inserted in the adventitia. On the surgical needle, a suture was mounted. Before cutting, the needle was removed but the suture remained in place. This suture was used as a marker for sectioning location.

Coronary arteries were pressure-fixed

Subsequently, the coronary arteries were pressure-fixed (80 mmHg) and imaged segments were stained for the presence of collagen and fat (picro Sirius red and polarized microscopy), smooth muscle cells (α-actin), and macrophages (CD 68).

Elastograms were calculated as described before (de Korte 1998b). The local strain was calculated from the gated radio frequency traces and displayed color-coded from blue for 0% strain via red to yellow for 2% strain and plotted as a complementary image to the

IVUS echogram. The resolution of the strain measurement in the radial direction was 200 μm.

Observers blinded for the outcome of each respective technique analyzed elastograms and histology.

Observers blinded for the outcome of each respective technique analyzed elastograms and histology. The thickness of the plaque cap and the atheroma size were measured using quantitative analysis of light microscopic images (Clemex Vision PE 3.5). To compare histology with elastography, matching between IVUS pictures and histology was performed using anatomical or artificial landmarks like calcium spots or the above-described suture. The matching was performed without knowledge of the elastographic results. Cross sections (n=4), for which a match between histology and IVUS echogram was not obvious, were excluded from the study.

In histology, a vulnerable plaque was defined as a plaque whose content consists of more than 40% atheroma covered by a thin cap with moderate to heavy macrophage infiltration, as described by Davies (Davies 1995). A thin cap was defined as smaller than 250 μm (Mann 1996). Smooth muscle cells (SMCs), collagen, and macrophages were graded as none, minor, moderate, and heavy according to their staining (Pasterkamp 1998).

In elastography, the potentially vulnerable location was defined as the region with the highest strain at the surface with adjacent low-strain regions (Figure 1). These spots were correlated with tissue components, which indicate vulnerability.

A ROC curve analysis was performed to evaluate the value of local strain for the prediction of plaque vulnerability

For statistical analysis, SPSS 11.0.1 (SPSS Inc, Chicago, MI, USA) was used. Continuous variables are presented as median values and corresponding 25th and 75th percentiles. A receiver operator characteristic (ROC) curve analysis was performed to evaluate the value of local strain for the prediction of plaque vulnerability. According to this method, sensitivity (number of identified vulnerable plaques per total number of vulnerable plaques) and specificity (number of identified nonvulnerable plaques per total number of nonvulnerable plaques) were determined over the entire range of strain measurements using each observed value as a diagnostic threshold and plotted against each other. The area under the obtained curve, which may range from 0.5 to 1.0, represents the diagnostic accuracy of local strain. The strain value with the highest sum of sensitivity

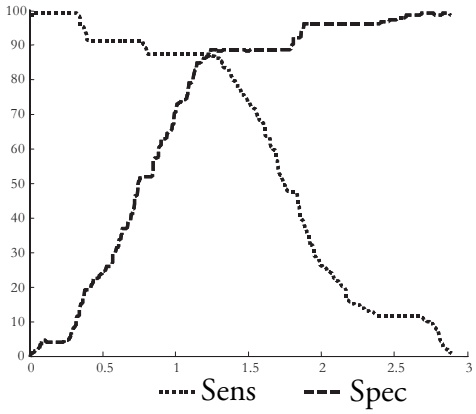

Fig 2: Relation between strain, sensitivity (Sens) and specificity (Spec)

and specificity was considered to best discriminate between vulnerable and nonvulnerable plaques.

Subsequently, multiple linear regression analyses were performed to evaluate the relationship between local strain and several plaque components, such as macrophages, smooth muscle cells, collagen content, and cap thickness. Regression coefficients with corresponding standard errors are reported, as well as significance levels. Nonlinear regression was used to test the relation between cap thickness and strain according to the model of Loree et al. (Loree 1992). The Kolmogorov-Smirnov test was used to assess normal distribution.

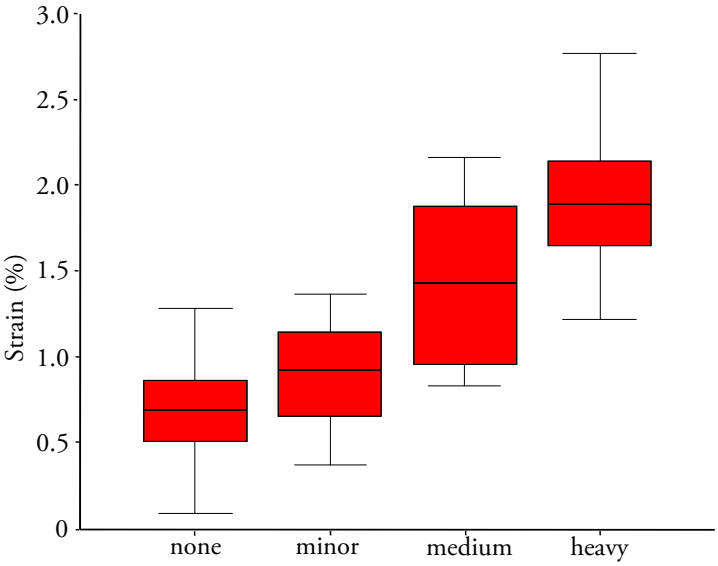

Fig 3: Relation between strain (percent) and macrophages of the potentially vulnerable locations.

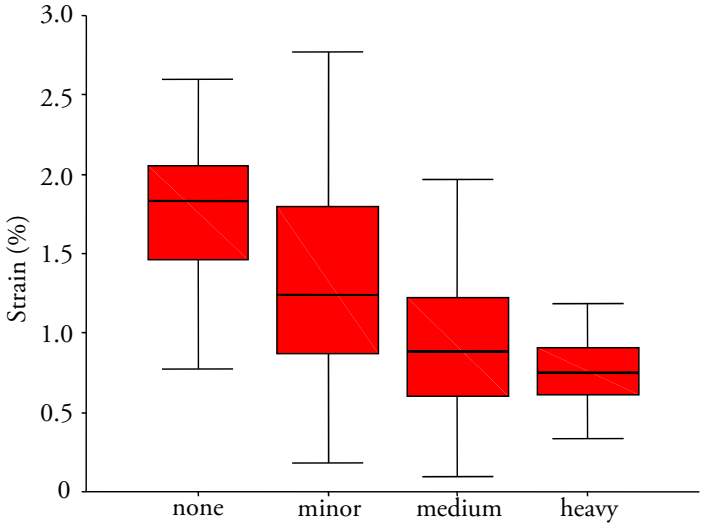

Fig 4: Relation between strain (percent) and smooth muscle cells of the potentially vulnerable locations.

Results

Predictive value of intravascular elastography to detect vulnerable plaque

Average strain was obtained in the high-strain region of the plaques (n=54) of 24 diseased coronary arteries and compared with the histological grading of vulnerability. Twenty six vulnerable plaques and 28 nonvulnerable plaques were found. The optimal sensitivity and specificity were obtained for a threshold value of 1.26% strain (Figure 2). The area under the curve of the ROC analysis was 0.85 (95% CI, 0.74 to 0.97).

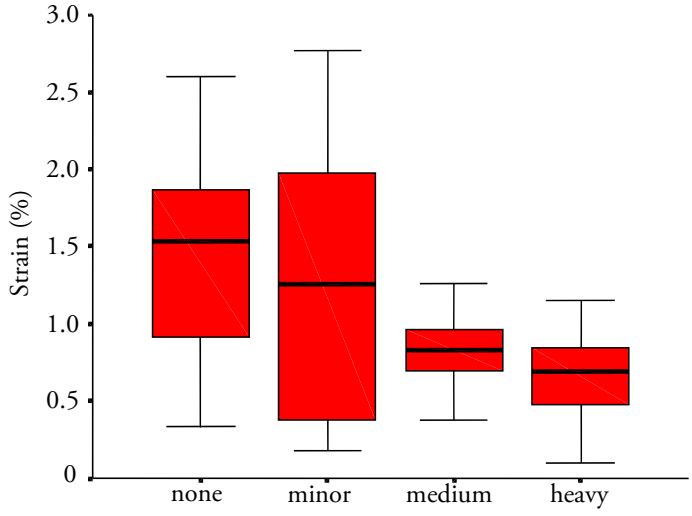

Fig 5: Relation between strain (percent) and collagen of the potentially vulnerable locations.

Regarding vulnerable plaques, elastography was positive in 23 cases but negative in 3 cases. This results in a sensitivity of 88%. Nonvulnerable plaque were seen by histology in 28 cases and detected by elastography in 25 cases but were falsely diagnosed as positive in 3 cases. This results in a specificity of 89%. Intravascular elastography has a positive predictive value of 88% and negative predictive value of 89% based on comparison with histology. Comparing vulnerability in elastograms with cap thickness measured in histology, vulnerable plaques have a statistically thinner cap (258.7±18.1 μm) than nonvulnerable plaques (362.7±29.7 μm), with $P< 0.005$.

Relation between features associated with plaque vulnerability and strain

The box-and-whisker plots show the relation between the 4 classes of macrophage content divided versus strain (Figure 3), SMC versus strain (Figure 4), and collagen versus strain (Figure 5). The relation between strain and cap thickness is reported in Figure 6. There is an inverse relationship between strain and cap thickness. A

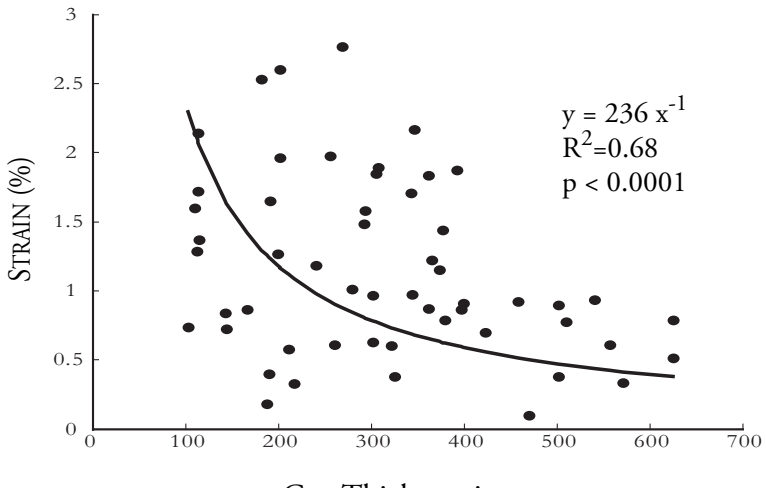

Fig 6: Relation between strain (percent) and cap thickness (micrograms)

curve estimation, based on finite element modelling (Loree 1992), showed R=0.68 with P<0.0001. It should be noticed that a cap >400 μm results in a strain <1%, whereas the data are more scattered for lower cap thickness. The *R* of the linear regression model with all tissue components mentioned above as independent variables and strain as dependent variable is 0.48, with a value of $P<0.0001$. Detailed analysis is given in Table 1.

Model	Coefficient	SD	p value
Cap thickness, µm	-0.0004	0.001	0.14
Macrophages	0.552	0.192	0,006
SMC	-0.738	0.177	0.0001
Collagen	-0.217	0.177	0.227

Table 1: Description of the Linear Regression Model Regarding the Influence of Tissue Components (Cap Thickness, Macrophages, SMCs, Collagen) on Strain

Discussion

There is a need for a technique to diagnose the vulnerability of a plaque. With the availability of such a technique, a vulnerable plaque can be identified and followed and treatment can be monitored. Studies have shown that different strain values were obtained with intravascular elastography for different plaque components in vitro and in vivo (de Korte 2002a+b).

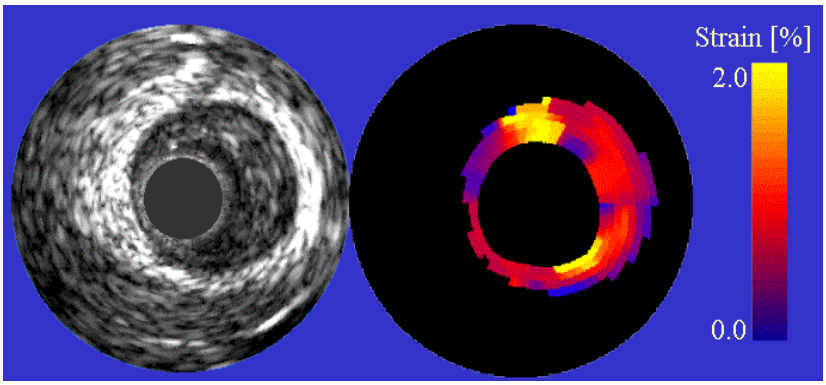

Fig 7: A typical observational example of an eccentric plaque with high strain spots on the shoulders is given.
The image was recorded in a patient with unstable angina pectoris (Braunwald IIIb).

One aim of the study was to assess the predictive value of IVUS elastography to identify the vulnerable plaque. This study demonstrates that intravascular elastography can accurately diagnose vulnerable plaques, as defined by Davies (Davies 1995) in vitro with a

high sensitivity and specificity. Because detection of vulnerability is presently not feasible in vivo with other available techniques, intravascular elastography may offer an unique opportunity to learn more about the aetiology of plaque rupture and to assess the effect of pharmacological agents on plaque stabilization.

We measured the mechanical properties of plaques, as depicted by the strain in an elastogram.

Rupturing of a lipid-rich plaque may initiate the development of acute cardiac ischemic events. We measured the mechanical properties of plaques, as depicted by the strain in an elastogram. The vulnerable plaque is characterized by a high strain value on the surface of the plaque (Figure 7); conversely, a stable plaque has a low strain caused by a stable cap.

Another aim of the study was to find out which anatomical features in particular generate the high strain spots in an elastogram. To answer this question, elastograms and histology were compared in 54 cross sections of human coronary arteries. The principal findings of this part of the study were as follows. First, there is a high correlation between the strain in the cap of coronary plaques and the amount of macrophages. Second, there is an inverse correlation between the amount of SMC and strain. Third, plaques, which are declared vulnerable in elastography, have a thinner cap than non-vulnerable plaques and a higher macrophage concentration.

High correlation between strain and macrophages

The high correlation between strain and macrophages can be explained by weakening of the cap. Macrophages play a central role in the degradation process of the extra cellular matrix by secreting proteolytic enzymes (Galis 1994). In our study, this is reflected by the relationship between the amount of macrophages and the level of strain in the high strain spot in the elastogram.

High strain is correlated with a low amount of SMC

Compared with macrophages, less is known about the influence of SMCs on the vulnerable plaque. Nevertheless, it has been suggested that plaques are more likely to break if fewer SMCs are present (Davies 1993). The reason is not quite clear, but it seems that SMCs play an important role in preserving the integrity of the extra cellular matrix in the cap (Geng 1997) (Seshiah 2002). Furthermore, mechanical overstretching has proven to induce apoptosis in isolated vascular smooth muscle cells (Sotoudeh 2002). In our study, this phenomenon may be exemplified by the fact that high strain is correlated with a low amount of SMCs.

Significant relation between strain and collagen

There is also a significant relation between strain and collagen. However, after correcting for the confounding effect of macrophages and smooth muscle cells, no statistically significant effect of collagen on strain could be demonstrated. Thus, these results demonstrate that high strain is mainly caused by the presence of macrophages and the paucity of smooth muscle cells.

Inverse relation between cap thickness and strain.

Rupture of the plaque occurs mostly at the thinnest part of the cap. In our study, we found an inverse relation between cap thickness and strain. Loree et al. (Loree 1992) have already shown using a finite element model that a reduction of the fibrous cap thickness under 250 μm dramatically increases peak circumferential stress in the plaque. However, this relation was never demonstrated by measurements in coronary plaques. In our study, the cap thickness of plaques that are considered vulnerable was 250 μm. Furthermore, no regions with a strain higher than 1% were found in plaques with a cap thickness of greater than 260 μm.

In this study, all patients died from noncoronary causes. This population was chosen to detect rupture-prone plaques and not already-ruptured plaques. However, taking into account that plaque rupture is a process triggered by inflammation, using cap thickness as an exclusive marker may be too simple. The often-used upper bound of 65 μm, as defined by Burke et al. (Burke 1997), described that it was not likely to have ruptured caps thicker than 65 μm. However, their conclusion was not that caps that are larger than 65 μm could not be considered vulnerable. Davies et al. (Davies 1993) focused more on the presence of inflammation rather than the cap thickness, which degrades the integrity and leads to a rupture. Nevertheless, in vulnerable patients who died from coronary artery disease, Mann and Davies (Mann 1996) found that the mean minimal cap thickness, i.e., the thinnest part of a cap, was 250 μm. In view of this, we considered caps thinner than 250 μm with moderate or heavy infiltration of macrophages as rupture prone. Studies have shown that inflammation contributes extensively to mechanical behaviour of fibrous caps (Lendon 1991). Therefore, an exact cap thickness and the relation to triggering processes-like inflammation have to be exactly investigated in the future.

The impact of a diagnostic technique is highly dependent on its feasibility in vivo. Intravascular elastography has been applied in pa-

tients (de Korte 2002b). Because IVUS is a commercially available technique that is routinely used by cardiologists, no additional catheters are needed to perform elastography. Elastography is able to detect vulnerable plaque features. This may enable us to follow the natural history of plaques suspected to be vulnerable (Figure 7). Furthermore, the influence of treatment of vulnerable plaques can be studied. Because palpography is based on computer processing, it can be easily implemented in the daily diagnostic procedure of patients with acute coronary syndrome.

Motion, either from the heart or the catheter, can lead to unreliable results in the clinical setting.

Motion, either from the heart or the catheter, can lead to unreliable results in the clinical setting. These motion artifacts can be avoided by acquisition of the signals in end diastole, where a pressure change still exists but the catheter motion reaches its minimum (de Korte 2002b). Furthermore, contrary to light-based techniques, ultrasound at the frequency used in this study does not suffer from the presence of blood in the artery.

However, the use of intravascular elastography is limited by its invasive nature. In the future, noninvasive tests like computed tomography or MRI may serve as screening tests to identify high-risk lesions and triage the patients to a more invasive testing once they have reached sufficient spatial and parametric resolution.

OCT

Other intravascular techniques are presently under development to detect vulnerable plaque features. Optical coherence tomography has a much higher resolution (approximately 10 μm) than IVUS and may provide a more detailed description of the morphology of a plaque. However, it has limited penetration depth and requires flushing the lumen with saline or inflating a balloon before images can be acquired (Jang 2002).

Angioscopy

The same problems occur with angioscopy, where flushing is needed to identify yellow plaques, which are associated with acute coronary syndromes (Uchida 1995).

Thermography

Thermography can detect plaques with high temperature, which is related to inflammation (Casscells 1996). Results of preliminary investigation in humans have been reported (Stefanadis 2001). However, the method needs additional validation, especially regarding the influence of external parameters like intracoronary blood flow.

Near-infrared spectroscopy

Near-infrared spectroscopy obtains pictures based on absorbance of light by organic molecules. This technique has proven to detect plaque components with a high accuracy in vitro, although blood particles may hinder light waves to reach the plaque (Moreno 2002), a fact that limits all light-emitting diagnostic tools in their ability to detect plaque components.

Several groups have investigated the potential of radiofrequency signal analysis for tissue characterization (Nair 2001) (Landini 1986) (Wilson 1994) (Jeremias 1999) Wickline 1994) (Bridal 2000) (Spencer 1997). Many of these studies revealed the potential to identify calcified plaques, but although promising, none of them has converged yet to a technique with sufficient spatial and parametric resolution to identify a lipid pool covered by a thin fibrous cap. The power of elastography is that it is assessing the weak spot of a plaque and thus not needing high resolution.

Limitations

Strain estimation in this study is based on tissue mechanics ex vivo. The level of deformation of tissue in vivo may be different to the in vitro measurements. This may be attributable to lack of external parameters, such as innervations, tonus, and pulsatility. Future studies will address these questions. To extrapolate the results to a clinical situation, a prospective study is needed as in vivo validation. All measurements of this study were performed at room temperature (23°C). In a previous study, we found that this temperature difference in vitro does not affect strain measurements (Schaar 2002).

The phrase and definition of vulnerable plaque are critically chosen. From a prospective view, it is unknown which plaques are rupture prone. The result of the ROC analysis may have been different if another definition were chosen. The arteries are preconditioned by repetitively pressurizing them from baseline. The arteries were initially pressurized at 80 mm Hg and then pressurized 10 seconds later to 100 mm Hg. The effects of preconditioning and hysteresis were not assessed in these experiments, limiting our ability to directly extrapolate to steady-state pulsatile environment. Although there is a difference between the static and dynamic mechanical properties of vascular tissue, the ratio between the different plaque components remains similar (Lee 1991) (Lee 1992). Nevertheless,

in a pulsatile environment, the locations with increased strain may change between static or pulsatile experiments. However, the optimal threshold value (1.26% strain) for detecting a vulnerable plaque cannot be directly transferred from static in vitro experiments to pulsatile in patient recordings. This is corroborated by the initial elastographic in vivo acquisitions, where similar strain values were measured as in the in vitro experiments but with a significantly lower pressure differential (de Korte 2002a). This study shows that you can get sensitivity and specificity of approximately 90%. For in vivo measurements in patients, the strain threshold still has to be determined.

Plaques, in which elastography was assessed, were selected from the IVUS pictures. However, because the coronary artery specimens were short and recording close to the sheets was avoided, only a limited number of plaques were suited for recording and a preselection of certain plaque features was hindered.

Conclusions

Intravascular elastography identifies successfully vulnerable plaque features in postmortem coronary arteries. Thus, intravascular elastography may play an important role in diagnosing the vulnerable plaque and help to gain deeper insight in the pathophysiology of acute coronary syndrome and identify the high-risk patient.

If unstable angina, plaque progression, and myocardial infarction are to be understood and prevented, vulnerable plaques must be identified and stabilized. Endeavours to prevent acute events are limited by identifying the high-risk plaque. The identification of vulnerable plaques may allow establishing therapies to reduce the risk of cardiac death in the future and opens the door to a preventive strategy for our patients.

Part III
Validation in Vivo

Chapter 5

Identification of Atherosclerotic Plaque Components With Intravascular Ultrasound Elastography In Vivo A Yucatan Pig Study

Based on:

Johannes A. Schaar, Chris L. de Korte, Frits Mastik, Chaylendra Strijder; Gerard Pasterkamp, Eric Boersma, Patrick W. Serruys, Anton F.W. van der Steen
Characterizing Vulnerable Plaque Features With Intravascular Elastography
Circulation (2003) 108, 2636-2641

The composition of an atherosclerotic plaque is an important determinant for clinical syndromes. Determinants of ruptured plaques are a large lipid core covered by a thin fibrous cap with a dense infiltration of macrophages (Davies 1993). Although some promising invasive and noninvasive techniques (Pasterkamp 2000) are being developed, no technique is currently clinically available to identify these vulnerable plaques.

Intravascular ultrasound (IVUS) has proven to be a powerful technique to assess the geometry of the vessel wall and plaque. However, the sensitivity and specificity to detect lipid cores remains low (Komiyama 2000) (Prati 2001). IVUS elastography assesses the local radial strain in the tissue caused by an intraluminal pressure differential. In vitro experiments revealed different strain values in fibrous and fatty plaques in human coronary and femoral arteries (de Korte 2000a). Feasibility experiments in patients showed that reproducible elastograms could be obtained (de Korte 2002b).

The aim of this study was to validate IVUS elastography in vivo with an atherosclerotic Yucatan minipig model. Additionally, we studied whether atheroma and macrophages were related with strain values.

Methods

Animals

Six atherosclerotic Yucatan pigs, average weight 40 kg, were studied. To induce atherosclerosis, pigs were put on an atherogenic diet. Two weeks thereafter, the external iliac and femoral arteries were denuded with a 4-F endothelial Fogarty catheter. The atherogenic

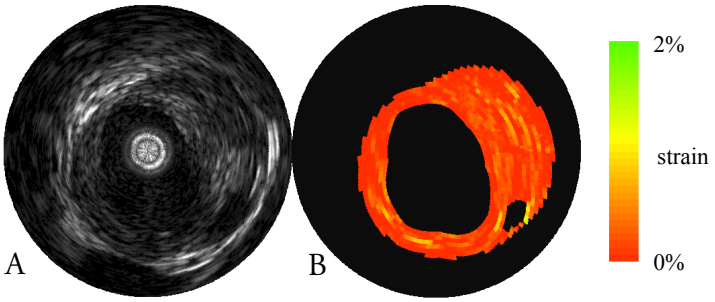

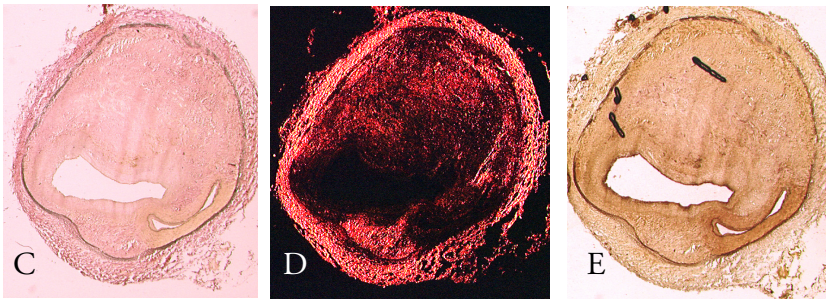

Fig 1: IVUS echogram (A) and elastogram (B) of cross-section with an advanced fibrous lesion. Low-strain values were found in this plaque. The plaque is mainly composed of collagen and no macrophages were found. Histology picro-Sirius red [C], picro-Sirius red imaged with polarized light microscopy [D], and acid phosphatase [E]) reveals that the plaque was imaged froma false lumen that was created during the intervention. The region in the elastogram with no strain values corresponds to the original lumen.

diet was continued for 9 to 10 months after which femoral and internal iliac arteries were stented for the purpose of another study. Subsequently, the atherogenic diet was replaced by a regular diet. No intervention was performed in the denuded external iliac arteries that were visualized for the present study. The following 42 days, 3 pigs were treated with a drug and 3 pigs served as controls for the purpose of another study. ANOVA revealed that the intake of the drug had no influence on the measurements performed in this study. After the elastographic acquisition, animals were euthanized and vessels were harvested. The Ethical Committee on Animal Experimentation of the Faculty of Medicine, Utrecht University, approved the investigation.

Atherogenic Diet

In addition to essential nutrients, vitamins, salts, 2% cholesterol, 18% casein, and 6% peanut oil formed the basic atherogenic components of the diet.

Anesthesia

During denudation, intervention, and termination, the animals were anesthetized with intravenous midazolam 0.3 mg/kg per h and

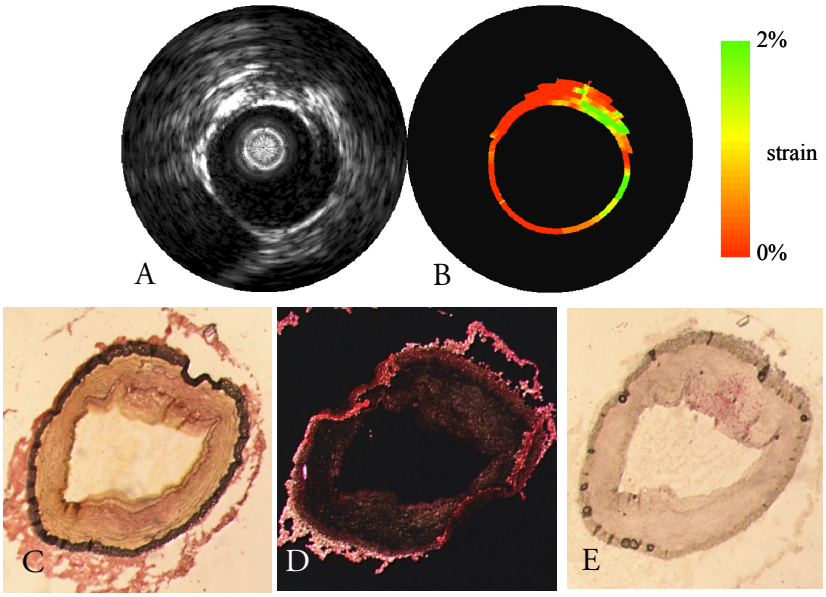

Fig 2: IVUS echogram (A) and elastogram (B) of an early fatty plaque. The strain in this plaque is high, which indicates soft material. Histology (picro-Sirius red [C], picro-Sirius red imaged with polarized light microscopy [D], and acid phosphatase [E]) reveals a lack of collagen in this plaque and a heavy staining of macrophages. The geometry of the cross-section is distorted, because of shrinkage caused by freezing.

sufentanil 2.5 µg/kg per h and ventilated with a mixture of O_2:air=1:1 and 1% halothane after a premedication with 4 mg/kg azaperone, 10 mg/kg ketamine, and 4 mg/kg thiopental.

Elastographic Acquisition

At termination, the arterial tree was accessed through a left carotid approach. An arterial 8-F sheath was introduced into the descending aorta, and an 8-F guiding catheter was advanced to the aortic bifurcation. Through the guiding catheter, contrast angiography was performed and a 20-MHz Visions catheter (JoMed, Rancho Cordova, CA, USA) was advanced. IVUS data were acquired in the external iliac and the proximal, unstented part of the femoral artery. The position of the IVUS catheter was registered with angiography and radiopaque rulers.

Frames that contained 512 angles with high-frequency raw ultrasound signals (7.5 mm) were acquired at 30 frames/second. The data were captured together with the pressure and ECG signals with a workstation that contained a framegrabber (Coreco Inc) connected to the digital interface of an InVision Echo machine (JoMed, Cordova, CA, USA). Blood pressure was measured with the introduction sheath that was located distally from the aortic arch. Each acquisition of 4 seconds that contained 120 frames was stored on a CD-ROM for off-line processing. The animals were euthanized by an overdose of pentobarbital.

After euthanization, the surrounding tissue was removed from the arteries without changing the position of the legs. The investigated cross-sections were identified by angiography by comparison with the stored angiogram and the anatomic landmarks and radio-opaque rulers. The investigated locations were marked with suture in the adventitia. Next, the artery was excised and frozen in liquid nitrogen.

Histology

Cross-sections (7 μm) were stained for general morphology (elastin van Gieson), collagen (picro-Sirius red and imaged with polarized light), and macrophages (acid phosphatase). The lipid content was assessed by the empty spaces in the picro-Sirius red stain imaged with polarized light microscopy (Davies 1993). A lesion was classified as fatty when >40% of the plaque area consisted of fat. A lesion had positive macrophage staining when the acid phosphatase stain revealed clusters of cells with >10 cells. A lesion was classified as advanced when occupying an area within the internal elastic lamina of >40%; otherwise, it was classified as early lesions. Plaques were classified as absent, early fatty lesions, early fibrous lesions, and advanced fibrous plaques by observers blinded to the elastographic results. In this animal model, no advanced fatty plaque and no calcified components were found.

Data Analysis

Elastograms were determined with 2 frames acquired near end-diastole because motion of the catheter is minimal in this phase (de Korte 2002b). Strain values up to 2% were obtained for a pressure differential of 4 mmHg (±0.5) (100 milliseconds interframe time). These strain values are detectable with the chosen window length (Cespedes 1999). For each angle, the radial strain is determined with cross-correlation analysis of the high frequency ultrasound data (de Korte 2000c). All signal processing was performed in Matlab (MathWorks). The strain values were color coded from red for low strain via yellow to green for 2% strain and were plotted as a complementary image to the IVUS echogram. The resolution of an elastogram in the radial direction is 200 μm.

The strain value of a plaque was determined by averaging all strain values found in the plaque. Additionally, the presence of a high-strain spot (strain >1%) in the elastogram was related to the presence of fat and macrophages. The alignment of the ultrasound data

and the histologic cross-sections was performed by the use of the IVUS echogram and the histology as described earlier (de Korte 2000a+b).

Statistics

All statistical analysis was performed with SPSS statistical software. Values are expressed as mean and the range. Bivariable linear regression analysis was performed to study the relation between the presence of fat and macrophages and the mean radial strain. Receiver operating characteristic analysis was performed to assess the optimal strain value and to evaluate the predictive power to identify fatty plaques. Furthermore, the sensitivity and specificity of a high-strain spot to identify fat and macrophages was determined.

Results

In 50% of the arterial segments, early plaques were found (n=12). Nine of these early lesions were classified as fatty. Advanced fibrous lesions were found in 25% of the segments (n=6), and the remaining 25% contained no plaque (n=6). Macrophages were found in cross-sections with early plaque (n=11) and in 1 fibrous plaque.

	Strain %	
Plaque	Mean	Range
Absent (n = 6)	0.21	0.13–0.33
Early fatty lesions (n = 9)	0.46	0.28–0.80
Early fibrous lesions (n = 3)	0.24	0.21–0.27
Advanced fibrous plaque (n = 6)	0.22	0.17–0.28

Table 1: Mean Strain Value in Plaque Types and Normal Artery

Typical examples of an advanced fibrous plaque and an early fatty plaque are shown in Figures 1 and 2. The elastogram (Figure 1) shows low-strain values, which indicate relatively hard material. The histology reveals the presence of collagen. Macrophages and fat are not found. High-strain values were found in a cross-section with early fatty plaque (Figure 2).

Higher average strain values were found in the fatty plaques with fatty material than in the other pathologies that showed similar mean strain values (Table 1). Regression analysis revealed a highly significant difference in average strain values between plaques with and without fat (P=0.007). After correction for the confounding effect of fat, the presence of macrophages had no additional effect (P=0.966). Receiver operating characteristic analysis revealed a maximum sensitivity of 100% with a corresponding specificity of 80% to identify fatty plaques for a strain value of 0.35%. The area under the curve was 0.952.

	Fat		Macrophages	
High Strain Spot	Present	Absent	Present	Absent
Present	9	3	11	1
Absent	0	12	1	11

Table 2: Relation Between a High Strain Spot and Fat or Macrophages

A high-strain spot has 75% sensitivity and 100% specificity to identify fat (Table 2). A 92% sensitivity and 92% specificity was found to identify the presence of macrophages.

Discussion

In this study, IVUS elastography is validated in vivo with an atherosclerotic Yucatan minipig model. An earlier in vitro study revealed different mean strain values in fibrous, fibrofatty, and fatty plaques in human coronary and femoral arteries (de Korte 2000a). In this in vivo study, significant higher strain values were found in fatty plaques than in fibrous plaques.

In this animal model, only homogeneous plaque types and no calcified material were found. Because human plaques are mainly heterogeneous, these results cannot be directly transferred to the human situation. However, the main components of rupture prone plaques (i.e., fibrous and fatty tissue and macrophages) were all present in this model.

Elastography has a high sensitivity to identify fatty material: A maximum sensitivity of 100% with corresponding specificity of 80% was achieved when the threshold was set at a mean strain in the plaque of 0.35%. This sensitivity and specificity is higher than values obtained with conventional IVUS in vitro. Prati et al. (Prati 2001) found a sensitivity of 65% and a specificity of 95%. In another study (Komiyami 2000), a sensitivity and a specificity of 53% and 72%, respectively, were found. This corroborates our findings in vitro in which we found a high correlation between strain and plaque composition and no relation between echogenicity and plaque components (de Korte 2000a).

No independent relation between mean strain of the plaque and macrophages was found. These results indicate that the mean strain value of the plaque is dominated by the tissue type (fibrous or fatty). However, a high-strain spot has a sensitivity and specificity of 92% to identify macrophages. It should be realized that the presence of macrophages should not necessarily be interpreted as plaque inflammation. However, increased strain values probably refer to the presence of active macrophages, because these cause plaque weakening.

Conclusions

With the use of in vivo intravascular elastography, higher mean strain values were found in fatty plaques than in fibrous plaques. Elastography has a high sensitivity and specificity to identify fatty plaques. The presence of macrophages results in localized high-strain spots.

Chapter 6

Three-Dimensional Palpography of Human Coronary Arteries

Based on:

Johannes A Schaar, Chris L. de Korte, Frits Mastik, Luc C. A. van Damme, Rob Krams, Patrick W. Serruys and Anton. F. W. v. d. Steen
Three-Dimensional Palpography of Human Coronary Arteries
Herz (2005) 30, 125-133

Rupture of a thin-cap fibroatheroma (suspected to be a vulnerable, high-risk or rupture-prone plaque) is a major cause of acute coronary syndrome and stroke (Schaar 2004b). Much current research activity is focused on the identification and treatment of these vulnerable plaques, before rupture occurs, in order to prevent clinical events. At present, there is no clinically available technique with a high sensitivity and specificity to identify such plaques.

There is evidence that most vulnerable plaques are suspected to be characterized by the presence of a large atheroma that is shielded from the blood by a thin fibrous cap (Davies 1996). Inflammation involving accumulation of macrophages weakens the cap and increases the susceptibility of these plaques to rupture (Lendon 1991). These highly deformable plaques may rupture, if the cap is unable to withstand the oscillatory stress due to the pulsatory nature of the blood pressure. In support of this concept, regions with increased circumferential stress are found in plaques with the typical morphology of a vulnerable plaque (Arroyo 1999). An increase in circumferential stress is associated with an increase in the radial strain (deformability) of the tissue.

Intravascular elastography is a technique that allows assessment of the local strain of the plaque using intravascular ultrasound (de Korte 2000a). In contrast to other techniques that assess only one or more of the plaque features like geometry, composition or inflammation, elastography may be capable of identifying the deformable plaque by direct assessment of the immediate cause of rupture. An in vitro study revealed 88% sensitivity and 89% specificity using elastography to identify the vulnerable plaque (Schaar 2003a). Recently, elastography was validated in vivo using an atherosclerotic animal model (de Korte 2002a) and the feasibility of clinical appli-

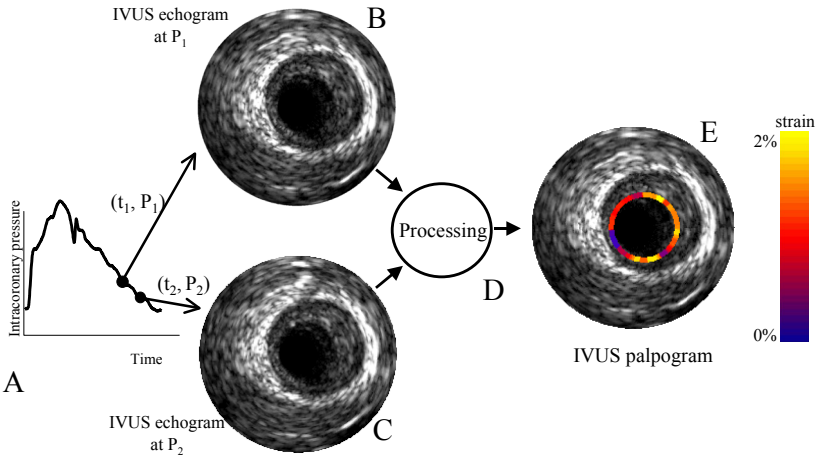

Fig 1A to 1E: Principle of palpography. The artery is deformed by the physiologically pulsating intraluminal pressure (A). Intravascular ultrasound (IVUS) echograms are produced from radio frequency (rf) signals acquired at high (B) and low (C) pressure. Using cross-correlation analysis of these rf signals, the strain (deformation) in the inner layer of tissue is determined (D). This strain is color-coded and superimposed on the IVUS echogram at the lumen/vessel wall boundary (E). In this particular example, high strain is found at the shoulders of this eccentric plaque.

cation was shown in patients undergoing cardiac catheterization (de Korte 2002b) (Schaar 2004a). In these studies, strain was measured

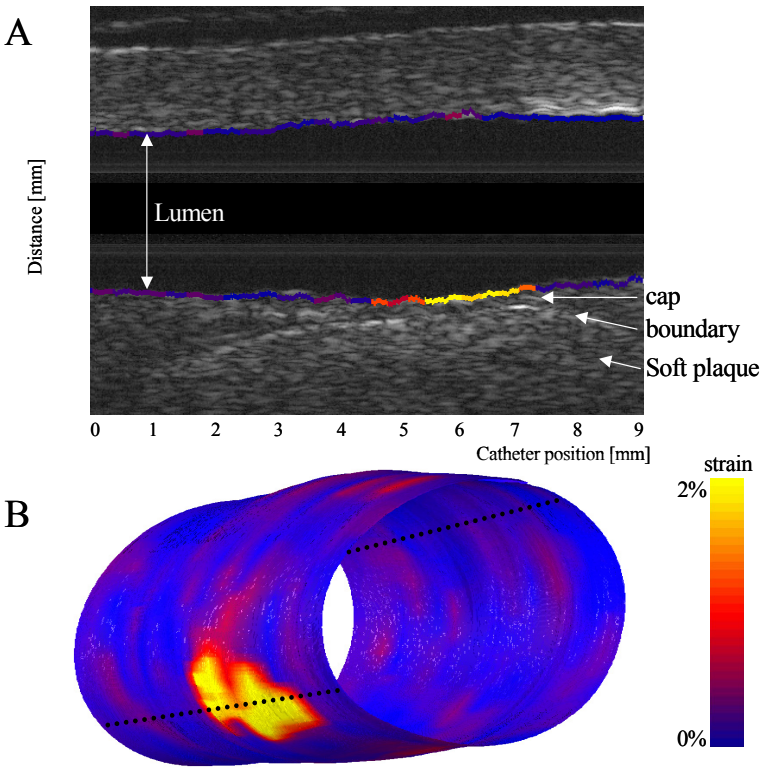

Fig 2A and 2B: Longitudinal IVUS image with superimposed palpogram (A) and three-dimensional palpogram (B) of a tissue-mimicking phantom. The longitudinal view shows the soft plaque that is covered by a harder cap. The superimposed palpogram shows high strain values in the thinnest part of the cap. The three-dimensional palpogram shows low strain values in the phantom with a high-strain region corresponding to the area with the thin cap.The dotted line indicates the cross-sectional imaging plane of the longitudinal echogram.

at one cross section of a single plaque. This is clearly not sufficient to assess whether a patient is at risk, as multiple deformable plaques frequently coexist in a single patient.

Since this catheter-based technique provides only a single cross-sectional image, the catheter needs to be pulled back to obtain three-dimensional information. However, moving the catheter during acquisition introduces out-of-plane motion that is considered the main source for decorrelation of the signals and thus produces a decrease in the quality of the strain estimate (Konofagou 1998).

Therefore, the position of the transducer has to be kept as stable as possible and only motion in the direction of the beam is allowed during elastographic acquisitions (Ophir 1991). For that reason, it was considered impossible to obtain valid intravascular elastograms while performing a continuous pullback of the catheter. In the present study, we describe a scanning technique that provides a full three-dimensional reconstruction of the distribution of high-strain regions in atheromatous plaques in coronary arteries in vivo. Direct detection of these high-strain regions may improve risk stratification for patients that are at high risk of myocardial infarction.

Material and Methods

We developed and evaluated three-dimensional intravascular ultrasound palpography using phantom experiments and measurements in atherosclerotic rabbits. Furthermore, we performed initial studies in patients during interventional procedures.

Phantom Experiments

A phantom with the morphology of a vessel wall containing a soft plaque was made of PolyVinyl Alcohol Cryogel (Chu 1997). The soft area was isolated from the lumen by a thin cap. The thickness of the cap varied from 2 mm to 100 μm. The phantom was put in a water tank and strain was applied using a pulsatile intraluminal pressure. Palpographic data was acquired at a pullback speed of 1 mm/s.

Animal Experiments

3 days before denudation the rabbits started a high (2%) cholesterol diet, for a period of 2 months. On the day of experimentation, NZW rabbits (n = 8; weight: 3.1 ± 0.2 kg) were premedicated with fentanyl (0.315 mg/ml) and fluanisone (10 mg/ml; Hypnorm® 0.5

Fig 3A and 3B: Orthogonal regression analysis of the strain values acquired during subsequent acquisitions. Combining all acquisitions revealed the relation $\varepsilon_2 = 0.92\ \varepsilon_1 + 0.01$ (n = 624, $R^2 = 0.81$), with ε_1 being the strain measured during first acquisition and ε_2 being the strain measured during second acquisition (A). The residual plot (B) shows that the standard deviation of the measured strain with respect to the estimated average strain value is 0.04%.

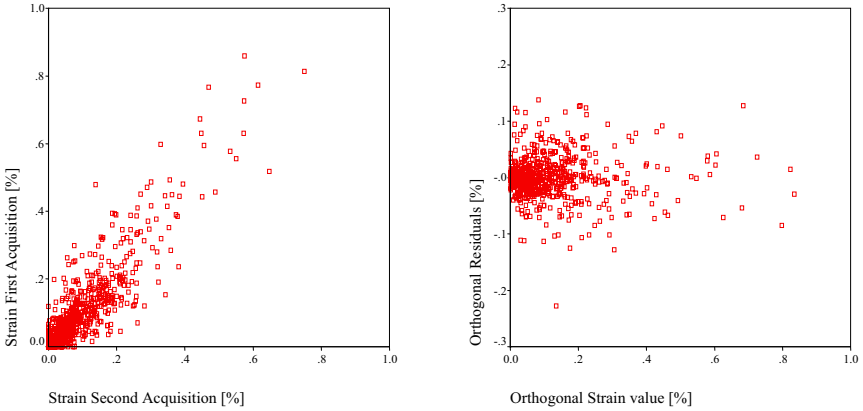

ml/kg i.m.) and anaesthetized with propofol i.v. (10 mg/ml, infusion rate 10–15 ml/h, Abbott, Hoofddorp, The Netherlands) and fentanyl i.a. (0.2 mg/kg/h, B. Braun, Melsungen, Germany) and a 2 : 1 mixture of N_2O : O_2 after intubation (3.0-mm tube). The marginal ear artery was cannulated for arterial pressure measurement with a fluid-filled catheter (Amatek Inc., Philadelphia, PA, USA), and for arterial blood withdrawal. The reduction in mean arterial blood pressure induced by the anaesthetics was compensated for by an infusion of epinephrine (1 mg/ml, infusion rate 2–12 ml/h, Centrafarm, Etten Leur, The Netherlands) titrated to achieve a mean arterial pressure of 70 mmHg. A 4-F guiding catheter was advanced from the dissected femoral artery to the renal artery. After performing angiography, a Fogarty balloon (3 F, Applied Medical, Laguna Hills, CA, USA), attached to a manometer (2–2.5 A) was located just below the renal artery and endothelial denudation was performed by pulling back and twisting the inflated Fogarty balloon three times over a length of 5 cm. After an 8-week follow-up period, the right carotid artery was dissected for the introduction of a 5-F sheath. An angiographic overview image of the infrarenal aorta was performed and markers were located to indicate the previously denuded region. The intravascular ultrasound catheter was positioned in the atherosclerotic part of the aorta and a pullback at 1.0 mm/s was performed. The catheter was removed, inserted again and positioned for the second acquisition. During these acquisitions, pressure was measured using a fluid-filled line, connected to the 5-F introduction sheath.

Subsequently, the rabbit was sacrificed (Euthasate®, 20 ml/kg) and perfusion fixation (formaldehyde 4%) was performed in the aorta at a controlled arterial pressure of 70–80 mmHg for 20–30 min. Next, the infrarenal aorta was dissected and stored in 4% formaldehyde for further analysis. All experiments were performed in accordance with institutional regulations and the "Guiding principles for the care and use of animals" as approved by the Council of the American Physiological Society.

After dissection, the tissue was embedded in 4% formaldehyde. To compare the location of tissue slices with the elastography-derived three-dimensional reconstruction, we measured the degree of axial vessel shrinkage by comparing the length of the vessel segment, as obtained by radiopaque markers, before and after excision. Immunohistochemistry was performed applying monoclonal antibodies for macrophages (RAM-11, DAKO, Glostrup, Denmark), for smooth muscle cells (α-actin IA4, DAKO) and for collagen (picrosirus red, Klinipath, Duiven, The Netherlands). The latter stain was evaluated after polarizing the light. Quantitative software was developed applying the Clemex Vision software package. The first 600 μm of tissue from the internal elastic membrane was selected for analysis. Areas of macrophages, smooth muscle cells and collagen were calculated and related to the area of the region of interest and reported as densities (%). A high-strain area was defined as an area with an average strain > 0.5%. This corresponds to the upper 5% of the observed strain values.

Patient Studies

Pullbacks at 1.0 mm/s were performed in patients (n = 2) referred for an interventional procedure after signing informed consent. The local medical ethics committee approved this study. Three-dimensional palpograms were acquired before the therapeutic procedure.

Statistical Analysis

Scanning an identical part of the rabbit aorta twice tested the reproducibility of three-dimensional palpography. Between acquisitions, the catheter was removed, reintroduced and the same part was scanned again. Quantitative analysis of the reproducibility of the three-dimensional strain map was performed using orthogonal regression (Slager 2000)

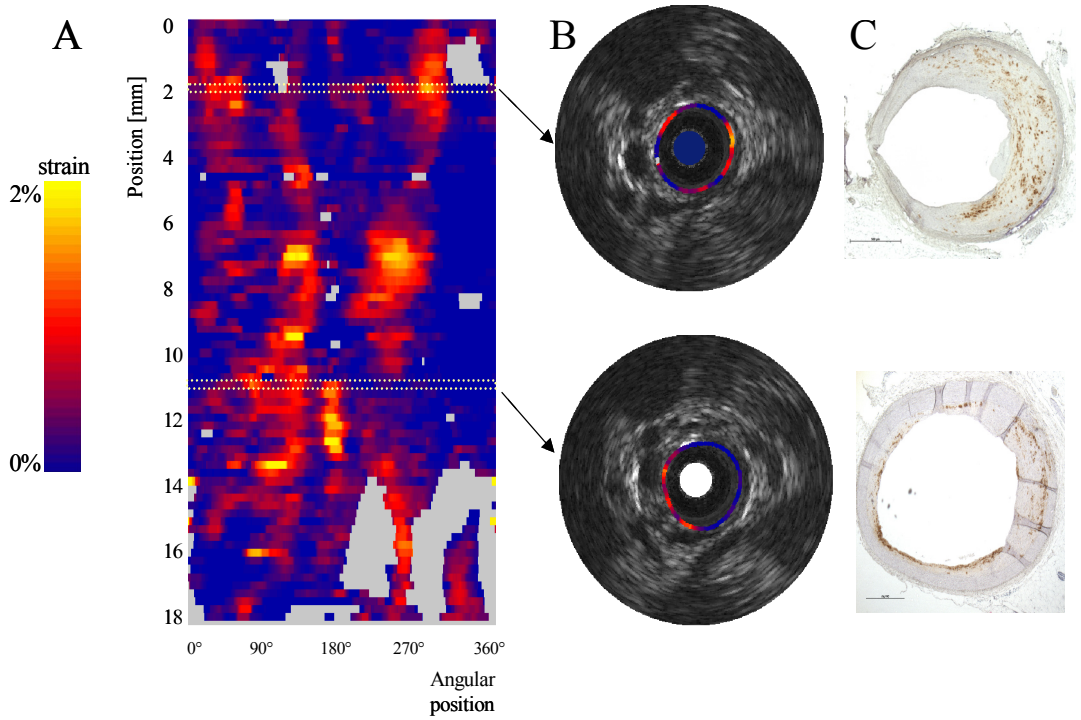

Fig 4A to 4C: Three-dimensional palpography of a rabbit aorta. The three-dimensional palpogram is cut open and plotted as a two-dimensional strain map (A). The palpogram of two regions with high strain is superimposed on the IVUS echogram (B). Comparison with histology (C) reveals a high correlation between presence of superficial macrophages (brown in RAM11 staining) and high-strain regions. Note that the macrophages deeper in the core of the plaque are not correlated with high strain. Analysis of the echograms revealed that the gray regions in this two-dimensional strain map correspond to a bifurcation region.

Calculating a Palpogram

All data were acquired using an Avanar 20 MHz catheter (Volcano, Rancho Cordova, CA, USA). Radio frequency (rf)-data were obtained with a Magellan Workstation. For calculating reproducible strain estimates, data acquired in the decreasing part of the pressure cycle were selected automatically and analyzed for phantoms, animals, and patients. In animals and patients we limited processing to data from subsequent frames with high similarities, as quantified by a likelihood curve to decrease the influence of catheter motion on the three-dimensional palpogram. High likelihood values correspond to the end-diastolic phase of the heart cycle (de Korte 2002).

Strain is determined using cross-correlation analysis of subsequent ultrasound data (de Korte 2000). Since the strain between frames is

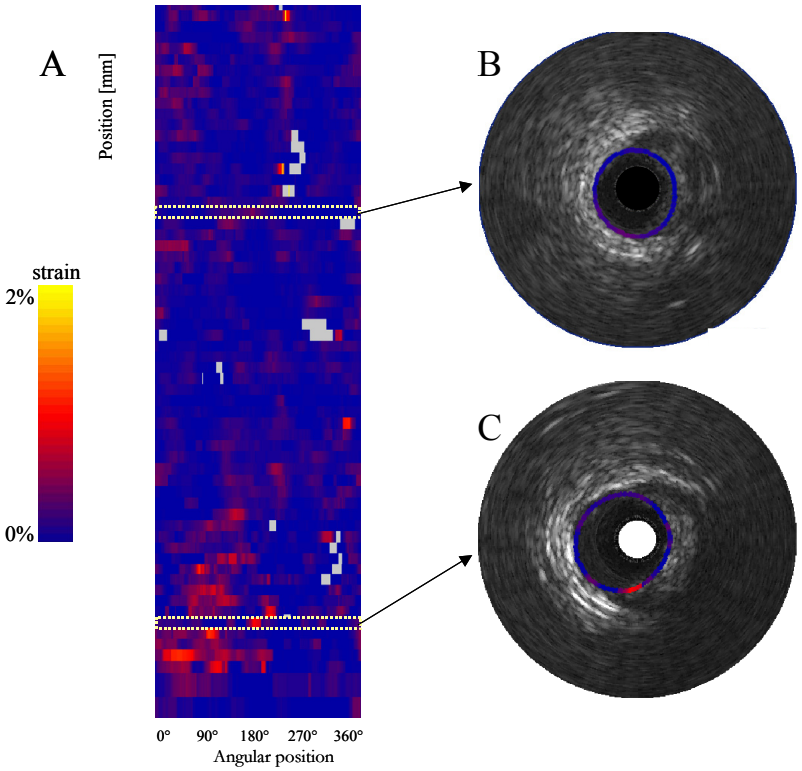

Fig 5A to 5C: Three-dimensional palpography of a human coronary artery obtained in vivo. The three-dimensional palpogram is cut open and plotted as a two-dimensional strain map (A). The strain map shows low- and high-strain regions. A two-dimensional palpogram superimposed on the IVUS echogram of a distal cross section with a large eccentric plaque (B) reveals no high strain values. Although the proximal plaque (C) has a similar appearance in the echogram, the palpogram shows high strain at one shoulder, indicating an unstable plaque. The gray regions in the two-dimensional strain map correspond to regions where side branches are present as identified from the echograms.

low, the conventional echogram is not suitable for this analysis. However, using the rf raw ultrasound signals that contain not only the amplitude but also the phase information, minute strains can be determined (lower bound for strain estimation of this intravascular ultrasound system is 0.05%) (Cespedes 1995). Intravascular ultrasound images contain 512 angles with ultrasound information. For each ultrasound signal, the boundary between lumen and vessel wall is automatically detected using a frame-by-frame gradient-based algorithm. From this point, the strain in the inner 600 µm of tissue is determined. This 600 µm is divided into two windows. For each window, the displacement between the acquisition obtained at low and high pressure is calculated. The difference in displacement results in the radial strain of the tissue. Repeating this procedure for all 512 angles results in a partial palpogram. This partial palpogram

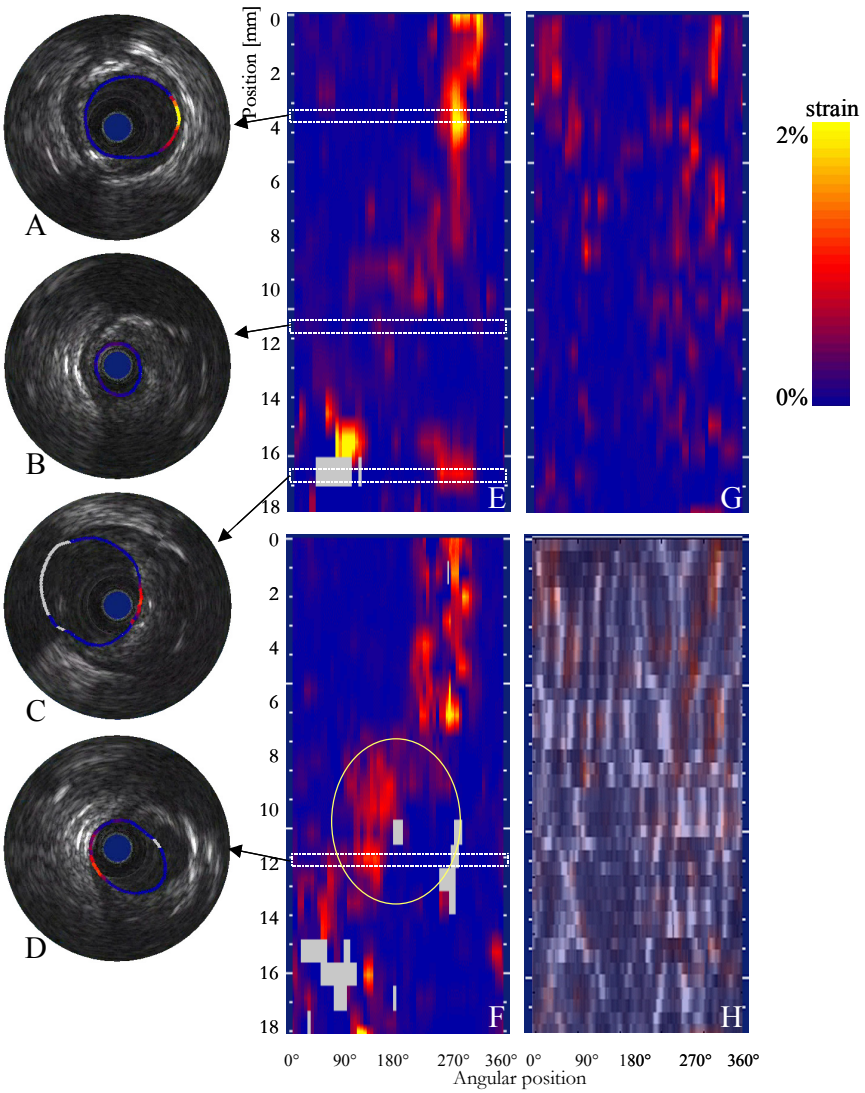

Fig 6A to 6H: Three-dimensional palpography of a human coronary artery obtained in vivo. The three-dimensional palpogram is cut open and plotted as a two-dimensional strain map (E to H). The strain map before intervention (E) shows high- and low-strain regions. A two-dimensional palpogram superimposed on the IVUS echogram of a distal cross section with a large eccentric plaque (A) reveals high strain values at the shoulder. The proximal lesion (B) has low strain values. The side branch visible in the echogram (C) causes erroneous strain values indicated with gray. After the procedure, increased strain values are found (F) in the region where atherectomy was performed (indicated with the circle) at the shoulder of the plaque (D). After stenting, low strain values are found in the entire segment (G). However, high strain values are still present at the shoulders of the distal plaque: the overlay of the IVUS echogram demonstrates that this high strain is found in tissue not covered

have missing strain values for some angles due to erroneous strain estimates. These erroneous strain estimates are automatically detected using a previously described principle (de Korte 2000). All partial palpograms for one heart cycle were averaged to determine a compound palpogram (Doyley 2001) (Figure 1).

Three-Dimensional Palpography

If a pullback is performed, each compound palpogram represents the strain information for a certain cross section [van der Steen 1997). The longitudinal resolution of the three-dimensional acquisitions is dependent on the heart rate and the pullback speed. A heart rate of 60 beats/min. and a pullback speed of 1.0 mm/s results in a palpogram for each 1.0 mm. The influence of performing a pullback was investigated using a phantom experiment. The correlation between signals acquired at the different intraluminal pressures was determined for a static position of the catheter and while performing a pullback. The peak value of the cross-correlation function can directly be related to signal-to-noise ratio (the better the signal-to-noise ratio, the higher the peak value of the cross-correlation function) (Cespedes 1997). If the signal-to-noise ratio is known, the standard deviation of the strain estimate can be determined using the lower bound of strain estimation (Cespedes 1995).

In coronary arteries, the natural motion of the catheter due to increasing blood flow and the contraction of the heart is as follows: during the systolic phase, the blood flow is low, the heart is contracting, and the catheter moves toward the ostium. In the diastolic phase, blood flow is increasing, the heart is relaxing, and the catheter moves deeper into the coronary artery away from the ostium (Arab-Zadeh 1999). For intravascular palpography, data are acquired in the diastolic phase of the heart cycle. In this phase, the motion due to pulling back the catheter is in the opposite direction to the natural motion of the catheter. Therefore, the pullback will decrease the out-of-plane motion and may not deteriorate but increase the quality of the palpogram.

During the experiments, data is continuously acquired at a pullback speed of 1.0 mm/s using a mechanical pullback device (Trakback II, Volcano Imaging, Rancho Cordova, CA, USA). Simultaneously, the ECG and intraluminal pressure are registered. The data is subdivided in heart cycles using the R-wave of the ECG signal.

After calculating all the compound palpograms of the full scan, the data can be plotted as a three-dimensional structure representing the lumen/vessel wall boundary (Figure 2B) or as a color-coded map representing the angles versus longitudinal position (Figure 4). Furthermore, a longitudinal crosscut can be made having the echo

information with the strain information on the lumen/vessel wall boundary (Figure 2A).

Results

A tissue-mimicking phantom with the typical morphology of a thin-cap fibroatheroma was scanned to evaluate the possibility to assess reliable palpographic data while introducing motion that is perpendicular to the imaging plane. The phantom allows quantitative evaluation of three-dimensional palpography, since it provides exact knowledge of geometry and acoustic and mechanical properties of the tissue. Although performing an acquisition while moving the catheter introduces no bias, the standard deviation of the strain estimate is increased from 0.10% to 0.14% (for strain values ranging from 0 to 2%). The three-dimensional palpogram (Figure 2B) shows a large increase in strain at the site with minimal cap thickness. The longitudinal cross section (Figure 2A) shows a good delineation of the soft inclusion. An inverse relation between cap thickness and strain was observed, thereby confirming experiments from Loree et al. (Loree 1992), who already demonstrated an inverse relationship between cap thickness and peak circumferential stress using finite element model simulations. In conclusion, the in vitro experiments showed that catheter motion does not bias the three-dimensional palpograms, identify soft and hard tissue and produce data in accordance with the literature.

We validated three-dimensional palpography in vivo using experiments in the aorta of an atherosclerotic rabbit model. First, the reproducibility of three-dimensional palpography was investigated by performing repetitive pullbacks in the same region of the aorta for all rabbits. Orthogonal regression revealed a high correlation between repeat acquisitions in all rabbits ($R^2 = 0.81$, $p < 0.001$; Figure 3A). Residual analysis revealed a standard deviation of the difference between acquisitions of 0.04% (Figure 3B). This error is two times smaller than the error of the strain estimate, thus indicating an excellent reproducibility. In three animals, additional pullbacks at a speed of 0.5 mm/s and 1 mm/s were performed. These acquisitions revealed that the speed had no influence on the palpographic values.

Second, correlating the measured strain values with histological features validated palpographic results. Palpograms with low strain (0–0.3%) were found in aortic segments with low-deformable plaques (rich in collagen and smooth muscle cells with almost no macrophages). Regions with increased strain (0.5–1%) were observed in segments with deformable plaque (atheroma, highly infiltrated by macrophages; Figure 4). Increased macrophage density was found in cross sections with a high-strain spot ($p = 0.009$).

In conclusion, these animal experiments showed that it is feasible and accurate to perform three-dimensional palpography in vivo. Furthermore, these experiments showed that three-dimensional palpograms identify regions with inflammation, which is a marker for vulnerable plaques.

In the atherosclerotic rabbit experiments we proved that three-dimensional palpography is feasible in an aorta in vivo. In these experiments the catheter motion is minimal as compared to acquisitions in coronary arteries in patients. However, acquisitions in patients ($n = 2$) provided evidence that three-dimensional palpography in coronary arteries is feasible. In a patient with unstable angina pectoris, plaques with low and high strain values were found (Figure 5). Three-dimensional palpography identified a deformable region in the distal part of this coronary artery (between 3 and 4 mm) at one of the shoulders of this plaque. The large eccentric plaque between 12 and 13 mm is characterized by low strain values. This information is not available from the conventional echogram, since in both cases it reveals an eccentric plaque with low echogenicity at the shoulders. After an atherectomy procedure at the proximal plaque, increased strain values are found that may be caused by damage to the structure of the plaque due to the intervention. After stenting, this region is characterized by low strain values except for the deformable shoulder of the distal plaque visible between the stent struts.

A three-dimensional acquisition of 6 cm in the dominant epicardial part of the LAD in a patient with unstable angina pectoris revealed plaques with low and high strain values (Figure 6). Three-dimensional palpography identified a soft region in the proximal part of this coronary artery (between 47 and 55 mm) corresponding to a mechanically unstable shoulder of this plaque. This information

is not available from the conventional echogram, since in both cases it reveals an eccentric plaque with low echogenicity at both shoulders.

Discussion

Plaque vulnerability is currently considered a ubiquitous phenomenon and therefore lesions can be present anywhere in the coronary tree (Buffon 2002). Therefore, it is important to have a technique that can identify these vulnerable plaques in all three major epicardial coronaries. Intravascular ultrasound elastography has proven to be able to identify fatty and fibrous plaques both in vitro (de Korte 2000) and in vivo (de Korte 2002). However, this technique only provides information on the strain distribution in a single cross section of the vascular wall. Using three-dimensional palpography, the deformable plaque can be scanned and imaged three-dimensionally in vivo allowing investigation of the distribution of strain over the total plaque surface.

Over time, the geometry and composition of the plaque may change. If the analysis is based on one cross section, repositioning of the catheter using angiography can only be performed in an unreliable manner. Conventional three-dimensional intravascular ultrasound has proven that longitudinal monitoring is clinically feasible using acquisitions with side branches as anatomic landmarks. Therefore, three-dimensional palpography will allow longitudinal monitoring of plaque development. Furthermore, the capacity to obtain a three-dimensional representation of the strain allows identification of the most deformable part of a particular plaque.

Producing a three-dimensional palpogram takes three times as long as performing the pullback procedure (typically 3–5 min.). Although the current processing time is already fast enough to be clinically useful, long-term prospective studies are needed to prove that high-strain spots are associated with increased risk and demonstrate that this diagnostic tool has prognostic value.

Limitations

Palpograms cannot be determined in all cases. Erroneous strain estimates are determined, when the arterial wall is thin in the absence of plaque, when tissue is in the shadow region behind a large calcified deposit, or when the out-of-plane motion of the catheter is

large. However, a thin arterial wall and presence of a large calcified deposit are not related to plaque vulnerability. The algorithm automatically identifies these erroneous strain estimates, resulting in gray regions in the palpograms.

High-strain regions are not only expected at locations with a deformable plaque, but also at regions with different mechanical behaviour due to either particular artery geometries or underlying anatomic structures. We found regions with increased strain at bifurcations and in non-diseased coronary artery segments where there was a vein directly outside the adventitia. Since these situations can be identified on the conventional intravascular echogram, this causes no fundamental problem because the three-dimensional palpograms are acquired and displayed in conjunction with the echogram.

The data are meant to prove feasibility in a clinical environment. Due to the limited number of patients in the study no conclusion on the clinical significance of the technique can be made.

Conclusion

Three-dimensional palpography provides information on the presence and distribution of high- and low-strain areas in coronary arteries in patients. Since high strain is highly correlated with increased numbers of macrophages and decreased cap thickness, three-dimensional palpography might identify plaques that are prone to rupture.

Chapter 7

Reproducibility of 3D Palpography in Humans

Based on:

Johannes A Schaar, Frits Mastik, Evelyn Regar, Patrick W. Serruys, Anton F.W. van der Steen
Reproducibility of 3D Palpography in Humans
submitted

Intravascular palpography can measure strain using cross-correlation analysis of radio-frequency ultrasound signals recorded at different intravascular pressures (de Korte 1998b). The underlying principle is that the strain of the tissue as a result of a pressure variation is a function of its mechanical properties. The local strain of the tissue is displayed color-coded (palpogram) on the lumenal boundaries of the IVUS echogram (Doyley 2001) (Cespedes 1995).

Rupture of thin-cap fibroatheromas (TCFA) is the main cause of acute coronary syndrome and myocardial infarction. Identification of this form of vulnerable plaque is therefore essential to enable the development of treatment modalities to stabilize such plaque (Kolodgie 2004). In palpography a typical strain pattern has been described which has a high (88%) sensitivity and specificity (89%) for the detection of these thin cap fibroatheromas (TCFA) (Schaar 2005).

Rupture of thin cap fibroatheroma is related to weakening of the cap of an atheromatous plaque (Falk 1999) (Loree 1992). This process may be triggered by an accumulation of inflammatory cells such as macrophages, which produce metalloproteinases (Libby 1995). Rupture of caps is particularly prone to occur in regions with increased mechanical stress (Burleigh 1992). This stress is caused by the pulsatile intravascular blood pressure, which strains the vessel wall (Lendon 1993).

Three-dimensional intravascular palpography allows scanning of coronary arteries in patients to identify and localize mechanically highly deformable regions (Schaar 2005). Patients with stable angina have less highly deformable plaques than patients with unstable angina and patients after acute myocardial infarction (Schaar 2004a).

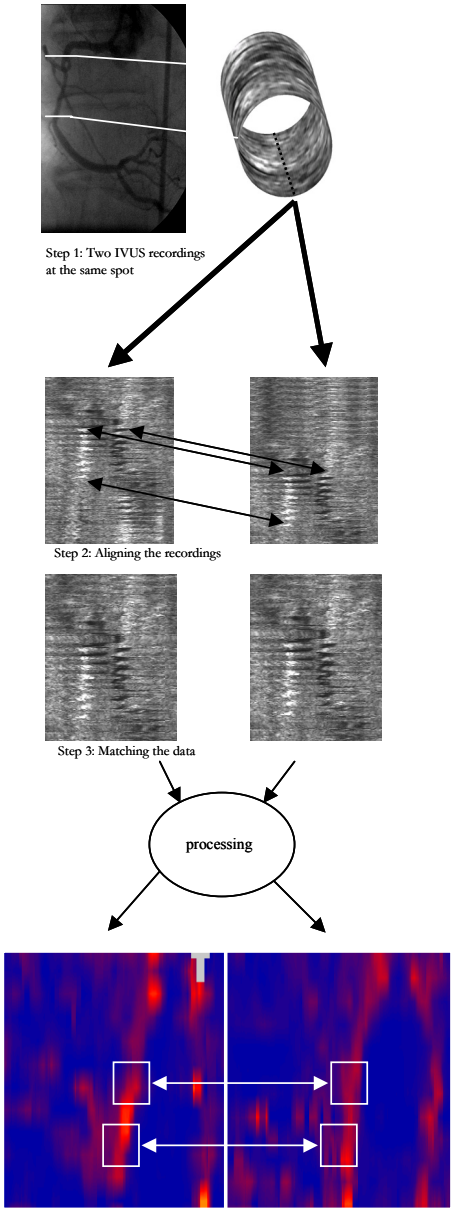

Fig 1: Description of the different steps testing the reproducibility of palpography

The reproducibility of a method is a prerequisite for further scientific evaluation and usage in clinical trials (Popper 2002).

In the current paper we evaluate the reproducibility of three-dimensional palpography in coronary arteries of patients.

Methods

Single center prospective and observational study

This study was a single center prospective and observational study, which was approved by the medical ethics committee of the ErasmusMC. All patients provided written informed consent. The palpographic recordings were acquired after successful intervention. The region, in which palpography was performed, was defined on the basis of identifiable landmarks, such as side branches or edges of stents. All data were acquired using a 20 MHz Jovus Avanar F/X IVUS catheter (Volcano, Rancho Cordova, CA, USA), which was connected to an InVision Gold IVUS console. Recordings were obtained at a pullback speed of 1 mm/sec using a mechanical pullback device (Trackback II, Volcano, Rancho Cordova, CA, USA). Simultaneously, the ECG and intraluminal pressure signals were recorded. Acquisition was done with a custom made dedicated workstation connected to the digital interface of the IVUS machine recording fundamental IVUS data (rf-data). Analysis was done as previously described (Schaar 2004a).

Matching was done on the IVUS frames

At analysis of the second recording the begin end the end of the region of interest were matched based on the previously described landmarks. Within the ROI, for every millimeter along the full pullback length, the matching cross section of the follow up recording was determined (see figure 1). This matching was done on the IVUS frames reconstructed from rf-data unaware of the palpographic results. The matching included also a correction of the rotational orientation of the follow up registration to allow an analysis not only for the entire cross section, but also for positions along the circumference of the lumen. The resulting strain values were depicted in a strain map (see figure 1). Along the longitudinal axis the position in the artery is displayed, while on the horizontal axis the position of the strain values according to the circumference of the cross section is displayed. Over this strain map a grid of 16 by 6 elements was put. On each of this elements the median strain was calculated, which was used as the variable for further analysis.

For statistical analysis, SPSS 11.0.1 (SPSS Inc., Chicago, USA) was used. The Bland and Altman plot was used to assess the reproducibility of a method by comparing repeated measurements.To de-

scribe the relationship between the two recordings a linear regression analysis was performed.

Results

In 14 patients 19 recordings with a length of 1.8 cm were done resulting in 909 sections to compare. The Blant-Altman test showed a mean of 0.042 of strain differences with a standard deviation of 0.07 (see figure 2). The regression analysis between the 909 sections revealed an R-square of 0.89 with a $p < 0.0001$ (see figure 3). The t-test showed no significant difference between the data with a p =

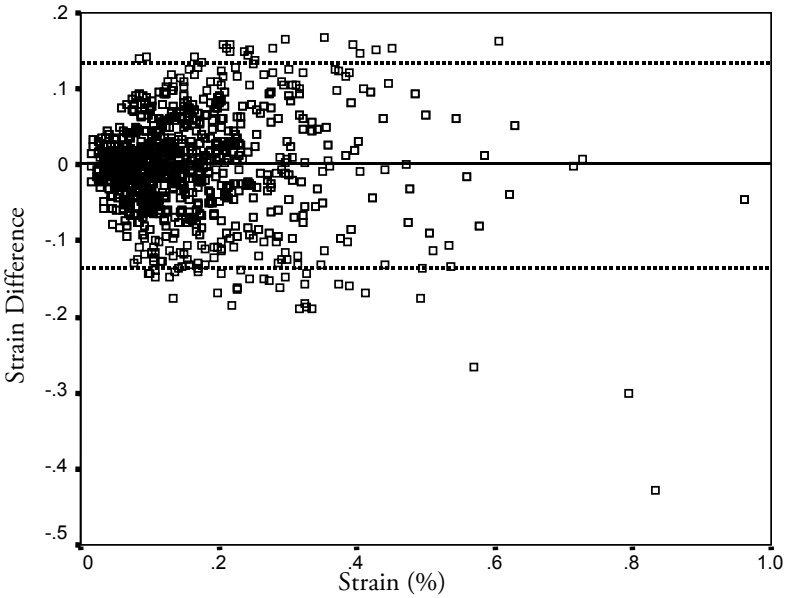

Fig 2: Blant Altman test of 909 palpographic recordings

0.07. The Pearson correlation of the data showed a R = 0.84 with a $p < 0.0001$.

Discussion

Reproducibility is a fundamental and indispensable requirement of a technique

Reproducibility is a fundamental and indispensable requirement of a technique, which is used for decision making in a clinical environment. For a technique like 3D palpography absolute reproducibility cannot be reached in coronary arteries since disturbing factors like small pressure differences, catheter motion, the movement of

the heart and electrical noise will influence the results. Nevertheless for patient follow up, which is needed to study treatment effects, the right parameters have to be chosen and their reproducibility needs to be assessed. The results of this study represent different approaches to look at reproducibility of strain data in human coronary arteries. The Blant-Altman analysis reveals a very good reproducibility since the variation of the data was low given by a low standard deviation. Another way looking to the data is regression analysis, which shows the relation of the two recordings, giving a more that 80% overlap of the data. Comparing the results of both recordings leaves us with no statistical difference using a t-test. The different approaches to evaluate the reproducibility were chosen since the ideal test does not exist for this kind of dataset. Nevertheless, we think that looking from different angles to the subject gives us enough confidence to claim that intravascular palpography is a reproducible enough technique to be used in the clinic. This study tested the question, if palpography recordings in patients are reproducible. Future investigations will address the intra- and inter observer variability of the technique.

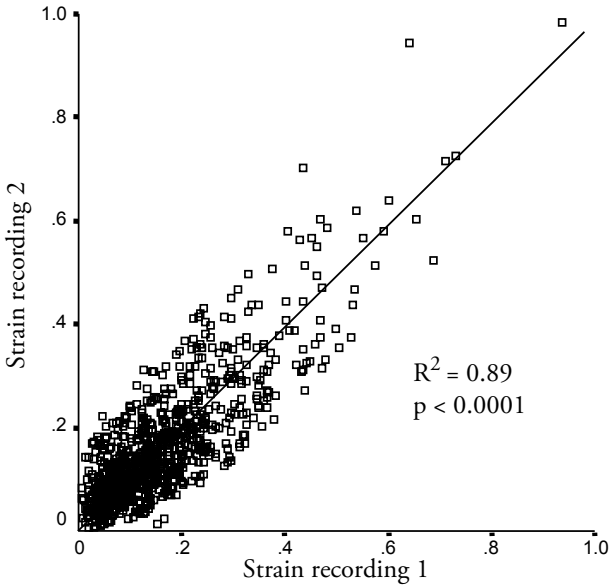

Fig 3: Regression analysis of 909 palpographic recordings

Conclusion

Three-dimensional intravascular palpography is reproducible up to the quality to be useful in the clinical environment as well as in clinical trials.

Three-dimensional intravascular palpography is reproducible

Part IV
Clinical Application

Chapter 8

Incidence of High-Strain Patterns in Human Coronary Arteries

Based on:

Johannes A Schaar, Evelyn Regar, Frits Mastik, Eugene P McFadden, Francesco Saia, Clemens Disco, Chris L de Korte, Pim J de Feyter, Antonius FW van der Steen, Patrick W Serruys
Incidence of High-Strain Patterns in Human Coronary Arteries. Assessment With Three-Dimensional Intravascular Palpography and Correlation With Clinical Presentation
Circulation (2004) 109, 2716 - 19

Accumulating evidence suggests that acute coronary syndromes, the clinical presentation of which ranges from unstable angina to sudden cardiac death, are commonly related to thrombosis superimposed on rupture or erosion of atheromatous plaques. Anatomopathological studies have shown that such events are associated with ruptured thin-cap fibroatheroma, plaque erosions, and the presence of superficial calcium spots (Virmani 2001).

Plaque rupture is related to weakening of the cap of an atheromatous plaque (Falk 1999) (Loree 1992). This process may be triggered by an accumulation of inflammatory cells such as macrophages, which produce metalloproteinases (Libby 1995). Rupture of caps is particularly prone to occur in regions with increased mechanical stress (Burleigh 1992). This stress is caused by the pulsatile intravascular blood pressure, which strains the vessel wall (Lendon 1993).

Intravascular palpography can measure strain using cross correlation analysis of radio frequency ultrasound signals recorded at different intravascular pressures (de Korte 1998b). The underlying principle is that the strain of the tissue is a function of its mechanical properties. The local strain of the tissue is displayed color coded (palpogram) on the luminal boundaries of the intravascular ultrasound (IVUS) echogram (Doyley 2001) (Cespedes 1995).

In palpography, a typical strain pattern has been described that has a high sensitivity and specificity (89%) for the detection of thin-cap fibroatheroma in vitro in postmortem coronary arteries (Schaar 2003a).

We designed the present study to evaluate the incidence of this typical strain pattern in patients undergoing percutaneous coronary in-

tervention (PCI) for stable angina, unstable angina, or acute myocardial infarction (AMI).

Methods

Three-Dimensional Palpography

A 20-MHz IVUS catheter connected to an InVision echo apparatus (both from Volcano Inc., Rancho Cordova, CA, USA) was used to obtain palpograms in patients undergoing PCI. Palpograms were obtained as described previously (van der Steen 2003). Digital radio frequency data were acquired using a custom-designed workstation. The local strain was calculated from the gated radio frequency traces using cross-correlation analysis and displayed, color coded, from blue (for 0% strain) through yellow (for 2% strain) via red. This color-coded circumferential image was superimposed on the cross-sectional IVUS image. The resolution of the strain measurement in the radial direction is 400 μm.

The cross-sectional data can be reconstructed as a 3D structure representing either the lumen vessel-wall boundary or as a color coded map representing the angles versus longitudinal position. Furthermore, a longitudinal crosscut can be made having the echo information with the strain information on the lumen vessel-wall boundary (Figure 1).

When a pullback is performed, each palpogram represents the strain information for a certain cross section over the full cardiac cycle. The longitudinal resolution of the 3D acquisitions depends on heart rate and pullback speed. With a heart rate of 60 bpm and a pullback speed of 1.0 mm/s, the longitudinal resolution is 1.0 mm. Movement of the catheter in the artery during acquisition introduces out-of-plane motion. For palpography, this motion is the main source of signal decorrelation and thus a source of error in strain estimation (Konofagou 1998). Ideally, the position of the transducer should be as stable as possible, with motion only in the direction of the beam during acquisitions.

In coronary arteries, the natural motion of the catheter, related to blood flow pattern during systole and diastole and to the contraction of the heart, is predictable. During systole, blood flow is low, the heart is contracting, and the catheter moves toward the ostium.

In the diastolic phase, blood flow is increasing, the heart is relaxing, and the catheter moves distally away from the ostium (Arbab-Zadeh 1999). For intravascular palpography, data are acquired in the diastolic phase of the heart cycle. In this phase, catheter motion related to the motorized pullback opposes the natural motion of the catheter, related to the cardiac cycle. During the recordings, data were continuously acquired at a pullback speed of 1.0 mm/s using a mechanical pullback device (Trak Back II, Volcano Therapeutics) with simultaneous recording of the ECG and the aortic pressure. The data set is subdivided into heart cycles by use of the R wave of the ECG signal.

Analysis included the complete length of the study vessel, starting with the IVUS pullback distally (in the left anterior descending coronary artery [LAD] at segment 7, American Heart Association classification, and in the right coronary artery [RCA] at segment 3) and ending at the ostium.

Definition of the High-Strain Spot

A region was defined as a high-strain spot when it had high strain (>1.2% at 4 mm Hg pressure difference) that spanned an arc of at least 12° at the surface of a plaque (identified on the IVUS recording) adjacent to low-strain regions (<0.5% at 4 mm Hg pressure difference). The highest value of strain was taken as the strain level of the spot.

Study Population

This cross-sectional study included 55 patients. Seventeen patients had stable angina and underwent elective coronary angioplasty. Nineteen patients had unstable angina, defined as symptomatic transient ST-segment depression with normal biochemical markers of myocardial damage. In stable and unstable patients, palpography was performed in the treated vessel before intervention. Nineteen patients presented with acute ST-segment elevation MI and underwent primary angioplasty <12 hours after onset of symptoms. Palpography was performed in a non-culprit vessel.

No patient was taking anti inflammatory drugs other than aspirin. Our institutional review board approved the protocol, and all patients gave written informed consent.

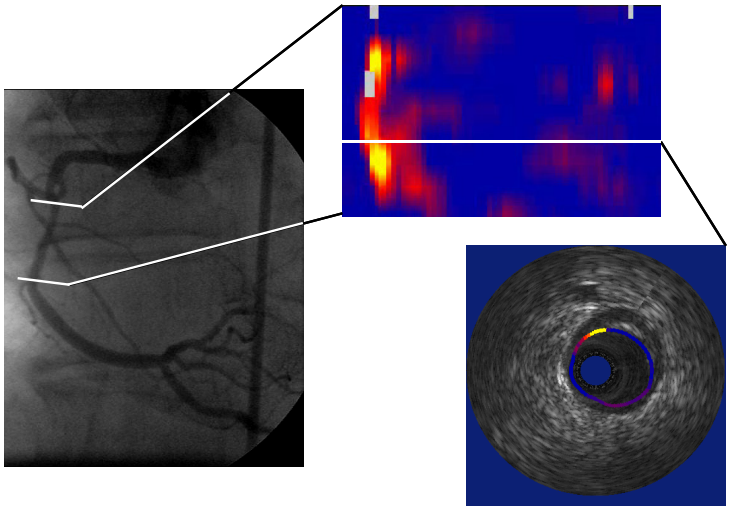

Fig 1: Angiogram (A) shows an intermediate plaque. (B) 3D palpogram of vessel segment between white lines in angiogram. (C) Cross section of 2D palpogram plus echogram as indicated in 3D palpogram. A high-strain plaque on shoulders of eccentric plaque (yellow) can be clearly identified.

Lipid and hsCRP Measurements

Venous blood samples were obtained before catheterization. Lipid levels (total cholesterol, LDL) and high-sensitivity C-reactive protein (hsCRP) were determined routinely with standard methods (Rothkrantz-Kos 2002).

Statistical Analysis

For statistical analysis, SAS version 8.02 (SAS Institute) was used. Data are expressed as mean ±SD. Variables were tested for normal distribution with the Shapiro-Wilk test. Values of $P<0.05$ were considered statistically significant. Continuous variables are also presented as median values with the corresponding 25th and 75th percentiles. To test for independence between categorical groups, Fisher's exact test was used. Univariate ANOVA was used to compare continuous data among groups.

Results

We studied 55 patients (29 male, 26 female). Patients were divided into 3 groups on the basis of clinical presentation (stable or unstable angina, AMI). Mean age (mean, 61±9 years) did not differ among groups. In the stable angina group, the study vessel was the LAD in 8 patients and the RCA in 9 patients. In the unstable angina group, the study vessel was the LAD in 10 patients and the RCA in 9 patients. In patients with AMI, the non–infarct-related study vessel was the RCA in 9 and the LAD in 10 patients.

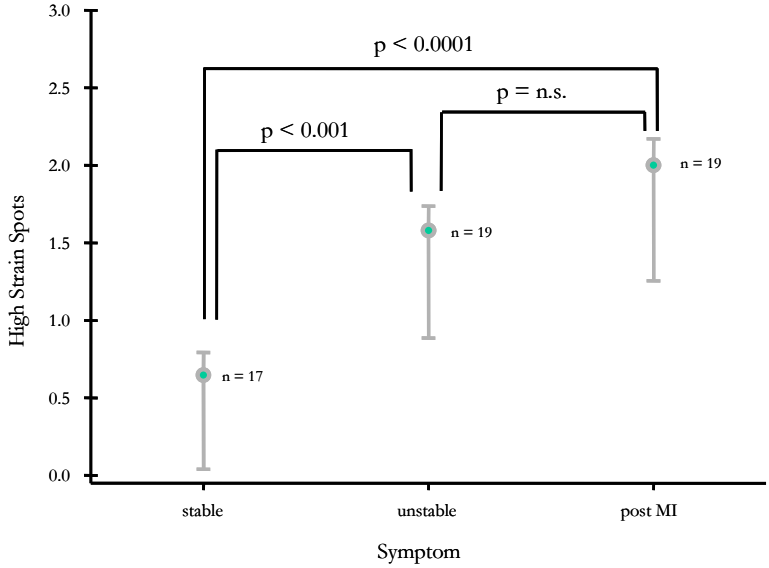

Fig 2: Relation between number of high-strain spots and clinical presentation.

Palpography in 55 vessels (28 LAD, 27 RCA) identified 97 typical high-strain patterns (spots). In 8 vessels, no high strain spot was detected; in 21 vessels, 1 spot; in 29 vessels, 2 spots; and in 6 vessels, 3 spots.

Patients with stable angina had 0.6±0.6 highly deformable plaques, with the typical high-strain pattern of a suspected vulnerable plaque. Significantly more highly deformable plaques (1.6±0.7) were found in unstable angina patients (P=0.0019) and in AMI (P<0.0001) patients (2.0±0.7) compared with stable angina patients (Figure 2). There was no significant difference between unstable and AMI patients with regard to the number of highly deformable lesions (P=0.27). Gender had no influence on the number of highly deformable lesions (P=0.90).

There was no significant difference (P=0.54) in the overall number of high-strain spots detected in the LAD (n=1.6±0.9) and the RCA (1.3±0.9). The mean length of vessel studied did not differ significantly (P=0.496, ANOVA) among groups: stable angina, 52±14 mm; unstable angina, 51±13 mm; and AMI, 47±14 mm.

hsCRP levels differed significantly among groups (P<0.0001). They were significantly higher in patients with unstable angina (1.2±0.8 µg/mL; P=0.02) or AMI (1.8±0.5 µg/mL; P<0.0001)

compared with patients with stable angina (0.6±0.4 μg/mL). hsCRP levels also differed significantly between the unstable angina group and the AMI group (P=0.03). The number of high-strain spots per artery was positively correlated with the hsCRP level (R^2=0.65, P<0.0001). For zero high-strain spots, the hsCRP level was 0.3±0.2 μg/mL; for one, 0.8±0.5 μg/mL; for two, 1.7±0.5 μg/mL; and for three, 2.2±0.3 μg/mL. With multivariate analysis, the interaction between clinical presentation, number of deformable plaques, and hsCRP was tested. The clinical presentation did not have a significant effect on the relationship between number of high-strain spots and hsCRP levels (P=0.06). Separate analysis showed, in the stable angina patients, a Pearson correlation of 0.69 with a value of P<0.002; in the unstable angina group, of 0.83 with a value of P<0.0001; and in the AMI group, of 0.50 with a value of P<0.031.

There was no relation between individual risk factors such as hypercholesterolemia (P=0.82), smoking (P=0.73), diabetes (P=0.31), and hypertension (P =0.42) and the number of high-strain spots. The level of LDL among groups did not differ significantly (P=0.26). In the stable angina group, 70.6% were on statins; in the unstable angina group, 68.4%; and in the AMI group, 52.6%. A univariate analysis showed no significant influence of statin use on the number of high-strain spots (P=0.153).

Discussion

This is the first clinical study using 3D palpography to assess the incidence of possible vulnerable plaque, defined as plaques with high-strain spots. The major findings of the study are that the incidence of high-strain spots is related both to clinical presentation and to levels of hsCRP, a marker of inflammation.

Intravascular palpography, by its capacity to evaluate the mechanical properties of the plaque, can detect thin-cap fibroatheromas. Validation studies in vitro and in vivo have shown that palpography can identify such plaques with high sensitivity and specificity (Schaar 2003a) (de Korte 2002a). Until now, this method was applied only to the analysis of single cross sections. Because atherosclerosis is a 3D process, the extension of palpography from a 2D to a 3D technique was a necessary prerequisite to its introduction as a

potential clinical modality. This technique now permits us to assess the number of suspected vulnerable plaques in the entire coronary artery.

Incidence of High-Strain Patterns: Relation to Clinical Presentation

We found that the incidence of high-strain patterns was strongly related to the clinical presentation. Patients with acute coronary syndromes (unstable angina, AMI) had significantly more high-strain patterns than did patients with stable angina. In the unstable group, there was no significant difference in the number of high-strain patterns in the nonculprit vessel of AMI patients compared with the culprit vessel in unstable angina patients; this supports the hypothesis that inflammation in acute coronary syndromes is a multifocal process (Buffon 2002). The number of high-strains spots we describe is consistent with the number of thin-cap fibroatheromas observed in autopsy studies (Virmani 2003) (Falk 1983) and with the number of yellow plaques observed in angioscopic studies (Takano 2001) (Asakura 2001) (de Feyter 1995).

Incidence of High-Strain Patterns: Relation to hsCRP Levels

Inflammation plays an important role in destabilizing plaques. A clear connection between inflammation and cap stability has been described (Lendon 1991). There is increasing evidence that hsCRP not only is a reactive marker but also has proatherogenic characteristics by its pro-oxidative effect (Kobayashi 2003). hsCRP has a positive predictive value for cardiac events in patients presenting with unstable angina (Liuzzo 1994) (Ridker 1998a). We found a positive correlation between the number of high-strain patterns and levels of hsCRP. Our study was not powered to validate a relationship between hsCRP and the number of suspected vulnerable plaques. Furthermore, the high hsCRP level in the AMI group may partly reflect an increase in hsCRP because of myocyte necrosis. However, this reactive increase starts approximately 16 hours after the onset of MI (Oldgren 2003), whereas blood samples for hsCRP levels in the present study were obtained <12 hours after the onset of symptoms (Nijmeijer 2001).

Future prospective studies should address the value of intravascular palpography in the detection of rupture-prone thin-cap fibroatheromas, in the prediction of clinical events, and as a tool to follow the natural progression and the effect of pharmacological or other interventions (MacNeill 2003).

Limitation of the Study

We assessed only 1 coronary artery per patient. Risk stratification ideally requires evaluation of the total vulnerable plaque burden. Because of the invasive character of intravascular palpography, this assessment can be justified only if the predictive power of the technique is high enough. Nevertheless, assessment of all coronary arteries in 1 patient is feasible and safe with IVUS, a widely available technique (rioufol 2002). The left circumflex artery was not investigated in this study because of the increased motion of this vessel. A motion compensation method is being developed for future studies.

Conclusions

Three-dimensional intravascular palpography can detect high-strain spots, consistent with plaque vulnerability, in vivo in human coronary arteries. The incidence of such possible vulnerable plaques is correlated with both clinical presentation and markers of inflammation. Additional validation is needed to assess the predictive value of the technique to identify vulnerable patients.

Chapter 9

Rationale and Methods of the Integrated Biomarker and Imaging Study (IBIS)

Based on:

Carlos AG Van Mieghem, Nico Bruining, Johannes A Schaar, Eugene McFadden, Nico Mollet, Filippo Cademartiri, Frits Mastik, Jurgen MR Ligthart, Gaston A Rodriguez Granillo, Marco Valgimigli, Georgios Sianos, Willem J van der Giessen, Bianca Backx, Marie-Angele M. Morel, Gerrit-Anne Van Es, Jonathon D Sawyer, June Kaplow, Andrew Zalewski, Anton FW van der Steen, Pim de Feyter, Patrick W Serruys
Rationale and methods of the integrated biomarker and imaging study (IBIS): Combining invasive and non-invasive imaging with biomarkers to detect subclinical atherosclerosis and assess coronary lesion biology
Int J Cardiovasc Imaging 2005 (in press).

Although coronary atherosclerosis is common, clinical events are relatively rare and not linearly related to either the extent or severity of atherosclerosis. The majority of acute coronary events arise from non-flow limiting lesions and are often the first clinical manifestation of previously sub clinical atherosclerosis (Ambrose 1988) (Haft 1988) (Little 1988) (Falk 1995) (Kullo 1998). These observations, among others, led to the concept of the vulnerable atherosclerotic plaque, a plaque that has a high probability of causing a clinical event (Naghavi 2003b+c) (Schaar 2004b). The most common post-mortem histological features in such plaques are the presence of a thin fibrous cap, a lipid-rich core, and infiltration by inflammatory cells (Virmani 2000) (Ross 1999a) (Kolodgie 2001) (Libby 2002a+b) (Davies 1996). Less common pathological substrates for fatal clinical events are plaque erosion, nodular calcification and intraplaque haemorrhage (Virmani 2000)(Kolodgie 2003).

Coronary angiography is the standard technique to define the presence and to assess the extent of coronary atherosclerosis; however, it can only detect plaques that impinge on the lumen. Given the diffuse nature of coronary atherosclerosis and the phenomenon of arterial remodelling, an extensive amount of plaque can be present yet go undetected on angiography (Glagov 1987) (Schoenhagen 2001). To detect potentially vulnerable plaque before it impinges on the lumen, other diagnostic modalities are needed (Nissen 2001) (de Feyter 2000). Furthermore, accurate evaluation of the composition or biomechanical characteristics of such plaques could aid in the detection of high-risk lesions.

Several circulating plasma biomarkers related to increased inflammatory burden, platelet activation or endothelial activation correlate with the risk of cardiovascular events both in patients who have previously had an acute coronary event and in apparently healthy individuals (Ross 1999b) (Pearson 2003) (Ridker 2002) (Ridker

2003) (Biasucci 1996) (Cesari 2003) (Bayes Genis 2001). Despite these epidemiological results, little data exist on the relation between circulating biomarkers and local biomechanical or other structural characteristics of coronary plaques.

The aim of the IBIS study is to characterize non flow limiting subclinical coronary lesions by invasive and non-invasive imaging techniques in conjunction with multiple biomarkers.

General and Clinical Criteria
Braunwald class IA, IIA, IIIA (Unstable angina caused by noncardiac illness)
Pregnant women or women of childbearing potential who do not use adequate contraception
Known allergies to aspirin, clopidogrel bisulfate (Plavix^{TM}), Ticlopidine (Ticlid^{TM}), heparin, stainless steel, copper or a sensitivity to contrast media, which cannot be adequately premedicated
Life expectancy of less than one year or factors making clinical and/or angiographic follow-up difficult
Planned coronary bypass surgery or major non-cardiac surgery
Impaired renal function (creatinine >2 mg/dl or >150 µmol/L)
A history of bleeding diathesis or coagulopathy
Previous disabling stroke within the past year

Table 1a: Exclusion criteria

Criteria related to invasive imaging
Severe 3-vessel coronary artery and/or left main disease with ‡50% stenosis
Minimal lumen diameter <2 mm in the segments to be analyzed within the study vessel
Diameter stenosis >70% or total occlusion of the study vessel
In case the study-vessel has been stented previously more than 1/3 (outside the length of the stent plus 5 mm proxintal and distal to the stent) of the study vessel should be available for examination
Ejection fraction <30%

Table 1b: Exclusion criteria

CRITERIA RELATED TO INVASIVE IMAGING
Moderate to severe tortuosity (moderate: 2 bends >75_ or one bend >90_) of the proximal vessel in the segment(s) to be analyzed
Known tendency to coronary vasospasm

Table 1b: Exclusion criteria

CRITERIA RELATED TO NON-INVASIVE IMAGING
Heart rate >70 beats/min. 1 h after administration of an oral beta-blocker
Contra-indication to iodinated contrast material (.g. known allergy, serum creatinine >150 μmol/l, thyroid disorders)
Inability to hold breath for 20 s
Irregular heart rate (e.g. atrial fibrillation or very frequent PVCs)

Table 1c: Exclusion criteria

Methods

Patients and study protocol

From March to November 2003 we enrolled 90 patients in IBIS a prospective, single center, non-randomized, observational study. No formal ample size calculations have been performed. Follow-up will be completed in summer 2004. Patients 18 years of age or older were eligible for inclusion if (1) they presented with stable angina pectoris, documented silent ischaemia or an acute coronary syndrome (unstable angina pectoris, non ST segment elevation or ST segment elevation myocardial infarction) and (2) they underwent successful percutaneous coronary intervention (PCI) of one or more lesions in the native coronary circulation. Successful PCI was defined as attainment of residual diameter stenosis <20% (visual assessment), TIMI 3 flow and no residual dissection. Exclusion criteria are listed in Table 1. Patients who met all the inclusion criteria and none of the exclusion criteria were enrolled. The study was performed in accordance with the principles set out in the Declaration of Helsinki and was approved by the Medical Ethics Committee of

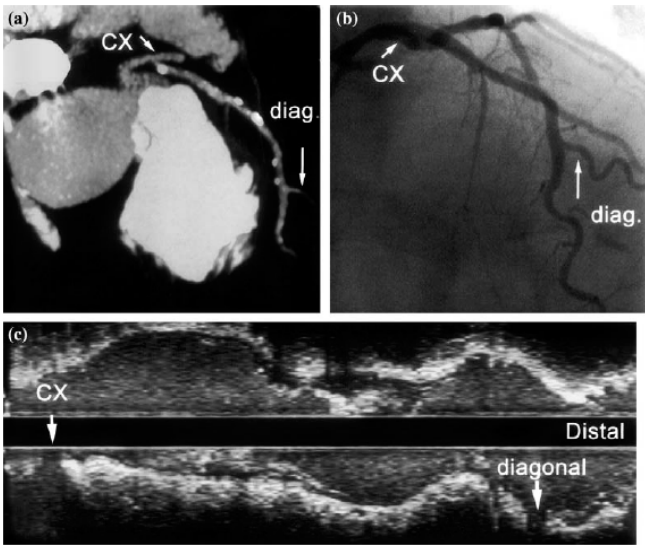

Fig 1: The region of interest (ROI) within the study vessel, in this example the LAD, as determined by MSCT (A) is appropriately matched with the angiographic (B) and IVUS (C) image. This ROI is demarcated by clear distal (in this example the first diagonal branch) and proximal (in this example the ostium of the Cx) anatomical landmarks. LAD=left anterior descending artery; Cx=circumflex artery; diag=diagonal branch.

the Erasmus MC. All patients gave written informed consent.

A coronary artery, other than the vessel that was the target for PCI, was designated as 'the study vessel'. In order of preference, the left anterior descending artery (LAD), right coronary artery (RCA) or circumflex artery (CX, including large intermediate branches) were selected. In addition, interrogation of the PCI vessel could be undertaken at the discretion of the investigator. All invasive imaging procedures (coronary angiography, IVUS, and palpography) were performed immediately after the PCI procedure or the morning following the PCI (where PCI was performed for STEMI). MSCT was preferably performed prior to invasive imaging; otherwise it was done within 21 days after PCl. Blood samples were obtained, whenever possible, prior to PCI from the arterial sheath before administration of unfractionated heparin. In order to correlate the different imaging techniques, a region of interest (ROI) in the study vessel was defined. This was based on the MSCT scan; a side branch was chosen as the distal boundary of the region of interest and a second side branch, or the ostium of the vessel, as the proximal boundary. An example is provided in Figure 1.

Clinical follow-up visits were scheduled at 3 and 6 months. At each visit, an ECG and blood samples for biomarker analysis were obtained and data collected on clinical events. At 6 months, repeat MSCT was performed, followed by repeat invasive imaging procedures on the study vessel.Whenever clinically driven angiography

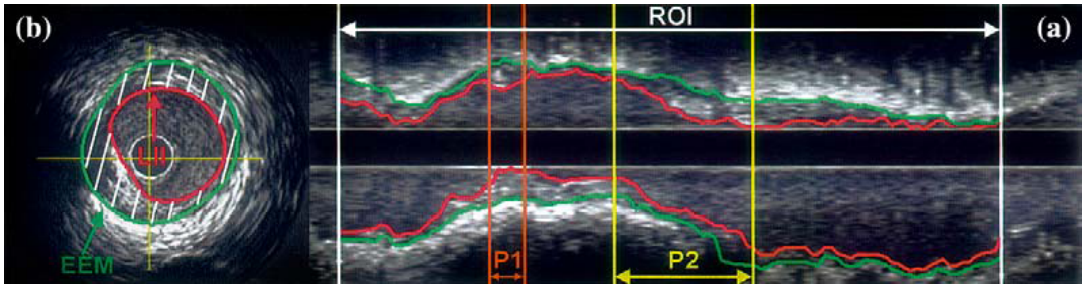

Fig 2: Longitudinal view (a) of the ROI on IVUS, as obtained by the Intelligate™method. The tissue between the external elastic membrane (EEM), depicted in green, and the lumen–intima interface, depicted in red, is defined as the coronary plaque plus media volume. For the purpose of this study, significant coronary plaque was defined as a plaque that occupied >50% of the area within the EEM. This is indicated in the longitudinal view by P1 (plaque 1) and P2 (plaque 2) and shown in a cross-sectional image of P2 (b). LII = lumen–intima interface.

was performed before the 3-month follow-up, patients were asked to return for the previously scheduled angiogram at 6 months. When angiography was performed after 3 months follow-up, this angiogram was considered as the final follow-up angiogram. All different invasive imaging techniques (angiography, IVUS, palpography) were repeated at follow-up; when PCI of the 'study vessel' was indicated at follow-up, the imaging procedures were performed before intervention. Patients who failed to attend the follow-up visits were contacted by phone or by letter or information was obtained

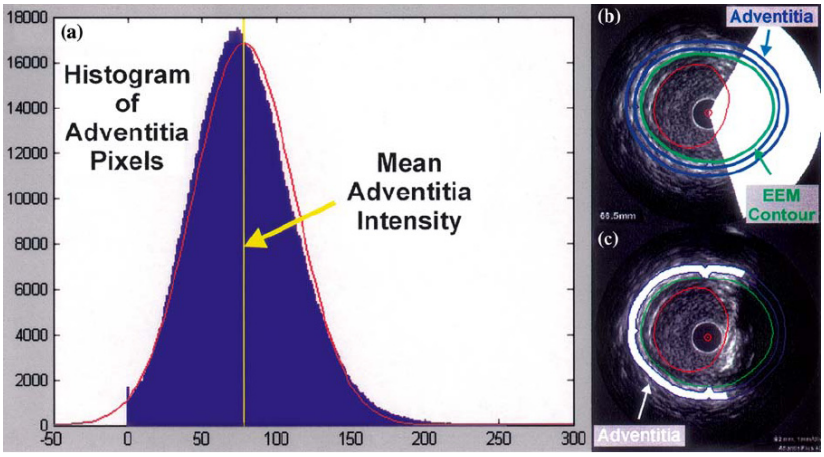

Figure 3. Panel A shows a histogram of the distribution of the grey level intensities of the pixels in the adventitia, which is located outside the EEM contour, in all the cross-sections of the ROI. In order to obtain a reliable reference value, parts of the adventitia with reduced intensity, due to acoustic shadowing, are excluded. When the distribution of the grey values in the histogram follows a normal distribution, shown here as a red line, the ultrasound images can be reliably used for image based tissue characterization. An example of a calcified plaque with acoustic shadowing of the adventitia is provided in panel B and C. The non-shadowed part of the adventitia is colored white (panel C).

through the general practitioner, the patient's next of kin or referring cardiologist. The patient was considered lost to follow-up if all these avenues were unsuccessful.

Coronary angiography

Conventional selective coronary angiography was performed with standard techniques. In order to obtain accurate and reproducible quantitative coronary angiographic (QCA) measurements, each angiogram was preceded by the intra-coronary injection of nitrates (1–3 mg isosorbide dinitrate) and the catheter tip was cleared of contrast. QCA analysis was performed by the core laboratory using the Cardiovascular Angiography Analysis System II algorithm (CAAS II), as previously described in detail (de Feyter 1991).

QCA: Definitions

The mean and minimal lumen diameters of the ROI were measured in all individual suitable projections. The average of these values for all available projections was calculated to provide an overall mean and minimal luminal diameter for the ROI diameter. A plaque was defined as luminal narrowing that resulted in >20% diameter sten-

Fig 4: Examples of tissue types as defined by the computer-aided grey scale analysis program. Panels 1A, 2A and 3A show the delineation of the lumen-intima (red), EEM (green) and adventitia (blue). Panels 1B, 2B and 3B are the corresponding cross sections and depict the different tissue types in different colors: red structures are hypoechogenic; green spots are hyperechogenic. Panel 3B also explains the principle of unknown tissue, colored yellow: tissue that cannot be characterized due to acoustic shadowing from calcium. The histograms (C panels) are divided in three portions, each portion showing the main tissue type of the plaque. 1C, the majority of the plaque is located in the left portion of the histogram and is therefore hypoechogenic. 2C, example of hyperechogenic plaque. 3C, example of a mainly hypoechogenic plaque, with a rim of calcium

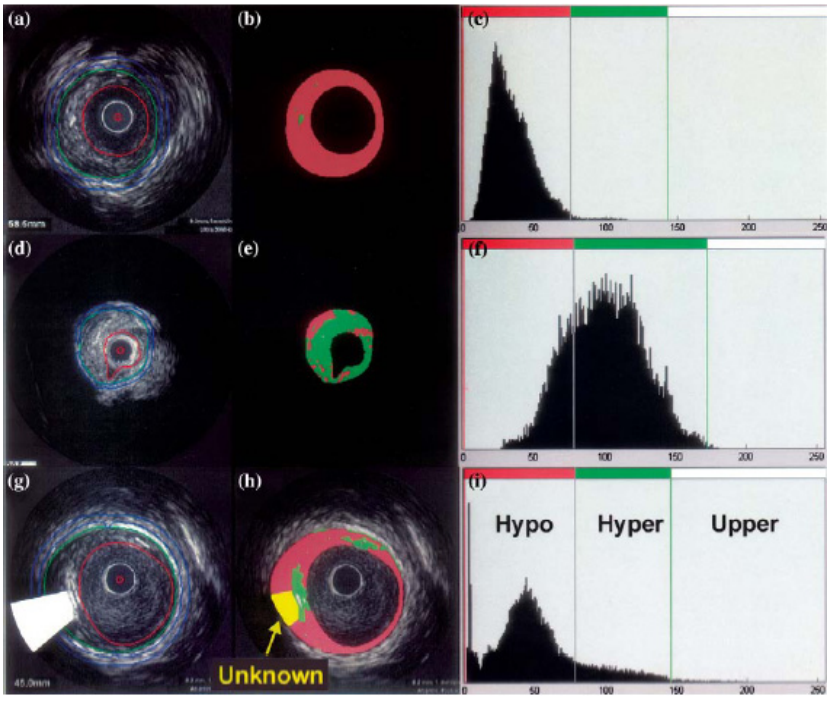

osis within the ROI with respect to the interpolated reference diameter. The reproducibility for QCA has previously been reported (Reiber 1994).

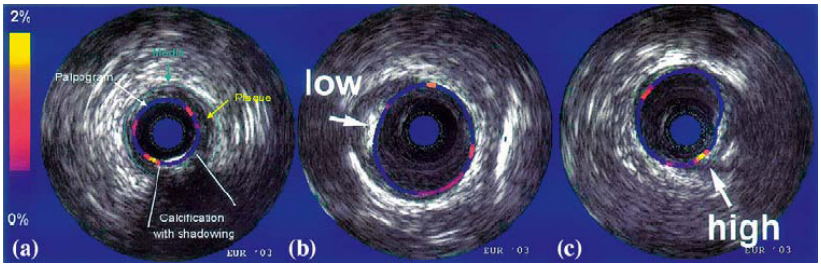

Fig 5: (a), the intravascular palpogram is superimposed on the IVUS image. This technique measures the deformation of the underlying vessel wall and plaque in the radial direction. The resulting strain values are plotted as a color-coded contour at the lumen vessel boundary. (b) is an example of a plaque with a low strain on the surface. (c) shows a plaque with high strain.

An additional qualitative analysis will be performed on the pre-intervention angiogram(s) to assess the presence and severity of atherosclerosis, based on angiography, in the study population in order to allow comparison of the 'tota1 plaque burden' on angiography with that on MSCT. All segments of the coronary tree were analyzed by an independent experienced cardiologist. Each segment was classified as normal (smooth or tapering borders), as atheromatous without an identifiable plaque (<20% diameter stenosis visually), as atheromatous with a distinct but <50% stenosis, as atheromatous with a >50% stenosis but without occlusion or as occluded.

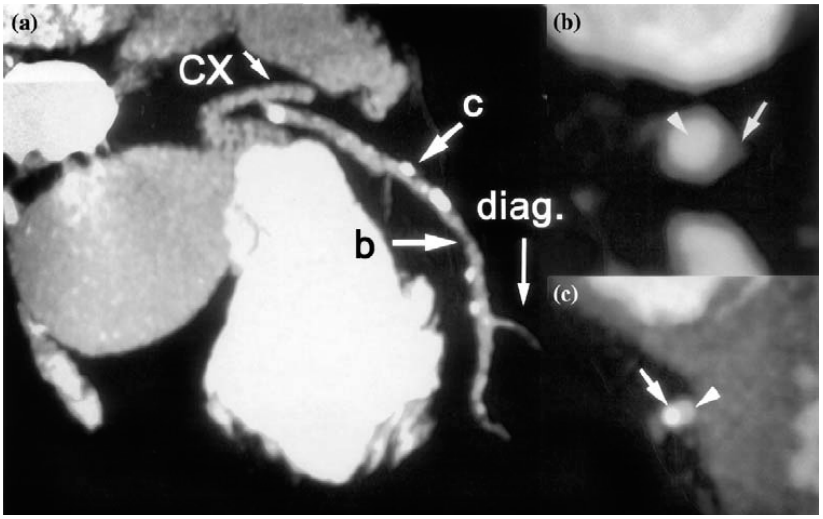

Fig 6: (a), using the same region of interest as in Figure 1, different plaque types can be identified on MSCT. (b), cross-section at location 1, showing non-calcified plaque (23 HU). C, cross-section at location 2, showing calcified plaque (579 HU)

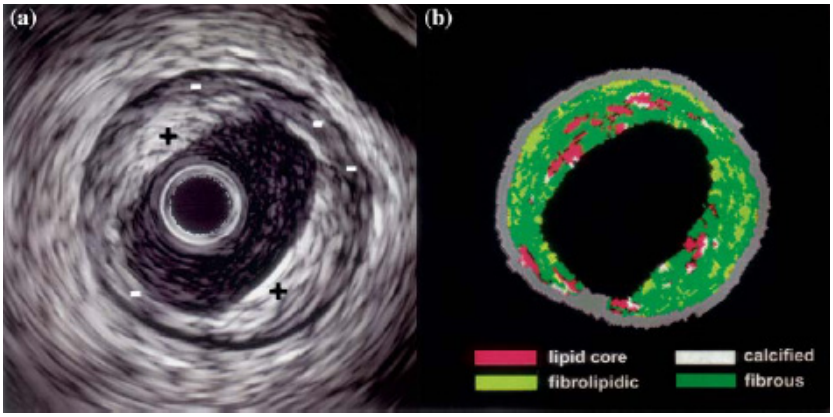

Fig 7: Atheroma morphology by IVUS (a) and IVUS virtual histology (VH) (b). (a), Concentric plaque with soft ()) and fibrous (+) components. (b), The same cross-section in IVUS VH shows that this plaque has a more heterogeneous composition: fibrous (green), fibrolipidic (light green), lipid core (red) and calcified (white) components can be identified

IVUS imaging

The IVUS catheter used was a commercially available mechanical sector scanner with a 30 or 40 MHz transducer (Ultracross™ 2.9F 30 MHz catheter or CVIS Atlantis™ SR Pro 2.5F 40 MHz catheter, Boston Scientific Corporation, Santa Clara, USA), connected to

Fig 8: Integration of the different imaging modalities, used in IBIS, into one graph provides a more comprehensive view on coronary atherosclerosis. Visualizing the same coronary artery segment, it becomes clear that the coronary angiogram grossly underestimates the coronary plaque burden: a significant amount of plaque on IVUS (plaque/EEM ratio >50%) and MSCT (plaque thickness >2 mm) produces only a mild lumen reduction on angiography. The palpogram provides additional information on the plaque surface: in this patient two high strain areas (ROC 4) were identified. The ROI is shown in the x-axis (in this patient 22 mm). The percent EEM-area reduction (on IVUS) and diameter reduction (on angiography) is depicted on the left *y*-axis. The right *y*-axis visualizes the plaque thickness in mm (MSCT) and the ROC score (palpography). Distal and proximal indicate the distal and proximal reference point the coronary artery, with respect to the coronary ostium.

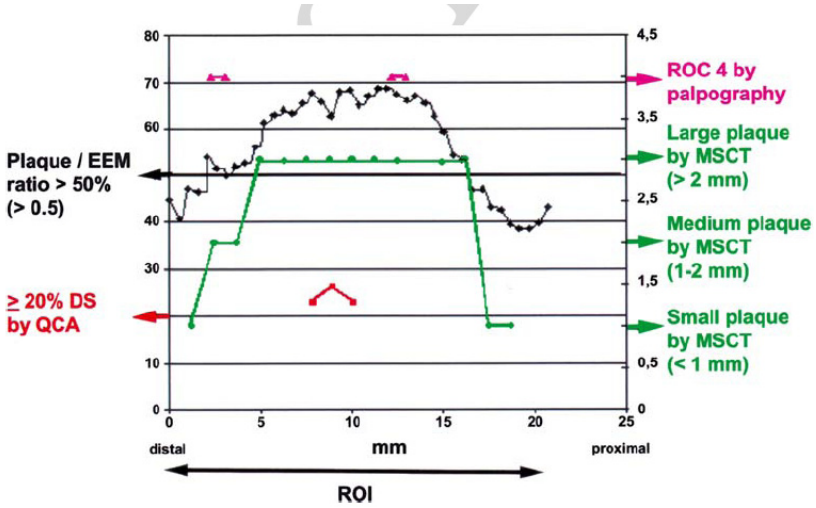

the Galaxy™ ultrasound console from Boston Scientific. Using an automated pullback device, the transducer was withdrawn at a continuous speed of 0.5 mm/s. Cine runs before and during contrast injection were performed to define the position of the IVUS catheter before the pullback was started. IVUS data were acquired after the intracoronary administration of isosorbide dinitrate and the data were stored on S-VHS videotape. The videotapes were digitized on a computer system, transformed into the DICOM medical image standard and stored on an IVUS Picture Archiving and Communications System (PACS).

Quantitative coronary ultrasound (QCU) analysis

QCU analysis was performed by the core laboratory using validated software (Curad, version 3.1, Wijk bij Duurstede, the Netherlands), which allows semi-automated detection of luminal and external elastic membrane boundaries in reconstructed longitudinal planes (L-mode views) (Hamers 2001). Due to catheter motion during the cardiac cycle, non-gated IVUS pullbacks result in a saw-tooth-appearance of the coronary segment on the longitudinal views and thus interfere with the contour detection algorithms used in most QCU software packages. This phenomenon can also lead to inaccurate measurements. In order to obtain a smooth appearance of the vessel wall structures in the longitudinal views, the Intelligate™ imagebased gating method was applied (Bruining 1998) (de Winter 2004). This validated technique eliminates catheter-induced image artefacts, by retrospectively selecting end-diastolic frames, thus resulting in more reliable volumetric measurements. Assuming a heart rate of 60 beats per minute and given a pullback speed of 0.5 mm/s, the Intelligate™ method selects 2 IVUS frames per millimeter for data analysis. After performing QCU, the borders of the external elastic membrane (EEM) and the lumen–intima interface enclose a volume that was defined as the coronary plaque plus media volume (Figure 2). The intra- and inter observer variability in our institution for measurements of lumen, EEM and plaque + media cross-sectional area has been reported in a previous study (von Birgelen 1997). Because of recent adjustments and improvements in the whole IVUS imaging chain, from catheter until final analysis, the observer-related variability data will again be determined for a subset of patients included in the IBIS study (de Winter 2004) (Bruining 2004).

IVUS plaque characterization: Computer-aided grey-scale analysis

In addition to plaque volume, IVUS also provides information on plaque echogenicity, a potential source of information on plaque composition. The acoustic characterization of a coronary plaque has been investigated by in vitro and in vivo studies that support a role for echogenicity as a predictor of-histological plaque composition (Nissen 2001) (Nishimura 1990) (Prati 2001) (Okimoto 2002) (Schartl 2001). In the present study, we used a computer-aided grey scale value analysis program for plaque characterization (de Winter 2003). Using the mean grey level of the adventitia as a threshold, five main tissue types can be characterized (Figure 3): (1) hypoechogenic tissue has a mean grey level lower than that of the adventitia, (2) hyperechogenic tissue, defined as tissue with a mean grey value higher than that of the adventitia, (3) calcified tissue, defined as a tissue with a mean grey value higher than that of the adventitia with associated acoustic shadowing, (4) unknown tissue, defined as tissue shadowed by calcification and (5) 'upper' tissue, defined as tissue that has a mean grey value higher than the mean adventitial intensity plus two times its standard deviation but is not typical calcified tissue with acoustic shadowing. An example of a recording illustrating some of the types of tissue described is presented in Figure 4.

Plaque size and composition by IVUS: Definitions

For the purpose of the IBIS protocol, significant plaque was defined as the presence of echolucent media and echogenic plaque area that resulted in a >50% reduction in the cross-sectional area circumscribed by the external elastic membrane (EEM). Plaque composition was classified, as defined previously, based on tissue echogenicity. Plaque within the ROI was considered calcified if it contained calcium in at least two consecutive cross-sections (0.5 mm < calcified plaque < 1 mm) and was scored in a binary fashion.

Palpography

Intravascular palpography is a new parametric imaging technique based on lVUS that assesses the local mechanical properties of the vessel wall and plaque. The underlying principle is that soft material will deform more compared with hard material when force is applied to the tissue. The naturally occurring pulsatile arterial pressure provides the force. The relative deformability of coronary plaque components can be estimated by measuring the relative displacements of radio frequency (RF) signals, recorded during IVUS acquisition, at two different pressure levels (de Korte 2002a). Post-processing of RF signals derives data regarding deformation of the

tissue and allows the construction of a 'strain' image in which 'harder' (low strain) and 'softer' regions (high strain) can be identified. The local strain is displayed color coded from blue for 0% strain via red to yellow for 2% strain as a complementary image to the IVUS echogram (Figure 5) (Schaar 2003a). The resolution of the strain measurement in the radial direction is 200 μm. In vitro and in vivo studies have validated the technique and found higher strain values in fatty as compared to fibrous plaques (de Korte 2000a+2002a+2002b). A recent in vitro study demonstrated the diagnostic potential of palpography to identify thin cap fibroatheromas (Schaar 2003a). All data in IBIS were acquired using a 20 MHz Jovus Avanar F/X IVUS catheter (Volcano, Rancho Cordova, CA, USA), which was connected to an In Vision Gold IVUS console. Recordings were obtained at a pullback speed of 1 mm/s using a mechanical pullback device (Trackback II, Volcano, Rancho Cordova, CA, USA). Simultaneously, the ECG and intraluminal pressure signals were recorded. Acquisition was done with a custom made dedicated workstation connected to the digital interface of the IVUS machine. Each acquisition was stored on a separate DVD. Processing and analysis of the data was done independently by observers unaware of the results of the other techniques. The reproducibility of three-dimensional palpography at our institution has been recently reported (Schaar 2003b).

Palpography: Definitions

The strain value that best discriminates a plaque at risk of rupture has a threshold of 1.26% (Schaar 2003). Strain values were classified according to the ROC classification (Rotterdam Classification) as low strain spots (ROC I: 0.0–<0.6%), moderate strain spots (ROC II: 0.6–<0.9%), medium strain spots (ROC III: 0.9–<1.2%), or high strain spots (ROC IV: >1.2%).

Multislice spiral computed tomography (MSCT)

Intravenous contrast injection with multislice coronary tomography allows non-invasive visualization of coronary arteries including visualization and evaluation of non-calcified and calcified plaques (Schroeder 2001) (Nieman 2002). Patients with resting heart rates >60 beats/minute received a single oral dose of 100 mg metoprolol (Selokeen, AstraZeneca Pharmaceuticals, UK), 1 h prior to the MSCT scan. All scans were performed using a true 16-row detector MSCT scanner (Sensation 16, Straton) with a gantry rotation time of 375 ms. Other scan parameters were: 16 · 0.75 detector collimation, table feed 3.0 mm/rotation, tube voltage 120 kV, tube current

500–600 mAs. A bolus of 140 ml Iodixanol with an Iodine content of 320 mgI/ml (Visipaque 320, Amersham Health, UK) was intravenously injected in an antecubital vein at 4 ml/s. A bolus tracking technique was used to synchronize the arrival of contrast material inside the coronary arteries and the start of the scan: a ROI was positioned inside the ascending aorta and the mean density within the ROI was monitored at intervals of 1.25 ms after the start of the injection. The patient was instructed, via an automated prerecorded message, to perform a breath hold when the mean density reached a predefined threshold (+100 HU), and the scan started 4 s later. All data were acquired during a single breath hold of 20 s, and images were reconstructed using retrospective ECG gating. An image reconstruction algorithm was used, which uses data obtained in half gantry rotation time resulting in a temporal resolution of up to 188 ms. To obtain motion-free images, standard reconstruction windows were selected during the mid-to-end diastolic phase (350, 400, and 450 ms prior to the next R-wave), but additional image reconstruction windows were explored when deemed necessary. The dataset with least motion-artefacts was selected and loaded into an off-line workstation (Leonardo, Siemens, Forchheim, Germany). Then, a ROI in the study vessel was selected on multiplanar reconstructed (MPR) images, using easily identified anatomic landmarks (sidebranches or the ostium). Thereafter, the dataset was loaded into a semi-automated vessel-tracking software program and a central lumen line was created throughout the ROI. Ten, twenty, or thirty cross-sectional MPR images (depending on the length of the ROI) were reconstructed orthogonal to this central lumenline, and used for image analysis. A cardiologist and a radiologist, unaware of the results of other imaging modalities, independently evaluated the cross-sectional images. Disagreements were resolved by consensus. The image quality of all cross-sectional images was classified as reliable, adequate, or unreliable. Images with unreliable image quality were excluded from further analysis.

MSCT: Definitions

Reliable cross-sectional MSCT images were visually evaluated for the presence of plaque; plaque was further classified based on size – as small, medium, or large-and composition – non-calcified, calcified, or mixed. A plaque was defined as a visually apparent abnormal space-occupying lesion, within the wall of the coronary artery that was clearly distinguishable both from the adjacent epicardal fat and from the coronary lumen. The mean Hounsfield unit (HU) of

a plaque was defined as the average HU of the individual cross-sections with plaque. Plaque size was further classified, based on their measured maximal thickness, as small (<1 mm), medium (1–2 mm),
or large (>2 mm). Plaque was defined as calcified if it contained high-density (>130 HU) components (Figure 6). Plaque tissue with both calcified and non-calcified components was classified as mixed. HU of non-calcified and calcified tissue components were measured in all cross-sections with medium and large plaques by positioning a ROI as far as possible from the lumen and adjacent epicardial fat. The j-values in our institution for inter- and intra-observer agreement regarding plaque size, using the 16-row detector MSCT scanner, have been determined in a group of 78 patients and are 72% and 74%, respectively.

Finally, the total plaque burden of the entire coronary tree was assessed on MSCT. All coronary segments were assessed. Where not possible (vessel <2 mm, vessel segment distal to an apparent total occlusion, motion or other artefact rendering interpretation unreliable), this was noted. Plaque was defined as mentioned above and was further classified as non-calcified, mixed, or calcified. Where MSCT was performed after the intervention, evaluation of plaque burden in the stented segments was obviously not possible. In these patients, an independent observer assessed the pre-intervention coronary angiogram as follows: the segments that had been stented were scored, by imputation. The segment(s) that were the site of the culprit lesion were classified as having a large plaque. In some patients, segments that were stented had no significant stenosis on angiography. This mainly reflected our practice of stenting from 'normal' to 'normal' with drug-eluting-stents; in other situations, multiple stents were implanted to cover a dissection or to protect a compromised side branch. These segments were considered as non-assessable or the presence of plaque. Qualitative assessment for calcium was performed, as described above, in all stented segments.

IVUS Virtual Histology (IVUS-VH): An IBIS substudy

IVUS VH is an intravascular ultrasound derived technique that analyses the radio frequency component of the reflected ultrasound signal. As compared with standard IVUS, this imaging modality has the potential for more detailed assessment of different plaque components. In preliminary in vitro studies, four plaque types (fibrous, fibrolipidic, lipid core and calcium) as defined by histology

could be correlated with a specific spectrum of the radio frequency signal (Nair 2002) (Moore 1998). The different plaque components are assigned colour codes: fibrous, fibrolipidic, lipid core, and calcified regions are labelled green, light green, red and white, respectively (Figure 7). This technique, given its ability to identify lipid-rich plaques, could be of great value in identifying potentially vulnerable plaque.

IVUS VH derives its data from the RF output of a conventional IVUS console and is ECG-gated for accurate data analysis. Since validation of the technique so far only exists for a 30 MHz system, the same 30 MHz IVUS catheter, used for the acquisition of the IVUS data, was utilized. The RF and ECG signal were transferred from the Boston Scientific console to a dedicated IVUS VH (Volcano) platform. The IVUS VH data were stored on a CD-ROM and sent to the Imaging Core Lab at Cardialysis for off-line analysis by one independent observer.

IVUS Virtual Histology: Definitions and endpoints

In analogy with QCU, the tissue in between the EEM and lumen–intima interface was defined as the coronary plaque plus media. Classification of the coronary plaque into its four components within the ROI was assessed independently from the media. Since IVUS VH was not incorporated at the start of the IBIS protocol, the results of this technique will only be reported as a substudy. The primary endpoints of this substudy are: (1) the volumetric correlation with QCU, (2) the correlation of the different plaque components with clinical presentation and biomarkers. (3) the correlation between plaque composition and strain pattern observed on palpography. Furthermore, the design of the IBIS study provides the means to address changes in plaque composition.

Biomarker and blood analysis

Cardiac enzymes (including troponin), hemoglobin, hematocrit, red blood cell (RBC) count, white blood cell (WBC) count, platelet count, urea, creatinine, total cholesterol, HDL cholesterol (HDL-C) and triglycerides were analyzed by the local laboratory. Plasma concentration of LDL cholesterol (LDL-C) was calculated by the use of the Friedewald formula [LDL-C = total cholesterol minus HDL-C minus (triglycerides/5)].

Plasma and sera used for biomarker analysis was centrifugally separated within 30 min of draw and stored at -70 ^{0}C. Analytes were

measured using commercial ELISA kits from R&D Systems except where noted. Plasma high sensitivity interleukin 6 (hs IL-6), tumor necrosis factor alpha (TNFa), serum high sensitivity C-reactive protein (hsCRP- Diagnostic Systems Laboratories), lipoprotein phospholipase A2 (LpPLA2- GSK), ultra sensitive pregnancy associated plasma protein A (PAPP-A-Diagnostic Systems Laboratory), matrix metalloproteinase 9 (MMP-9), soluble CD40L (sCD40L-Bender MedSystems) and monocyte chemoattratact protein (MCP-1), were measured in the Human Biomarker Centre, GlaxoSmithKline, using protocols provided by the manufacturer. Results from the standardized ELISA assays were measured on a MRX Revelation microplate reader with 4.2 software. Plasma LpPLA2 activity assay measures the proportional release of aqueous 3H acetate resulting from the enzymatic cleavage of the 3H acetyl-platelet activating factor substrate using methodology developed at GlaxoSmithKline. All simple analyses were done in batches representing the three time points (baseline, 3 and 6 months follow-up). Internally developed matrix matched or kit provided controls were incorporated to ensure consistency in the assay performance.

NT pro BNP was measured in EDTA plasma by Quest Diagnostics using a two-site electro-chemiluminescent assay. The lipoprotein subclass distribution was analyzed by Liposciences Inc. using NMR based technology. The analysis provided to us for the IBIS trial used the newest NMR LipoProfile II methodology.

In addition, serum batched by patient sets from all baseline and follow-up visits, were measured using an analyte defined (closed format protein chip. Protein chips provide capability for the analysis of between 10 and 157 different chemokines, cytokines and growth factors depending on the platform. Our analyses to date include the ZyomyxTM protein chip. The limits of quantification for the above analytes are as follows: 2.5 uIU/mL for PAPP-A, 0.18 ng/ml for MMP-9, 0.0048 mg/l for CRP, 6.31 pg/ml for MCP-l, 0.78 ng/ml for sCD40L, 0.057 pg/ml for IL-6, 0.88 pg/ml for TNF-a, and 3.92 nmols/min/ml for LpPLA2 activity.

Off-line analysis of imaging techniques: Principles and resolution of problems

No previous study has attempted to identify and characterize either coronary atherosclerosis or potentially vulnerable coronary plaques with such a wide range of invasive and non-invasive imaging techniques (Figure 8) in conjunction with multiple analyses of classic and novel biomarkers. In the present study all imaging techniques were analyzed independently. The QCA and QCU were performed by an independent Core Lab (Cardialysis) using standard operating procedures and validated methodology. The IVUS based tissue echogenicity, palpography, and MSCT analyses were performed independently by the research groups that developed or refined the techniques in our institution.

Ideally, we aimed to study a common ROI >30 mm long for all techniques. This was possible for the majority of patients but specific difficulties related to each technique required either a redefinition of the original ROI, before database lock, or the use of a shorter ROI within the initially defined region, in some patients. For all patients, the initial ROI was to be determined on MSCT. However, in some cases the landmarks on MSCT were not identifiable on IVUS. This primarily occurred in the RCA when the ostium was chosen as a landmark on MSCT but was not reliably identified on IVUS because the distal tip of the guiding catheter was within the coronary artery. In a few cases, the ROI could not be determined on MSCT. This was mainly related to un-interpretable images due to artefact related to high heart rates, irregular heart rates, or cardiac motion (exclusively in the RCA). Finally, in some cases, MSCT was not performed.

Imaging techniques: Parameters measured at baseline

IVUS

Mean plaque area in the ROI as defined by QCU was used for comparisons among imaging techniques and for exploratory analyses on the relation between clinical and biological variables and the extent of subclinical atheroma in the ROI. To this end, mean plaque area (MPA) was calculated as the difference between mean total vessel area (A_{TV}) and mean total lumen area (ATL). Total plaque volume (TPV) was calculated as the sum of the differences between external elastic membrane (EEM) and lumen areas across all frames in the region of interest (Nissen 2004). The plaque variables we measured and their definitions are presented in Table 2. Calcified plaque was

measured in the ROI based on the presence or absence of calcium in each 5 mm segment.

VOLUMETRIC VARIABLES (mm^3)
Absolute plaque volume (mm^3)
Total plaque volume (TPV) = $\sum(EEM_{CSA}) - (Lumen_{CSA})$
Relative (percent) plaque volume (%)
Relative plaque volume (RPV) = $\frac{\sum(EEM_{CSA}) - (Lumen_{CSA})}{EEM_{CSA}} x100$
AREA VARIABLES (mm^2)
Mean plaque area (MPA) = Mean total Vessel Area (A_{TV}) - Mean total Lumen Area (A_{TL})

Table 2. IVUS Coronary Plaque Measurements

MSCT

The ROI was subdivided into 5 mm segments. Each 5 mm segment was classified as plaque free or as containing a small, medium, or large plaque. Each plaque was classified as non-calcified, calcified, or mixed. Finally the longitudinal extent of calcium was expressed as an integer score based on the presence or absence of calcium in each 5 mm segment.

Comparison of QCU with MSCT

Based on QCU-derived measurements of coronary atheroma (i.e. plaque and media), the ability of MSCT to detect coronary plaques resulting in 50% EEM area reduction and to detect calcification was assessed. To ensure that the same plaques were assessed by the different techniques and to allow correlations, the ROI within the study vessel was subdivided into 5 mm segments as outlined above. The QCU and MSCT data were compared in corresponding 5 mm segments in the ROI.

Using these definitions, the ability of MSCT to detect plaque (binary classification; plaque present or absent) was compared with

that of IVUS (binary classification, coronary plaque area >50% of area enclosed by the EEM, yes/no). The effect of the presence or absence of calcium detected on IVUS on the specificity and sensitivity of MSCT plaque detection was also assessed, using a binary classification: calcium present/absent on MSCT or IVUS within the 5 mm segments.

QCA The overall mean and minimal lumen diameters of the ROI were measured. The number of plaques, defined as luminal narrowing that resulted in >20% diameter stenosis within the ROI, was also assessed.

Tissue echogenicity The major variables measured using the tissue echogenicity program were absolute hypo-echogenic and hyper-echogenic plaque volume (mm^3). Other variables measured, defined in the methods section, were upper volume and unknown volume (mm^3). These variables were also assessed for contiguous 5 mm segments within ROI.

Palpography The number of ROC III and IV scores was measured in the ROI and in individual 10 mm segments of the ROI (ROC 3/4 density).

Safety The occurrence of Major Adverse Cardiac and Cerebral Events (MACCE) was assessed after the procedure, at discharge, and at 3 and 6 months, as were the individual components: death, MI, revascularization by PCI or CABG, hospitalization for ischaemia and/or anginal symptoms, and stroke. They were classified, where possible, as related to the 'study vessel', the PCI vessel, or a non-PCI/non-study-vessel. The definition of myocardial infarction was identical to that defined in the ACC/ESC joint document on the redefinition of myocardial infarction (Alpers 2000). Major bleeding and vascular complications were also prospectively recorded using standard definitions (Serruys 1996).

Statistics For the comparison between and within techniques for each patient, for each analysis technique, and each time point, the same ROI, selected by the Core Lab, will be studied. Comparisons between techniques and within techniques (baseline vs. follow-up) will be performed with use of either two-by-two tables (sensitivity, specificity) for qualitative outcomes or linear regression analysis (regression coefficient, scatter plots) for quantitative outcomes. For

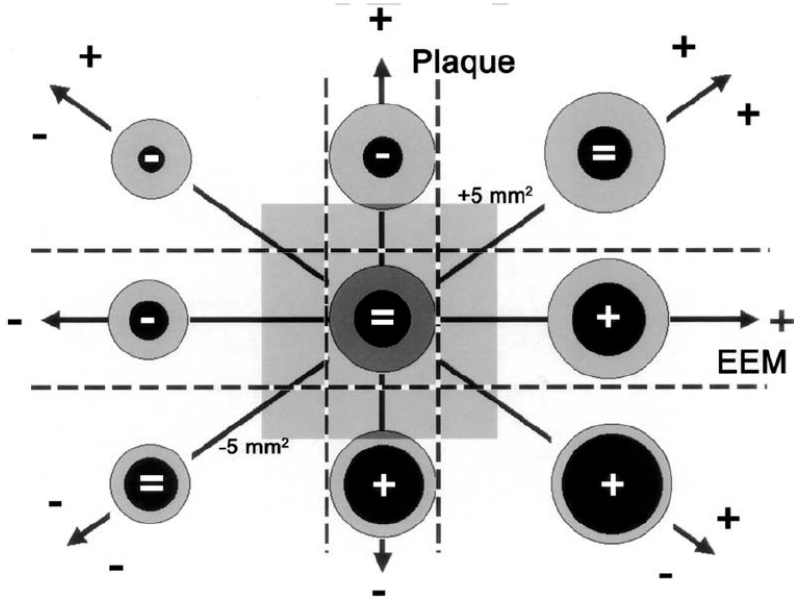

Fig 9: Schematic outline of the remodelling process in coronary atherosclerosis, as assessed by IVUS. In theory nine remodelling patterns can be defined, as depicted. Determinants of the coronary artery lumen diameter are the change in plaque size and the process of vascular remodelling, which is the change in the size of an artery over time. The change in the vascular lumen is indicated in the figure by the + (increase), - (decrease) or = (unchanged) signs. By taking into account the, still to be determined, observer related variability of the IVUS data in this study, as indicated by the (hypothetical) dotted lines, the natural history of the remodelling process can be defined for the IBIS population. The shaded box in grey indicates a change of 5 mm^2 along the x- and y-axis

the analysis on a per patient level, including biomarkers, clinical parameters, and imaging technique results, the data will be summarized by vessel (ROI) and for 5 mm increments of the ROI. For each 5 mm increment in each technique it was judged whether or not plaque could be detected. On the vessel level, plaque was defined as plaque in any of the 5 mm increments of the ROI. Circulating biomarkers will be correlated with imaging endpoints using the univariate Pearson correlation coefficients. We will also use Box and Whisker plots to compare biomarker distributions in predefined subgroups of the study population (diabetic status, anginal status, etc.). Statistical analyses will be performed with use of SAS version 8.

Discussion

Coronary atherosclerosis remains one of the major causes of mortality and morbidity in the Western Hemisphere. Advances in medical research have resulted in the introduction of new pharmacological agents that have significantly contributed to our ability to decrease the risk of clinical events related to atherosclero-

sis. Furthermore, the discipline of interventional cardiology has evolved from an experimental technology that was an option in highly selected patients to a discipline that complements and may soon largely replace coronary artery bypass surgery.

In parallel, advances in our understanding of the mechanisms underlying atherosclerosis have clearly demonstrated that clinical events are not necessarily related to the severity of luminal narrowing in large epicardial coronary arteries. The potential contribution of a low-grade inflammation, infectious agents, genetic factors, and other putative mechanisms to the occurrence of atherosclerosis-related clinical events is the subject of intense investigation.

Finally, the recognition that death or myocardial infarction is often related to plaque rupture at the site of non-flow limiting subclinical atherosclerosis has evolved into the concept of the vulnerable atherosclerotic plaque. Post-mortem studies have shown that plaque rupture at the site of thin-cap fibroatheromas is the most common mechanism that leads to death from atherosclerosis. However, it has also been clearly shown that such ruptures often remain clinically silent and contribute to lesion progression. As atherosclerosis is a diffuse process that involves many vascular beds and several sites within the coronary vasculature, better identification of plaque compositional characteristics is needed. The quest to identify reliable technique(s) to detect plaques that are at high risk of causing future clinical events is currently the subject of intense research activity. Ideally, biomarkers in peripheral blood, singly or in combination, could be used to identify patients at risk for new or recurrent clinical events such as sudden death or acute myocardial infarction. Appropriate non-invasive or invasive techniques could then be used to further refine risk stratification.

The aim of the IBIS study is to evaluate the feasibility and safety of both invasive (quantitative coronary angiography, intravascular ultrasound with tissue echogenicity and palpography) and non-invasive (multislice spiral computed tomography) imaging techniques to characterize non-flow limiting coronary lesions. The performance of MSCT to identify and characterize coronary plaque will be directly compared with that of IVUS, the current gold standard. Multiple classical and novel biomarkers will be measured and their levels will be correlated with the results of the different imaging

techniques. In addition, the potential utility of novel techniques such as tissue echogenicity and palpography will be evaluated. Beyond these specific goals, the longitudinal character of the IBIS study will be utilized to assess the natural history of arterial remodelling (Figure 9). Serial studies, like IBIS, that measure changes in vessel area at the same site over time are the ideal way to assess the remodelling process since they are not subjected to the limitations of using a reference site (Mintz 2001) (Ward 2000). A few IVUS studies with serial long-term (>12 months) follow-up in patients with atherosclerotic coronary artery disease have recently been reported (von Birgelen 2003+2004). They substantiate the earlier knowledge that changes in the arterial lumen correlate more closely with the direction and magnitude of the remodelling process than with plaque size.

Study limitations

We used two different IVUS catheters in the present study. During the first 3 months of patient inclusion IVUS imaging was done using a 40-MHz catheter; all subsequent baseline and all follow-up analyses were done using the 30-MHz system. This approach was driven by the decision to include IVUS VH as an additional imaging technique 3 months after the start of the IBIS study. Ideally, the same IVUS catheter used at baseline should again be selected for the follow-up procedure. However, since both IVUS catheters were operated on the same display system (Galaxy™ console, Boston scientific), this should not affect IVUS measurements (Bruining 2004).

Plaque assessment by MSCT was based on visual evaluation. While automated programs with the possibility of manual contour correction, such as used for QCA and IVUS, are under development for MSCT imaging, none are currently available for use.

IVUS examinations performed with a 40-MHZ IVUS catheter will not be used for evaluation by IVUS VH since validation only exists for the 30-MHZ system.

Where the initial ROI on MSCT could not be used for correlation with the other imaging techniques due to a problem with the identification of the landmarks, a new ROI was defined on MCST by the Core Lab in conjunction with an independent cardiologist, fa-

miliar with but not involved in the analysis of the various techniques. Where MSCT was not performed or could not be interpreted, a ROI was defined on IVUS using proximal and distal anatomic landmarks.

Chapter 10

Baseline Results of The Integrated Biomarker and Imaging Study (IBIS)

Based on:

Eugène P McFadden, Pim J de Feyter, Patrick W. Serruys, Carlos AG Van Mieghem, Johannes A Schaar, Nico Bruining, Nico Mollet, Filippo Cademartiri, Gaston Rodriguez Granillo, Anton FW van der Steen, Willem J van der Giessen, Georgios Sianos, Bianca Backx, Marie-Angèle M Morel, Clemens MC Disco, Gerrit-Anne van Es, Jonathon D Sawyer, June Kaplow, Andrew Zalewski
Integrating Biomarkers with Invasive and Non-Invasive Coronary Plaque Imaging: The IBIS Study (Integrated Biomarker and Imaging Study)
submitted

Potential of novel coronary imaging techniques

Atherosclerosis is a systemic disease whose clinical sequelae are unpredictable and only weakly related to its extent or severity. Pathological studies have related specific coronary plaque characteristics to fatal ischemic events but conventional imaging techniques cannot reliably identify them prospectively (Virmani 2000). While population based studies have shown that circulating biomarker levels predict clinical events in apparently healthy subjects or patients with coronary disease, individual biomarker profiles are less useful to guide management (Ridker 2003). Given the limitations of current methods for risk stratification, the potential of novel coronary imaging techniques to refine risk stratification in individual patients and ultimately guide local preventive strategies has attracted attention from the medical and scientific community (Casscells 2003b) (Wang 2004).

Comparison of MSCT angiography and IVUS

We investigated an integrated approach that included novel invasive and state-of-the-art non-invasive coronary imaging combined with circulating biomarkers to assess non flow-limiting atherosclerotic lesions in patients, with diverse clinical presentations, referred for percutaneous coronary intervention (PCI). We compared non-invasive Multi Slice Computed Tomography (MSCT) angiography and invasive intravascular ultrasound (IVUS) for detection of clinically silent coronary plaques and used novel invasive IVUS-based imaging (echogenicity and palpography) to assess plaque characteristics. Finally, we explored correlations between clinical presentation, imaging parameters, and circulating biomarkers.

METHODS

This pilot study was a prospective, observational and single center trial. Briefly, patients with stable angina, unstable angina, non-ST segment elevation myocardial infarction (NSTEMI), or ST segment elevation MI (STEMI) referred for PCI were eligible for in-

clusion. Major clinical exclusion criteria included significant renal (creatinine >2mg/dl) dysfunction, life expectancy less than one year or factors that made follow-up difficult. Major imaging-related exclusion criteria included coronary anatomy that precluded safe IVUS examination of a suitable region of interest (ROI) or criteria that precluded acquisition of diagnostic MSCT images (irregular heart rhythm or inability to breath hold for 20 seconds). The Medical Ethics Committee of the Erasmus MC approved the study protocol and all patients gave written informed consent. The coronary study vessel, preferentially a vessel not targeted for PCI, was, in order of preference, the LAD, RCA or LCX. The region of interest (ROI) was defined on the basis of identifiable landmarks, such as branches or the vessel origin.

Quantitative Coronary Angiography

Coronary angiograms were obtained in multiple views after the intracoronary injection of nitrates. Quantitative analyses were performed by a core laboratory (Cardialysis, Rotterdam, The Netherlands) with the use of edge-detection techniques. Mean and minimum luminal diameters and diameter stenosis were measured in at least two, preferentially orthogonal, projections and averaged.

Intra Coronary Ultrasound

IVUS was performed with commercially available catheters (Ultracross^{TM} or CVIS Atlantis^{TM} SR Pro, Boston Scientific, Santa Clara, USA) and an automated pullback device (0.5 mm/s). Data were stored on S-VHS videotape, digitized and transformed into the DICOM medical image standard, and archived. QCU analysis was performed by the core laboratory using validated software (Curad, version 3.1, Wijk bij Duurstede, The Netherlands) and retrospective image-based gating (de Winter 2004). The borders of the external elastic membrane (EEM) and of the lumen were traced. The area they enclosed was defined as the coronary plaque plus media area (subsequently referred to as plaque area). Significant plaque was defined as plaque area whose area occupied 50% or more of the cross-sectional area circumscribed by the EEM. Quantitative parameters were reported for the entire ROI and for slices with significant plaque.

Plaque Echogenicity

We used a computer-aided, gray-scale value, analysis program for plaque characterization.6 Based on the mean gray level (brightness) of the adventitia, plaque was classified as brighter (hyperechogenic) or less bright (hypoechogenic) than the adventitia. Calcified plaque was defined as plaque brighter than the adventitia with associated acoustic shadowing. The percentage of hypoechogenic plaque was calculated for the entire ROI and for slices with significant plaque, with use of previously reported methodology (de Winter 2003) (Schartl 2001).

Palpography

Palpography assesses the relative deformability of coronary plaque components using data acquired during an IVUS pullback (1 mm/s) with a commercially available catheter (20MHz Jovus Avanar F/X, Volcano, Rancho Cordova, CA, USA). Using previously described and validated methodology, strain values were classified according to the Rotterdam Classification (ROC) (de Korte 2002a+b) (Schaar 2003+2004a).

Multislice Spiral Computed Tomography

All scans were performed on a 16-row detector MSCT scanner (Sensation 16, Straton). The scan protocol and image reconstruction parameters were recently published (Mollet 2004). Technical advances allowed us, in this study, to adapt tube output to patient weight. The dataset with least motion artifacts was loaded on an off-line workstation (Leonardo, Siemens, Forchheim, Germany) and the ROI identified on multiplanar reconstructions (MPR), using anatomic landmarks. Data sets were loaded on a semi-automated vessel-tracking software program and a central lumen line created throughout the ROI. Ten through 30 cross-sectional MPR (depending on ROI length), reconstructed orthogonal to this line, were analyzed independently by two observers. Disagreements were resolved by consensus. Plaque was defined as an abnormal mass within the artery wall, clearly distinguishable from epicardial fat and the coronary lumen and classified, based on manually measured maximal thickness, as small (<1 mm), medium (1-2 mm), or large (>2 mm). Calcification was defined as the presence of high-density, >130 Hounsfield Unit, components.

Biomarkers

Blood for biomarker analysis was taken at the time of the interventional procedure, centrifuged within 30 minutes and stored at -70C. Analytes were measured using commercial ELISA kits from R&D Systems except where noted. Plasma high sensitivity interleukin 6 (IL-6), and serum high sensitivity C-reactive protein (hsCRP Diagnostic Systems Laboratories), lipoprotein phospholipase A2 (Lp-PLA2) and tumor necrosis factor-a (TNF-a) were measured in the Human Biomarker Center (GlaxoSmithKline, PA, USA) using protocols provided by the manufacturer. Results from the standardized ELISA assays were measured on a MRX Revelation microplate reader with 4.2 software. Plasma Lp-PLA2 activity assay measures the proportional release of aqueous 3H acetate re-

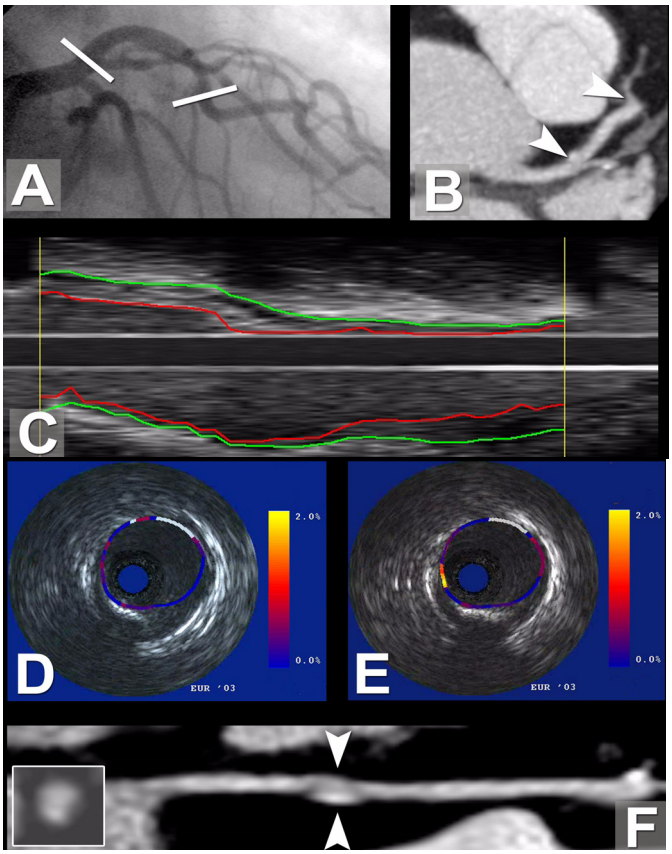

Fig 1: Example of imaging findings in a patient in whom intervention was performed on the right coronary artery. The study segment was the proximal left anterior descending coronary artery. The borders of the region of interest were the ostium of the left anterior descending and a large septal branch. These are indicated by the lines on the angiogram (Panel A) and by the arrows on the Multiplanar MSCT reconstruction (Panel B). Panel C shows a gated longitudinal intravascular ultrasound reconstruction. The vertical lines mark the boundaries of the region of interest. The red line indicates the lumen-intima interface and the green line the external border of the plaque plus media. Representative color-coded circumferential palpography data, superimposed on the intravascular ultrasound cross-sections. Strain values are color-coded from 0% (blue), through yellow (2%) via red. Panel D shows non-deformable eccentric plaque with acoustic shadowing compatible with calcification. The blue line indicates a non-deformable plaque with 0% strain. Panel E shows eccentric partly calcified plaque with a high strain (yellow) spot on one shoulder of the plaque (nine o clock). On the other shoulder (four o clock) the blue color (0% strain) indicates that the plaque is not deformable in this region. The gray color, in the arc without plaque, indicates that no strain value is available. Typical findings on echogenicity are presented in Panels F and G. The bottom panel (I) shows the MSCT reconstruction and inset a cross-section in an area with calcified plaque.

sulting from the enzymatic cleavage of the 3H acetyl-platelet activating factor substrate using methodology developed at GlaxoSmithKline. NT pro BNP was measured in EDTA plasma by Quest Diagnostics using a two site electrochemiluminescent assay. The limits of quantification were 0.0048 mg/L for hsCRP, 0.057 pg/mL for IL-6, 3.92 nmols/min/mL for Lp-PLA2 activity, 10 pg/ml for NT pro BNP, and 41 pg/mL for TNF-a.

Statistical Analysis

Discrete variables are presented as counts and percentages. Continuous variables are presented as means ± SD, unless otherwise indicated. IVUS data were summarized by ROI and for the part of the ROI with significant plaque. Measurements of systemic biomarkers are presented as Box-Whisker plots. Comparisons between MSCT

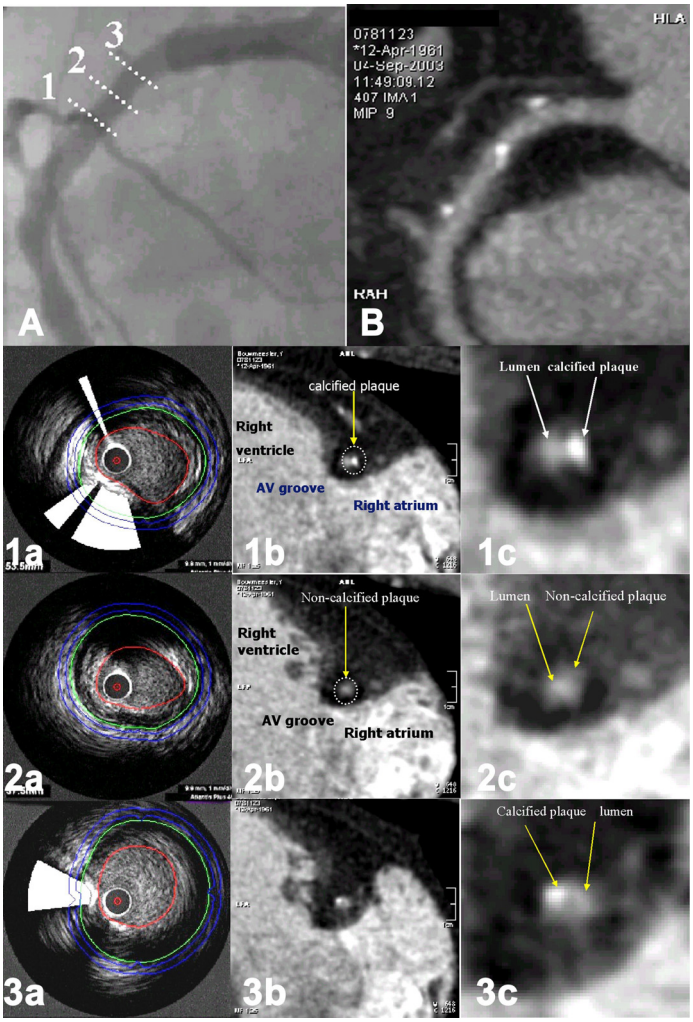

Fig 2: This illustrates MSCTA and IVUS findings in a region of interest in the proximal right coronary artery. The conventional angiogram is shown in Panel A and a Multiplanar Reconstruction (MPR) of the MSCT in Panel B; the white spots seen on the MPR reconstruction are calcified areas. Below, the Panels in 1, 2, and 3 show cross-sectional IVUS (a), cross-sectional MSCT (b), and magnified cross-sectional MSCT images in the regions indicated by the corresponding numbered lines in the conventional angiogram (Panel A). Regions 1 and 3 show plaque with calcified components, as shown on the IVUS by the acoustic shadowing, whereas the plaque in Region 2 is not calcified.

and IVUS were performed with use of two-by-two tables (sensitivity, specificity). Comparisons between quantitative outcomes were performed with use of scatterplots and linear regression analysis (regression coefficient). As biomarker data were not normally distributed, analyses were performed after natural logarithmic transformation. We made scatterplots of quantitative angiographic and IVUS outcomes versus the log-transformed value of the biomarkers and calculated the univariate correlation coefficients. Differences in means among groups were analyzed by a two-sample t-test or by one-way analysis of variance. Adjustment for multiple comparisons was performed with use of the Bonferroni correction. A P value of less than 0.05 (two-sided) was considered to indicate statistical significance. Statistical analyses were performed with use of SAS Version 8.

RESULTS

Demographic data

The demographic, clinical, and angiographic characteristics of the patients are reported in Table 1. QCA and IVUS parameters in the ROI, by vessel studied, are reported in Table 2. Although the mean diameter stenosis on QCA was only 25±11%, IVUS examination revealed significant plaques (i.e., >50% reduction of vessel cross-

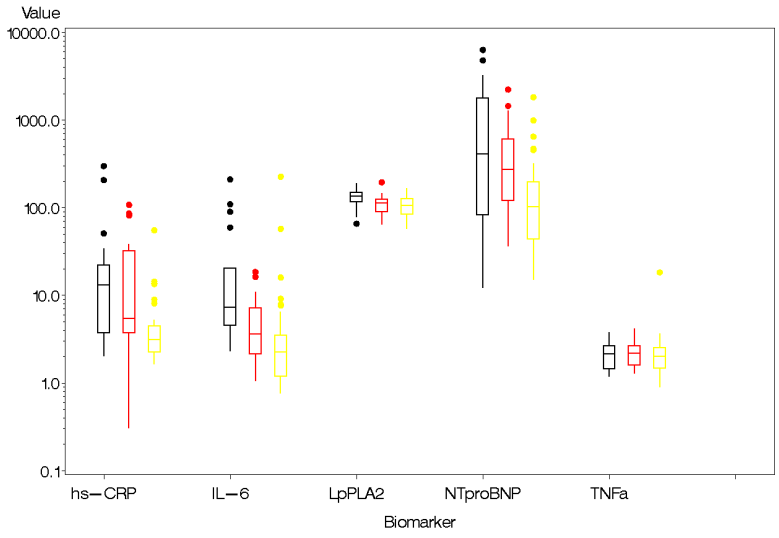

Fig 3: Relation between the systemic values of the biomarkers we measured and the clinical presentation that prompted referral for intervention. Data are presented as box-whisker plots, with 25th and 75th percentiles (box) and 10th and 90th percentiles (I). There were significant differences among patient groups with acute myocardial infarction (black), unstable angina (red), and stable angina (yellow) for systemic values of hsCRP (P=0.0003), IL-6 (P=0.0001), LpPLA2 (P=0.035), and NTproBNP (P=0.0012).

sectional area) in 75% (61/81) vessels, within the study segment (mean length: 32.8±15.9 mm). There were 113 discrete significant plaques. The findings in IVUS slices with significant plaque are also presented in Table 2. Biomarker data was obtained in 83/84 (99%) patients. For imaging techniques, data suitable for analysis was obtained for all patients (QCA), 81/84 (96%) patients (IVUS), 80/84 (95%) patients (echogenicity), and 69/84 (82%) patients (palpography). MSCT, performed in 70/84 patients, was of diagnostic quality for plaque imaging in 64/70 (91%).

Novel Invasive Imaging

The results of echogenicity and palpography are reported in Table 3. In the entire ROI and in slices with significant plaque, the predominant plaque component was hypoechogenic plaque whose mean brightness was less than that of the adventitia (Table 3). The percentage of hypoechogenic plaque was 92.7±3.5 for patients (n=17) undergoing intervention for STEMI, 92.4±4.0 for patients with unstable angina (n=25), and 89.5±4.6 for stable (n=38) angina patients (p=0.013 for STEMI vs stable, p=0.09 for STEMI vs unstable/stable). On palpography, high strain spots (ROC 3/4), that reflect abnormal biomechanical plaque characteristics, were common (4.0±4.1 per ROI, range 0-16) and at least one ROC 3/4 strain spot was detected in 78% of studied segments. The ROC scores and the density of ROC 3/4 strain spots (mean per 10mm ROI) were distributed similarly among epicardial coronary arteries

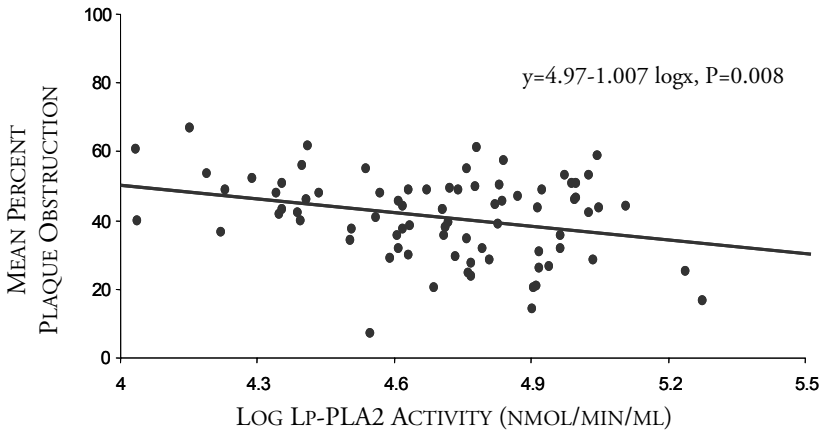

Fig 4: Correlation between Percentage Values for Mean Percent Plaque Obstruction, defined as EEM_{area} - $Lumen_{area}$) divided by EEM_{area}, in the Region of Interest and log transformed Systemic Values for Lp-PLA2 activity. Mean Percent Plaque Obstruction was significantly ($P<0.05$) correlated with the Systemic Values for Lp-PLA2 activity

(Table 3). However, the density of ROC 3/4 strain spots was 2.1±2.1 for patients (n=14) presenting with STEMI, 1.4±1.7 for patients with unstable angina (n=21), and 1.2±1.1 for stable (n=33) angina patients (p=0.003 for STEMI vs stable, p=0.02 for STEMI vs unstable/stable). Representative imaging findings are presented in Figure 1.

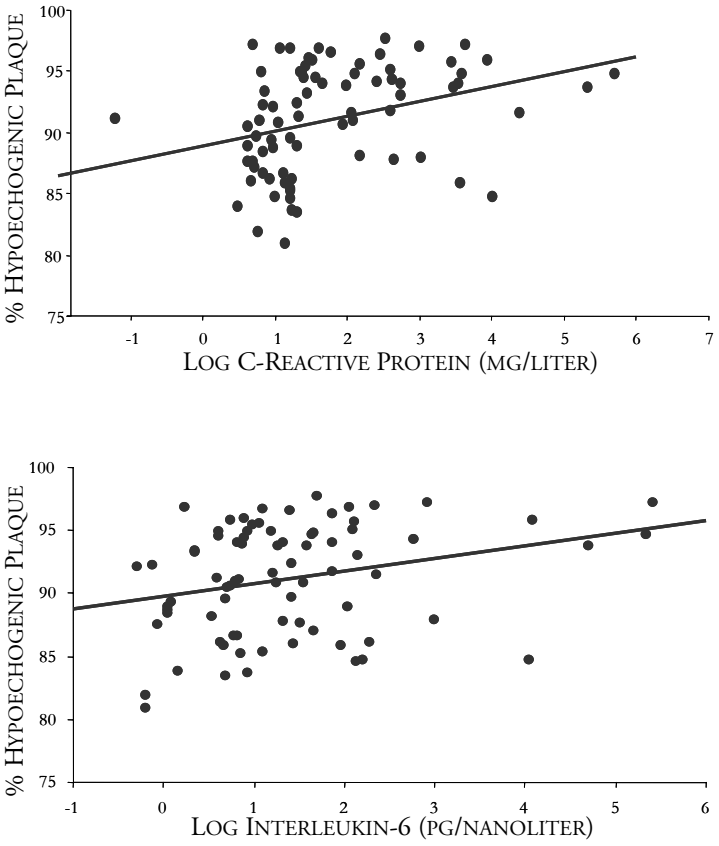

Fig. 5: Correlation between Percentage Values for Hypoechogenic Plaque in the Region of Interest and log transformed Systemic Values for C-Reactive Protein and Interleukin-6. The Percentage of Hypoechogenic Plaque was significantly (P<0.05) correlated with the Systemic Values for C-Reactive Protein (Top Panel) and Interleukin-6 (Bottom Panel).

MSCTA vs IVUS

MSCT and IVUS were compared in 61 patients. The sensitivity and specificity of MSCT to detect plaque identified on IVUS (>50% mean cross-sectional area obstruction or the presence of calcification on 2 consecutive slices on IVUS) was calculated per entire ROI and for 3mm sub-segments (Table 4.). The sensitivity and specificity of MSCT for detection of plaque in the ROI were 85% and 71%, respectively. The positive and negative predictive values of MSCT for detection of plaque were 75% and 72% for the entire ROI, (75%) 71% and (72%) 71% for (5mm) 3mm slices. Repre-

sentative findings are presented in Figure 2. The sensitivity of MSCT to detect plaque was 64% (28/44) for small (<1mm), 77% (73/95) for medium (1-2 mm), and 86% (25/29) for large plaques (>2 mm).

Biomarkers

The relation of soluble biomarkers to conventional and novel imaging parameters is presented in Table 5 and their relation to clinical status at the time of intervention is presented in Figure 3. There were significant relationships between systemic levels of hsCRP (P=0.0003), IL-6 (P=0.0001), Lp-PLA2 (P=0.035), and of NT pro BNP, (P=0.0012) and clinical presentation. Biomarker levels showed no significant relationship to any conventional angiographic (mean MLD or mean percent diameter stenosis) parameter or to mean plaque area on IVUS. However, mean percent area obstruction on IVUS was inversely related (P=0.008) to systemic levels of Lp-PLA2 (Figure 4). There were also significant correlations (Figure 5) between plaque echogenicity and systemic levels of hsCRP (p=0.003) and IL6 (p=0.016).

DISCUSSION

This study is the first to combine novel invasive techniques, state-of-the-art non-invasive MSCTA, and measurements of multiple biomarkers to characterize sub-clinical coronary atherosclerosis. As expected, the majority of non-culprit vessels in patients referred for coronary intervention had large plaques on IVUS, despite only mild angiographic disease. The majority of these plaques were identified on non-invasive imaging with use of MSCTA. Most importantly, features potentially indicative of high-risk plaque were both widespread and highly prevalent in coronary vessels examined by NIVUS-based imaging. Although only a short segment of the coronary tree was imaged, several intriguing relationships between clinical and biological parameters and putative indicators of structural instability or plaque composition were noted.

Conventional invasive imaging modalities cannot reliably identify plaques with potential to cause future clinical events. However, systemic levels of inflammatory biomarkers, notably CRP, can refine risk stratification and CRP adds to coronary risk prediction based on non-invasive detection of coronary calcification (Ridker 2002)

(Reilly 2003). Recommendations that measurement of CRP be incorporated into risk stratification algorithms, combined with widespread availability of non-invasive coronary imaging, will likely result in an increasing number of referrals to cardiologists for further evaluation (Pearson 2003). In parallel, the advent of drug-eluting stents has rekindled enthusiasm among interventional cardiologists for the concept of prophylactic intervention on vulnerable plaque (Casscells 2003b)(Wang 2004)(Meier 1995)(Hoye 2004). In this context, the potential of novel imaging techniques to guide such strategies has stimulated innovative research.

Subclinical Atherosclerosis: Insights from Novel Invasive Techniques

Pathologic studies suggest that rupture of thin-capped fibroatheromas is a common substrate for clinical events (Virmani 2000). We have validated in vitro the potential of palpography to identify thin-capped fibroatheromas (de Korte 2002a+b). Subsequently, we showed that the number of high-strain spots in epicardial vessels was correlated with clinical presentation (Schaar 2004a). The present study extends these findings by demonstrating that, within arbitrarily selected segments of non-culprit vessels, structurally vulnerable plaques were quite common (mean of 4.0±4.1, range 0-16), despite only mild angiographic disease. It confirms our previous observations that patients with STEMI have a significantly higher number of structurally vulnerable plaques than other patients with different presentations, in coronary regions remote from the site of occlusive thrombosis. These findings are consistent with other observations that there are widespread abnormalities, in non-culprit vessels or remote myocardium of patients with acute coronary syndromes (Buffon 2002) (Abbate 2004). The high prevalence of structurally vulnerable plaque found in this study, together with post-mortem observations showing clinically silent plaque rupture is relatively common, suggest that isolated rupture is unlikely to account for rather infrequent ischemic events (Davies 1984).

Several studies have indicated that echogenicity is related to the histological components of both carotid and coronary plaques (El-Barghouty 1996) (Gronholdt 1998) (Rasheed 1995) (Prati 2001), and that carotid plaque echolucency (low echogenicity) was associated with neurological events, both spontaneous and related to percutaneous carotid stent placement (Polak 1998) (Gronholdt 2001) (Mathiesen 2001). Recent studies suggested a link between carotid

plaque echogenicity and coronary plaque instability (Honda 2004) (Lombardo 2004). For carotid studies, a highly reproducible quantitative computer-assisted index of echogenicity, based on gray-scale values of blood and of adventitia, has gained widespread acceptance (Sabetai 2000).

While carotid plaque echogenicity can be assessed non-invasively, assessment of coronary plaque echogenicity requires invasive techniques and has been restricted to research settings. A recent study systematically studied, for the first time, coronary plaque echogenicity in a protocol with mandated IVUS follow-up and showed that treatment with atorvastatin resulted in quantifiable changes in coronary plaque echogenicity, compatible with changes in plaque composition (Schartl 2001). These findings offered a potential explanation for the clinical efficacy of statins despite only modest effects on plaque volume (Cannon 2004)(Nissen 2004). In the present study, we used a quantitative computer-assisted index of echogenicity, based on gray-scale values of adventitia (de Winter 2003). The predominant plaque component, in the arterial segment we evaluated, was hypoechogenic plaque. Although we found significant correlations between plaque echogenicity and clinical presentation, the preponderance of hypoechogenic plaque in the vessel we studied suggests that plaque echogenicity lacks the discrimination necessary for robust risk stratification. It might, however, prove useful as a surrogate indicator of changes in plaque composition on serial studies (Schartl 2001).

Subclinical Atherosclerosis: Role of Non-Invasive Imaging

MSCTA can identify significant coronary lesions with high sensitivity and specificity (Nieman 2002). Recent studies have shown its potential for detecting non-obstructive coronary plaques in highly selected patients (Achenbach 2004)(Schoenhagen 2003). Our results extend these findings by showing that non-obstructive coronary plaque can be detected, in an arbitrarily selected ROI, with moderately high sensitivity and specificity in a less selected population and that the size of such plaques can be assessed noninvasively. As diffuse subclinical coronary atherosclerosis is common, our data do not support the indiscriminate use of MSCTA as a tool for risk stratification at the present time, notwithstanding its demonstrated potential as a diagnostic tool in selected patients.

Assessment of Subclinical Atherosclerosis: Potential of Biomarkers

Population-based studies have demonstrated the predictive value of circulating biomarkers in evaluating the risk of coronary heart disease. A few small studies suggested that plasma biomarkers might reflect plaque composition (Weiss 2001)(Blake 2003). Levels of soluble biomarkers are affected by many patient-specific (e.g., background therapy, obesity) and disease-specific factors (e.g., presence of an acute coronary syndrome). Nevertheless, we found significant correlations between inflammatory biomarkers (hsCRP, IL-6) and the IVUS-derived hypoechogenicity index. The extent of hypoechogenic plaque in our study was somewhat higher than previously reported (Schartl 2001). Although we have no clear explanation for these findings, it is plausible that increases in systemic levels of these biomarkers, by altering endothelial permeability, might transiently affect plaque echogenicity. Overall, these observations raise the possibility that imaging parameters, in conjunction with measurements of biomarkers, may open new avenues of research that might elucidate established mechanisms or shed light on novel mechanisms involved in the complex relation between subclinical atherosclerosis and ischemic events.

Limitations

Our patient population was intentionally heterogeneous and the study was not designed to correlate compositional imaging endpoints with clinical outcomes. Second, our attempt to relate systemic biomarkers, measured at a single time point, to imaging in an arbitrarily selected region of interest can only be regarded as hypothesis generating. Third, while our results underscore the heterogeneity of coronary atheroma, much larger studies are needed to clarify the role of novel plaque imaging techniques in clinical practice.

Implications of the Study

Despite considerable advances, patients with documented coronary atherosclerosis have a significant risk of future ischemic events (Cannon 2004). Our results demonstrate that abnormal findings detected by novel invasive plaque imaging are both widespread and rather frequent in coronary vessels with only mild angiographic disease. These observations argue against a preventive strategy to treat vulnerable non-obstructive plaque with catheter-based intervention such as drug-eluting stent implantation (Wang 2004). First, it is likely that findings suggestive of plaque vulnerability are not limit-

ed to the short arterial segment that underwent detailed interrogation; second, neither the clinical benefit nor the cost effectiveness of such a strategy has been proven. The ability to prospectively identify structurally vulnerable plaques provides a means to clarify their natural history. This perspective, coupled with studies of endothelial function and inflammatory biomarkers may increase our understanding of the mechanisms of future clinical events. Furthermore, imaging studies have potential to serve as surrogate endpoints and to assist in dose selection of emerging pharmacologic interventions with unprecedented mechanisms of action (Nissen 2003).

DEMOGRAPHICS AND PAST MEDICAL HISTORY		
	N	%
Male	67	79.8
Mean age (range)	58.9	(28 - 77)
Previous MI	35	41.7
Previous CABG	1	1.2
Previous PCI	12	14.3
Diabetes mellitus	11	13.1
History of stroke	1	1.2
Family history of coronary disease	46	54.8
Hypertension*	39	46.4
Hypercholesterolemia**	71	84.5
Previous smoker	29	34.5
Current smoker	30	35.7
CLINICAL STATUS AT ENROLMENT		
Stable angina	35	41.7
Silent ischemia	4	4.8
Unstable angina	27	32.1
ST-segment elevation MI	18	21.4

Table 1: Patient characteristics (n = 84)

Extent of disease***		
Non significant	5	5.9
Single-vessel	51	60.7
Two-vessel	25	29.8
Three-vessel	1	1.2
Left Main (plus two-vessel)	2	2.4

*Blood pressure > 160/95 mmHg or treatment for hypertension, ** total cholesterol > 5.5 mmol/l (215 mg/dl) or treatment for hypercholesterolemia, ***Significant disease was defined as angiographically significant (>50% visual estimation) stenosis in a major epicardial vessel or in branches > 2.5 mm diameter. MI myocardial infarction; CABG, coronary artery bypass grafting; PCI, percutaneous coronary intervention.

Table 1: Patient characteristics (n = 84)

Vessel	Total (84)	LAD (37)	LCX (15)	RCA (32)	P value
Length (mm)	28.63 ± 14.30	24.20 ± 12.63	25.67 ± 12.31	35.13 ± 14.91	0.004
Mean Diameter (mm)	2.78 ± 0.68	2.55 ± 0.61	2.95 ± 0.62	2.96 ± 0.71	0.02
Minimal Diameter (mm)	2.32 ± 0.64	2.15 ± 0.55	2.43 ± 0.70	2.47 ± 0.67	0.09
DS (%)	25 ± 10	25 ± 11	25 ± 12	24 ± 10	0.95
DS <20%	27 (32%)	12 (32%)	6 (43%)	9 (28%)	
DS 20 – 50%	56 (67%)	25 (68%)	8 (53%)	23 (72%)	0.23
DS >50%	1 (1%)	0	1 (7%)	0	

Table 2a: Quantitative Angiographic Parameters in the Region of Interest

Vessel	Total (81)	LAD (37)	LCX (13)	RCA (31)	P value
R.O.I. length (mm)	32.8 ± 15.9	27.9±14.4	31.1±13.6	39.4±16.6	0.009

Table 2b: Intravascular Ultrasound Parameters in the Region of Interest

EEM area (mm^2)	16.9 ± 4.6	15.6±4.4	17.0±5.1	18.4±4.4	0.04
Lumen area (mm^2)	9.9 ± 3.7	8.5±2.6	10.3±3.5	11.6±4.3	0.002
(EEM-Lumen) area (mm^2)	6.9 ± 2.7	7.1±2.8	6.6±3.0	6.8±2.4	0.86
'Plaque' present*	61 (75%)	32 (86%)	8 (62%)	21 (68%)	0.09
Plaques/ROI	1.4±1.1	1.5±1.0	1.2±1.2	1.4±1.3	0.82
Plaques/ROI (range)	0-5	0-5	0-3	0-5	

*'Plaque' is defined as an (EEM_{area} - $Lumen_{area}$)/ EEM_{area}, expressed as a percentage, > 50%

LAD: left anterior descending, LCX: left circumflex, RCA: right coronary artery

Table 2b: Intravascular Ultrasound Parameters in the Region of Interest

Number of Plaques	Total (113)	LAD (54)	LCX (16)	RCA (43)	P Value
EEM area (mm^2)	15.9 ± 4.5	15.3±4.2	17.1±6.6	16.2±4.0	0.32
Lumen area (mm^2)	7.0 ± 2.2	6.6±2.1	7.5±3.1	7.3±2.0	0.16
(EEM-Lumen) area (mm^2)	8.9 ± 2.6	8.7±2.5	9.5±3.6	8.9±2.2	0.52
(EEM_{area}-$Lumen_{area}$)/ EEM_{area} (%)	56.2 ± 4.5	56.9±5.2	56.1±2.8	55.2±3.9	0.18
Mean Length 'plaque'* (mm)	6.9± 6.2	6.3 ±6.1	7.0±5.1	7.7±6.7	0.53

*'Plaque' is defined as an (EEM_{area} - $Lumen_{area}$)/ EEM_{area}, expressed as a percentage, > 50%

LAD: left anterior descending, LCX: left circumflex, RCA: right coronary artery

Table 2c: Intravascular Ultrasound Parameters: Plaque-based analysis

Artery	Total	LAD	LCX	RCA	P Value
	n = 80	n = 36	n = 13	n = 31	

Table 3a: Results of Echogenicity For the Entire Region of Interest

% Hypo-echogenic Volume	91.1 ± 4.4	89.9 ± 4.4	90.3 ± 5.2	92.8 ± 3.5	0.001
Calcium present	47 (58%)	22 (61%)	7 (54%)	18 (58%)	0.90

Table 3a: Results of Echogenicity For the Entire Region of Interest

	Total	LAD	LCX	RCA	P Value
	N = 60	n = 31	n = 8	n = 21	
% Hypoechogenic Volume	89.5 ± 5.6	89.1± 5.4	87.6 ± 7.3	90.7 ± 5.1	0.12
Calcium present	41 (68%)	20 (65%)	5 (63%)	16 (76%)	0.56

Table 3b: Results of Echogenicity For Intravascular Ultrasound Slices With Significant Plaque

Artery	Total	LAD	LCX	RCA	P Value
	n = 68	n = 30	n = 11	n = 27	
Any ROC III/IV spot	53 (78%)	23 (77%)	8 (73%)	22 (81%)	0.45
Number (range)	4.0 ± 4.1 (0-16)	3.6 ± 3.9 (0-16)	3.1 ± 3.2 (0-9)	4.9 ± 4.6 (0-15)	0.33
Number/10mm ROI	1.4 ± 1.5	1.5 ± 1.6	1.5 ± 1.7	1.4 ± 1.4	0.92

ROC: Rotterdam Classification, ROI: Region of Interest

Table 3c: Results for Palpography For the Entire Region of Interest

		Significant Plaque on IVUS*	
		No	Yes
MSCT	No Plaque	211	86
	Plaque	77	189

* Mean Percent Plaque Area ≥ 50% or Calcium Present

Sensitivity: 69%; Specificity: 73%

Table 4a: Performance of Multi Slice Computed Tomography in 3 mm Subsegments of the Region of Interest versus IVUS for the Detection of Plaque.

		Significant Plaque on IVUS*	
		No	Yes
MSCT	No Plaque	119	46
	Plaque	42	126

* Mean Percent Plaque Area ≥ 50% or Calcium Present

Sensitivity: 73%; Specificity: 74%

Table 4b: Performance of Multi Slice Computed Tomography in 5 mm Subsegments of the Region of Interest versus IVUS for the Detection of Plaque.

	QCA	IVUS	Echo genicity	Palpo graphy

Table 5: Overview of the relation of log transformed values of systemic biomarkers to conventional and novel imaging parameters

	Mean per cent diameter stenosis	Mean per cent area obstruction	Percent Hypo-echogenic plaque	Number of ROC III/IV spots per 10 mm ROI
Hs-CRP	-0.18	-0.17	0.33**	-0.06
IL-6	0.04	0.01	0.27***	0.10
Lp-PLA_2	0.01	-0.30*	0.16	0.21
NT ProBNP	0.03	-0.15	0.18	-0.07
TNF-α.	-0.04	0.03	-0.06	0.00

*P=0.008, **P=0.003, ***P=0.016

Table 5: Overview of the relation of log transformed values of systemic biomarkers to conventional and novel imaging parameters

Chapter 11

Follow Up Results of The Integrated Biomarker and Imaging Study (IBIS)

Based on:

Carlos AG Van Mieghem, Johannes A Schaar, Eugène P McFadden, Pim J de Feyter, Nico Bruining, Nico R Mollet, Filippo Cademartiri, Dick Goedhart, Sebastiaan de Winter, Gaston Rodriguez Granillo, Marco Valgimigli, Frits Mastik, Anton F van der Steen, Willem J van der Giessen, Georgios Sianos, Bianca Backx, Marie-Angèle M. Morel, Gerrit-Anne van Es, June Kaplow, Andrew Zalewski, Patrick W. Serruys
Non-invasive Detection of Subclinical Coronary Atherosclerosis Coupled With Assessment, Using Novel Invasive Imaging Modalities, of Changes in Plaque Characteristics Over Time: The IBIS Study (Integrated Biomarker and Imaging Study)
submitted

Atherosclerosis is a systemic disease whose clinical sequelae are unpredictable and only weakly correlated with its extent or severity. Furthermore, sudden death or acute coronary syndromes are frequently the first manifestation of previously subclinical atherosclerosis and the majority of such events occur as a result of plaque rupture at sites with noncritical luminal narrowing (Ambrose 1988). Pathologic studies have correlated specific coronary plaque characteristics with fatal ischemic events, but conventional imaging techniques such as quantitative angiography and quantitative intravascular ultrasound (IVUS) cannot reliably identify high-risk, rupture-prone, plaques prospectively (Virmani 2000). Thus, the development of novel invasive coronary imaging modalities, to detect structural and compositional plaque characteristics that might predict future plaque behavior, has attracted attention from the medical community (Cassells 2003) (Madjid 2004). In parallel with the advances in novel invasive imaging, non-invasive multislice computed tomographic angiography (MSCTA) has matured to the extent that it can reliably identify flow-limiting coronary lesions in relatively unselected patients.

Based on conflicting interpretations of current knowledge, there are two opposing schools of thought with respect to the potential of targeted local intervention to improve prognosis in the vulnerable plaque/patient (Wang 2004) (Buffon 2002). Novel imaging could provide information both on the incidence of vulnerable plaque (Schaar 2004) characteristics and on their evolution over time that would help clarify this debate.

The aim of this study was fourfold. First, to determine the potential of MSCTA in the detection of subclinical, non-flow limiting coronary atherosclerosis; second to assess, with two novel IVUS-based imaging modalities (palpography and IVUS echogenicity tissue characterization) the prevalence of high risk features in such plaque

at baseline; third, to assess the potential of both techniques to detect temporal changes in high risk characteristics. Finally, we attempted to relate changes in imaging parameters to changes in systemic biomarker levels.

METHODS

Study Design and Patient Selection

This was a prospective, observational, and single center, pilot study involving patients with stable angina, unstable angina, or ST segment elevation myocardial infarction (STEMI) who were referred for PCI of one or more lesions in the native coronary circulation. The study design has been described in detail elsewhere (Van Mieghem 2005). The Medical Ethics Committee of the Erasmus-MC Rotterdam approved the study protocol and all patients provided written informed consent. The study vessel, preferentially a coronary vessel not targeted for PCI, was, in order of preference, the left anterior descending, right, and circumflex coronary artery. At the discretion of the operator, a second artery could be studied. The region of interest was defined on the MSCTA, using landmarks, such as branches or the vessel origin. At six months the patient underwent the same invasive imaging procedures (angiography, intravascular ultrasound, palpography and echogenicity) as at baseline. Patients who had angiography less than three months after inclusion were asked to undergo invasive imaging again at six months.

Quantitative Coronary Angiography and Intravascular Ultrasonography

Coronary angiograms were obtained in multiple views after the intracoronary injection of nitrates. Quantitative analyses were performed by a core laboratory (Cardialysis, Rotterdam, The Netherlands) with the use of edge-detection techniques (Cass II.). Mean and minimum luminal diameters and diameter stenosis were measured in at least two, preferentially orthogonal, projections, and averaged.

IVUS was performed with commercially available catheters (30 MHz, Ultracross^{TM},or 40 MHz, Atlantis^{TM} SR Pro, Boston Scientific, Santa Clara, CA) using standard procedures (Van Mieghem 2005) with an automated pullback device (0.5 mm/s). Data were stored on videotape, transformed into the Digital Imaging and Communication in Medicine (DICOM) image standard, and archived.

Quantitative analysis was performed by the core laboratory using validated software (Curad, version 3.1, Wijk bij Duurstede, The Netherlands) and retrospective image-based gating (de Winter 2004). The borders of the external elastic membrane and of the lumen were traced. The area they enclosed was defined as the coronary plaque plus media area (subsequently referred to as plaque area). Significant plaque was defined as a plaque that occupied 50% or more of the cross-sectional vessel area circumscribed by the external elastic membrane (EEM area obstruction). Other IVUS analyses included lumen area, vessel area and plaque volume over the entire region of interest. The inter observer variability was determined for a subset of patients in this study. Inter observer variability for IVUS was assessed by re-analyzing the baseline and follow-up IVUS recordings of 16 patients by a different core lab analyst. The 16 patients (32 recordings) were randomly selected among recordings that fulfilled the following 2 criteria: (1) region of interest >30 mm long, and (2) both pullbacks were performed with the same type of IVUS catheter (30 MHz catheter, as all follow-up examinations were performed with 30 MHz).

Novel IVUS-based Plaque Imaging: Echogenicity

We used a computer-aided, gray-scale value analysis program for plaque characterization (de Winter 2003). Based on the mean gray level (brightness) of the adventitia, plaque was classified as brighter (hyperechogenic) or less bright (hypoechogenic) than the adventitia. Calcified plaque was defined as plaque brighter than the adventitia with associated acoustic shadowing. The variables measured in the previously defined region of interest included hypoechogenic plaque volume and hyperechogenic plaque volume (mm^3), and relative plaque echogenicity, calculated as (hypoechogenic plaque volume/ sum of hypoechogenic and hyperechogenic plaque volume) x 100.

Novel IVUS-based Plaque Imaging: Palpography

Palpography data were acquired during an intravascular ultrasonography pullback (1 mm/s) with a commercially available catheter (20MHz Jovus Avanar, Volcano, Rancho Cordova, CA). Using previously described and validated methodology, plaque strain values were assigned a ROtterdam Classification (ROC) score ranging from 1 to 4 (ROC I: 0-0.6%; ROC II: 0.6-<0.9%; ROC III:0.9-<1.2%; ROC IV: >1.2%).9-12 The vulnerability of a vessel was described by the Schaar-Mastik-van der Steen- (SMS)-Index. It was calculated as the total number of ROC III and IV scores that were

counted in all cross sections that were acquired at 1 mm intervals in the full ROI. This number was divided by the length of the ROI and multiplied by 10 to normalize to the pullback length. This SMS-Index describes the longitudinal extent of highly deformable plaques and is taken as a measure for vulnerability e.g. in a specific coronary artery.

Multislice Spiral Computed Tomography

All scans were performed on a 16-row detector scanner (Sensation 16, Straton, Siemens, Forchheim, Germany). The scan protocol and image reconstruction parameters were recently published (Mollet 2004). Technical advances allowed us to adapt tube output to patient weight. The dataset with least motion artifacts was loaded on an off-line workstation (Leonardo, Siemens, Forchheim, Germany) and the region of interest identified on multiplanar reconstructions, based on anatomic landmarks. Data sets were loaded on a semi-automated vessel-tracking software program and a central lumen line created throughout the region of interest. Ten through 30 cross-sections were reconstructed orthogonal to the center of the lumen and analyzed independently by two observers. Disagreements were resolved by consensus. Plaque was defined as an abnormal mass within the artery wall, clearly distinguishable from epicardial fat and the coronary lumen. Based on manually measured maximal thickness, plaques were classified as small (<1 mm), medium (1-2 mm), or large (>2 mm). Calcification was defined by the presence of high-density components (>130 Hounsfield Unit).

Lipoprotein levels and Biomarkers

Plasma concentrations of total cholesterol and high-density lipoprotein cholesterol (HDL-C), and triglycerides were measured in the local laboratory. The Friedewald formula was used to derive low-density lipoprotein cholesterol (LDL-C) levels. Blood samples for additional biomarker analysis were stored at –70°C. Serum C-reactive protein (Diagnostic Systems Laboratories), plasma interleukin 6 and tumor necrosis factor-α (R&D Systems), were measured in the Human Biomarker Center (GlaxoSmithKline, PA, USA) based on protocols provided by the manufacturer. Lipoprotein associated phospholipase A_2 (Lp-PLA_2) activity assay was measured by the proportional release of aqueous 3H acetate resulting from the enzymatic cleavage of the ^{3}H acetyl-platelet activating factor substrate (100 μM). N-terminal pro brain natriuretic peptide was measured with use of a two site electro-chemiluminescent assay. The limits of quantification were 0.0048 mg/L for C-reactive

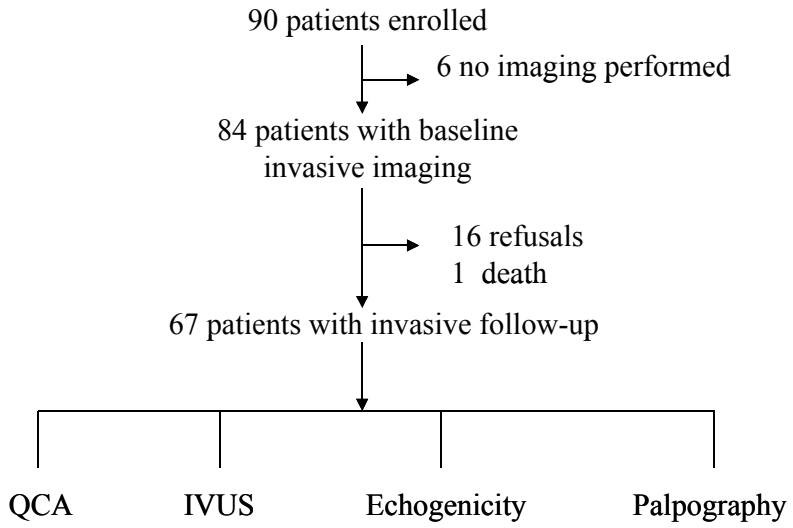

Fig 1: Flow Chart detailing the imaging procedures at the different time points.

protein, 0.057 pg/mL for interleukin-6, 3.92 nmol/min/mL for Lp-PLA_2 activity, 10 pg/ml for N-terminal pro brain natriuretic peptide, and 0.88 pg/mL for tumor necrosis factor-α.

Definition of Events and Follow-Up for Major Adverse Cardiac Events

The occurrence of Major Adverse Cardiovascular Events (MACE) was assessed after the procedure, at discharge, and at 3 and 6 months, as were the individual components: death, MI, revascularization by PCI or CABG, hospitalization for ischaemia and/or anginal symptoms, and stroke. The diagnosis of myocardial infarction was consistent with the ACC/ESC definition (Alpert 2000). Major bleeding and vascular complications were also prospectively recorded using standard definitions.

	QCA	IVUS	ECHOGENICITY	PALPOGRAPHY
Baseline	67 (74)	63 (69)	63 (67)	53 (58)
Follow up	67 (74)	62 (64)	55 (60)	57 (60)
Matched results	67 (74)	58 (63)	55 (60)	49 (52)

Values in de Table are number of patients (number of vessels)

Statistical Analysis

Discrete variables are presented as counts and percentages. Continuous variables are presented as means ± SD, unless otherwise indicated. Comparisons between quantitative outcomes were performed with use of scatterplots and linear regression analysis (regression coefficient). Where appropriate, biomarker analyses were performed after natural logarithmic transformation. Correlations between imaging end points and circulating biomarkers were assessed, and univariate Pearson correlation coefficients were calculated. Comparisons among patient subgroups, grouped by clinical presentation, with findings on palpography and on echogenicity, were performed at both vessel and patient level. In the latter case, the imaging findings from two regions of interest in the same patient were averaged. Differences in means among groups were analyzed by a two-sample t-test or by one-way analysis of variance. A P value of less than 0.05 (two-sided) was considered to indicate statistical significance. No formal hypotheses were tested in this exploratory study, therefore p-values are given as such, without any correction for multiplicity of testing. Statistical analyses were performed with use of SAS Version 8

RESULTS

Patient population

A flow diagram detailing the number of patients undergoing multimodality coronary imaging is presented in Figure 1. Sixty-seven patients underwent serial invasive imaging of non-culprit segments of coronary artery at baseline and 196±19 days later. Not all patients (n = 67) had all imaging modalities available for comparison. Nine patients had one or both IVUS recordings that were not further analyzable due to artifact or use of an incorrect scale. An additional 3 patients could not be analyzed for IVUS echogenicity due to extensive calcification overshadowing a large part of the adventitia which is used as a reference for the interpretation of gray-scale values of surrounding tissue. Reasons for inaccurate palpogram readings (n=18) were related to extensive catheter motion during data acquisition.

Baseline characteristics of patients who completed the study are shown in Table 1. They were comparable to those of the entire cohort of 84 patients enrolled at baseline (not shown). Medical therapy during 6 months of follow-up included antiplatelet therapy (aspirin 91%, clopidogrel 94%), statins (99%), ACE-inhibitors or

angiotensin-2 receptor antagonists (51%) and beta-blockers (24%). Mean total cholesterol, LDL cholesterol, HDL cholesterol and triglyceride values for patients who completed the study are presented in Table 2. There were no significant differences in total and LDL cholesterol parameters in the overall patient population; however, patients who presented with STEMI had a significant decrease in mean LDL cholesterol.

Non-invasive Angiography versus Intravascular Ultrasonography at Baseline

Non-invasive angiography and intravascular ultrasonography were compared, at baseline, in 61 patients (67 vessels). The sensitivity and specificity of non-invasive angiography to detect significant plaque identified on intravascular ultrasonography (> 50% EEM area obstruction or the presence of calcification on two consecutive slices) was calculated for the entire ROI and for 5mm sub-segments (Table 3). The sensitivity, specificity, positive and negative predictive values of non-invasive angiography for detection of any significant plaque was 86, 69, 90, and 61% respectively. These values were similar for the sub-segmental analysis. The sensitivity of non-invasive angiography to detect plaque was 60% (30/50) for small (<1mm), 76% (80/105) for medium (1 to 2 mm), and 79% (26/33) for large (>2 mm) plaques.

Reproducibility of IVUS Measurements

Inter observer variability results for IVUS (n= 31 pullbacks) showed no systematic error, and good reproducibility. Mean differences in area (mm^2) measurements were: –0.04±0.56 for EEM, 0.02±0.50 for lumen, and –0.06±0.59 for plaque. Mean difference in plaque volume (mm^3) was –2.43±22.

Conventional Imaging: Quantitative Coronary Angiography and IVUS Imaging

There were no statistically significant changes, from baseline to follow-up, in the angiographic variables measured in the region of interest (Table 3). Likewise, IVUS-derived measurements (Table 4) remained unchanged in matched segments, except for a small decrease in vessel area (p=0.04). When patients were grouped according to initial diagnosis (i.e., STEMI, unstable angina, stable angina), there were no significant changes in either angiographic or IVUS measurements between baseline and follow-up (data not shown).

Novel IVUS-based Imaging

Temporal changes in plaque characteristics based on IVUS-based palpography and echogenicity are shown in Tables 4 and 5. At baseline, the predominant plaque component was hypoechogenic tissue

(91.6% of plaque volume). There was no significant change between baseline and follow-up in the absolute volume of hypoechogenic or hyperechogenic plaque. On palpography recordings, the SMS-index decreased significantly between baseline and follow-up. This decrease, in the overall population, was largely driven by changes in the subgroup of patients with STEMI; this group had both the highest SMS-index at baseline and the most marked relative decrease during follow-up, compared to patients with other clinical presentations. At the 6 month follow-up, the SMS-index was comparable among clinical subgroups.

Biomarkers and Imaging Techniques

Table 6 shows values for the biomarkers measured at baseline and after 6 months. Not surprisingly, several inflammatory mediators (CRP, IL-6, Lp-PLA_2) and a marker of hemodynamic stress (NT-proBNP) decreased over time, particularly in patients presenting with acute coronary syndromes. With palpography there were no significant correlations noted between circulating biomarkers and imaging parameters. Among lipid parameters (total cholesterol, LDL-C, HDL-C, and triglycerides), a correlation with the change in IVUS-derived plaque area was only noted for the change in HDL-C (Pearson correlation coefficient 0.37, $P<0.05$, data not shown).

Adverse Events

There were no deaths during the study and no complications attributable to invasive imaging of the non-culprit study vessel.

DISCUSSION

The major findings of the study were fourfold. First, using IVUS as a gold standard, noninvasive MCST angiography can identify atherosclerotic plaque, in vessels with only minimal angiographic disease, with high sensitivity and moderate specificity. Second, further investigation of such plaque with novel IVUS-based imaging techniques (palpography and echogenicity) showed that features potentially indicative of vulnerable plaques are both widespread and highly prevalent. Third, while conventional imaging using quantitative coronary angiography and IVUS demonstrates no significant changes in either lumen or plaque dimensions, the biomechanical properties of the plaques, assessed by palpography, showed significant changes over a relatively short (six-month) follow-up pe-

riod. Finally, biomarker levels showed no biologically significant correlations with baseline values or temporal changes in novel imaging parameters.

Despite considerable therapeutic advances, patients with documented coronary atherosclerosis have a significant risk of future ischemic events. Neither IVUS nor angiographic variables have proved useful to predict the site of such future clinical events. Furthermore, many adverse cardiac events, such as death or acute MI, occur as the first presentation of coronary disease due to vessel occlusion at sites with noncritical atherosclerotic narrowing. In this context, the potential of novel imaging techniques to identify high-risk plaque and potentially guide management strategies has stimulated innovative research.

Subclinical Atherosclerosis: Role of Noninvasive Imaging

The development of noninvasive angiography, with MSCT, has reached a stage where it can be used, in selected patients, to reliably identify significant epicardial coronary atherosclerosis (Nieman 2002). Recent studies have shown its potential for detecting non-obstructive coronary plaques in highly selected patients (Achenbach 2004) (Schoenhagen 2003). Our results extend these findings by showing that non-obstructive coronary plaque can be detected, in an arbitrarily selected region of interest, with moderately high sensitivity and specificity in a broader patient population and show that the size of such plaques can be assessed noninvasively. However, when examined in more detail, with novel invasive techniques, we found that vulnerable features were very common. This observation provides additional arguments to support recommendations discouraging the indiscriminate use of non-invasive coronary imaging to detect subclinical atherosclerosis at the present time (O'Rourke 2000).

Subclinical Atherosclerosis: Insights from Novel Invasive Techniques

Pathologic studies suggest that rupture of thin-capped fibroatheromas is a common substrate for clinical events (Virmani 2000). We have previously validated the potential of palpography to identify thin-capped fibroatheromas *in vitro* (de Korte 2002a+b) (Schaar 2003). Subsequently, we showed that the number of high-strain spots in culprit epicardial vessels was correlated with clinical presentation (Schaar 2004a).The present study extends these findings by demonstrating that, within arbitrarily selected segments of non-culprit vessels, structurally vulnerable plaques were quite common,

despite only mild angiographic disease. The most marked changes occurred in patients with an acute MI, most of whom were statin-naive at the time of the initial presentation (86%). Although acute MI patients had an extend of high strain spots at baseline, 6 months later all subgroups were comparable regardless of the initial presentation. The implication of our finding that abnormal strain patterns persist over time is unclear. Clarification of this question will require larger studies with longer follow-up. It might be speculated that it reflects the inadequacy of standard medical care. This hypothesis would be consistent with recent data that indicate the need for intensive intervention for LDL cholesterol (<70 mg/dL) and inflammation (CRP <2mg/L) to achieve the best clinical outcomes in the course of therapy with statins in post ACS patients (Nissen 2005) (Ridker 2002).

Prior studies suggested that echogenicity is related to the histological components of carotid and coronary plaques, and that carotid plaque echolucency (low echogenicity) is associated with neurological events, both spontaneous and related to percutaneous carotid stent placement (El-Barghouty 1996) (Gronholdt 1998)(Rasheed 1995)(Polak 1998)(Gronholt 2001)(Mathiesen 2001). For carotid studies, a highly reproducible quantitative computer-assisted index of echogenicity, based on gray-scale values of blood and adventitia, has gained widespread acceptance (Seabatai 2000). While carotid plaque echogenicity can be assessed non-invasively, assessment of coronary plaque echogenicity requires invasive techniques and has been restricted to research settings. A recent study systematically studied, for the first time, coronary plaque echogenicity in a protocol with mandated intravascular ultrasonography follow-up and showed that treatment with atorvastatin resulted in quantifiable changes in coronary plaque echogenicity, compatible with changes in plaque composition (Schartl 2001). In the present study, we used a quantitative computer-assisted index of echogenicity, based on gray-scale values of adventitia and demonstrated that hypoechogenic tissue was the predominant plaque component (de Winter 2003). We found no significant change in absolute hypoechogenic or hyperechogenic plaque volume over the average 6-month period. At first sight, our findings contradict the observations of Schartl et al., who found a small but significant increase in the hyperechogenic plaque component (Schartl 2001). However, their study had a longer follow-up period and patients had intensive, carefully-mon-

itored, statin therapy. Another recent study from our institution convincingly demonstrated changes in plaque echogenicity over a much longer (4 year) follow-up period (Aoki 2005). In any case, the high preponderance of hypoechogenic plaque (>90% of the plaque volume) coupled with the lack of significant change during follow-up suggests that plaque echogenicity lacks the discrimination necessary either for robust risk stratification or for use as a surrogate indicator of changes in plaque composition on serial studies.

Limitations

Our patient population was intentionally heterogeneous and the study was underpowered to correlate compositional imaging end points with clinical outcomes. Follow-up was incomplete (67/84, 80%), but compares favourably with recent serial IVUS studies.[31,32] Moreover, baseline characteristics of the 67 patients with completed follow-up were the same as in the overall study population. The present study did not demonstrate changes in plaque size. Recently published studies carried out in patients with acute coronary syndrome or in patients with more aggressive lipid-lowering therapy demonstrated clear regression of coronary atherosclerosis (Okazaki 2004)(Nissen 2003)(Jensen 2004). Another potential limitation was the rather modest intensity of therapy with statins, reflecting clinical practice settings. Data from recent trials, such as REVERSAL and PROVE-IT, indicate that intensive treatment with statins affects plaque size and event rates, respectively (Nissen 2004)(Cannon 2004). Whether more intensive statin therapy applied to the IBIS cohort would further reduce the observed compositional changes remains to be determined.

Conclusions

This study confirms the potential of current MSCT technology to noninvasively detect large coronary plaques within coronary segments without significant lumen impairment. In contrast to conventional imaging modalities that frequently reveal static luminal and plaque dimensions, novel IVUS-based plaque palpography can detect significant alterations in coronary plaque characteristics over a relatively short time interval. This study highlights the dynamic changes in the strain of coronary plaques that are remote from the culprit lesions in patients with myocardial infarction. Whether the persistence of a high-strain pattern is a harbinger of cardiovascular events remains to be determined in future much larger studies. The novel imaging modalities utilized in this study provide insights into plaque biology, whereas temporal changes detected using these mo-

dalities may eventually serve as intermediate end points in interventional trials.

Demographics and Clinical History	Patients (N=67)
Male sex - no. (%)	57 (85%)
Age - yr. (SD)	58 ± 11
Previous myocardial infarction - no. (%)	27 (40%)
Previous coronary bypass surgery - no. (%)	1 (1%)
Previous percutaneous coronary intervention - no. (%)	11 (16%)
History of diabetes - no. (%)	6 (9%)
History of stroke - no. (%)	1 (1%)
Family history of coronary disease - no. (%)	36 (54%)
Hypertension* - no. (%)	29 (43%)
Hypercholesterolemia† - no. (%)	57 (85%)
Previous smoker - no. (%)	23 (34%)
Current smoker - no. (%)	26 (39%)
Statin therapy at baseline – no. (%)	50 (75%)
Clinical Status at Enrolment	
Stable angina - no. (%)	32 (48%)
Unstable angina - no. (%)	21 (31%)
ST-segment elevation myocardial infarction - no. (%)	14 (21%)
Extent of Disease‡	
Non significant disease– no. (%)	4 (6%)
Single-vessel disease – no. (%)	36 (53.7%)
Two-vessel disease – no. (%)	21 (31.3%)
Three-vessel disease – no. (%)	3 (4.5%)
Left main stem (plus two-vessel) disease – no. (%)	3 (4.5%)

*Blood pressure > 160/95 mmHg or treatment for hypertension, † total cholesterol >215 mg/dl or treatment for hypercholesterolemia, ‡ Significant disease was defined as >50% (visual estimate) stenosis in a major epicardial vessel or in branches > 2.5 mm diameter

Table 1: Baseline Characteristics of Patients With Invasive Follow Up Evaluation

	Total Cholesterol	LDL	HDL	Triglycerides
Entire cohort (n=64)	(n)	(n)	(n)	(n)
Baseline	4.58±1.24 (64)	2.93±1.16 (64)	1.03±0.36 (64)	1.62±0.95 (64)
Follow-up	4.43±0.82 (50)	2.71±0.77 (49)	1.14±0.37 (49)	1.87±0.93 (49)
Change	-0.15±1.32 (50)	-0.27±1.15 (49)	0.11±0.23 (49)	0.24±0.90 (49)
P value	NS	NS	0.001	0.008
STEMI				
Baseline	5.44±0.97 (13)	3.76±0.85 (13)	1.13±0.31 (13)	1.62±0.78 (13)
Follow-up	4.32±0.90 (12)	2.66±0.80 (11)	1.03±0.27 (11)	1.84±0.76 (11)
Change	-1.06±1.02 (12)	-0.93±1.06 (11)	-0.09±0.16 (11)	0.31±0.66 (11)
P value	0.003	0.006	NS	NS
Unstable angina				
Baseline (n=21)	4.33±1.17	2.79±0.94	0.95±0.30	1.63±0.91
Follow-up (n=15)	4.40±0.69	2.60±0.65	1.22±0.41	1.73±0.98
Change (n=15)	0.19±1.40	-0.12±1.03	0.25±0.17	0.07±0.91
P value	NS	NS	<0.001	NS
Stable angina				
Baseline (n=30)	4.38±1.27	2.66±1.27	1.04±0.41	1.61±1.06
Follow-up (n=23)	4.51±0.89	2.80±0.84	1.14±0.40	1.99±0.99
Change (n=23)	0.09±1.24	-0.06±1.20	0.12±0.24	0.32±1.01
P value	NS	NS	0.026	0.014

Table 2: Changes in lipid parameters

		Significant Plaque on Intravascular Ultrasonograph	
		No	Yes
MSCT Plaque	Yes	11 (140)	7 (49)
	No	5 (52)	44 (136)

The values in parentheses are those for 5mm subsegments. Sensitivity: 86% (74%); specificity: 69% (73%), positive predictive value 90% (72%), negative predictive value 61% (74%).

* Significant plaque was defined as mean plaque area obstruction (Vessel area - Lumen area/ Vessel area) x 100 > 50% or the presence of calcium on intravascular ultrasound

Table 3a: Multislice computed tomography for the detection of significant coronary plaque: Comparison with intravascular ultrasonography for the entire region of interest and for its 5 mm subsegments

	Length (mm)	Mean Diameter (mm)	Minimal Diameter (mm)	Diameter Stenosis (%)
Baseline	27.2±13.1	2.78±0.64	2.31±0.64	25±11
Follow-up	27.2±13.1	2.84±0.76	2.38±0.71	25±11
Change	0.0±2.5	0.06±0.36	0.06±0.36	0.0±8
P value	NS	NS	NS	NS

Table 3b: Quantitative Angiographic Parameters (n=67)

Variable	Length	Vessel Area *	Lumen Area	Plaque Area †	Hypo Volume	Hyper Volume	Plaque Volume
Units	mm	mm^2	mm^2	mm^2	mm^3	mm^3	mm^3
Baseline	29.3±14.4	16.9±4.8	10.0±3.75	6.9±2.7	171±104	15±11	195±117
Follow-up	29.2±14.2	16.5±4.6	9.7±3.52	6.8 ±2.6	177±98	12±14	190±107
Change	-0.1±1.62	-0.4±1.7	-0.3±1.57	-0.1±1.1	6±53	-3±13	-5.2±33
P value	NS	0.04	NS	NS	NS	NS	NS

* Vessel area denotes the area circumscribed by the external elastic membrane; † Plaque area denotes Vesselarea-Lumen area including echolucent media.

Table 4. Quantitative Intravascular Ultrasonography (n=58) and Echogenicity (n=55) Parameters

	Baseline	Follow Up	p-value
STEMI (n=12)	2.30 ± 1.80	1.15 ± 1.37	0.0003
Unstable (n=16)	1.78 ± 1.78	1.41 ± 1.69	0.29
Stable (n=24)	1.21 ± 1.06	1.17 ± 1.14	0.56
p-value	0.02	0.91	

Table 5: Plaque Characterization Palpography for the Entire Population Classified by Clinical Presentation (n=52) using the SMS index given as mean ± SD

Entire cohort (n=65)	CRP	IL-6	Lp-PLA$_2$	TNF-a	proBNP
Baseline	13.22 (20.63)	10.34 (30.22)	116.26 (28.74)	2.16 (0.72)	394 (728)
Follow-up	5.81 (7.41)	5.55 (16.41)	83.82 (26.78)	3.49 (4.72)	158 (183)
Change	-7.58 (20.08)	-4.92 (18.26)	-32.51 (28.37)	1.29 (4.85)	-236 (719)
P value	0.0014	0.0001	<0.0001	0.16	0.0022
STEMI (n=14)					
Baseline	12.59 (9.37)	12.70 (22.73)	132.57 (21.24)	2.25 (0.85)	842 (1360)
Follow-up	5 (3.68)	2.89 (2.27)	89.36 (19.54)	3.75 (8.04)	204 (173)
Change	-7.59 (7.73)	-9.82 (23.04)	-43.20 (26.87)	1.51 (8.29)	-624 (1343)
P value	0.0040	0.0017	<0.0001	0.64	0.36
Unstable angina (n=20)					
Baseline	24.69 (31.64)	5.73 (4.89)	114.20 (29.97)	2.22 (0.73)	369 (347)
Follow-up	5.47 (5.55)	2.77 (2.72)	84.25 (30.50)	2.37 (1.51)	114 (103)
Change	-19.21 (31.22)	-2.96 (5.39)	-29.95 (30.72)	0.14 (1.38)	-262 (384)
P value	0.0038	0.0062	0.0003	0.65	0.0009
Stable angina (n=31)					
Baseline	6.12 ((9.80)	12.25 (41.09)	110.22 (28.86)	2.09 (0.67)	217 (369)
Follow-up	6.42 (9.61)	8.65 (23.64)	80.94 (27.45)	4.23 (3.96)	164 (223)
Change	0.17 (7.45)	-3.94 (21.27)	-29.23 (27.12)	2.06 (4.08)	-47 (329)
P value	0.91	0.59	<0.0001	0.0085	0.58

CRP: C-reactive protein, IL-6: interleukin 6, Lp-PLA2; lipoprotein-associated phospholipase A2, NT-proBNP: N-terminal pro brain natriuretic peptide, TNF-a: tumor necrosis factor alpha. With the exception of LpPLA2 all p-values were calculated on the log-transformed values. The number in between brackets is the standard deviation.

Table 6: Biomarker results

Chapter 12

Palpography in The Integrated Biomarker and Imaging Study (IBIS)

Based on:

Johannes A Schaar, Frits Mastik, Eugène P McFadden, Dick Goedhart, Pim J de Feyter, Andrew Zalewski, Anton FW van der Steen, Patrick W Serruys

Three -Dimensional Intravascular Palpography: Results of the Integrated Biomarker and Imaging Study

submitted

The most common post-mortem histological features in plaques, which caused myocardial infarction, are the presence of a thin fibrous cap, a lipid-rich core, and inflammatory cells. These plaques are called thin cap fibroatheromas (TCFA) (Virmani 2000)(Schaar 2004b). These TCFA's have certain mechanical properties, which can be measured by three-dimensional intravascular palpography (Schaar 2005).

Palpography assesses the local mechanical properties of tissue using its deformation caused by the intraluminal pressure (Doyley 2001). The technique was validated in vitro using diseased human coronary and femoral arteries (de Korte 2000). Especially between fibrous and fatty tissue, a highly significant difference in strain was found (de Korte 2000a). Additionally, the predictive value to identify the vulnerable plaque was investigated. A high strain region at the lumen vessel wall boundary has an 88% sensitivity and 89% specificity for identifying these plaques (Schaar 2003a). Patients with myocardial infarction or unstable angina have more high strain spots in their coronary arteries than patients with stable angina (Schaar 2004a).

The majority of acute coronary events arises from non-flow limiting lesions and is often the first clinical manifestation of previously subclinical atherosclerosis (Ambrose 1988). Our knowledge on the mechanism, how these plaques develop is rather limited.

The Integrated Biomarker and Imaging Study (IBIS) was designed to investigate non flow-limiting atherosclerotic lesions in patients, with diverse clinical presentations, referred for percutaneous coronary intervention (Van Mieghem 2005). These plaques were investigated at baseline and 6 month follow up. To assess plaque

characteristics of these lesions, we explored correlations between clinical presentation and Palpography results. We hypothesize that there will be no significant difference of the palpographic results between baseline and follow up since no specific intervention was done in this observational investigator driven study.

Methods

This study was a single center prospective and observational study, which was approved by the medical ethics committee of the ErasmusMC Rotterdam. All patients provided written informed consent. In brief, patients 18 years of age or older with stable angina, unstable angina, non-ST segment elevation or ST segment elevation myocardial infarction, who underwent successful percutaneous coronary intervention (PCI) of one or more lesions in the native coronary circulation, were eligible for inclusion.

Major clinical exclusion criteria were significant renal dysfunction, prior coronary intervention in the region of interest, life expectancy less than one year or factors that made follow-up difficult. Major imaging-related exclusion criteria were coronary anatomy that precluded safe intravascular ultrasonographic examination of a suitable region of interest. The coronary study vessel, preferentially a vessel not targeted for intervention, was, in order of preference, the left anterior descending, right and circumflex coronary artery. At the discretion of the operator, a second artery could be studied.

The region of interest was defined on the basis of identifiable landmarks, such as side branches or the vessel ostium. Follow up procedures were done at 6 months. All data in IBIS were acquired using a 20 MHz Jovus Avanar F/X IVUS catheter (Volcano, Rancho Cordova, CA, USA), which was connected to an InVision Gold IVUS console. Recordings were obtained at a pullback speed of 1 mm/sec using a mechanical pullback device (Trackback II, Volcano, Rancho Cordova, CA, USA). Simultaneously, the ECG and intraluminal pressure signals were recorded. Acquisition was done with a custom made dedicated workstation connected to the digital interface of the IVUS machine recording fundamental IVUS data (rf-data). Each acquisition was stored on a separate DVD. Processing and analysis of the data were done by different personnel, than those who did the recording. Analysis was done as previously

described7 and unaware of the clinical patient data and other results of the study. The reproducibility of three-dimensional palpography has been recently reported (Schaar 2003b+2005).

ROC Classification and SMS-Index

Strain values were classified according to the ROC classification (ROtterdam Classification) as low strain spots (ROC I: 0.0 - <0.6%), moderate strain spots (ROC II: 0.6 - <0.9%), medium strain spots (ROC III: 0.9 - <1.2%), or high strain spots (ROC IV: >1.2%). The vulnerability of a vessel was described by the Schaar-Mastik-van der Steen- (SMS)-Index. It was calculated as the number of ROC III and IV scores that was measured in the ROI every mm and averaged over the length of the ROI and multiplied by 10 to normalize to the pullback length in cm. This SMS-Index describes the longitudinal extent of highly deformable plaques and is taken as a measure for vulnerability e.g. in a specific coronary artery.

Matching Landmarks

At follow up analysis first the begin end the end of the region of interest were matched based on the previously described landmarks. Within the ROI, for every millimeter along the full pullback length, the matching cross section of the follow up recording was determined. This matching was done on the fundamental IVUS frames reconstructed from rf-data unaware of the palpographic results. The matching included also a correction of the rotational orientation of the follow up registration to allow an analysis not only for the entire cross section, but also for positions along the circumference of the lumen.

The likelihood ratio test with a PROC MIXED model in SAS V8.02 was used to analyse the change of ROC scores within the different clinical groups. The SMS index differences between the clinical groups at baseline and at follow up as well as the differences between baseline and follow up recordings were calculated using the f-test.

Results

In 48 patients 52 coronary arteries were studied

We studied in 48 patients 52 coronary arteries. Patients were divided into three groups on the basis of clinical presentation (stable or unstable angina, AMI). Twelve coronary arteries from patients with

STEMI, 16 from patients with unstable angina and 24 from patients with stable angina were investigated.

	Baseline	Follow Up	p-value
STEMI (n=12)	2.30 ± 1.80	1.15 ± 1.37	0.0003
Unstable (n=16)	1.78 ± 1.78	1.41 ± 1.69	0.29
Stable (n=24)	1.21 ± 1.06	1.17 ± 1.14	0.56
p-value	0.02	0.91	

Table 1: SMS index given as mean ± SD

SMS index higher n the STEMI group

Results of the SMS index at baseline and follow up are given in Table 1. The main finding is that at baseline the SMS index is significant different between the groups (p=0.02), while in follow up no difference could be observed (p=0.91). Furthermore there is a significant decrease in the SMS index in the STEMI group at follow up (p=0.0003), while this could not be seen within the other groups.

	Observations	Baseline	Follow Up	p-value
STEMI (n=12)	231	2.10 ± 1.05	1.57 ± 0.87	0.0004
Unstable (n=16)	260	1.83 ± 0.98	1.67 ± 0.95	0.24
Stable (n=24)	507	1.68 ± 0.92	1.54 ± 0.91	0.63
p-value		0.002	0.72	

Table 2: Comparison of individual ROC scores is given as mean ± SD

998 cross sections at baseline and follow up

We scored the highest ROC score at 998 cross sections at baseline and follow up. The results are given in Table 2. The main finding is that at baseline the peak ROC score is significant different between the groups (p=0.002), while in follow up no difference could be observed (p=0.72). Furthermore there is a significant decrease in peak ROC scores in the STEMI group at follow up (p=0.0004), while this effect could not be seen within the other groups. The

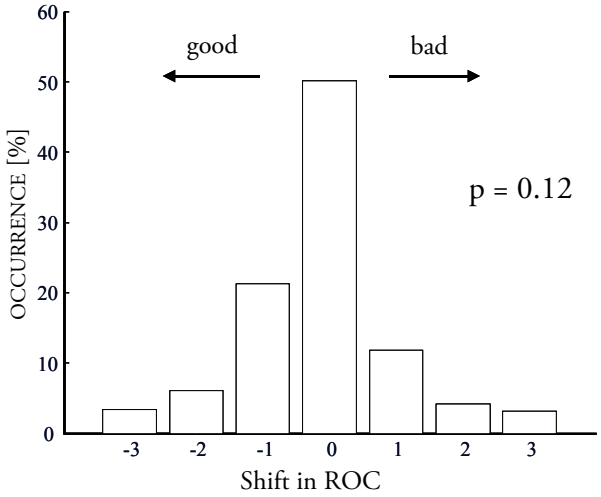

Fig 1: ROC shift of patients with stable angina in 507 observations

mean change of ROC scores in the group with stable angina was not significant (p = 0.12) with a mean of -0.14 see figure 1. The mean change of ROC scores in the group with unstable angina was not significant (p = 0.1577) with a mean of -0.1577 (see figure 2), while in patients with STEMI the shift was significant (p=0.0099) in the direction of lower ROC scores (mean = - 0.5325) (see figure 3).

Discussion

This is the first clinical follow up study using 3D palpography. This pilot study was performed blinded to assess (a) the change of the SMS-index and (b) the change of individual ROC scores, as well as (c) their relation to clinical presentation.

Follow up trials with palpography are feasible

The major findings of this study are that follow up trials with this new technique are feasible in a blinded matter and plaque deformability changes to a certain extend towards lower strain values predominantly in the group of patients with myocardial infarction.

Three-dimensional Intravascular palpography, by its capacity to evaluate the mechanical properties of the plaque, can detect thin-cap fibroatheromas. Validation studies in vitro and in vivo have shown that palpography can identify such plaques with high sensitivity and specificity and assess the number of suspected vulnerable

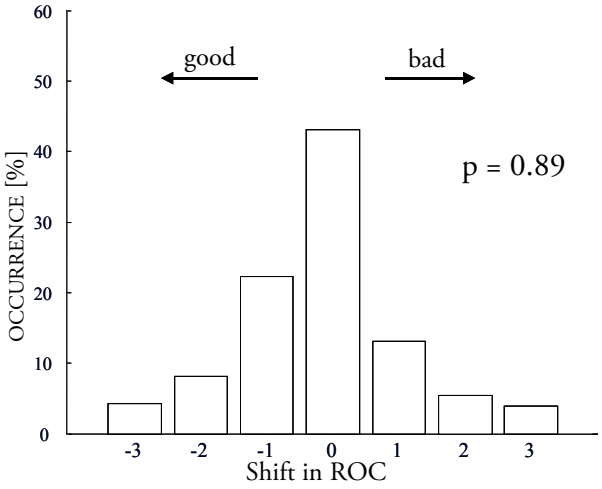

Fig 2: ROC shift of patients with unstable angina in 260 observations

plaques in the entire coronary artery or a region of interest (Schaar 2003a + 2004a).

The SMS-index: Relation to clinical presentation

At baseline the SMS index was significantly different showing a higher value for patients with myocardial infarction compared to the ones with unstable or stable angina. This supports data, which we have previously reported (Schaar 2004a), but shows in addition that there is a significant bigger extent of plaque deformability in patients with myocardial infarction that in patients with stable or unstable angina. After 6 month the index has not changed for patients with stable and unstable angina, but is significantly reduced in the group of patients with myocardial infarction. This may be due to the fact that patients in the latter group were presented at in-

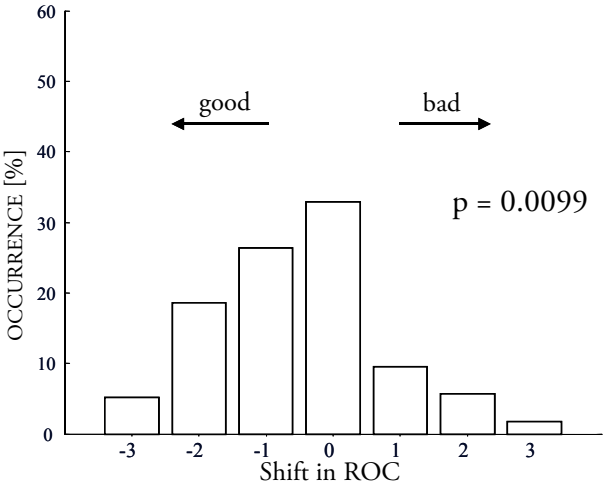

Fig 3: ROC shift of patients with STEMI in 231 observations

dex with a therapy regime, which was extensively modified after initial interventional treatment. Furthermore this data support the hypothesis that vulnerability is a pan-artery process (Buffon 2002) and current treatment regimes can reduce it, but not eliminate it taking into account that at follow up the SMS index was not significantly different between the groups.

The ROC-score: Local changes of plaque deformability

The development of a method, which enables us to compare atherosclerosis in coronary arteries per millimeter slices, gives us the opportunity to assess rather small changes of deformability in a big number of observations without suffering from longitudinal motion artifacts. We observed changes in deformability on both sides of the spectrum: Low strain areas changed into high strain areas and high strain areas into low strain areas, while in the majority of plaques no or only minor changes of deformability could be shown. This can be explained by the fact that atherosclerosis is a dynamic process dependent on a variety of mechanisms, which may influence deformability either by enhancing it like chronic inflammation or decreasing it like treatment with drugs. In the group of patients with stable and unstable angina the change in ROC scores was rather balanced, while in the group with myocardial infarction the change towards lower ROC scores was prevailed. This may be explained by treatment intensification in this particular patient group, but this study was certainly not powered to evaluate effect of certain treatment modalities and the described changes may be also the consequence of natural causes. Future studies will address this problem.

Intravascular ultrasound (IVUS) techniques have proven to give deep insight into plaque morphology (Rioufol 2004) (Nissen 2005). Since palpography is a supplementary technique, it can be expected that we will gain even deeper insight into plaque development in the future.

Limitations of the study

The analysts were aware of the fact that they are looking to follow up results. This may have induced a bias in the analysis. Nevertheless the investigators were blinded towards the clinical patient presentation and interpretation of palpographic parameters allows only limited degrees of freedom.

Conclusion

With intravascular three-dimensional palpography the extend of deformable plaques can be measured at baseline and follow up procedures. Patients with myocardial infarctions have a bigger extend of deformability than patients with unstable or stable angina. In all groups deformable plaques remain, which leaves room for improvement regarding the therapy of patients with atherosclerosis.

Part V

Future applications

Chapter 13

In Vivo Assessment of Thrombus Age Using Intravascular Palpography

Based on:

Johannes A Schaar, Frits Mastik, Elza D van Deel, Cornelis J Slager, Patrick W Serruys, Dirk J Duncker, Anton FW van der Steen
In Vivo Assessment of Thrombus Age Using Intravascular Palpography
submitted

Disruption of coronary atherosclerotic plaques is recognized as the initial trigger of coronary thrombosis and may lead to acute coronary syndrome (Davies 1996). Although the mechanisms of plaque rupture and thrombus formation in lesions have been intensively investigated (Schaar 2004b), the in vivo assessment of thrombus age in an arterial system was not performed yet. It is well known that thrombi harden by aging (Browse 1999). It can be assumed that this mechanical stabilization can be measured by using elasticity measurements and we hypothesize that quantitative strain measurement can determine thrombus age in an animal model of arterial thrombosis.

This quantitative assessment of strain of biological material is feasible with intravascular palpography, a new IVUS derived imaging technique (de Korte 2002a). Palpography assesses the local mechanical properties of tissue using its deformation caused by the intraluminal pressure (Schaar 2004a).

Materials and Methods

The present experiments were performed conform with the "Guide for Care and Use of Laboratory Animals" published by the US National Institutes of Health (NIH publication No. 85-23, revised 1996) and under the regulations of the Erasmus Medical Center Rotterdam.

Eight overnight-fasted crossbred Landrace Yorkshire pigs of either sex (46±2 kg) were sedated with ketamine (20 mg/kg i.m), and midazolam (0.5 mg/kg, i.m.), anaesthetized with sodium pentobarbital (15 mg/kg i.v.) and intubated for ventilation with O2 and N2O (1:2).

Catheters were inserted into the superior caval vein for infusion of saline and sodium pentobarbital (10-15 mg/kg·h-1) to maintain anaesthesia. Furthermore 9F sheets were placed one in the right- and one in the left carotid artery. Through these sheets two 20 MHz phased array intravascular ultrasound catheters (Avanar, Volcano Therapeutics, Rancho Cordova, CA, USA) were positioned in the right and left femoral artery and left in place over the whole length of the experiment. The sheets were also used for measuring arterial pressure and arterial blood sampling to maintain PO_2, CO_2 and pH within the physiological range.

The femoral arteries were exposed surgically. Thrombosis was induced by placement of an electrode on the outer vessel wall by applying an electrical field to generate thrombosis formation (Romson 1980) (Lanza 1996) using a controlled electrical DC current (9 mA) for 30 seconds. The site of injury was chosen by the location of the tip of the IVUS catheter. The current caused a vessel injury with the signs of endothelial erosion. Over this erosion a wall standing thrombus was formed, which left a lumen in which the blood pressure acted as the driving force to strain the thrombus. Radio-frequency (RF) ultrasound data were acquired at 30 frames per second. Data were recorded and stored at 7 time points after thrombus introduction (5, 20, 45, 75, 105, 150, 210 min.). Cross-correlation based analysis of the RF data revealed the radial strain of the lumenal layer of the thrombus as described before (Doyley 2001).

At the end of the study the animals were sacrificed by infusion of an overdoses pentobarbital.

For statistical analysis SPSS 11.0.1 (SPSS Inc., Chicago, IL, USA) was used. The continuous variable strain is presented as median value with corresponding 25th and 75th percentiles in figure 1 and as mean ± standard deviation in the text. Multiple comparisons were done using the Bonferroni test.

Results

In 10 out of 13 vessels a thrombus was formed at the side where an anode caused a DC current through the femoral wall (fig 1 now fig 3). Initially thrombi are soft and stiffened dramatically in the first 20 minutes with a strain reduction of about 50% (fig 2 and 3). The

strain between frames in a thrombus decreased from (0.27 ± 0.17) at 5 minutes through (0.17 ± 0.08) at 20 minutes to (0.12 ± 0.09) after 45 minutes. At 75 minutes the strain was 0.13 ± 0.10, at 105 minutes 0.15 ± 0.08. Further stiffening took considerable more time, but could be observed towards the end of the experiment. The strain was 0.10 ± 0.07 at 150 min. and the lowest (0.05 ± 0.01) at

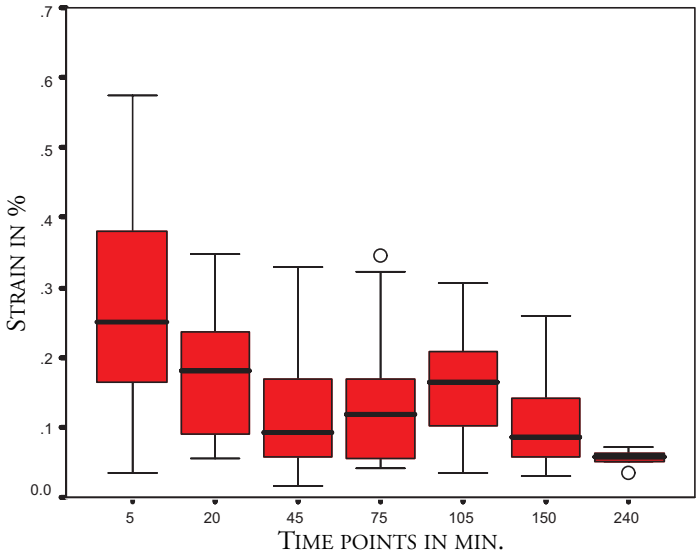

Fig 1: Median strain data are given at the different time points of acquisitions. The box represents the interquartile range, which contains the 50% of values, while the whiskers are lines that extend from the box to the highest and lowest values excluding outliers.

240 minutes. The difference in strain was significant between the time point at 5 minutes vs. all other measurement points (20 min. $p<0.038$; 45 min. $p<0.0001$; 75 min. $p<0.003$; 105 min. $p< 0.018$; 150 min. $p<0.0001$; 240 min. $p<0.0001$). Other significant differences could not be found. The inverse relation between the time and strain over the first 3 hours is highly significant ($R^2=0.59$; $p < 0.0001$).

Discussion

This is the first time that the generation and organization of an arterial thrombus in vivo is shown (Figure 3). We used an animal model inducing electric vascular injury, which generates platelet-rich thrombi similar to that observed in the coronary arteries of patients with acute myocardial infarction. The major findings of this study are that a thrombus gets stiffer over time and a vast part of the organization process takes place within 20 min. after thrombus in-

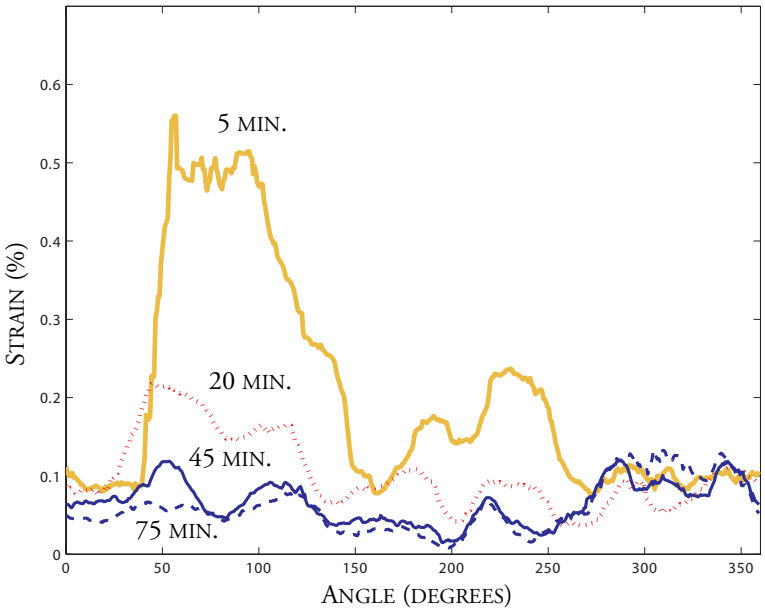

Fig 2: Actual strain data over the circumference of one vessel are given. Between 50 and 150 degrees the strain is the highest at the beginning, while the strain decreases over time

troduction and that this process can be monitored using intravascular palpography.

Intravascular palpography, by its capacity to evaluate the mechanical properties of biological tissues, can detect e.g. thin-cap fibroatheromas. Validation studies in vitro and in vivo have shown that palpography can identify such plaques with high sensitivity and specificity. However this thin-cap fibroatheromas cause only 70% of all myocardial infarction. Plaque erosion, which is the second most possibility to get a thrombosis (25%), cannot be detected by current IVUS derived techniques like palpography. However IVUS is capable to detect thrombosis by using integrated attenuation values, texture analysis of radio frequency data or video densitometric data to differentiate between various types of thrombus. All these approaches give us no information on the age of the thrombus in the early phase of development. How important this information is on treatment success is proven by several thrombolysis studies showing that complete early reperfusion is associated with reduced in-hospital mortality (Vogt 1993) (Morrison 2000). The scanning of coronary arteries after stenting the culprit lesion in order to identify remaining thrombi may help to customize anticoagulation therapy when the age of the thrombus is known.

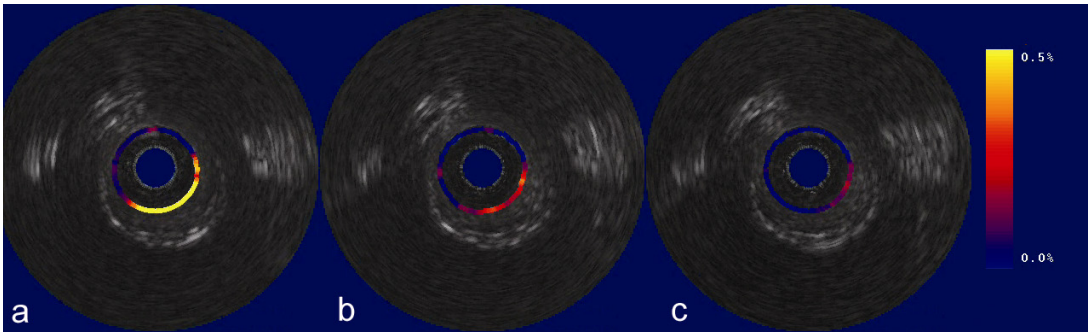

Fig 3: At the beginning of the experiment (a) strain is the highest at the thrombus outer side between the 3 and 7 o'clock position. The strain decreases after 20 minutes (b). At the end of the experiment (c) the thrombus is entirely stiff

The stabilization of thrombi is mainly caused by transformation of the thrombus. In an animal model it was shown by western analysis of thrombus extracts that nearly 50% of fibrinogen was cleaved to fibrin and extensively cross-linked within 30 min. of injury with no evidence of fibrinolysis (McBane 2000). Our investigation is confirming these earlier investigations showing strain reduction of the thrombus by about 50% in the first 20 minutes suggesting the stabilization of the thrombus due to fibrin cross linking.

Although the constitution of our experimental thrombosis resembles natural fresh thrombi in patients and the time course of stiffening corresponds to fibrin cross-linking, we have no prove that the time course of our model is identical to natural thrombus formation. However this study shows that the thrombus stiffens over time and that this process can be assessed by palpography. A direct translation between strain in this experimental thrombus and a thrombus in a clinical scenario still needs to be assessed.

The observations in this study open up the stage for more detailed clinical trials.

Chapter 14

Assessment of Vulnerable Plaque Composition

Based on:

Radj A Baldewsing, Johannes A Schaar, Frits Mastik, Cees WJ Oomens, Antonius FW van der Steen
Assessment of Vulnerable Plaque Composition by Matching the Deformation of a Parametric Plaque Model to Measured Plaque Deformation
IEEE Trans Med Imaging. 2005; 4: 514-28

The majority of acute coronary syndromes, such as unstable angina, myocardial infarction or sudden cardiac death, are caused by coronary thrombosis (Davies 2000) (Falk 1995). More than 60% of these thrombi are caused by rupture of vulnerable, thin-cap fibroatheroma (TCFA) plaques (Virmani 2000). Their morphological features are a large lipid core, covered by a thin fibrous cap. Considered as major determinants for their rupture are their material composition, geometry, and cap inflammation caused by infiltration of macrophages (Davies 2001). As such, identification of these rupture-determinants is of vital diagnostic importance (Schaar 2004).

IVUS elastograms cannot be interpreted directly as plaque component images

IntraVascular Ultrasound (IVUS) elastography is a technique that determines arterial radial strain by cross-correlation processing on a pair of IVUS radio-frequency signals; each signal is measured with an IVUS catheter at a different intraluminal pressure (de Korte 2003)(Brusseau 2002)(Saijo 2004)(Perry 2003)(Shapo 1996)(Choi 2002)(Ryan 1997)(Talhami 1994). This arterial radial strain is visualized in a so-called (strain) elastogram. IVUS elastography is clinically available and has proven to be capable of detecting the presence of human TCFAs in vitro with a sensitivity of 88% and specificity of 89%, merely by inspecting the elastogram for a specific strain pattern that consists of high strain with adjacent low strain on the surface of a plaque (Schaar 2003a). In vivo animal experiments and in vitro human experiments demonstrated that discrimination between fibrous and fatty plaques is possible, merely by determining the average radial strain value of the plaque (de Korte 2000a + 2002a). The in vivo animal experiments also showed that the presence of a high strain spot (average radial strain > 1%) at the plaque surface had a sensitivity of 92% and a specificity of 92% for identifying macrophages. Although these studies have shown that a specific radial strain pattern and the average radial strain of a plaque

can provide valuable information, there doesn't exist a one-to-one relation between the local radial strain value in an IVUS elastogram and the local tissue component type (calcified, fibrous, fatty or tissue infiltrated by macrophages). The underlying reason is that the local stresses that induce local radial strain depend upon the structural configuration of the artery and the material properties and geometry of its plaque components. Furthermore, radial strain depends on the catheter position used during imaging (Baldewsing 2004a)(de Korte 1996+1999)(Ophir 1996). Thus, IVUS elastograms cannot be interpreted directly as plaque component images.

Image of the Young's modulus distribution

Such an image can be interpreted as a morphology and material composition image of a plaque, due to the large differences between Young's moduli of plaque components, like calcifications, healthy arterial tissue, lipids or tissues weakened by infiltration of macrophages (de Korte 2000a)(Lendon 1991)(Lee 1991+1992)(Fung 1981). Many researchers have used displacement and/or strain components that were derived from simulated or measured ultrasound data or other imaging modalities in combination with tissue deformation equations, to compute a Young's modulus image. Usually a 'direct' or 'iterative' reconstruction method is employed. With a direct reconstruction method the deformation equations are rewritten to express the moduli as unknowns. Subsequently, they are solved by means of an analytical formula or by a discretization or numerical integration approach. With iterative reconstruction, the moduli values of each individual mesh element or groups of mesh elements in a finite element model representation of the tissue are iteratively updated such that the computed model output eventually closely matches the experimentally measured data (e.g., displacement and/or strain components). Many groups have applied these methods on a two dimensional cross-section of a homogeneous rectangular medium with a circular or rectangular inclusion using a direct method (Cohn 2000)(Raghavan 1994)(Skovoroda 1995)(Sumi 2000)(Zhu 2003)(Wellman 1999) or an iterative method (Bishop 2000)(Doyley 2000)(Kallel 1996)(Fu 2000). Some applied an iterative method to breast (Plewes 2000)(Samani 2001)(Miga 2003), prostate (Sarvazyan 1998), brain (Van Houten 1999) or heart (Moulton 1995). However, only a few groups considered arteries. Some of them used an iterative method (Beattie 1998) (Vorp 1995) (Chandran 2003) (Soualmi1997), others a direct method (Bank 1999) (Kanai 2003) (Wan 2001).

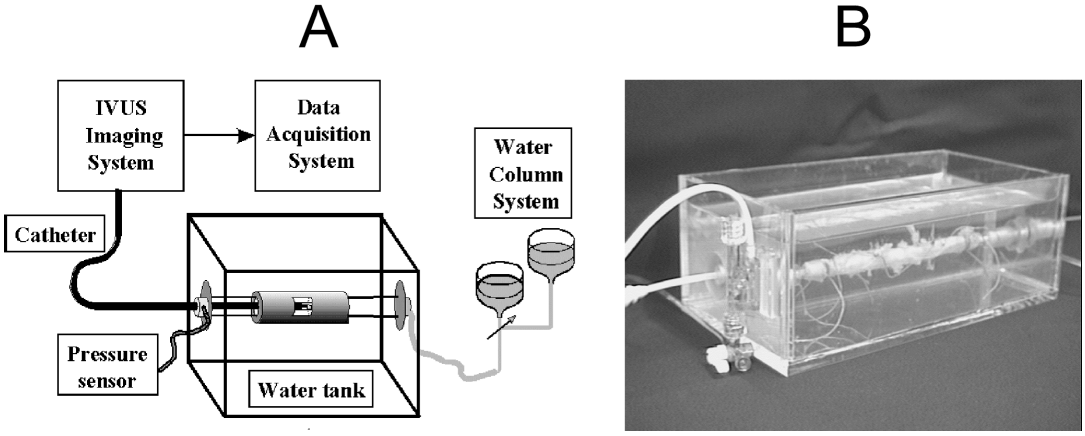

Fig. 1: (A) Experimental set-up consisting of a water column system, water tank, pressure sensor, catheter, IVUS imaging system and data acquisition system. (B) Photograph of the water tank containing an atherosclerotic human artery; all arterial side branches are closed with suture

Both inversion techniques suffer to different degree from stability problems like non-uniqueness and non-convergence. Various groups (Skovoroda 1995) (Kallel 1996) (Moulton 1995) (Beattie 1998) (Barbone 2002+2004) (Sumi 1995) have mentioned possible causes, such as measurement noise, a limited number of measured displacement or strain components, boundary data that is erroneous or of an incorrect type, a Finite Element Model (FEM) with too many (physically not interpretable) parameters, or an inappropriate FEM.

A new reconstruction method specially suited for TCFA

The ultimate clinical goal is to obtain a diagnostically useful and easily interpretable modulus image of an arbitrary complex atherosclerotic plaque using a modulus imaging method, which suffers as little as possible from stability problems. To proceed towards this goal and to be able to investigate and quantify reconstruction problems in a systematic way, we developed a new reconstruction method specially suited for TCFAs (Davies 2000) (Schaar 2004b) (Virmani 2003). Our method uses an iterative reconstruction approach to produce a Young's modulus image. To this end, the deformation output, calculated with a Parametric Finite Element Model (PFEM) representation of a TCFA plaque, is matched to plaque deformation measured with IVUS elastography. The PFEM uses a minimum number of morphology and material composition parameters, but is still able to model a variety of these TCFAs. The

resulting Young's modulus image of the plaque shows both the morphology and Young's modulus value of three main plaque components, namely lipid, cap and media and is therefore fast and easy to interpret in clinical settings.

Aim of this study

The aim of this study is twofold: Firstly, to describe the new reconstruction method. Secondly, to demonstrate its ability to successfully reconstruct Young's modulus images from elastograms obtained from five plaques. These elastograms are simulated using finite element models, measured from vessel-mimicking material, and measured from human coronary arteries in vitro and in vivo.

Materials

A. Simulated Arteries with Plaque

Two different finite element models were constructed for a realistic TCFA; one TCFA was defined using circles, the other by tracing TCFA histology.

B. Phantom with Plaque

One vessel-mimicking phantom with an eccentric, soft region embedded in a stiff wall was made from 10% PolyVinyl Alcohol (PVA) Cryogel (Chou 1997) as described in (Baldewsing 2004b). Carborundum (SiC) particles (3-10 mm) were added as scattering material. The static Young's moduli were measured in a custom designed tension set up. The static Young's modulus was 4.2 kPa for the plaque and 16.8 kPa for the wall. The pressure-free phantom had a length of 150 mm, an outer diameter of 18 mm, and an inner diameter of approximately 4 mm.

C. Human Coronary Arteries with Plaque

A coronary artery segment with a TCFA was excised from one patient who died of a non-coronary cause. Furthermore, in vivo measured IVUS radio-frequency data were obtained from a non-culprit coronary artery of one patient referred for percutaneous transluminal coronary angioplasty. The IVUS data revealed the presence of a large eccentric plaque.

METHODS

A. Elastography Simulations and Measurements

Elastography Simulations

Elastograms were simulated for two TCFAs using the finite element package SEPRAN (Sepra Analysis, Technical University Delft, The Netherlands). Linear elastic, isotropic, nearly incompressible (Poisson's ratio n=0.4999), plane strain finite element models were used for this purpose, because it has been demonstrated (Baldewsing 2004b) that such models are appropriate to simulate radial strain elastograms that are measured in vitro from human atherosclerotic coronary arteries using IVUS elastography. The geometry of the first TCFA was defined by using circles. The geometry of the second TCFA was defined by tracing the histology of an excised human coronary artery with a TCFA. The material properties of the TCFA components (Table 1) and pressure differential of 20 mmHg were taken from values reported in (Baldewsing 2004a+b). Histology revealed a layer of collagen and a layer of smooth muscle cells resulting in the two Young's moduli values for different regions in the cap. The finite element mesh consisted of plane-strain triangular finite elements with extended quadratic interpolation functions. The averaged finite element size was approximately 0.1 mm. The radial strain was calculated with respect to the geometric center of the lumen border.

Material Parameter	Plaque 1	Plaque 2
E lipid [kPa]	50	25
E cap [kPa]	2000	1500/1250
E media [kPa]	1500	1000
ν cross section	0.4999	0.4999

Table 1: Young's modulus (E) and Poisson's ratio (ν) used in Finite Element Models for Arterial Plaque Cross-sections.

Elastography Measurements with Phantom and In Vitro Artery

The experimental setup for performing elastography measurements with the phantom and in vitro artery consisted of a water tank equipped with two insertion sheaths (fig. 1). The water tank was connected via the distal sheath to a water column system, which contained distilled water for the phantom and a de-gassed physiological saline solution for the in vitro artery. The phantom and in vitro artery were subsequently mounted between the two sheaths. Also the arterial side-branches were closed with suture material to prevent leakage (Schaar 2002). The column system was used to apply intraluminal pressures and to perform preconditioning. Preconditioning of the artery was done by loading the artery with 100 mmHg pressure and subsequently unloading it to ambient pressure, for at least five cycles (Lally 2004). A 20-MHz 64-element phased array IVUS catheter (Volcano Inc., Rancho Cordova, CA, USA) connected to an InVision echo apparatus (Volcano Inc., Rancho Cordova, CA, USA) was inserted in the proximal sheath. The pressure was monitored using a pressure sensor that was also connected to the proximal sheath.

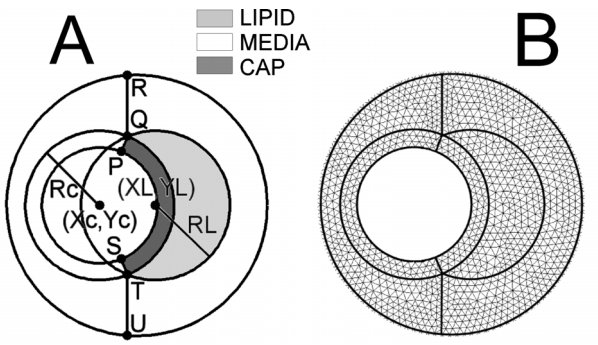

Fig. 2: Parametric Finite Element Model for a Vulnerable Plaque. (A) Each circle is parameterized by its center (X,Y) and a radius R. The dynamic control points P, Q, R, S, T, and U are used to define the three plaque components. (B) Finite element mesh regions corresponding to geometry in A. Letters L and c denote lipid and cap, respectively.

Elastography measurements for the in vitro artery were done within 24 hours post mortem and directly after preconditioning (Schaar 2003a). First, an IVUS echo frame was acquired at an intraluminal pressure of 5 mmHg for the phantom and 80 mmHg for the artery. After 10 seconds, another IVUS echo frame was acquired at 6 mmHg for the phantom and 100 mmHg for the in vitro artery. Each echo frame consisted of 512 angles of raw radio-frequency (RF) data-lines sampled at 100 MHz in 12 bits. Each line contained 1024 data points (corresponding to 7.6 mm imaging depth). The intraluminal pressures were chosen to strain the phantom and the artery up to a maximum of 2.5%. This strain value is an upper limit

for properly calculating the local radial strain using the cross-correlation method described by de Korte et al. (de Korte 1998) with a window length of 60 RF data points, 50% window overlap and a 20-MHz center frequency of the ultrasound signal. This cross-correlation technique was applied to the ultrasound data to calculate the local radial strain. First, the radial tissue displacement along the ultrasound beam was determined. Then, finite differences of these displacements resulted in the local radial strain. Since a window length of 60 RF data points was used with 50% window overlap, the spatial resolution of the strain determination was 30 RF data points in the radial direction (approximately 200 μm). Strain estimates of the phantom, in vitro artery and in vivo artery were clipped respectively between 0% (color coded in black) and an upper strain value (color coded in white).

The histology of the in vitro artery was created from the tubular segment that was elastographically imaged. This segment was pressure-fixed at 80 mmHg, sectioned, and counter-stained for the presence of collagen and lipid (picro Sirius red and polarized microscopy), smooth muscle cells (a actin) and macrophages (CD 68).

Elastography Measurements In Vivo

A multiframe averaging method similar to the one described in Doyley et al. (Doyley 2001) was used to compute a compounded elastogram. First, IVUS echo frames were acquired at 30 fps. Next, at the diastolic phase of a cardiac cycle, when catheter motion is minimal, a consecutive sequence of 7 echo frames was selected. Each consecutive frame pair was highly correlated, i.e., the sum-of-absolute-differences between the RF-envelopes of a consecutive frame pair divided by the sum of RF-envelopes of the first frame was less than 0.1. Furthermore, the total incremental rotation of the catheter was less then 1 degree. The measured intraluminal pressure was 53 mmHg for the first frame and 60 mmHg for the seventh frame; intraluminal pressure difference between consecutive frames was 1 mmHg. From each consecutive frame pair an elastogram was computed using the method describe above for the phantom and in vitro artery. Finally, a compounded elastogram was computed by averaging the 6 elastograms; throughout the paper this elastogram is denoted as 'in vivo measured elastogram'.

B. Parametric Model-Based Reconstruction Method

The main components of the reconstruction method were the Parametric Finite Element Model (PFEM) for a plaque, the forward problem calculation, and minimization algorithm used:

PFEM for a Plaque:

1) PFEM for a Plaque: An idealized TCFA (Virmani 2003) was used as model for a plaque. Our model is a variation of the PFEM used by Loree et al. (Loree 1992). Our PFEM geometry consisted of a media area containing a lipid pool, which was covered by a cap. The borders of the lipid, cap, and media areas were defined using circles (fig. 2A). Lipid was defined as region QTQ, cap as region PQTSP and media as the remaining area. Each circle was parameterized by its center with Cartesian coordinates (X,Y) and radius R. Arterial tissue was modelled in the PFEM as linear elastic, isotropic, nearly incompressible (Poisson's ratio ν=0.4999), plane strain material (Baldewsing 2004a+b). The lipid, cap, and media regions were assumed homogenous. The Young's modulus values of these regions were denoted as E_L, E_C, and E_M, respectively.

Forward Problem

2) Forward Problem (i.e., Radial Strain Image Calculation): First, parameters were specified that define the geometry and Young's modulus values of the PFEM, and pressure boundary conditions. Then, a mesh topology file was created from these parameters using MATLAB (release 12.1, the MathWorks, Inc.). Next, the finite element package SEPRAN used this file to calculate a finite element mesh consisting of plane-strain triangular elements (e.g., fig. 2B) with extended quadratic interpolation functions. Then, it calculated the Cartesian strain tensor components in these mesh points. Finally, MATLAB converted these Cartesian components to their polar equivalents using the catheter center as origin. The radial strain component field was subsequently interpolated onto a reference grid, i.e., square equidistant grid of 100 by 100 points. This radial strain field was called a PFEM elastogram. For each reconstruction, the size of the square reference grid was chosen such that it tightly surrounded the arterial wall region. The whole process from defining the PFEM parameters up to the calculation of the PFEM elastogram was fully automatic. The simulated and measured elastograms were also interpolated onto the corresponding reference grid.

Minimization Algorithm

A Constrained Sequential Quadratic Programming minimization algorithm (Optimization Toolbox, MATLAB) was used, that auto-

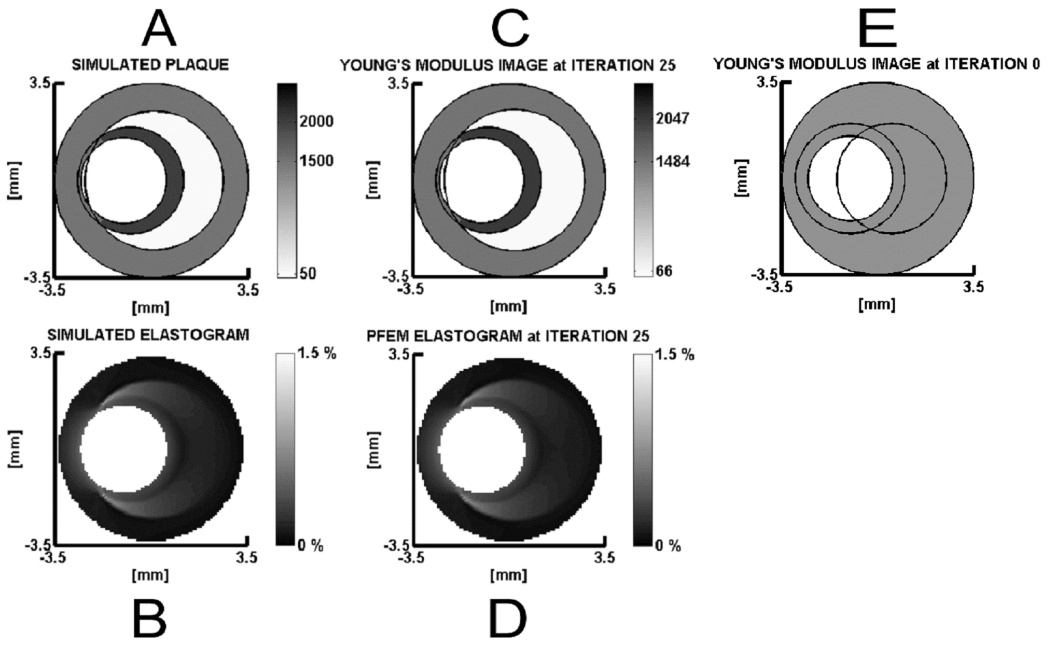

Fig. 3: Reconstruction from a simulated elastogram of a thin-cap fibroatheroma that consists of circles. (A) Young's modulus image in kPa used for simulating the plaque. (B) Simulated elastogram computed using A. (C) Reconstructed Young's modulus image in kPa. (D) PFEM elastogram computed using C; the RMS error is 0.016%. (E) Initial state at start of the reconstruction process: The Young's modulus of the lipid, cap and media plaque component is 1185 kPa.

matically searches a local minimum of a non-linear objective function, i.e., quantification of the difference between PFEM elastogram and a simulated or measured input-elastogram, by iteratively updating the PFEM parameters. At every iteration the six PFEM geometry and three PFEM material parameters were all simultaneously updated. The objective function was defined as the Root-Mean-Squared (RMS) error between PFEM elastogram and input-elastogram. The RMS error was calculated from the strain values that belong to those reference grid points that are shared by the input-elastogram (i.e., simulated or measured elastogram) and the PFEM elastogram. At every iteration the RMS error decreases. The average time between two iterations was 45 seconds on a computer with a 3 GHz Xeon processor.

A detailed mathematical description of the algorithm can be found in the Optimization Toolbox of MATLAB. The basic steps were as follows. At each major iteration a simultaneous update for all parameters was computed by solving a quadratic subproblem. This

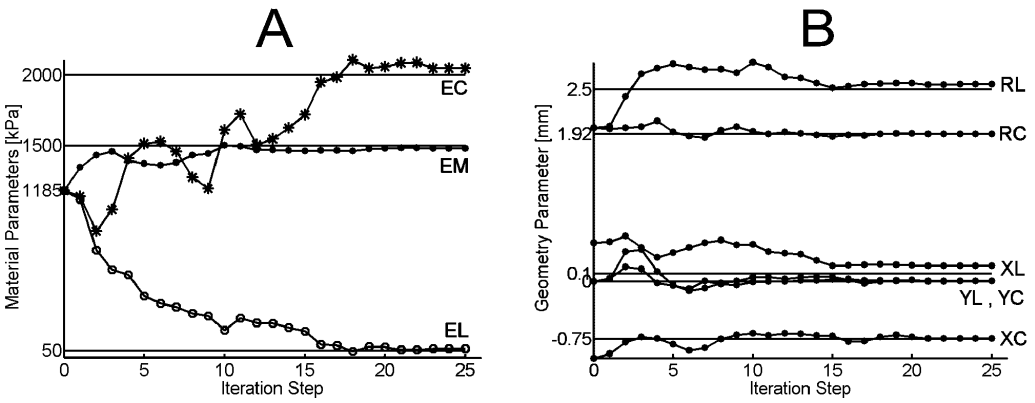

Fig. 4: PFEM-parameters versus iteration-step curves for the simulated thin-cap fibroatheroma that consists of circles. (A) Material parameters: Young's moduli for lipid pool (E_L), cap (E_C) and media (E_M). (B) Geometry parameters: Center coordinates and radius of the lipid pool circle (X_L,Y_L) and R_L, and cap (X_C,Y_C) and R_C. The solid lines are the parameters values used to create the simulated thin-cap fibroatheroma.

subproblem was generated by approximating the Hessian matrix of the Lagrangian function, using a quasi-Newton updating method. The solution of this subproblem was then used to form a search direction for a line search method, which resulted in the update.

Positioning of PFEM Lumen and Media Circle

For all reconstructions, the PFEM lumen circle was defined (i.e., its center coordinates and radius was determined) as the largest circle within the lumen border. Similarly, the PFEM media circle was defined as the smallest circle enclosing the media contour. For both the in vitro and in vivo artery, the media contour was defined as the

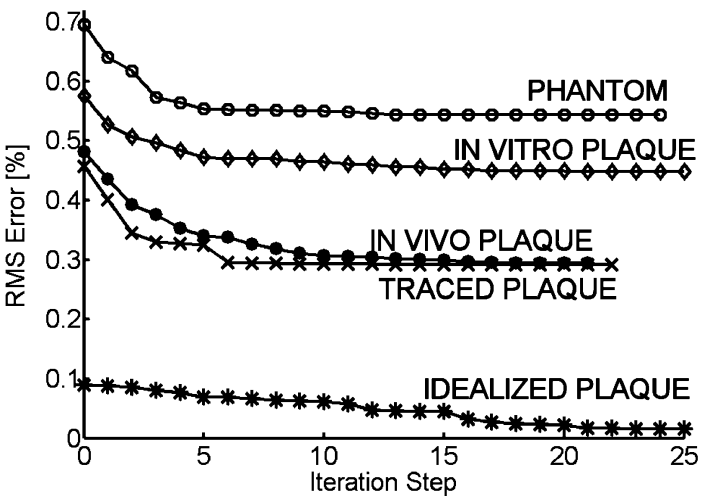

Fig. 5: RMS-error versus iteration-step curves for each of the five reconstructions presented in this paper. The idealized plaque denotes the simulated thin-cap fibroatheroma that consists of circles and the traced plaque denotes the simulated thin-cap fibroatheroma that is traced from arterial histology.

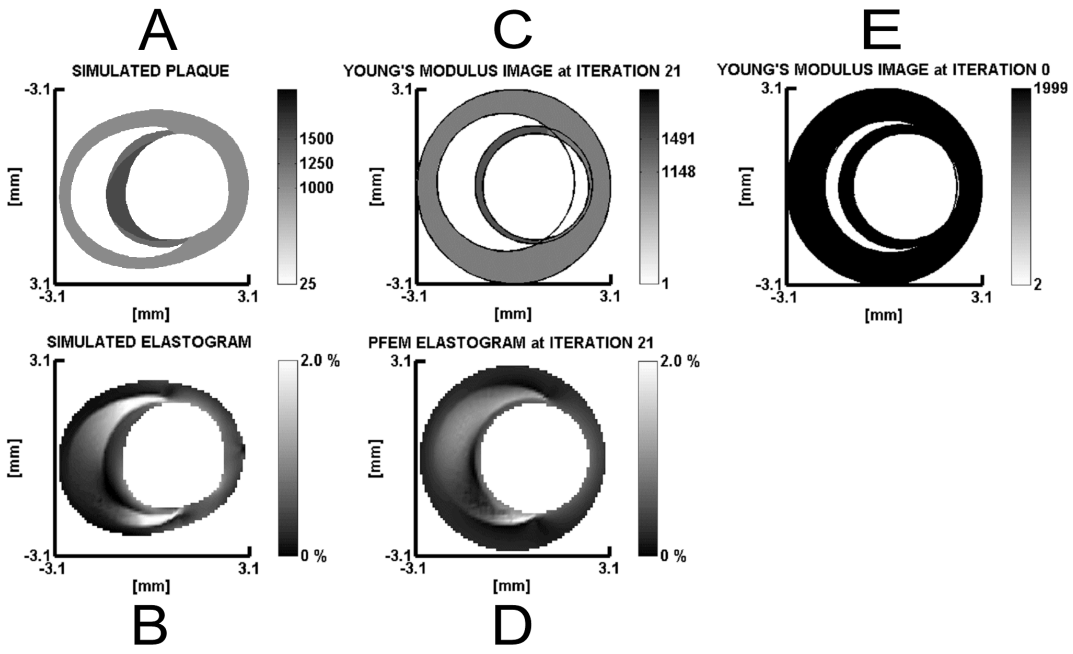

Fig 6: Reconstruction using a simulated elastogram of a thin-cap fibroatheroma that is traced from arterial histology. (A) Young's modulus image in kPa traced from histology and used for simulating the plaque. (B) Simulated elastogram computed using A. (C) Reconstructed Young's modulus image in kPa. (D) PFEM elastogram computed using C; the RMS error is 0.29%. (E) Initial state at start of the reconstruction process.

media-adventitia border, which was visible in the echogram as an echolucent contour with distal brightening. In case of the phantom, whose diameter was 18 mm and thus exceeded the 15.2 mm diameter of the echogram, the part of the wall boundary that was visible in the echogram was extrapolated. For the two simulated arteries, the media contour was already defined during their creation.

Nonlinear and Linear Constraints

In order to maintain the morphology of an idealized TCFA (fig. 2A) and to automatically calculate a proper finite element mesh (e.g., fig. 2B) during the minimization process, the following nonlinear geometry constraints were enforced upon the PFEM geometry parameters: (i) The lipid circle must have exactly two intersection points with the cap circle (Q and T). (ii) The cap circle must always contain the lumen circle. (iii) The lipid circle must always be inside the media circle. The other dynamic mesh-control points (P, R, S, and U in fig. 2A) were automatically calculated and used to define the three plaque regions. Point P (and analogously S) was defined as the projection of point Q onto the lumen circle.

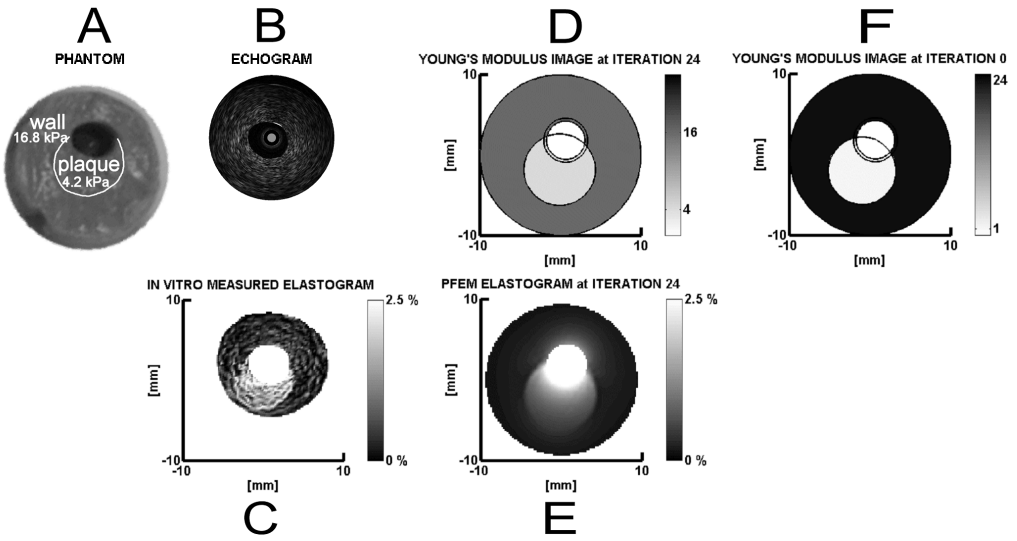

Fig. 7: Reconstruction using a measured elastogram from a vessel-mimicking phantom; it has a soft region embedded in a stiff wall. (A) Young's modulus image. (B) Echogram. (C) Measured elastogram. (D) Reconstructed Young's modulus image in kPa. (E) PFEM elastogram computed using D; the RMS error is 0.54%. (F) Initial state at start of the reconstruction process.

Point R and U were located on the media circle such that line QR and TU bisected the angle between two direction-vectors that were defined as the outward normal of respectively the lipid and cap circle at point Q and T. The separation of the media region by the two line pieces RQ and TU was done to make the finite element meshing of the media region more robust.

Minimization process

Furthermore, to speed-up the minimization process, the range of each PFEM parameter was restricted to stay within a user-defined lower bound and upper bound value. These bounds were, by definition, linear constraints and chosen as follows. The centers of the cap and lipid pool circles were restricted to stay within the smallest square that fitted around the PFEM media circle. The radii of the cap and lipid pool were non-negative and bounded by the radius of the PFEM media circle. The Young's moduli were all chosen to be positive. For the two simulated arteries, the upper bound was set arbitrarily at 500 kPa higher than the Young's modulus of the stiffest plaque components, namely that of the cap. Similarly, the upper bound of the phantom was set at 25 kPa, which is arbitrarily higher than the measured Young's moduli of its components, namely 4.2 and 16.8 kPa. For the in vitro artery, the same upper bound was

used as for the simulated artery that was traced from histology, because they showed resemblance in their geometry and their elastograms showed similar maximal strain at the same pressure differential of 20 mmHg. Finally, the in vivo artery showed approximately the same maximum strain as the in vitro and the two simulated arteries, however at a 20 times lower pressure differential, namely 1 mmHg, therefore the upper bound was set proportionally lower, at 300 kPa.

The minimization algorithm was terminated after 25 iterations or if the decrease in RMS error was less than 10^(-8).

Initialization of Reconstruction Method

At the start of each reconstruction an initial state is required for the PFEM geometry and material parameters that are varied by the minimization algorithm, namely the lipid and cap circle parameters and the Young's modulus of the lipid, cap and media region. Each initial state was chosen so that it differed from the actual underlying plaque composition. For all the reconstructions, the cap and lipid pool circles were put arbitrarily in the direction of the plaque. For all reconstructions, except the first, an initial modulus contrast was used between the plaque components, by setting the modulus of the

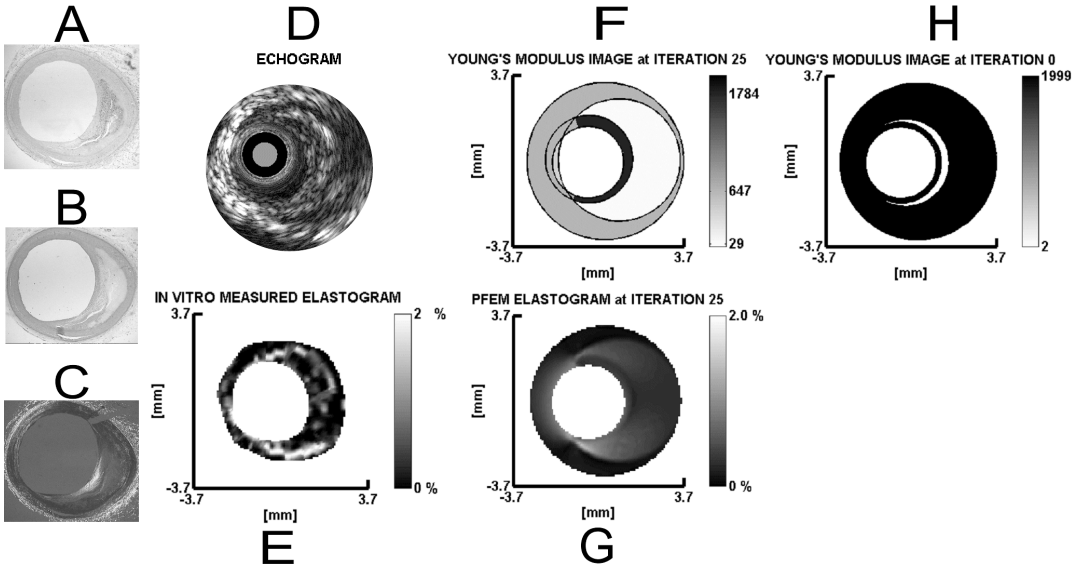

Fig. 8: Reconstruction using an *in vitro* measured elastogram from a human coronary artery with a thin-cap fibroatheroma. (A) Macrophages. (B) Smooth Muscle Cells. (C) Collagen. (D) Echogram. (E) *In vitro* measured elastogram. (F) Reconstructed Young's modulus image in kPa. (G) PFEM elastogram computed using F; the RMS error is 0.45%. (H) Initial state at start of the reconstruction process.

cap and media close to the upper-bound value and the modulus of the lipid close to the lower-bound value. Finally, the phantom only consisted of two regions: a soft homogenous region within a stiff homogenous wall. To model this situation appropriately, the following additional constraints were enforced upon the PFEM during the minimization: (i) the cap circle was kept fixed during the minimization and (ii) the Young's modulus of this cap region was kept equal to the Young's modulus of the lipid region.

C. Uniqueness Estimation

For the in vivo case, the actual underlying plaque composition was unknown. Therefore, multiple reconstructions were performed using a set of different initial states. This was done (i) to enhance the chance of finding a successful reconstruction, i.e., finding a reconstruction with a PFEM elastogram that highly resembles the measured elastogram and (ii) to estimate the uniqueness of a successful reconstruction. The initial states were defined, as follows: The cap circle had the same center as the lumen circle and was given a cap thickness of 100, 200 or 300 μm. The lipid circle was the same for all initial states, was slightly positioned in the direction of the plaque and occupied only a small area of the plaque. The initial Young's modulus values for the lipid pool (E_L), cap (E_C) and media (E_M), were set at the following values: 0.1 or 10 kPa for E_L and 100, 150, 200, 250 or 299 kPa for E_C; the initial EM value was set equal to the initial EC value. These initial parameter values for cap thickness, E_L and E_C(=E_M) resulted in 3*2*5 = 30 different initial states.

RESULTS

A. Simulated Plaques

Plaque 1

Figure 3A shows a simulated arterial TCFA that is defined by circles. The circumferential geometry and relatively high stiffness of the cap causes the arterial stress to concentrate on the cap, especially at its edges and around the corners of the lipid pool (Richardson 1989); this redistribution mechanism causes the typical regions of high radial strain at the corners of the lipid pool in figure 3B and the relatively low strain at the center of the lipid pool (Loree 1992).

This elastogram shows a perfect example of the specific strain pattern, which consists of high strain with adjacent low strain on the surface of the plaque, that has proven to detect the presence of human TCFAs *in vitro* with a sensitivity of 88% and specificity of 89% (Schaar 2003a). The reconstructed Young's modulus image (fig. 3C) highly resembles the morphology and material composition of the simulated arterial TCFA in figure 3A (respectively, E_L=66, E_C=2047, and E_M=1484 kPa versus E_L=50, E_C=2000, and E_M=1500 kPa). Also the input-elastogram (fig. 3B) and the PFEM elastogram (fig. 3D) show a high resemblance. The initial state (fig. 3E) has no Young's modulus contrast between the three plaque components. Figure 4 shows the evolution of the PFEM material and geometry parameters during the reconstruction process; figure 4B shows quantitatively that the geometry of each plaque component is closely approximated. Figure 5B shows for each reconstruction presented in this paper the RMS error, which always decreases during the reconstruction process.

Plaque 2

Figure 6A shows a simulated TCFA that was traced from arterial histology. Just as plaque 1 it results in a simulated elastogram (fig. 6B) with similar typical regions of high and low strain. The Young's modulus image (fig. 6C) shows that both the morphology (which is not delineated by circles) and material composition of the simulated TCFA (fig. 6A) are successfully approximated (respectively, E_L=1, E_C=1491, and E_M=1148 kPa versus E_L=25, E_C=1500 (and cap side-regions 1250), and E_M=1000 kPa). Also a high resemblance between input-elastogram (fig. 6B) and PFEM elastogram (fig. 6D) is visible. The initial state (fig. 6E) has a large Young's modulus contrast between lipid and the other two plaque components and both the cap and lipid circle are positioned slightly in the direction of the plaque.

B. Phantom

Vessel-mimicking phantom

Figure 7A shows the composition of the vessel-mimicking phantom that has a soft region embedded in a stiff wall. The echogram (fig. 7B) cannot discriminate between the two mechanically different regions. However, the measured elastogram (fig. 7C) reveals the presence of the soft region by means of the high strain region. This region shows a typical radial strain decay that results from a decreas-

ing stress; this natural stress decrease is due to the circumferential vessel geometry. Only a limited range of phantom material is contained in the elastogram due to the limited imaging depth of the catheter (approximately 7.6 mm). The heterogeneous strain texture throughout the elastogram is caused by measurement noise and the gradient based calculation of strain. The Young's modulus image in figure 7D shows that both the circular morphology and material composition of the phantom are successfully approximated (respectively, E_L=4 and E_M=16 kPa versus E_L=4.8 and E_M=16.8 kPa). A high resemblance is obtained between input-elastogram (fig. 7C) and PFEM elastogram (fig. 7E). The initial state (fig. 7F) has a large Young's modulus contrast between the soft region (i.e., lipid) and stiff wall (i.e., media) and the lipid circle is positioned near the location indicated by the high strain region in the measured elastogram (fig. 7C).

C. Human Coronary Arteries with Plaque

In Vitro Plaque: Figs. 8A-C show that the *in vitro* plaque is a TCFA with a stiff media containing an even stiffer cap which overlays a soft lipid pool. The echogram (fig. 8D) reveals the plaque location but cannot be used to discriminate between its components, e.g., cap and lipid pool. Similarly as with plaque 1 and 2, the measured elastogram (fig. 8E) suggests the presence of the TCFA by means of the specific strain pattern. The heterogeneous strain texture throughout the elastogram is due to measurement noise and the gradient-based calculation of the strain. The Young's modulus image (fig. 8F) shows that both the morphology and stiffness contrast of the arterial plaque components are in qualitative agreement with, respectively, the morphology and stiffness contrast information provided by the histology of the plaque. Both the measured elastogram (fig. 8E) and PFEM elastogram (fig. 8G) show a low strain region at the center of the plaque and a high strain region at both corners of the plaque. However, both high strain regions in the PFEM elastogram are not as thin and elongated as in the measured elastogram. The initial state (fig. 8H) has a large Young's modulus contrast between lipid and other two plaque components and both the cap and lipid circle are positioned slightly in the direction of the plaque.

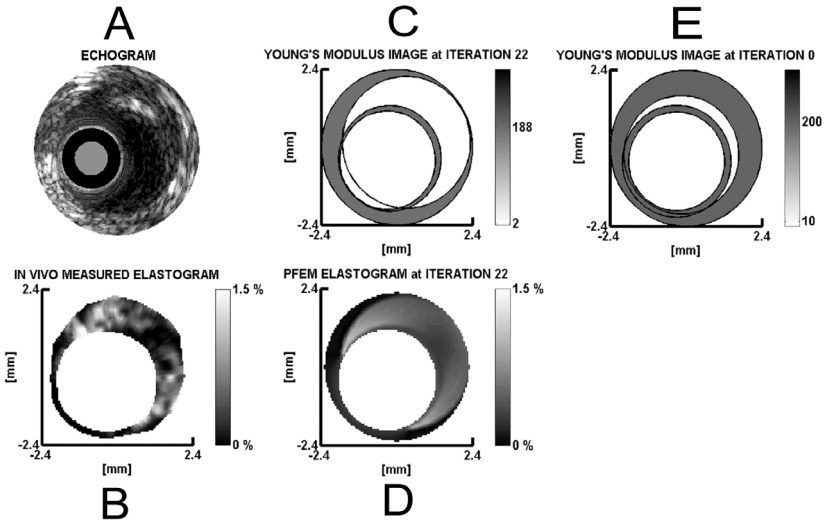

Fig. 9: Reconstruction using an *in vivo* measured elastogram of a human coronary artery with a vulnerable plaque. (A) Echogram. (B) *In vivo* measured elastogram. (C) Reconstructed Young's modulus image in kPa. (D) PFEM elastogram computed using C; the RMS error is 0.29%. (E) Initial state at start of the reconstruction process.

In Vivo Plaque

The echogram (fig. 9A) reveals the presence of a large eccentric plaque between 10 and 5 o'clock, but cannot discriminate between the possible cap and lipid component of the plaque. Similarly as with plaque 1, plaque 2 and the *in vitro* plaque, the *in vivo* measured elastogram (fig. 9B) shows the specific strain pattern that suggests the presence of a TCFA. The reconstructed Young's modulus image (fig. 9C) is a likely candidate for the real underlying plaque composition, since the measured elastogram (fig. 9B) and PFEM elastogram (fig. 9D) show two co-localizing regions of high strain at the corners of the plaque and a region of low strain at the center of the plaque. The initial state has a large Young's modulus contrast between lipid and other plaque components and the lipid circle is positioned slightly towards the plaque.

D. Uniqueness of In Vivo Plaque Reconstruction

From the 30 reconstructions, only 5 were successful, i.e., five showed a PFEM elastogram that highly resembled the measured elastogram. These five PFEM elastograms had the following features clearly in common with the measured elastogram (i) a region of high strain at each corner of the plaque and (ii) a region of low strain at the center of the plaque (e.g., figs. 9D, 10B, 10C). Their RMS errors lay between 0.29% and 0.30%, which was lower than the RMS errors of the 22 unsuccessful reconstructions ranging from

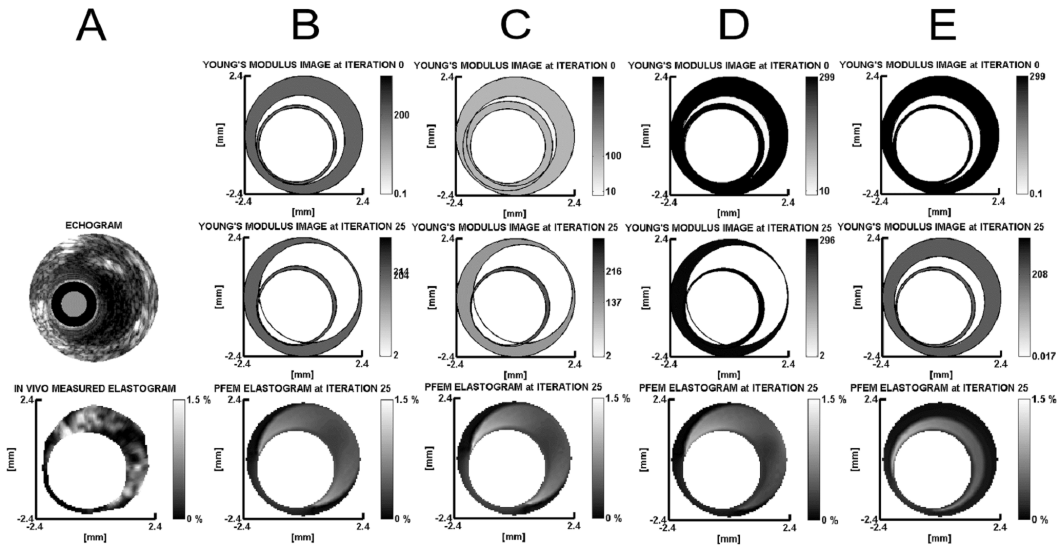

Fig. 10: Typical successful and unsuccessful reconstruction results obtained from the *in vivo* measured elastogram of the human coronary artery with a vulnerable plaque. (A) Echogram and *in vivo* measured elastogram. Columns (B) and (C) each shows a successful reconstruction; the RMS error for both is 0.29%. (C) An unsuccessful reconstruction whose PFEM elastogram has only one region with high strain in common with the measured elastogram; the RMS error is 0.32% (D) Another unsuccessful reconstruction whose PFEM elastogram does not have a region of low strain at the centre of the plaque in common with the measured elastogram; the RMS error is 0.38%. All Young's moduli are in kPa.

0.31% up to 0.37%. The majority of unsuccessful reconstructions resulted in a PFEM elastogram with only one region of high strain at the corner of the plaque (e.g., fig 10D) or lacked a region of low strain at the center of the plaque (e.g., fig 10E). Within each of the 5 successful reconstructions, the morphology (size, shape and position) of a plaque component (i.e., lipid pool or cap) was visually almost identical (e.g., figs. 9C, 10B, 10C). Furthermore, there was a consistent large modulus contrast between the lipid pool and the other two stiffer components (i.e., cap and media). E_L varied only between 1.8 and 2.4 kPa with a mean+/-SD of 2.1+/-0.2 kPa. There was less consistency in both E_C and E_M, since E_C varied between 145 and 280 kPa with a mean+/-SD of 209+/-44 kPa and E_M between 137 and 209 kPa with a mean+/-SD of 179+/-27 kPa.

DISCUSSION

A new reconstruction method to image the morphology and material composition of vulnerable plaques

We have described a new reconstruction method to image the morphology and material composition of vulnerable plaques. This method needs a plaque's elastogram, i.e., radial strain image, in order to reconstruct the plaque's Young's modulus distribution. It accomplishes this by iteratively matching the radial strain image output of a parametric plaque finite element model to the elastogram. Reconstructions using elastograms obtained from simulated plaques, a vessel-mimicking phantom with a plaque and an *in vitro* human coronary plaque demonstrated that this method could closely approximate the morphology and material composition of the three main plaque components, namely lipid pool, cap, and media. Furthermore, the reconstruction of a plaque, using an *in vivo* measured elastogram from a patient, was described. Finally, this elastogram was used as a realistic example to investigate the uniqueness of the reconstruction method.

Young's Moduli of Plaque Components

In this study, the sets of Young's moduli values that were used for the two simulated plaques (Table 1), for the phantom (E_L=4.2 kPa, E_M=16.8 kPa), and those that were reconstructed from the *in vitro* plaque (E_L=29, E_M=647, E_C=1784 kPa) and *in vivo* plaque (E_L=2, E_M=188, E_C=188 kPa), all had a Young's modulus value for the non-fibrous plaque component (e.g., lipid pool) that was much lower than the fibrous (e.g., media and cap) plaque components: Such a stiffness difference has been consistently observed by researchers that performed measurements or used a modulus reconstruction approach to determine static moduli values for human atherosclerotic plaque components (Table 2).

	NON-FIBROUS	FIBROUS	CALCIFIED
Loree et al. (1994b) Circumferential tensile E	927 ± 468 (n=12)	2312 ± 2180 (n=9)	1466 ± 1284 (n=5)
Lee et al. (1992) Radial compressive $E^{A, D, E}$	41.2 ± 18.8 (n=14)	81.7 ± 33.2 (n=18)	354 ± 245.4 (n=11)
de Korte et al. (2000a) Incremental pressure-strain $E^{A, D}$	222 (n=13)	493 (n=62)	
Kanai et al. (2003) Incremental circumferential $E^{B, D}$	81 ± 40 (n=9)	1000 ± 630 (n=9)	
Beattie et al. (1998) Bi-linear isotropic $E^{B, D}$	3.81, strain<18.2% 38.8, strain>18.2% (n=4)	483, strain<8.2% 1820, strain>8.2% (n=7)	3990, strain<5.3% 10700, strain>5.3% (n=1)

Young's moduli (E) are in kPa and given as mean +/- standard deviation ('n' = number of samples).

[A]Measured, [B]Reconstructed, [C]In vivo, [D]In vitro, [E]Only plaque-cap

Table 2: Measured and Reconstructed Static Young's moduli (E) of Human Atherosclerotic Plaque Components.

The following methods were applied to obtain the Young's moduli values listed in Table 2: Loree et al. (1994b) used uni-axial mechanical tensile testing on specimens at a physiological applied circumferential tensile stress of 187.5 mmHg. Lee et al. (1992) used uniaxial mechanical compressive testing on specimens that were classified by their IVUS appearance; the modulus was defined as the ratio between the increase in equilibrium-stress, namely from 30 to 90 mmHg, to the resulting strain after creep. De Korte et al. (de Korte 2000a) used IVUS elastography to measure the radial strain that resulted by increasing the pressure from 80 to 100 mmHg. Kanai et al. (Kanai 2003) used a direct reconstruction method to measure local thickness changes of vessel wall layers with an 'ultrasonic phased tracking' method during physiological pressurization. Moduli were subsequently computed with an analytical formula,

derived using the assumption that the artery was incompressible, isotropic and that the arterial pressure decreased linearly with the distance from lumen to adventitia. Beattie et al. (Beattie 1998) used an iterative FEM-based reconstruction method in combination with measured radial displacement fields (one at 40 mmHg and one at 80 mmHg intraluminal pressure). Plaque regions were assumed homogeneous and were identified *a priori* from histology, after having measured displacement fields by particle tracking on cross-sectional digital images. The following FEM material deformation features were used: isotropic, incompressible and plane stress.

This large variation in moduli values for a specific plaque component, and also for normal arterial wall (Gow 1979) (Mozersky 1072), can be attributed to factors that differ between research groups, such as Dobrin (Dobrin 1978) (Fung 1981) (Yamada 1970):

(i) Type of elastic modulus: dynamic, static, visco-elastic, anisotropic, incremental, pressure-strain, compressive, tensile, shear.

(ii) Type and host of artery: coronary, femoral, etc. from animal or human.

(iii) Environment: *in vitro*, *in vivo*, mechanical constraints, temperature.

(iv) History: preconditioning, (duration of) cold storage and age.

(v) Amount of pre-deformation/pressurization or longitudinal prestretch: arterial constituents stiffen with increasing tension.

(vi) Classification protocol: macroscopic classification into categories like fatty, fibro-fatty, fibrous, calcified etc. or microscopic classification into individual arterial constituents like smooth muscle cells, elastin, collagen, etc. In contrast to microscopic arterial constituents, global plaque constituents do not allow a clear and unique classification, because they are usually not small enough to be considered homogeneous.

(vii) Assumptions regarding the geometry of the arterial plaque components and the used constitutive material deformation models.

Despite these variations, discrimination between non-fibrous, fibrous and calcified plaque components is possible thanks to several-fold stiffness differences between these components. These differences are necessary for a successful application of reconstruction methods.

A pressure difference of 20 mmHg for the *in vitro* artery and only 1 mmHg for the *in vivo* artery resulted in both cases in elastograms with radial strains up to 2%. This result is in agreement with previous studies (de Korte 2000a+2003). The difference suggests that excising an artery may induce mechanical stiffening (Gow 1979) (Schaar 2002). This is possibly caused by differences in factors between situations *in vitro* and *in vivo* (e.g., cell inactivity or too much longitudinal pre-stretch). As expected from linear elasticity this pressure difference of a factor of 20 with similar strain is reflected in the reconstructed arterial Young's moduli values.

PFEM Material Deformation Features

In this study, we have used a linear elastic, isotropic, nearly incompressible, plain strain constitutive material model for (i) simulating the small-strain arterial deformation behaviour (strain<2.5%) at a level in the physiological intraluminal pressure range (50-150 mmHg) and (ii) for reconstructing the morphologies and Young's moduli of plaque components. Many other research groups have also used all, or only a subset, of these constitutive features for describing arterial deformation at a level in this pressure range, for example: linear elasticity (Chandran 2003) (Wan 2001) (Finet 2004) (Cheng 1993), isotropy (Lee 1994) (Veress 2000), (Huang 2001) (Lupotti 2003) (Kim 2004), (near) incompressibility (Holzapfel 1998) (Weizsacker 1988) and plane strain (Soualmi 1997) (Wan 2001) (Cheng 1993). The use of most of these modelling features can be justified, as follows:

Linear elasticity: When performing IVUS elastography, the measured arterial strains are low, i.e., the strain between two consecutive IVUS RF frames is less then 2.5%. Consequently, only a small part of the artery's non-

linear stress-strain behaviour is used and the arterial deformation can, therefore, be considered locally linear.

Incompressibility

According to Carew et al. (Carew 1968) arteries may be considered incompressible. Furthermore, our group has demonstrated (Baldewsing 2004a) that Poisson's ratio variations of vulnerable plaques, in the range 0.49-0.49999, had no significant influence on the strain pattern and strain values in simulated elastograms of those plaques.

Isotropy

Although arteries are anisotropic (i.e., their radial, circumferential and/or longitudinal Young's modulus values are different) when their deformation is considered over an intraluminal pressure range of 0 mmHg up to 200 mmHg (Yamada 1970), anisotropy can be considerably less prevalent when focusing on *in vivo* physiological intraluminal pressures. For example, Weizsacker and Pinto (Weizsacker 1988) showed that the overall response of vascular tissue is highly non-linear and anisotropic. However, they also concluded that for the range of deformations that occur *in vivo*, the arterial wall can be considered as incrementally isotropic. Furthermore, our group (Baldewsing 2004b) has demonstrated that a linear elastic, isotropic, nearly incompressible, plane strain constitutive material model can appropriately simulate the arterial small-strain behaviour within the physiological intraluminal pressure range during IVUS elastography measurements of atherosclerotic arteries *in vitro*. Furthermore, when isotropy may not be a good approximation for a certain artery, it is still likely that the erroneous reconstructed isotropic Young's moduli show a diagnostically useful stiffness contrast between the lipid pool and the media/cap components, merely because this contrast is large for real plaque components.

2D Plane Strain

A deforming 3D arterial tubular segment is in a condition of '2D plain strain' when those cross-sections that are perpendicular to its longitudinal axis exhibit only strains in the cross-sectional plane (e.g., circumferential and radial strain) and no strain in the direction perpendicular to it (e.g., longitudinal strain). Most large healthy vessels that do not suffer from external forces, maintain a constant longitudinal length *in vivo* due to the constraint provided by arterial side branches and perivascular connective tissue (Dobrin 1987). Consequently, the condition of '2D plane strain' is defendable for such vessels. However, for atherosclerotic coronary arteries

wrapped around the heart, this condition may not always be applicable because the following sources may introduce an unknown distribution of tensile and compressive longitudinal strain throughout some cross-sections: (i) deformation of the heart (ii) curvature of the coronary longitudinal axis (iii) longitudinal coronary plaque dimensions that are smaller than the diameter of the coronary. These longitudinal strains may result in an erroneous reconstruction when assuming a '2D plain strain' condition. Future comparative 3D-versus-'2D plane strain' simulation studies are needed to estimate the influence of those longitudinal strain sources.

Homogeneity

The lipid, cap and media plaque component regions were each assumed to be homogenous, i.e., within a region they had the same Young's modulus value. Many other groups have applied this homogeneity assumption for simulating stress within atherosclerotic plaques or for reconstructing their material properties, e.g., (Beattie 1998) (Chandran 2003) (Lee 1994) (Cheng 1993) (Hayashi 1997). We have deliberately required the homogeneity of each plaque component for the following reasons: (i) The assumption of homogeneity makes it possible to characterize each of the three plaque components by just one material parameter (i.e., Young's modulus). If this assumption would be dropped, then many moduli would be required for approximating the arterial Young's modulus distribution, namely one modulus for each small finite element in the arterial cross-section. A low number of reconstruction parameters is needed to increase the chance for obtaining a stable (i.e., highly unique and not overly sensitive to local minima) reconstruction (ii) For clinical applications, a clinician is aided by an arterial stiffness image that is fast and easy to interpret. The assumption of homogeneity contributes to that purpose. Of course, the drawback of the homogeneity assumption is that it narrows the class of plaques that can be reconstructed.

PFEM Geometric Features

In this study we have used an idealized thin-cap fibroatheroma as PFEM for a plaque; the borders of its plaque components are delineated with circles. This PFEM is a variation of the PFEM model used by Loree et al. (Loree 1992). It has only 15 parameters (i.e., three for each of the four PFEM circles and a Young's modulus for the each of the three plaque components), but can still model the

diagnostically important class of vulnerable plaques, having as morphological features a media area containing a lipid pool which is covered by a cap (Virmani 2002+2003). Although there exist other types of vulnerable plaques, such as eroded plaques or plaques containing calcified nodules, the idealized thin-cap fibroatheroma (TCFA) has been used as geometric model for the PFEM for the following reasons.

(i) TCFAs are considered to be the precursor lesion of rupture and they account for the majority of plaque rupture (Virmani 2002).

(ii) The use of an idealized thin-cap fibroatheroma PFEM, should be considered as a trade-off between (a) an important class of stably reconstructable plaques, namely the TCFAs and (b) a large class of non-stable reconstructable plaques.

(iii) The use of a circle for the PFEM lumen is an approximation for the lumen geometries of vulnerable plaques.

Non-obstructing vulnerable plaques have an almost perfect circular lumen

This approximation is not only practical for computational purposes (i.e., closed-form, analytical formulas are available for computing the dynamic control points of the PFEM in fig. 2A), but it is also often a good approximation for the shape of the lumen: IVUS studies have shown that normal arteries have an almost perfect circular lumen border (Nissen 1991). Furthermore, IVUS and pathological studies (Losorodo 1994) (Glagov 1987) have shown that during the accumulation of plaque within the normal vessel wall, arteries exhibit 'compensatory enlargement' or 'outward/positive remodelling', i.e., the lumen cross-sectional area is maintained while plaque accumulates; this compensation is maintained up to the point were the plaque area occupies approximately 40% of the (vessel wall + lumen) area. These observations, may partly explain why, during clinical trials, our group often observes that the majority of non-obstructing vulnerable plaques have an almost perfect circular lumen. Indeed, there does exist a small class of vulnerable plaques whose lumen shape is far from perfectly circular. For such plaques the application of a different, advanced PFEM model, whose lumen and/or media borders are manually traced or automatically contour-detected from the IVUS echogram, might be an appropriate solution. This is, however, at the expense of more processing, since

no closed-form solutions are then available for computing the dynamic control points P, R, S and U of the PFEM in fig. 2A.

(iv) Delineation of PFEM plaque component borders by curve-parameterizations other than circles (e.g., ellipses) potentially allows a closer approximation of arbitrarily shaped plaque components. However, the use of such parameterizations requires more defining parameters (e.g., an ellipse is described by 5 defining parameters, a circle by only 3). This will decrease the chance for obtaining a successful reconstruction, i.e., finding a reconstruction with a PFEM elastogram that highly resembles the measured elastogram, since a PFEM with more parameters, will introduce more local minima and will increase the non-uniqueness of a reconstruction.

The more non-circular the real lumen is, the more unreliable the reconstructed moduli are

The more non-circular the real lumen is, the more unreliable the reconstructed moduli are when using a circle for the PFEM lumen. This is due to local eccentricities that may cause local circumferential stress concentrations/spreading and, consequently, result in local increases/decreases of radial strain values, an effect that cannot be accounted for by the current PFEM. Nevertheless, the reconstruction results from the phantom and the simulated plaque that was traced from histology, demonstrated that a good approximation of both the geometry and Young's moduli for each plaque component was still possible, despite the fact that these components, including the lumen and media border, were not delineated by circles. A discrepancy in circularity between media borders is not expected to be of much impact, since the stress and strain are there much lower than near the lumen (due to natural stress decay caused by the circumferential geometry of the vessel wall).

Initialization Strategy

To maximize the chance for obtaining a successful reconstruction, all practically available *a priori* information in echograms and elastograms should be used to define an initial state for the PFEM: the lipid circle should be positioned towards the direction of plaque thickening. This strategy was applied for all reconstructions. Radial strain patterns in elastograms also indicate possible configurations for the PFEM components that will likely produce a PFEM elastogram that resembles the measured elastogram. This strategy was ap-

plied to improve the reconstruction in fig. 7. Finally, a Young's modulus contrast between the lipid and media/cap plaque components was used in all reconstructions (in fig. 3, the reconstruction was also successful without using initial Young's modulus contrast).

The closer the initial Young's modulus values are chosen to the actual values of the plaque components, the higher the chance for obtaining a successful and correct reconstruction. However, a reasonable initial choice is not practically retrievable from literature, since those values are too widespread (e.g., table 2). Thus, to determine reasonable initial values for a specific *in vitro* or *in vivo* situation, first multiple reconstructions should be performed for one plaque, using a wide range of different initial values for each plaque component, similar as was done for the *in vivo* human coronary plaque reconstruction. Then, the moduli of the most successful reconstruction can be used as a practical initial choice for reconstructions with other plaques.

Judgment of Reconstruction

The reconstruction method uses a minimization algorithm

The reconstruction method uses a minimization algorithm to find a local minimum of the RMS error between the simulated or measured elastogram and the PFEM elastogram. Without knowing the actual plaque composition one does not know how good a successful reconstruction approximates it or if a global minimum has been found. To get an indication if a global minimum has been found one may perform multiple reconstructions with different initial states and check if the majority of successful reconstructions approximate one Young's modulus image. The only way to judge how good a reconstruction approximates the actual unknown plaque composition is by comparing the similarity of structural patterns (e.g., regions of high and low radial strain) in both elastograms. This strategy was applied for the reconstruction using the *in vivo* measured elastogram

.

Uniqueness

A low RMS error might be a good criterion for selecting a successful reconstruction

The reconstruction results for the first three plaques (i.e., two simulated arteries and the phantom) have demonstrated that the reconstruction method can successfully approximate the geometry and stiffness of plaque components. However, it was not demonstrated or proven that these reconstructions were unique. Theoretically it is possible that different PFEM geometries and/or moduli of the plaque components give a similar PFEM strain elastogram or a very different PFEM strain elastogram that has the same RMS error (Barbone 2004). Practically, this seems highly unlikely because of the strong geometrical constraints that are imposed upon the PFEM model. The results from the *in vivo* case support this hypothesis because they demonstrated that the level of uniqueness for a successful reconstruction was high with respect to (i) the morphology of the reconstructed plaque components and (ii) the reconstructed stiffness contrast between the lipid pool and other two stiffer components. However, with respect to the absolute values of the reconstructed moduli of the stiff plaque components, the uniqueness level was only moderately high. Furthermore, from the 30 reconstructions that were performed, only those reconstructions with the lowest RMS errors were successful; this suggests that a low RMS error might be a good criterion for automatically selecting the most successful reconstruction(s) from a set of reconstructions.

Clinical implications and applications

A new way of intravascular tissue characterization

The current results suggest that our reconstruction method is a new way of intravascular tissue characterization that may be suitable for clinical applications, such as (i) tissue characterization: to allow the selection of proper interventional procedures and (ii) monitoring of atherosclerosis: to quantify the effect of pharmaceutical treatments aimed at stabilizing plaques, e.g., by stiffening (Loree 1994b) (Aikawa 1998) or reducing the lipids (Schartl 2001). Furthermore, this method allows investigation and explanation of strain artifacts in elastograms and it may be applied to quantify the amount of stiffening of arterial plaque components within the physiological intraluminal pressure range. Finally, this method only needs an elastogram as input. Therefore, any imaging modality capable of measuring elastograms may be used. Our reconstruction method

may potentially also be applied in other clinically relevant situations where circular objects are present in an almost homogeneous medium that is strained, e.g., superficial atherosclerotic arteries, such as the carotid or femoral.

Limitations

Although the presented reconstruction results are promising, there are still some issues related to the robustness of the reconstruction method that have to be quantified in future studies, such as

Measurement noise

(i) measurement noise: the results from the phantom and *in vitro* plaque showed that in the presence of measurement noise it was still possible to obtain a successful reconstruction. However, the contribution of measurement noise upon the degradation of a reconstruction has not been quantified.

Catheter position

(ii) Catheter position: the radial strain distribution in a simulated or measured elastogram depends upon the position of the catheter within the lumen (de Korte 1999). Consequently, different catheter positions within the same plaque result in different radial strain elastograms. Because these elastograms are different, it seems reasonable to expect that the corresponding reconstructions are different. However, this is unlikely, since the position of the catheter that is used for a simulation or measurement of an elastogram is also used in the PFEM.

CONCLUSION

A new reconstruction method is described for obtaining morphology and material composition images of arterial vulnerable plaques. This method reconstructs a Young's modulus image from a measured elastogram, i.e. radial strain image of a plaque, by iteratively matching an elastogram calculated with a parametric plaque finite element model to the measured elastogram. This method has successfully reconstructed Young's modulus images from elastograms that were

(i) simulated with finite element models of plaques,

(ii) measured from a synthetic plaque and

(iii) measured from an *in vitro* human coronary plaque. It has also been applied on an elastogram of a plaque measured *in vivo* in a patient.

Chapter 15

Consensus Statement

Based on:

Johannes A. Schaar, James E. Muller, John Ambrose, Juan J. Badimon, Eric Boersma, Renè Botnar, S. Ward Casscells, Antonio Colombo, Mat Daemen, Gerrit - Anne van Es, Erling Falk, Steven B. Feinstein, Pim J. de Feyter, Frank Gijsen, Giuseppe Giuffrida, Enrique Pablo Gurfinkel, Christian Hamm, Donald D. Heistad, Victoria L. Herrera, Joerg Herrmann, Albert Hofman, Ik Kyung - Jang, Samir Kapadia, Nicholas Kipshidze, Dominique de Kleijn, Michael J. Koenders, Rob Krams, Amir Lerman, Lars Lind, Elias Mallis, Frits Mastik, Kyouichi Mizuno, Marie - angèle Morel, Pedro R. Moreno, Andrew Newby, Gerard Pasterkamp, Evelyn Regar, Giuseppe Sangiorgi, Axel Schmermund, Paul Schoenhagen, Bernward A. Schoelkens, Yakov Schwartz, Patrick W. Serruys, Christodoulos I. Stefanadis, Gregg W. Stone, Corrado Tamburino, Jan Tuin, Shankar Vallabhajosula, Stefan Verheye, Geoffrey Vince, Renu Virmani, Pascal Vranckx, Allard C. van der Wal, Jan David Wald, Samuel Wickline, Robert L. Wilensky, Andrew Zalewski, Andreas M. Zeiher, Anton F. van der Steen
Consensus Statement of Second International Vulnerable Plaque Meeting, June 7-8, 2004, Taormina, Italy
submitted

A conference was held in which 75 participants from 12 countries spent two days reviewing progress in the field of research on the vulnerable atherosclerotic plaque. The discussions covered the pathophysiology, epidemiology, detection and treatment of this leading cause of cardiovascular morbidity and mortality.

The growing volume of research on this topic was apparent, as was substantial progress in many areas. There was general agreement that continued work in this area is essential because of the major progress in prevention of sudden cardiac death, non-fatal myocardial infarction, and stroke, that could be achieved, among those in the general population, and those already afflicted with cardiovascular disease. For those who are free of overt cardiovascular disease, the goal of this research is the identification of risk and preventive treatment of a first cardiac event. In those who have suffered a cardiac event and are studied in the catheterization laboratory, the goal is to lower their risk of a subsequent cardiac event to that of the general population. Prevention would be facilitated by improved determination of risk and initiatiation of treatment, including lifestyle changes, to stabilize vulnerable plaques that would otherwise be responsible for future events.

The participants identified the following areas in which research efforts should be accelerated:

Animal Models

Increased studies in existing animal models, especially the atherosclerotic Apo E deficient mouse, rabbit and pig.

Novel, robust animal models are needed to increase understanding of processes leading to formation and disruption of vulnerable plaques. This would facilitate identification of mechanism-based biomarkers, imaging and intervention strategies.

Characterization of the epidemiology

Improved characterization of the epidemiology of the disorder, including studies of autopsy material and plaques obtained at enderarterectomy

Development of diagnostic capabilities

Continued development of diagnostic capabilities using plasma markers, proteomics, gene expression and other non-invasive approaches that might be useful for screening, and invasive devices for precise evaluation of plaque characteristics.

Acceleration of Clinical Trials of Non-invasive Diagnostic Methods

Progress with, MSCT, MRI, PET/CT, EBCT and cardiovascular ultrasound enhanced with contrast agents now justifies more extensive study of these methods in patients to fully identify their potential for screening of the general population, identification of high-risk/vulnerable patients, and monitoring of therapy. Large trials in over 1,000s of individuals with follow-up studies to determine frequency of cardiovascular events are needed. The risks versus benefits of radiation exposure must be carefully considered for PET and CT methods.

Acceleration of Clinical Trials of Invasive Diagnostic Methods

Progress with many catheter-based invasive diagnostic devices, including those capable of assessing vascular function, was noted. These devices, which are in various stages of development, require further validation in clinical studies. The first level of validation required is the ability to differentiate signals from a disrupted (previously vulnerable) plaque from other plaques.

Once this capability is achieved, these devices should be tested for their ability to identify prospectively coronary artery plaques that are at increased risk of disruption, as determined by follow-up natural history studies. The most important endpoints for these studies are overall mortality, cardiovascular mortality, and documented non-fatal myocardial infarction. Other events such as unstable angina, PCI due to the presumed vulnerable plaque, and progression of stenosis and plaque volume are also of importance. These natural history trials will require studies in thousands of individuals followed for one or more years. They will be aided by the selection of individuals judged to be at high risk by other characteristics such as Framingham criteria, plasma markers and non-invasive findings. It is likely that successful identification of vulnerable plaque will require information from more than one modality. The focus of these

natural history trials should be on sites suspected to be vulnerable that are not associated with a flow limiting stenosis.

Features of Clinical Trials of Treatment of Vulnerable Plaque

It was noted that prior efforts to prevent cardiovascular disease through various pharmacologic treatments are likely to have achieved at least part of their positive effects through stabilization of vulnerable plaques, although these studies were conducted prior to availability of methods to characterize plaque vulnerability. Research is needed on novel pharmacologic approaches to stabilize vulnerable plaque.

The new vulnerable plaque diagnostic devices that are under development may assist pharmacologic studies by identifying high-risk groups in which randomized evaluation of a new therapy can be performed in a smaller number of patients.

It is possible that successful treatment of vulnerable plaque will require local as well as systemic therapy since focal areas of risk appear to be present. Stents offer promise for the treatment of vulnerable plaque, but their use for lesions producing less than 70% stenosis must take into account potential stent-related complications of subacute thrombosis and restenosis.

If an intracoronary diagnostic device could identify plaques at increased risk of disruption, treatment of the plaques with a stent or standard pharmacologic therapy could be randomly evaluated. At present, the available evidence does not justify routine stenting of non-flow limiting lesions because they are suspected to be vulnerable.

Summary

There has been considerable progress on vulnerable plaque research in the year since the First International Vulnerable Plaque Conference. Positive results in many areas indicate an increased likelihood that the goal of detection and treatment of vulnerable atherosclerotic plaque can be achieved. The goal is of increased importance because of the aging of the population.

An optimal rate of progress will require investment in the clinical trials that are now possible. The financial support and effort required to conduct these trials will be significant. Due to the magnitude of the disease public founding is recommended. However, if

these plaques, which are responsible for vast numbers of sudden deaths, myocardial infarctions and strokes, could be detected and treated before they cause disease, the costs of the trials, which should be supported by public funds as well as industry, would be more than justified by the great improvement in health throughout the world that would be achieved.

Part VI

Summary

Chapter 16

Discussion and Conclusion

Intravascular ultrasound palpography is a new imaging technique that allows visualization of the deformation of atherosclerotic plaques. The technique is based on principle of elastography that the strain as response of tissue to a mechanical force is dependent on its mechanical properties. Several techniques had been investigated (van der Steen 1998) to strain the vessel wall. Leaving the mechanical deformation to the intravascular pressure, which is reproducible, is occurring about sixty times per minute and is for free, seemed to be a reasonable idea.

Prior to this thesis it was formulated (de Korte 1998a) that elastography may have a place in detecting vulnerable plaques. The detection of vulnerable plaques is currently one of the major challenges in cardiology. Invasive and non-invasive techniques are currently evaluated and try to de-mystify the field. These techniques are reviewed in **chapter 1**.

Definitions

Agreement on nomenclature

The need for a well-accepted terminology and the outgrowth of the accompanying discussion is described in **chapter 2**. A group of investigators met for two days in Santorini, Greece, to discuss progress in the field of identification and treatment of high risk/vulnerable atherosclerotic plaques and patients. It was recognized that increased understanding of the pathophysiology of coronary thrombosis and onset of acute coronary syndromes has created the need for agreement on nomenclature. The participants spent considerable time discussing the topic and reached consensus on their own usage of the terms as described below. A culprit lesion in a cor-

onary artery can be considered, on the basis of angiographic, autopsy or other findings, to be responsible for the clinical event. In unstable angina, myocardial infarction and sudden coronary death, the culprit lesion is often a plaque complicated by thrombosis extending into the lumen.

Several forms of vulnerable plaques

Responsible for this event are several forms of plaques. An eroded plaque with loss and/or dysfunction of the lumenal endothelial cells leading to thrombosis. There is usually no additional defect or gap in the plaque, which is often rich in smooth muscle cells and proteoglycans. An inflamed thin-cap fibroatheroma (TCFA) is a plaque with a thin cap covering a lipid-rich, necrotic core. An inflamed TCFA is suspected to be a vulnerable plaque. A heavily calcified plaque, with the loss and/or dysfunction of endothelial cells over a calcified nodule makes the plaque vulnerable. This is the least common of the three types of suspected vulnerable plaques. The most common cause of thrombosis is an already ruptured plaque with deep injury with a real defect or gap in the fibrous cap that had separated its lipid-rich atheromatous core from the flowing blood, thereby exposing the thrombogenic core of the plaque. It was agreed that the terms high-risk plaque, vulnerable and thrombosis-prone plaque can be used as synonyms to describe a plaque that is at increased risk of thrombosis (or re-thrombosis). Since there is consensus on this terminology among several major scientists in the field, it is hoped that widespread adoption of this terminology may help communication between scientists throughout the field.

Validation in vitro

Human coronary and femoral arteries were used for in vitro validation

The foundation of this thesis was prepared by elastographic experiments, which were performed in excised human coronary (n=4) and femoral (n=9) arteries (de Korte 2000a). Data were acquired at room temperature at intraluminal pressures of 80 and 100 mmHg. Coronary arteries were measured using a solid state 20 MHz array catheter (Volcano, Rancho Cordova, CA, USA). Femoral arteries were investigated using a single element 30 MHz catheter (DuMed/EndoSonics, Rijswijk, The Netherlands). The rf-data were stored. The processing was done off-line. The visualized segments were stained on the presence of collagen, smooth muscle cells and macrophages. Matching of elastographic data and histology was performed using the IVUS echogram. The cross-sections were

segmented in regions (n=125) based on the strain value on the elastogram. The dominant plaque types in these regions (fibrous, fibro-fatty or fatty) were obtained from histology and correlated with the average strain and echo-intensity.

High strain values were co-localised with increased concentrations of macrophages

Mean strain values of 0.27%, 0.45% and 0.60% were found for fibrous, fibro/fatty and fatty plaque components. The strain for the three plaque types as determined by histology differed significantly (p=0.0002). This difference was independent on the type of artery (coronary or femoral) and was mainly evident between fibrous and fatty tissue (p=0.0004). The plaque types did not reveal echo-intensity differences in the IVUS echogram (p=0.992). Conversion of the strain into Young's modulus values resulted in 493kPa, 296 kPa and 222 kPa for fibrous, fibro/fatty and fatty plaques. Although these values are higher than values measured by Lee et al. (Lee 1992), the ratio between fibrous and fatty material is similar. Since fibrous and fatty tissue demonstrated a different strain value and high strain values were often co-localised with increased concentrations of macrophages, these results reveal the potential of identification of the vulnerable plaque features. This early validation work was done at room temperature, which rose continuously the question if this experiments could be translated into the "real world" since biological tissues may have at room temperature different material properties than in body temperature. We performed experiments **(chapter 3)** on specimens to determine the influence of freezing and measuring the tissues at room temperature (23 °C instead of 37 °C) on the elastic properties. Four human coronary, one carotid and one femoral arteries were first measured at 23 °C and next at 37 °C. Additionally they were stored at -80 °C for up to 24 h and finally measured at 23 °C. Qualitative and quantitative analysis of the elastograms obtained from fresh and frozen specimens measured at 23 °C revealed that storage of the specimen at -80 °C has no significant influence.

We concluded that in vitro experiments can be performed at room temperature after storage of the tissue at -80 °C without significant affection of the information with respect to measuring fresh ex vivo material at body temperature.

The most important step in the development of a vulnerable plaque is the rupturing process, which takes place at the surface of the tis-

sue. Since this acting force is applied on the lumen boundaries, a surface based assessment of the mechanical properties was developed. This robust technique is easier to interpret then elastograms and called palpography. Palpography derives mechanical information of the surface of the plaque, where the rupture may happen. This information is colour-coded and superimposed on the IVUS echogram.

Plaques, which are declared vulnerable in elastography, have a thinner cap than non-vulnerable plaques

From this point the identification of vulnerable plaques was of main interest making it necessary to perform additional validation **(chapter 4)**. Diseased coronary arteries (n=24) were measured in vitro. Palpographic data was acquired at intracoronary pressures of 80 and 100 mmHg. After the ultrasound experiments, the cross-sections were stained for collagen and fat, smooth muscle cells (SMC), and macrophages. In histology, a vulnerable plaque was defined as a TCFA. A plaque was considered vulnerable in elastography when a high strain region was present at the lumen-plaque boundary that was surrounded by low strain values. Using this definition, the vulnerability of the regions was assessed. We studied 54 cross sections. In histology, 26 vulnerable plaques and 28 non-vulnerable plaques were found; elastography was positive in 23 cases but negative in 3 cases. Non-vulnerable plaque were seen by histology in 28 cases and detected by elastography in 25 cases, but were falsely diagnosed as positive in 3 cases resulting in a sensitivity of 88%, and the specificity of 89% to detect vulnerable plaques defined as TCFA. Linear regression showed high correlation between the strain in caps and the amount of macrophages ($P<0.006$) and an inverse relation between the amount of smooth muscle cells and strain ($P<0.0001$). Plaques, which are declared vulnerable in elastography, have a thinner cap than non-vulnerable plaques ($P<0.0001$) (Schaar 2003a).

Taking together the evidence to detect tissue structures, which represent vulnerable plaques, we thought it is ethically justifiable to go into in vivo validation scenarios.

Validation in vivo

Iliac and femoral arteries of pigs were used for in vitro validation

IVUS elastography was validated in vivo **(chapter 5)** using an atherosclerotic Yucatan minipig (de Korte 2002a). External iliac and femoral arteries were made atherosclerotic by endothelial Fogarty denudation and subsequent atherosclerotic diet for the duration of 7 months. Balloon dilatation was performed in the femoral arteries and the diet was discontinued. Before termination, 6 weeks after balloon dilation and discontinuation of the diet, data were acquired in the external iliac and femoral artery in 6 Yucatan pigs. In total, 20 cross-sections were investigated. The tissue was strained by the pulsatile blood pressure. After the ultrasound experiments and before dissection, X-ray was used to identify the arterial segments that had been investigated by ultrasound. The specimens were frozen in liquid nitrogen. The cross-sections (7μm) were stained for collagen and macrophages. Plaques were classified as absent, as early fibrous lesion, as early fatty lesion or as advanced fibrous plaque. The mean strain in these plaques and normal cross-sections was determined to assess the tissue characterisation properties of the technique. Furthermore, the deformability of the acquisition was correlated with the presence of fat and macrophages. The deformability was characterised by the presence of a high strain region (strain is higher than 1%) at the lumen vessel-wall boundary.

High strain region had a high sensitivity (92%) and specificity (92%) to identify the presence of macrophages

Strains were similar in the plaque free arterial wall and the early and advanced fibrous plaques. Univariate Analysis of Variance revealed significantly higher strain values in cross-sections with early fatty lesions than in fibrous plaques ($p=0.02$) independently on the presence of macrophages. Although a higher strain value was found in plaques with macrophages than in plaques without macrophages, this difference was not significant after correction for fatty components. However, the presence of a high strain region had a high sensitivity (92%) and specificity (92%) to identify the presence of macrophages. Therefore, it was concluded that the tissue type dominates the mean strain value. Localised high strain values are related to local phenomena like inflammation.

Three-dimensional Palpography

During longitudinal monitoring of patients it is extremely difficult to find back the same spot

The distribution of the strain in the three dimensional geometry of an artery is an important tool to identify the presence of high strain spots **(chapter 6)**, the amount and the distribution. Especially, since the correlation between plaque vulnerability and parameters provided by the echogram is low, selection of cross-sections based on the IVUS echogram introduces selection bias and increases the chance to miss the vulnerable part. Additionally, during longitudinal monitoring of patients it is extremely difficult to find back the same spot after some months. Therefore, an acquisition method to get strain information of the full 3D coronary artery was developed.

Palpography has revealed excellent reproducibility

Experiments in rabbit aortas revealed that three-dimensional palpography is feasible in vivo. Despite the introduction of out-of-plane motion by the continuous pull back of the catheter, the similarity between successive frames acquired in the diastolic phase is high enough to calculate several palpograms per heart cycle. By combining these palpograms, one compound palpogram per heart cycle is determined (Doyley 2001). Furthermore palpography has revealed excellent reproducibility **(chapter 7)**. The region, in which palpography was performed two times, was defined on the basis of identifiable landmarks, such as side branches or edges of stents. This matching of these consecutive regions was done on the fundamental IVUS frames reconstructed from rf-data unaware of the palpographic results. In 14 patients 19 recordings with a length of 1.8 cm were done resulting in 909 sections to compare. Next to other statistical tests, which showed a good reproducibility the Blant-Altman test revealed a mean of 0.042 of strain differences with a standard deviation of 0.07. This data add evidence that palpography is a robust method to detect high strain spots in vivo.

Clinical application

AMI patients have significantly more high strain spots than stable patients

In a recent study in humans **(chapter 8)** three-dimensional palpograms were derived from continuous intravascular ultrasound pullbacks of entire coronary arteries. Patients (n=55) were classified by clinical presentation as having stable angina, unstable angina, or AMI. In every patient, one coronary artery was scanned (culprit vessel in stable and unstable angina, non-culprit vessel in AMI), and

the number of deformable plaques assessed. Stable angina patients had significantly fewer deformable plaques per vessel (0.6±0.6) than unstable angina patients (p<0.0019) (1.6±0.7) or AMI patients (p<0.0001) (2.0±0.7). Levels of C-reactive protein were positively correlated with the number of mechanically deformable plaques (R2=0.65, p<0.0001) (Schaar 2004a).

For further qualification in the clinical setting palpography took part in the IBIS (Integrated Biomarker and Imaging Study) trial **(chapter 9)**.

The SMS-Index describes the extent of highly deformable plaques and is taken as a measure for vulnerability

IBIS is a prospective, single-center, non-randomized, observational study The aim of the study was to evaluate both invasive (quantitative coronary angiography, intravascular ultrasound (IVUS) and palpography) and non-invasive (multislice spiral computed tomography) imaging techniques to characterize non-flow limiting coronary lesions. In addition, multiple classical and novel biomarkers were measured and their levels correlated with the results of the different imaging techniques. Strain values were classified according to the ROC classification (ROtterdam Classification) as low strain spots (ROC I: 0.0 - <0.6%), moderate strain spots (ROC II: 0.6 - <0.9%), medium strain spots (ROC III: 0.9 - <1.2%), or high strain spots (ROC IV: >1.2%). In the region of interest (ROI) the number of ROC III and IV scores were characterized using the Schaar-Mastik-van der Steen- (SMS)-Index. It was calculated as the number of ROC III and IV scores that were measured in the ROI at cross-sections positioned uniformly over the length of the ROI and averaged over the number of those cross-sections and finally multiplied by 10 to arrive at a value with an appealing range. This SMS-Index describes the extent of highly deformable plaques and is taken as a measure for vulnerability e.g. in a specific coronary artery.

The main findings of this trial **(chapter 10)** regarding palpography were consistent with other observations that there are widespread abnormalities, in non-culprit vessels or remote myocardium of patients with acute coronary syndromes. The high prevalence of structurally vulnerable plaque found in this study, together with post-mortem observations showing clinically silent plaque rupture is relatively common suggesting that isolated rupture is unlikely to account for rather infrequent ischemic events. Furthermore this study

demonstrates that, within arbitrarily selected segments of non-culprit vessels, structurally vulnerable plaques were quite common, despite only mild angiographic disease. It confirms our previous observations that patients with STEMI have a significantly higher number of structurally vulnerable plaques than other patients with different presentations, in coronary regions remote from the site of occlusive thrombosis.

After 6 month the SMS-index has not changed for patients with stable and unstable angina, but is significantly reduced in the group of patients with myocardial infarction.

After 6 month we have investigated the patients of IBIS again **(chapter 11 and chapter 12)**. This is the first clinical follow up study using 3D palpography. This pilot study was performed blinded to assess (a) the change of the SMS-index and (b) the change of individual ROC scores, as well as (c) their relation to clinical presentation. After 6 month the SMS-index has not changed for patients with stable and unstable angina, but is significantly reduced in the group of patients with myocardial infarction. This may be due to the fact that patients in the latter group were presented at index with a therapy regime, which was extensively modified after initial interventional treatment. Furthermore this data support the hypothesis that vulnerability is a pan-artery process (Buffon 2002) and current treatment regimes can reduce it, but not eliminate it taking into account that at follow up the SMS index was not significantly different between the groups.

Future applications

The process of plaque stiffening can be monitored using intravascular palpography

On the end all acute coronary syndromes are related to thrombotic events. Intravascular palpography, by its capacity to evaluate the mechanical properties of biological tissues, can detect e.g. thin-cap fibroatheromas, but 25% of all myocardial infarctions are caused by wall standing thrombi. We used an animal model **(chapter 13)** inducing electric vascular injury, which generates platelet-rich thrombi similar to that observed in the coronary arteries of patients with acute myocardial infarction. The major findings of this study are that a thrombus gets stiffer over time and a vast part of the organization process takes place within 20 min. after thrombus introduction and that this process can be monitored using intravascular palpography. The clinical application of this in vivo animal model has yet to be defined.

Palpography can not be used for tissue characterization

The future of intravascular diagnostic ultrasound will be tissue characterization. This can not be done by conventional IVUS or an IVUS related technique like palpography or elastography. This is mainly due to the fact that the arterial stress distribution is unknown and data cannot be directly translated into a morphological and compositional image. To overcome this limitation we have developed a method that reconstructs a Young's modulus image from an elastogram **(chapter 14)**. The reconstruction of the plaque is done by a minimization algorithm that matches the strain image output, calculated with a Parametric Finite Element Model (PFEM) representation of a TCFA, to an elastogram by iteratively updating the PFEM geometry and material parameters. This method has successfully reconstructed Young's modulus images from elastograms that were (i) simulated with finite element models of plaques, (ii) measured from a synthetic plaque and (iii) measured from an in vitro human coronary plaque. It has also been applied on an elastogram of a plaque measured in vivo in a patient. This new technique called modulography may develop into a reliable and robust technique to give us information about plaque content.

Vulnerable Plaque: Quo Vadis?

The directions along which the vulnerable plaque field may move into the future are expressed in a consensus statement of the leading vulnerable plaque experts **(chapter 15)**. There has been considerable progress on vulnerable plaque research in the last years. Positive results in many areas indicate an increased likelihood that the goal of detection and treatment of vulnerable atherosclerotic plaque can be achieved. The goal is of increased importance because of the aging of the population. Novel, robust animal models are needed to increase understanding of processes leading to formation and disruption of vulnerable plaques. These models could be tested for new invasive and non-invasive detection modalities and would serve as a base for clinical trials. These clinical trials have to address the stabilization process of plaques, e.g. by local as well as systemic therapy, but also their natural history. An optimal rate of progress will require investment in the clinical trials that are now possible. The financial support and effort required to conduct these trials will be significant.

Palpography: Quo Vadis?

The current limitations of the technique will guide us to further development of the technique. An issue is motion artifacts, which are caused by longitudinal motion of the catheter along the coronary artery, but also by rotational motion along the axis of the catheter. Furthermore motion is created by the pull-back procedure. Since the palpogram is calculated from two different radio frequency lines that are obtained from the same Region Of Interest (ROI) at different pressures, motion may inhibit finding the same ROI in both images. If this is the case there will be a missing value at this location in the palpogram. Motion detection and compensation will play an important role in near future palpography development. Using procedures like balloon inflation to stabilize the catheter seem to be clinically too complicated and may hinder the use in the daily practice.

Palpograms may be difficult to interpret by users since it gives a new parameter, which was not yet used in the clinic. A more objective way and simplified way to describe strain data may be useful to develop, which only highlights the high strains spots, which relate to vulnerable plaques. This may enhance practicability and reduce intra- and inter observer variability.

Furthermore, like all new evolving techniques, it will be fully integrated into the catheterization laboratory. A fully integrated cath lab will allow data and image fusion between modalities and the concomitant opportunities for clinical and pathophysiological cardiovascular research.

Palpography is an extensively validated technique, but so far the validation has been performed in just one centre. At present it is extended to multiple centres, which will reveal shortcomings, but also new opportunities for this technology.

Conclusion

Intravascular ultrasound palpography is a new technique capable to provide strain data of the vessel surface. Palpography:

- can detect inflamed thin cap fibroatheromas in vitro with a high sensitivity and specificity
- can detect fatty plaques with an increased mean strain value.
- can detect high-strain spots that are associated with the presence of macrophages
- can measure strain in three-dimensions in the coronary artery
- is reproducible
- can be applied in the clinic and detect high strains spots in follow up trials
- can detect thrombus age

Chapter 17

Discussie en Samenvatting

Intravasculair ultrageluid palpografie is een nieuwe afbeeldingstechniek die visualisatie toelaat van de deformatie van atherosclerotische plaques. De techniek is gebaseerd op het principe van elastografie, dat de deformatie van weefsel als gevolg van een mechanische kracht afhangt van zijn mechanische eigenschappen. Verschillende technieken zijn onderzocht om de vaatwand te vervormen. Het leek een redelijke gedachte om de mechanische vervorming over te laten aan de intravasculaire druk, die reproduceerbaar is, ongeveer zestig keer per minuut op treedt en kosteloos beschikbaar is.

Voorafgaand aan dit proefschrift, was reeds gesteld (de Korte 1998a) dat elastografie mogelijkerwijs een rol kan spelen in de detectie van vulnerabele plaques. Detectie van vulnerabele plaques is tegenwoordig een van de grootste uitdagingen in de cardiologie. Invasieve en niet-invasieve technieken worden op dit moment geevalueerd en deze proberen het onderzoeksgebied te de-mystificeren. Deze technieken worden nader bekeken in **hoofdstuk 1**.

Definities

Overeenstemming nomenclatuur

De vraag naar een algemeen geaccepteerde terminologie en de bijbehorende discussie wordt beschreven in **hoofdstuk 2**. Een groep van onderzoekers ontmoette elkaar voor twee dagen in Santorini Griekenland, om de voortgang in het veld van identificatie en behandeling van hoge risico/vulnerabele atherosclerotische plaques en patiënten te bediscussiëren. Het werd onderkend dat een verbeterd begrip van de pathofysiologie van coronair trombosis en het begin van acute coronair syndromen de vraag naar overeenstemming over nomenclatuur had gecreëerd.

De deelnemers besteden aanzienlijke tijd om het onderwerp te bediscussiëren en bereikten consensus over hun eigen gebruik van de termen zoals hieronder beschreven. Op basis van angiografie, autopsie of andere bevindingen, kan een verdachte laesie in een coronair vaatwand worden beschouwd als verantwoordelijk voor een klinische gebeurtenis. Bij onstabiele angina, myocard infarct en plotselinge dood door hartfalen, is de verdachte laesie vaak een plaque gecompliceerd door trombosis die doorloopt tot in het lumen.

Verschillende verschijningsvormen van vulnerabele plaques

Een aantal typen plaques zijn verantwoordelijk voor deze gebeurtenis. Een geërodeerde plaque met verlies en/of ontregeling van de luminale endotheelcellen leidend tot trombosis. Er is meestal geen additioneel defect of gat in de plaque die vaak rijk is aan gladde spiercellen en proteoglycans. Een ontstoken dunne-kap fibroatherma (TCFA) is een plaque met een dunne kap die een vet-rijk, necrotisch gebied bedekt. Een ontstoken TCFA wordt ervan verdacht een vulnerabele plaque te zijn. Een zwaar gecalcificeerde plaque, met verlies en/of ontregeling van endotheel cellen over een gecalcificeerde nodule maken de plaque kwetsbaar. Dit is het minst vaak voorkomende van de drie types plaque die ervan verdacht worden vulnerabel te zijn. De meest voorkomende oorzaak van trombosis is de ruptuur van een plaque met diepe schade waarbij een echte defect of gat in de fibreuze kap is ontstaan, die de lipide-rijke atheromateuze kern niet meer scheidt van de bloedbaan en dus de trombogene kern van de plaque bloot legt. Er werd overeengekomen dat de termen hoge-risico plaque, vulnerabele en trombosisvatbare plaque als synoniemen te gebruiken zijn voor de beschrijving van een plaque die een verhoogd risico van trombosis (of hertrombosis) heeft. Aangezien er een overeenstemming is bereikt over deze terminologie, tussen een aantal belangrijke wetenschappers in dit onderzoeksgebied, wordt er gehoopt dat een wijdverbreide ingebruikname van deze terminologie de communicatie tussen wetenschappers over het gehele onderzoeksgebied zal verbeteren.

Validatie in vitro

Humane coronairen en femoraal arteriën werden gebruikt voor invitro validatie

De basis van dit proefschrift werd voorbereid door elastografische experimenten, die ex-vivo werden uitgevoerd op humane coronair (n=4) en femoraal (n=9) arteriën(de Korte 2000a). Data werd verkregen bij kamertemperatuur bij een intraluminale druk van 80 en 100 mmHg. Coronair arteriën werden gemeten met een elektronisch gestuurde 20 MHz array catheter (Volcano, Rancho Cordova, CA, USA). Femoraal arteriën werden onderzocht met een enkelelements 30 MHz catheter. De rf-data werd opgeslagen. De processing werd off-line gedaan. De gevisualiseerde segmenten werden histologisch gekleurd voor de aanwezigheid van collagen, gladde spiercellen en macrofagen. Vergelijken van de elastografische data en histologie werd gedaan met behulp van het IVUS echogram. De doorsneden werden gesegmenteerd in gebieden (n=125) op basis van de strain waarde in het elastogram. De dominante plaque typen in deze gebieden (fibreus, fibreus-lipoïde of lipoïde) werden bepaald met de histologie en gecorreleerd met de gemiddelde strain en echo-intensiteit.

Hoge strain waarden vielen samen met verhoogde concentraties van macrofagen

Gemiddelde strain waarden van 0.27%, 0.45% en 0.60% werden gevonden voor fibreuze, fibreus-lipoïde of lipoïde plaque componenten. De strain waarde voor de drie plaque typen zoals bepaald met histologie verschilden significant (p=0.0002). Dit verschil was onafhankelijk van het type vaatwand (coronair of femoraal) en was hoofdzakelijk duidelijk tussen fibreus en lipoïde weefsel (p=0.0004). De plaque typen lieten geen echo-intensiteit verschillen in het IVUS echogram (p=0.992) zien. Omzetting van de strain naar Young's modulus resulteerde in 493kPa, 296 kPa en 222 kPa voor fibreuze, fibreus-lipoïde of lipoïde plaque componenten. Alhoewel deze waarden hoger zijn dan de waarden gemeten door Lee et al (Lee 1992), is de ratio tussen fibreus en lipoïde materiaal ongeveer hetzelfde. Aangezien fibreus en lipoïde weefsel een verschillende strain waarde toonden en hoge strain waarden vaak colokaliseerden met een verhoogde concentratie van macrofagen, laten deze resultaten de potentie zien om de eigenschappen van vulnerabele plaques te identificeren. Dit eerste validatie werk was uitgevoerd bij kamertemperatuur, hetgeen herhaaldelijk de vraag opperde of deze experimenten konden worden vertaald naar de “echte wereld”, aangezien biologisch weefsel bij kamertemperatuur andere materiaal eigenschappen kan hebben dan bij lichaamstem-

peratuur. Experimenten werden uitgevoerd (**hoofdstuk 3**) op specimens om de invloed te bepalen, op de elastische eigenschappen, van het bevriezen en van het meten van de weefsels op kamertemperatuur (23°C in plaats van 37 °C). Vier humane coronairen, een carotid en een femoraal arterie werden eerst gemeten bij 23°C en daarna bij 37 °C. Daarnaast werden ze voor 24 uur opgeslagen bij -80 °C en uiteindelijk gemeten bij 23 °C. Kwalitatieve en kwantitatieve analyse van de elastogrammen verkregen van verse en bevroren specimens gemeten bij 23 °C toonden aan dat het opslaan van de specimens bij -80 °C geen significante invloed had.

We concludeerden dat in vitro experimenten kunnen worden uitgevoerd bij kamertemperatuur na opslag van weefsel bij -80 °C zonder daarbij een significante invloed te hebben op de informatie ten aanzien van het meten van vers ex vivo materiaal bij lichaamstemperatuur.

De belangrijkste stap in de ontwikkeling van een vulnerabele plaque is het scheurings proces, hetgeen plaatsvindt aan het oppervlak van het weefsel. Aangezien de krachten die optreden aangrijpen op het lumen oppervlak, werd er een oppervlakte gebaseerde techniek ontwikkeld om de mechanische eigenschappen te meten. Deze robuuste techniek is gemakkelijker te interpreten dan een elastogram en wordt palpografie genoemd. Palpografie leid mechanische informatie af van het opppervlak van de plaque, daar waar de scheuring kan optreden. Deze informatie wordt kleur-gecodeerd en gesuperponeerd op het IVUS echogram.

Plaques die vulnerabel waren in elastografie, hebben een dunnere kap dan niet vulnerabele plaques

Vanaf dit moment was het de hoofdzaak om vulnerabele plaques te identificeren, hetgeen een additionele validatie vereiste (**hoofdstuk 4**). Zieke coronairen (n=24) werden gemeten in vitro. Palpografische data werd verkregen bij een intra-coronaire druk van 80 en 100 mmHg. Na de ultrageluid experimenten, werden de cross-secties gekleurd voor collageen en vet, gladde spiercellen (SMC), en macrofagen. In histologie werd een vulnerabele plaque gedefinieerd als een TCFA. Een plaque werd beschouwd als vulnerabel in elastografie wanneer een hoog strain gebied aanwezig op de lumen-plaque grens en dit hoge strain gebied werd omringd door lage strain waarden. Met gebruikmaking van deze definitie werd de vulnerabiliteit van de gebieden bepaald. We bestudeerden 54 cross-secties. In histologie werden 26 vulnerabele plaques en 28 niet-vulnerabele

plaques gevonden; elastografie was positief in 23 gevallen maar negatief in 3 gevallen. Niet-vulnerabele plaques werden gezien in histologie in 28 gevallen en gedetecteerd door elastografie in 25 gevallen, maar vals gediagnostiseerd als positief in 3 gevallen, hetgeen resulteerde in een sensitiviteit van 88% en een specificiteit van 89% om een vulnerabele plaque, gedefinieerd als een TCFA, te detecteren. Lineaire regressie toonde hoge correlatie tussen de strain in kappen en de hoeveelheid macrofagen (P<0.006) en een inverse relatie tussen de hoeveelheid gladde spiercellen en strain (P<0.0001). Plaques, die werden geclassificeerd als vunerabel in elastografie, hebben een dunnere kap dan niet-vulnerabele plaques (P<0.0001)(Schaar 2003a).

Alle bewijs materiaal, om weefsel structuren te detecteren die vulnerabele plaques representeren, bij elkaar genomen, leek het ons ethisch verantwoord om ons naar in vivo validatie scenario's te begeven.

Validatie in vivo

Iliac en femoraal arteriën van varkens werden gebruikt voor in vitro validatie

IVUS elastografie werd gevalideerd in vivo (**hoofdstuk 5**) met behulp van het atherosclerotische Yucatan dwergvarken(de Korte 2002a). Externe iliac en femoraal bloedvaten werden atherosclerotisch gemaakt door middel van endotheel Fogarty denudatie en het daaropvolgende atherosclerotische dieet voor de duur van 7 maanden. Ballon dilatatie werd uitgevoerd in de femoraal vaten en het dieet werd gestopt. Voor het einde van het experiment, 6 weken na ballon dilatatie en het stoppen van het dieet, werd data opgenomen van de iliac en femoraal vaten in 6 Yucatan varkens. In totaal werden 20 cross-secties onderzocht. Het weefsel werd gedeformeerd door de pulserende bloeddruk. Na de ultrageluid experimenten en voordat er dissectie plaatsvond werd X-ray gebuikt om de vaatwand segmenten te identificeren die onderzocht waren met ultrageluid. De weefsel specimens werden bevroren in vloeibaar stikstof. De doorsneden (7μm) werden gekleurd voor collageen en macrofagen. Plaques werden geclassificeerd als afwezig, als vroeg fibreuze laesie, als vroeg lipoïde laesie of als een ontwikkelde fibreuze plaque. De gemiddelde strain in deze plaques en normale cross-secties werden bepaald om de weefsel karakteriserings eigenschappen van de techniek te bepalen. Daarnaast, werd de deformeerbaarheid van de acquisitie gecorreleerd met de aanwezigheid van vet en macrofagen.

De deformeerbaarheid werd gekarakteriseerd door de aanwezigheid van een hoog straingebied (strain hoger dan 1%) bij de lumen-vaatwand grens.

Hoge strain gebieden hadden een hoge sensitiviteit (92%) en specificiteit (92%) om de aanwezigheid van macrofagen te identificeren

Strain waarden waren vergelijkbaar in het plaque-vrije vaatwand en de vroege en ontwikkelde fibreuze plaques. Univariate analyse van variantie toonde een significant hogere strain waarde in cross-secties met vroege lipoïde laesies dan in fibreuze plaques ($p=0.02$) onafhankelijk van de aanwezigheid van macrofagen. Alhoewel een hogere strain waarde werd gevonden in plaques met macrofagen dan in plaques zonder macrofagen, was dit verschil niet significant na correctie voor lipoïde componenten. Echter, de aanwezigheid van een hoog straingebied had een hoge sensitiviteit (92%) en specificiteit (92%) om de aanwezigheid van macrofagen te identificeren. Daarom werd er geconcludeerd dat het weefsel type de gemiddelde strain waarde domineert. Gelokaliseerde hoge strain waarden zijn gerelateerd aan lokale verschijnselen zoals ontsteking.

Drie-dimensionale Palpografie

Gedurende longitudinale monitoring van patiënten is het extreem moeilijk om dezelfde plek terug te vinden

De verdeling van de strain in de drie dimensionale geometrie van een bloedvat is een belangrijk instrument om de aanwezigheid (**hoofdstuk 6**), het aantal en de verdeling van hoge straingebieden te identificeren. De selectie van cross-secties gebaseerd op het IVUS echogram introduceert selectie bias en verhoogt de kans om een vulnerabele plaque te missen, vooral omdat de correlatie tussen de kwetsbaarheid van een plaque en de parameters die uit het echogram kunnen worden gehaald laag is. Bovendien is het extreem moeilijk om na een aantal maanden dezelfde plek terug te vinden tijdens het langdurig monitoren van patiënten. Daarom is er een acquisitie methode ontwikkeld om de strain informatie van de volledige 3D coronair arterie te verkrijgen.

Palpografie heeft uitstekende reproduceerbaarheid laten zien

Experimenten in konijnen aorta's lieten zien dat drie-dimensionale palpografie mogelijk is in vivo. Ondanks de introductie van beweging uit het beeldvlak tijdens de continue terug-trekking van de catheter is de overeenkomst tussen opeenvolgende frames, die verkregen zijn in de diastolische fase, hoog genoeg om een aantal palpogrammen te berekenen per hart cyclus. Door het combineren van deze palpogrammen, word één samengesteld palpogram per hartcyclus bepaald (Doyley 2001). Verder heeft palpografie een uit-

stekende reproduceerbaarheid laten zien (**hoofdstuk 7**). Het gebied, waarin palpografie twee keer werd uitgevoerd, was gedefinieerd op basis van identificeerbare herkenningspunten, zoals zij-takken of stents. Deze matching van opeenvolgende gebieden werd gedaan met de onderliggende IVUS frames, die geconstrueerd waren vanuit de rf-data, zonder daarbij op de hoogte te zijn van de palpografische resultaten. In 14 patiënten werden 19 opnames gedaan met een lengte van 1.8cm hetgeen resulteerde in 909 secties om te vergelijken. Naast andere statistische tests, die een goede reproduceerbaarheid toonden, liet de Blant-Altmann test een gemiddeld strain verschil zien van 0.042 met een standaard deviatie van 0.07. Deze data levert additioneel bewijsmateriaal voor de stelling dat palpografie een robuuste methode is om in vivo hoge straingebieden te detecteren.

Klinische toepassing

AMI patiënten hebben significant meer hoge strain spots dan stabiele patiënten

In een recente studie in mensen (**hoofdstuk 8**) werden drie-dimensionale palpogrammen afgeleid van intravasculair ultrageluid opnamen gedurende een continue terugtrek beweging van de catheter door de gehele coronair arterie. Patiënten (n=55) werden geclassificeerd door middel van hun klinische presentatie, namelijk als zijnde stabiele angina, onstabiele angina of AMI. In elke patient werd een coronair gescand (het verdachte bloedvat in stabiele en onstabiele angina, het niet verdachte bloedvat in AMI), en het aantal deformeerbare plaques werd vastgesteld. Stabiele angina patiënten hadden significant minder deformeerbare plaques per bloedvat (0.6±0.6) dan onstabiele angina patiënten ($p<0.0019$) (1.6±0.7) of AMI patiënten ($p<0.0001$) (2.0±0.7). Het niveau aan C-reactieve proteine was positief gecorreleerd met het aantal mechanisch deformeerbare plaques ($R2=0.65$, $p<0.0001$)(Schaar 2004a).

Voor verdere kwalificatie in de klinische omgeving nam palpografie deel aan IBIS (Integrated Biomarker and Imaging Study) trial (**hoofdstuk 9**).

De SMS-index beschrijft hoe uitgebreid de aanwezigheid van hoog vervormbare plaques is en wordt gebruikt als een maat voor vulnerabiliteit

IBIS is een prospectieve, enkel centrum, niet gerandomiseerde, observationele studie. Het doel van de studie was evaluatie van zowel invasieve (kwantitatieve coronair angiografie, intravasculair ultrageluid (IVUS) en palpografie) als wel niet-invasieve afbeeldingstechnieken (multislice spiral computed tomography) voor karakterisatie van niet-stromings reducerende coronair laesies. Daarnaast werden een aantal klassieke als ook nieuwe biomarkers gemeten en hun niveau gecorreleerd met de resultaten van de verschillende afbeeldings technieken. Strain waarden werden geclassificeerd volgens de ROC classificatie (ROtterdam Classificatie) als een laag strain gebied (ROC I: 0.0 - <0.6%), matig strain gebied (ROC II: 0.6 - <0.9%), medium strain gebied (ROC III: 0.9 - <1.2%), of hoog strain gebied (ROC IV: >1.2%). In het gebied van interesse (ROI) werd het aantal ROC III an IV scores gekarakteriseerd met behulp van de Schaar-Mastik-van der Steen- (SMS)-Index. Deze werd berekend als het aantal ROC III en IV scores die werden gemeten in de ROI op regelmatig over de lengte van de ROI gepositioneerde cross-secties en gemiddeld over het aantal van deze cross-secties en vermenigvuldigd met 10 om een waarde te krijgen met een aantrekkelijk bereik. Deze SMS-index beschrijft de uitgebreidheid van hoog deformeerbare plaques en word beschouwd als een maat voor vulnerabiliteit van bijvoorbeeld een specifieke coronair arterie.

De belangrijkste bevindingen van deze trial (**hoofdstuk 10**) met betrekking tot palpografie waren consistent met andere waarnemingen van wijdverspreide abnormaliteiten in niet-verdachte bloedvaten of verder verwijderd myocardium van patiënten met acute coronair aandoeningen. De hoge prevalentie van structureel vulnerabele plaques die gevonden werden in deze studie, te samen met het relatief vaak voorkomen van post-mortem waarnemingen van klinisch onopgemerkte plaquescheuringen, suggereert dat het onwaarschijnlijk is dat geïsoleerde plaquescheuringen het nogal infrequente voorkomen van ischemische gebeurtenissen kan verklaren. Bovendien toonde deze studie aan dat, binnen een beperkte selectie van segmenten van niet-verdachte bloedvaten, structureel vulnerabele plaques een redelijk een normaal verschijnsel waren, ondanks een slechts beperkt angiografische ziektebeeld. Het bevestigt onze hypothese dat patiënten met STEMI een significant hoger aantal structureel vulnerabele plaques hebben dan patiënten met andere ziektebeelden in coronair gebieden verder weg gelegen van de plek van de afsluitende trombose.

Na 6 maanden was de SMS-index niet veranderd voor patiënten met stabiele en onstabiele angina, maar was significant verlaagd in de groep patiënten met een myocard infarct

Na 6 maanden hadden we de patiënten van IBIS opnieuw onderzocht (**hoofdstuk 11 en hoofdstuk 12**). Dit is de eerste klinische follow-up studie met 3D palpografie. Deze pilot studie werd blind uitgevoerd om vast te stellen (a) de verandering van de SMS-index (b) de verandering van individuele ROC scores, als ook (c) hun klinische presentatie. Na 6 maanden was de SMS-index niet veranderd voor patiënten met stabiele en onstabiele angina, maar wel significant veranderd voor de groep van patiënten met een myocard infarct. Dit zou verklaard kunnen worden uit het feit dat patiënten in de laatste groep na de initiële interventionele behandeling op een uitgebreid veranderd therapeutisch regime werden gesteld. Daarnaast versterkt deze data de hypothese dat vulnerabiliteit een panarterie proces is en dat huidige behandelings regimes het kan reduceren, maar niet elimineren, rekening houdend met het feit dat de SMS-index bij follow-up niet significant verschillend was tussen de groepen.

Toekomstige toepassingen

Het proces van plaque verharding kan gemonitord worden met intravasculaire palpografie

Uiteindelijk zijn alle acute coronair syndromen gerelateerd aan trombogene gebeurtenissen. Intravasculair palpografie kan, vanwege zijn vermogen om de mechanische eigenschappen van biologisch weefsels te evalueren, dunne-kap fibroatheromas detecteren, echter 25% van alle myocard infarcten worden veroorzaakt door thrombi die aan de vaatwand hechten. Wij gebruikten een dier model (**hoofdstuk 13**) waarbij elektrische vasculaire beschadiging werd geïnduceerd, hetgeen bloedplaatjes rijke thrombi genereerde, soortgelijk aan die zijn geobserveerd in coronair arteriën van patiënten met een acuut myocard infarct. De belangrijkste bevindingen van deze studie zijn dat een trombus stijver wordt in de loop der tijd en dat een groot gedeelte van het organisatie proces plaatsvindt binnen 20 minuten na de introductie van de trombus en dat dit proces gevolgd kan worden met intravasculaire palpografie. De klinische toepassing van dit in vivo dier model moet nog worden bepaald.

De toekomst van intravasculair diagnostisch ultrageluid zal weefsel karakterisatie zijn. Dit kan niet gedaan worden met conventionele IVUS of een aan IVUS gerelateerde techniek zoals palpografie of elastografie. Dit is hoofzakelijk te wijten aan het feit dat de spanningsverdeling in een vaatwand onbekend is en dat data niet direct vertaald kan worden naar een morfologisch en compositioneel

beeld. Om deze beperking te boven te komen, hebben we een methode ontwikkeld die een Young's modulus beeld vanuit een elastogram reconstrueert (**hoofdstuk 14**). De reconstructie van de plaque wordt gedaan door een minimaliserings algoritme die het gemeten elastogram iteratief vergelijkt met het strain beeld berekend met een Parameterisch Eindige Elementen Model (PFEM) representatie van een TCFA, waarvan de PFEM geometrie en materiaal parameters worden aangepast. Deze methode heeft succesvol Young's modulus beelden gereconstrueerd vanuit elastogrammen die waren (i) gesimuleerd met eindige elementen modellen van plaques, (ii) gemeten van een synthetische plaque en (iii) gemeten in vitro van een humane coronair. Het is ook toegepast op een in vivo gemeten elastogram van een plaque in een patient. Deze nieuwe techniek, genaamd modulografie, kan zich ontwikkelen tot een betrouwbare en robuuste techniek om ons informatie te verschaffen over de samenstelling van de plaque.

Vulnerabele Plaque: Quo Vadis?

De richtingen waarin het vulnerabele plaque onderzoeksgebied zich kan ontwikkelen in de toekomst worden aangeven in een consensus verklaring van de leidende vulnerabele plaque experts (**hoofdstuk 15**). De laatste jaren is er veel vooruitgang geboekt in het onderzoek aan vulnerabele plaque. Positieve resultaten in veel onderzoeksgebieden geven aan dat er een verhoogde kans is om het doel, detectie en behandeling van vulnerabele atherosclerotische plaques, te bereiken. Het doel is des te belangrijker vanwege de vergrijzing van de populatie. Nieuwe, robuuste dier modellen zijn nodig om het proces te begrijpen dat leid tot de formatie en verstoring van vulnerabele plaques. Deze modellen kunnen getest worden door nieuwe invasieve en niet-invasieve detectie modaliteiten en kunnen dienen als een basis voor klinische trials. Deze klinische trials dienen het stabilisatie proces van plaques te onderzoeken, bijv. door lokale en systemische therapie, maar ook hun natuurlijk verloop. Een optimale voortgang zal investeringen vereisen in de klinische trials die nu mogelijk zijn. De financiële ondersteuning en moeite die vereist zijn om deze trials uit te voeren zullen aanzienlijk zijn.

Palpografie: Quo Vadis?

De beperkingen van de techniek zullen ons leiden om de techniek verder te ontwikkelen. Een onderwerp is bewegings-artefacten, deze worden veroorzaakt door longitudinale beweging van de catheter door de coronair, maar ook door rotatie om de as van de catheter. Daarnaast wordt beweging geïnduceerd door de terug-trek procedure. Daar het palpogram berekend wordt uit twee rf-signalen die verkregen zijn uit dezelfde Regio van Interesse(ROI) bij verschillende drukken, kan beweging verhinderen dat de zelfde ROI gevonden wordt in beide beelden. Wanneer dit het geval is zullen er op deze locatie in het palpogram missende waarden verschijnen. Bewegings detectie en compensatie zullen een belangrijke rol spelen in de ontwikkeling van palpografie in de naaste toekomst.

Het gebruik van ballon inflatie om de beweging van de catheter te stabiliseren lijkt klinisch te gecompliceerd en kan het gebruik in de dagelijkse praktijk hinderen.

Palpogrammen kunnen verschillend worden geïnterpreteerd door gebruikers aangezien het een nieuwe parameter geeft, die nog niet gebruikt is in de kliniek. Het kan nuttig zijn een meer objectieve manier en simpeler manier om strain data weer te geven te ontwikkelen, waarbij alleen de hoge strain gebieden worden benadrukt die gerelateerd zijn aan vulnerabele plaques. Dit zou de praktische bruikbaarheid verhogen en de intra -en interwaarnemer variabiliteit reduceren.

Verder zal het, net als alle nieuwe zich ontwikkelende technieken, volledig geintegreerd worden in het catheterisatie laboratorium. Een volledig geïntegreerd cathlab zal het mogelijk maken data en beelden tussen modaliteiten te fuseren en aanvullende mogelijkheden bieden voor klinisch en pathofysiologisch cardiovasculair onderzoek.

Palpografie is een uitvoerig gevalideerde techniek, maar tot nu toe heeft deze validatie slechts in één centrum plaats gevonden. Momenteel wordt de techniek over meerdere centra gedistribueerd, hierdoor zullen tekortkomingen aan het licht komen, maar het zal tevens nieuwe mogelijkheden voor de techniek bieden.

Conclusie

Intravasculair ultrageluid palpografie is een nieuwe techniek die in staat is om strain data van het vaatwand oppervlak te leveren.

Palpografie:

- kan ontstoken dunne kap fibroatheromas detecteren in vitro met een hoge sensitiviteit en specificiteit.
- kan lipoïde plaques detecteren, die een verhoogde gemiddelde strain waarde hebben.
- kan hoge strain gebieden detecteren, die geassocieerd zijn met de aanwezigheid van macrofagen.
- kan in drie dimensies strain in de coronair meten.
- is reproduceerbaar.
- kan toegepast worden in de kliniek en kan hoge strain gebieden detecteren in follow-up trials.
- kan de trombus leeftijd detecteren.

Part VII
Bibliography

(Abbate 2004) A. Abbate, E. Bonanno, A. Mauriello, R. Bussani, G. G. Biondi-Zoccai, G. Liuzzo, A. M. Leone, F. Silvestri, A. Dobrina, F. Baldi, F. Pandolfi, L. M. Biasucci, A. Baldi, L. G. Spagnoli and F. Crea (2004). "Widespread myocardial inflammation and infarct-related artery patency." Circulation 110(1): 46-50.

(Achenbach 2004) S. Achenbach, D. Ropers, U. Hoffmann, B. MacNeill, U. Baum, K. Pohle, T. J. Brady, E. Pomerantsev, J. Ludwig, F. A. Flachskampf, S. Wicky, I. K. Jang and W. G. Daniel (2004). "Assessment of coronary remodeling in stenotic and nonstenotic coronary atherosclerotic lesions by multidetector spiral computed tomography." J Am Coll Cardiol 43(5): 842-7.

(Aikawa 1998) M. Aikawa, E. Rabkin, Y. Okada, S. J. Voglic, S. K. Clinton, C. E. Brinckerhoff, G. K. Sukhova and P. Libby (1998). "Lipid lowering by diet reduces matrix metalloproteinase activity and increases collagen content of rabbit atheroma: a potential mechanism of lesion stabilization." Circulation 97(24): 2433-44.

(Alpert 2000) J. S. Alpert, K. Thygesen, E. Antman and J. P. Bassand (2000). "Myocardial infarction redefined--a consensus document of The Joint European Society of Cardiology/American College of Cardiology Committee for the redefinition of myocardial infarction." J Am Coll Cardiol 36(3): 959-69.

(Altman 1997) D. G. Altman (1997). Practical Statistics for Medical Research. London, Chapman & Hall: 136-142.

(Ambrose 1988) J. A. Ambrose, M. A. Tannenbaum, D. Alexopoulos, C. E. Hjemdahl-Monsen, J. Leavy, M. Weiss, S. Borrico, R. Gorlin and V. Fuster (1988). "Angiographic progression of coronary artery disease and the development of myocardial infarction." J Am Coll Cardiol 12(1): 56-62.

(Ambrose 1991) J. A. Ambrose (1991). "Prognostic implications of lesion irregularity on coronary angiography." J Am Coll Cardiol 18(3): 675-6.

(Arampatzis 2003) C. A. Arampatzis, J. M. Ligthart, J. A. Schaar, K. Nieman, P. W. Serruys and P. J. de Feyter (2003). "Images in cardiovascular medicine. Detection of a vulnerable coronary plaque: a treatment dilemma." Circulation 108(5): e34-5.

(Arbab-Zadeh 1999) A. Arbab-Zadeh, A. N. DeMaria, W. F. Penny, R. J. Russo, B. J. Kimura and V. Bhargava (1999). "Axial movement of the intravascular ultrasound probe during the cardiac cycle: implications for three-dimensional reconstruction and measurements of coronary dimensions." Am Heart J 138(5 Pt 1): 865-72.

(Arbustini 1999) E. Arbustini, B. Dal Bello, P. Morbini, A. P. Burke, M. Bocciarelli, G. Specchia and R. Virmani (1999). "Plaque erosion is a major substrate for coronary thrombosis in acute myocardial infarction." Heart 82(3): 269-72.

(Arroyo 1999) L. H. Arroyo and R. T. Lee (1999). "Mechanisms of plaque rupture: mechanical and biologic interactions." Cardiovasc Res 41(2): 369-75.

(Asakura 1990) T. Asakura and T. Karino (1990). "Flow patterns and spatial distribution of atherosclerotic lesions in human coronary arteries." Circ Res 66(4): 1045-66.

(Asakura 2001) M. Asakura, Y. Ueda, O. Yamaguchi, T. Adachi, A. Hirayama, M. Hori and K. Kodama (2001). "Extensive development of vulnerable plaques as a pancoronary process in patients with myocardial infarction: an angioscopic study." J Am Coll Cardiol 37(5): 1284-8.

(Baldewsing 2004a) R. A. Baldewsing, C. L. De Korte, J. A. Schaar, F. Mastik and A. F. W. Van Der Steen (2004). "Finite element modeling and intravascular ultrasound elastography of vulnerable plaques: parameter variation." Ultrasonics 42(1-9): 723-729.

(Baldewsing 2004b) R. A. Baldewsing, C. L. de Korte, J. A. Schaar, F. Mastik and A. F. W. van der Steen (2004). "A finite element model for performing intravascular ultrasound elastography of human atherosclerotic coronary arteries." Ultrasound Med Biol 30(6): 803-813.

(Bank 1999) A. J. Bank (1999). "Intravascular ultrasound studies of arterial elastic mechanics." Pathol Biol (Paris) 47(7): 731-7.

(Baraga 1992) J. J. Baraga, M. S. Feld and R. P. Rava (1992). "In situ optical histochemistry of human artery using near infrared Fourier transform Raman spectroscopy." Proc Natl Acad Sci U S A 89(8): 3473-7.

(Barbone 2002) P. E. Barbone and J. C. Bamber (2002). "Quantitative elasticity imaging: what can and cannot be inferred from strain images." Phys Med Biol 47(12): 2147-64.

(Barbone 2004) P. E. Barbone and N. H. Gokhale (2004). "Elastic modulus imaging: on the uniqueness and nonuniqueness of the elastography inverse problem in two dimensions." Inverse Problems 20: 283-296.

(Bayes-Genis 2001) A. Bayes-Genis, C. A. Conover, M. T. Overgaard, K. R. Bailey, M. Christiansen, D. R. Holmes, Jr., R. Virmani, C. Oxvig and R. S. Schwartz (2001). "Pregnancy-associated plasma protein A as a marker of acute coronary syndromes." N Engl J Med 345(14): 1022-9.

(Beattie 1998) D. Beattie, C. Xu, R. Vito, S. Glagov and M. C. Whang (1998). "Mechanical analysis of heterogeneous, atherosclerotic human aorta." J Biomech Eng 120(5): 602-7.

(Bergel 1961) D. H. Bergel (1961). "The static elastic properties of the arterial wall." Journal of Physiology 156: 445-457.

(Biasucci 1996) L. M. Biasucci, A. Vitelli, G. Liuzzo, S. Altamura, G. Caligiuri, C. Monaco, A. G. Rebuzzi, G. Ciliberto and A. Maseri (1996). "Elevated levels of interleukin-6 in unstable angina." Circulation 94(5): 874-7.

(Bishop 2000) J. Bishop, A. Samani, J. Sciarretta and D. B. Plewes (2000). "Two-dimensional MR elastography with linear inversion reconstruction: methodology and noise analysis." Phys Med Biol 45(8): 2081-91.

(Blake 2003) G. J. Blake, R. J. Ostfeld, E. K. Yucel, N. Varo, U. Schonbeck, M. A. Blake, M. Gerhard, P. M. Ridker, P. Libby and R. T. Lee (2003). "Soluble CD40 ligand levels indicate lipid accumulation in carotid atheroma: an in vivo study with high-resolution MRI." Arterioscler Thromb Vasc Biol 23(1): e11-4.

(Bom 1998) N. Bom, W. Li, A. F. van der Steen, C. T. Lancee, E. I. Cespedes, C. J. Slager and C. L. de Korte (1998). "Intravascular imaging." Ultrasonics 36(1-5): 625-8.

(Boppart 1998) S. A. Boppart, B. E. Bouma, C. Pitris, J. F. Southern, M. E. Brezinski and J. G. Fujimoto (1998). "In vivo cellular optical coherence tomography imaging." Nat Med 4(7): 861-5.

(Botnar 2000) R. M. Botnar, M. Stuber, K. V. Kissinger, W. Y. Kim, E. Spuentrup and W. J. Manning (2000). "Noninvasive coronary vessel wall and plaque imaging with magnetic resonance imaging." Circulation 102(21): 2582-7.

(Brezinski 1997) M. E. Brezinski, G. J. Tearney, N. J. Weissman, S. A. Boppart, B. E. Bouma, M. R. Hee, A. E. Weyman, E. A. Swanson, J. F. Southern and J. G. Fujimoto (1997). "Assessing atherosclerotic plaque morphology: comparison of optical coherence tomography and high frequency intravascular ultrasound." Heart 77(5): 397-403.

(Brezinski 2001) M. Brezinski, K. Saunders, C. Jesser, X. Li and J. Fujimoto (2001). "Index matching to improve optical coherence tomography imaging through blood." Circulation 103(15): 1999-2003.

(Bridal 2000) S. L. Bridal, B. Beyssen, P. Fornes, P. Julia and G. Berger (2000). "Multiparametric attenuation and backscatter images for characterization of carotid plaque." Ultrason Imaging 22(1): 20-34.

(Browse 1999) N. L. Browse, K. G. Burnand, A. T. Irvine and N. M. Wilson (1999). Deep venous thrombosis: pathology. In: Disease of the veins. N. L. Browse, K. G. Burnand, A. T. Irvine and N. M. Wilson. London, Arnold: 249-289.

(Bruining 1998) N. Bruining, C. von Birgelen, P. J. de Feyter, J. Ligthart, W. Li, P. W. Serruys and J. R. Roelandt (1998). "ECG-gated versus nongated three-dimensional intracoronary ultrasound analysis: implications for volumetric measurements." Cathet Cardiovasc Diagn 43(3): 254-60.

(Bruining 2004) N. Bruining, R. Hamers, T. J. Teo, P. J. de Feijter, P. W. Serruys and J. R. Roelandt (2004). "Adjustment method for mechanical Boston scientific corporation 30 MHz intravascular ultrasound catheters connected to a Clearview console. Mechanical 30 MHz IVUS catheter adjustment." Int J Cardiovasc Imaging 20(2): 83-91.

(Brusseau 2002) E. Brusseau, J. Fromageau, N. G. Rognin, P. Delachartre and D. Vray (2002). "Investigating elastic properties of soft biological tissues." IEEE Eng Med Biol Mag 21(4): 86-94.

(Buffon 2002) A. Buffon, L. M. Biasucci, G. Liuzzo, G. D'Onofrio, F. Crea and A. Maseri (2002). "Widespread coronary inflammation in unstable angina." N Engl J Med 347(1): 5-12.

(Burke 1997) A. P. Burke, A. Farb, G. T. Malcom, Y. H. Liang, J. Smialek and R. Virmani (1997). "Coronary risk factors and plaque morphology in men with coronary disease who died suddenly." N Engl J Med 336(18): 1276-82.

(Burke 2001) A. P. Burke, F. D. Kolodgie, A. Farb, D. K. Weber, G. T. Malcom, J. Smialek and R. Virmani (2001). "Healed plaque ruptures and sudden coronary death: evidence that subclinical rupture has a role in plaque progression." Circulation 103(7): 934-40.

(Burke 2003) A. P. Burke, R. Virmani, Z. Galis, C. C. Haudenschild and J. E. Muller (2003). "34th Bethesda Conference: Task force #2--What is the pathologic basis for new atherosclerosis imaging techniques?" J Am Coll Cardiol 41(11): 1874-86.

(Burleigh 1992) M. C. Burleigh, A. D. Briggs, C. L. Lendon, M. J. Davies, G. V. Born and P. D. Richardson (1992). "Collagen types I and III, collagen content, GAGs and mechanical strength of human atherosclerotic plaque caps: span-wise variations." Atherosclerosis 96(1): 71-81.

(Buschman 2000) H. P. Buschman, E. T. Marple, M. L. Wach, B. Bennett, T. C. Schut, H. A. Bruining, A. V. Bruschke, A. van der Laarse and G. J. Puppels (2000). "In vivo determination of the molecular composition of artery wall by intravascular Raman spectroscopy." Anal Chem 72(16): 3771-5.

(Cannon 2004) C. P. Cannon, E. Braunwald, C. H. McCabe, D. J. Rader, J. L. Rouleau, R. Belder, S. V. Joyal, K. A. Hill, M. A. Pfeffer and A. M. Skene (2004). "Intensive versus moderate lipid lowering with statins after acute coronary syndromes." N Engl J Med 350(15): 1495-504.

(Carew 1968) T. E. Carew, R. N. Vaishnav and D. J. Patel (1968). "Compressibility of the arterial wall." Circ Res 23(1): 61-68.

(Casscells 1996) W. Casscells, B. Hathorn, M. David, T. Krabach, W. K. Vaughn, H. A. McAllister, G. Bearman and J. T. Willerson (1996). "Thermal detection of cellular infiltrates in living atherosclerotic plaques: possible implications for plaque rupture and thrombosis." Lancet 347(9013): 1447-51.

(Casscells 1999) W. Casscells, M. David, G. Bearman, F. Clubb and J. G. Fujimoto (1999). Thermography. In: The Vulnerable Atherosclerotic Plaque. V. Fuster, Futura Publishing Company: 231-42.

(Casscells 2003a) W. Casscells, K. Hassan, M. F. Vaseghi, M. S. Siadaty, M. Naghavi, R. L. Kirkeeide, M. R. Hassan and M. Madjid (2003). "Plaque blush, branch location, and calcification are angiographic predictors of progression of mild to moderate coronary stenoses." Am Heart J 145(5): 813-20.

(Casscells 2003b) W. Casscells, M. Naghavi and J. T. Willerson (2003). "Vulnerable atherosclerotic plaque: a multifocal disease." Circulation 107(16): 2072-5.

(Cesari 2003) M. Cesari, B. W. Penninx, A. B. Newman, S. B. Kritchevsky, B. J. Nicklas, K. Sutton-Tyrrell, S. M. Rubin, J. Ding, E. M. Simonsick, T. B. Harris and M. Pahor (2003). "Inflammatory markers and onset of cardiovascular events: results from the Health ABC study." Circulation 108(19): 2317-22.

(Cespedes 1995) I. Cespedes, M. Insana and J. Ophir (1995). "Theoretical Bounds on Strain Estimation in Elastography." Ieee Transactions on Ultrasonics Ferroelectrics and Frequency Control 42(5): 969-972.

(Cespedes 1997) I. Cespedes, J. Ophir and S. K. Alam (1997). "The combined effect of signal decorrelation and random noise on the variance of time delay estimation." Ieee Transactions on Ultrasonics Ferroelectrics and Frequency Control 44(1): 220-225.

(Céspedes 1999) E. I. Céspedes, C. L. de Korte and A. F. W. van der Steen (1999). "Echo Decorrelation from Displacement Gradients in Elasticity and Velocity Estimation." IEEE Trans UFFC 46: 791-801.

(Chandran 2003) K. B. Chandran, J. H. Mun, K. K. Choi, J. S. Chen, A. Hamilton, A. Nagaraj and D. D. McPherson (2003). "A method for in-vivo analysis for regional arterial wall material property alterations with atherosclerosis: preliminary results." Med Eng Phys 25(4): 289-98.

(Cheng 1993) G. C. Cheng, H. M. Loree, R. D. Kamm, M. C. Fishbein and R. T. Lee (1993). "Distribution of circumferential stress in ruptured and stable atherosclerotic lesions. A structural analysis with histopathological correlation." Circulation 87(4): 1179-1187.

(Choi 2002) C. D. Choi, A. R. Skovoroda, S. Y. Emelianov and M. O'Donnell (2002). "An integrated compliant balloon ultrasound catheter for intravascular strain imaging." IEEE Trans Ultrason Ferroelectr Freq Control 49(11): 1552-60.

(Chu 1997) K. C. Chu and B. K. Rutt (1997). "Polyvinyl alcohol cryogel: an ideal phantom material for MR studies of arterial flow and elasticity." Magn Reson Med 37(2): 314-9.

(Cohn 2000) N. A. Cohn, B. S. Kim, R. Q. Erkamp, D. J. Mooney, S. Y. Emelianov, A. R. Skovoroda and M. O'Donnell (2000). "High-resolution elasticity imaging for tissue engineering." IEEE Trans Ultrason Ferroelectr Freq Control 47(4): 956-966.

(Davies 1984) M. J. Davies and A. Thomas (1984). "Thrombosis and acute coronary-artery lesions in sudden cardiac ischemic death." N Engl J Med 310(18): 1137-40.

(Davies 1993) M. J. Davies, P. D. Richardson, N. Woolf, D. R. Katz and J. Mann (1993). "Risk of thrombosis in human atherosclerotic plaques: role of extracellular lipid, macrophage, and smooth muscle cell content." Br Heart J 69(5): 377-81.

(Davies 1995) M. J. Davies (1995). "Acute coronary thrombosis--the role of plaque disruption and its initiation and prevention." Eur Heart J 16 Suppl L: 3-7.

(Davies 1996) M. J. Davies (1996). "Stability and instability: two faces of coronary atherosclerosis. The Paul Dudley White Lecture 1995." Circulation 94(8): 2013-20.

(Davies 2000) M. J. Davies (2000). "The pathophysiology of acute coronary syndromes." Heart 83(3): 361-6.

(Davies 2001) M. J. Davies (2001). "Going from immutable to mutable atherosclerotic plaques." Am J Cardiol 88(4A): 2F-9F.

(de Feyter 1991) P. J. de Feyter, P. W. Serruys, M. J. Davies, P. Richardson, J. Lubsen and M. F. Oliver (1991). "Quantitative coronary angiography to measure progression and regression of coronary atherosclerosis. Value, limitations, and implications for clinical trials." Circulation 84(1): 412-23.

(de Feyter 1995) P. J. de Feyter, Y. Ozaki, J. Baptista, J. Escaned, C. Di Mario, P. P. de Jaegere, P. W. Serruys and J. R. Roelandt (1995). "Ischemia-related lesion characteristics in patients with stable or unstable angina. A study with intracoronary angioscopy and ultrasound." Circulation 92(6): 1408-13.

(de Feyter 2000) P. J. de Feyter, K. Nieman, P. van Ooijen and M. Oudkerk (2000). "Non-invasive coronary artery imaging with electron beam computed tomography and magnetic resonance imaging." Heart 84(4): 442-8.

(de Feyter 2002) P. J. de Feyter and K. Nieman (2002). "New coronary imaging techniques: what to expect?" Heart 87(3): 195-7.

(de Korte 1996) C. L. de Korte, E. I. Céspedes, A. F. W. van der Steen and C. T. Lancée (1996). "Image artifacts in intravascular elastography." IEEE EMBS, Amsterdam, The Netherlands.

(de Korte 1998a) C. L. de Korte, E. I. Cespedes, A. F. van der Steen, G. Pasterkamp and N. Bom (1998). "Intravascular ultrasound elastography: assessment and imaging of elastic properties of diseased arteries and vulnerable plaque." Eur J Ultrasound 7(3): 219-24.

(de Korte 1998b) C. L. de Korte, A. F. van der Steen, E. I. Cespedes and G. Pasterkamp (1998). "Intravascular ultrasound elastography in human arteries: initial experience in vitro." Ultrasound Med Biol 24(3): 401-8.

(de Korte 1999) C. L. de Korte, E. I. Céspedes and A. F. W. van der Steen (1999). "Influence of catheter position on estimated strain in intravascular elastography." IEEE Trans Ultrason Ferroelectr Freq Control 46(3): 616-625.

(de Korte 2000a) C. L. de Korte, G. Pasterkamp, A. F. van der Steen, H. A. Woutman and N. Bom (2000). "Characterization of plaque components with intravascular ultrasound elastography in human femoral and coronary arteries in vitro." Circulation 102(6): 617-23.

(de Korte 2000b) C. L. de Korte, A. F. van der Steen, (van der Steen 2003) A. F. W. van der Steen, C. L. de Korte, , G. Pasterkamp, S. G. Carlier, F. Mastik, A. H. Schoneveld, P. W. Serruys and N. Bom (2000). "Characterization of plaque components and vulnerability with intravascular ultrasound elastography." Phys Med Biol 45(6): 1465-75.

(de Korte 2000c) C. L. de Korte, H. A. Woutman, A. F. van der Steen, G. Pasterkamp and E. I. Cespedes (2000). "Vascular tissue characterisation with IVUS elastography." Ultrasonics 38(1-8): 387-90.

(de Korte 2002a) C. L. de Korte, M. J. Sierevogel, F. Mastik, C. Strijder, J. A. Schaar, E. Velema, G. Pasterkamp, P. W. Serruys and A. F. W. van der Steen (2002). "Identification of atherosclerotic plaque components with intravascular ultrasound elastography in vivo: a Yucatan pig study." Circulation 105(14): 1627-1630.

(de Korte 2002b) C. L. de Korte, S. G. Carlier, F. Mastik, M. M. Doyley, A. F. van der Steen, P. W. Serruys and N. Bom (2002). "Morphological and mechanical information of coronary arteries obtained with intravascular elastography; feasibility study in vivo." Eur Heart J 23(5): 405-13.

(de Korte 2003) C. L. de Korte, J. A. Schaar, F. Mastik, P. W. Serruys and A. F. W. van der Steen (2003). "Intravascular elastography: from bench to bedside." J Interv Cardiol 16(3): 253-259.

(de Winter 2003) S. A. de Winter, I. Heller, R. Hamers, P. J. de Feyter, P. W. Serruys, J. R. T. C. Roelandt and N. Bruining (2003). "Computer assisted three-dimensional plaque characterization in ultracoronary ultrasound studies." Computers in Cardiology 30: 73-76.

(de Winter 2004) S. A. De Winter, R. Hamers, M. Degertekin, K. Tanabe, P. A. Lemos, P. W. Serruys, J. R. Roelandt and N. Bruining (2004). "Retrospective image-based gating of intracoronary ultrasound images for improved quantitative analysis: the intelligate method." Catheter Cardiovasc Interv 61(1): 84-94.

(Di Mario 1992) C. Di Mario, S. H. The, S. Madretsma, R. J. van Suylen, R. A. Wilson, N. Bom, P. W. Serruys, E. J. Gussenhoven and J. R. Roelandt (1992). "Detection and characterization of vascular lesions by intravascular ultrasound: an in vitro study correlated with histology." J Am Soc Echocardiogr 5(2): 135-46.

(Diamantopoulos 2003) L. Diamantopoulos, X. Liu, I. De Scheerder, R. Krams, S. Li, J. Van Cleemput, W. Desmet and P. W. Serruys (2003). "The effect of reduced blood-flow on the coronary wall temperature. Are significant lesions suitable for intravascular thermography?" Eur Heart J 24(19): 1788-95.

(Dobrin 1978) P. B. Dobrin (1978). "Mechanical properties of arteries." Physiol Rev 58(2): 397-460.

(Doyley 2000) M. M. Doyley, P. M. Meaney and J. C. Bamber (2000). "Evaluation of an iterative reconstruction method for quantitative elastography." Phys Med Biol 45(6): 1521-1540.

(Doyley 2001) M. M. Doyley, F. Mastik, C. L. de Korte, S. G. Carlier, E. I. Cespedes, P. W. Serruys, N. Bom and A. F. van der Steen (2001). "Advancing intravascular ultrasonic palpation toward clinical applications." Ultrasound Med Biol 27(11): 1471-80.

(El-Barghouty 1996) N. M. El-Barghouty, T. Levine, S. Ladva, A. Flanagan and A. Nicolaides (1996). "Histological verification of computerised carotid plaque characterisation." Eur J Vasc Endovasc Surg 11(4): 414-6.

(Falk 1983) E. Falk (1983). "Plaque rupture with severe pre-existing stenosis precipitating coronary thrombosis. Characteristics of coronary atherosclerotic plaques underlying fatal occlusive thrombi." Br Heart J 50(2): 127-34.

(Falk 1995) E. Falk, P. K. Shah and V. Fuster (1995). "Coronary plaque disruption." Circulation 92(3): 657-71.

(Falk 1999) E. Falk (1999). "Stable versus unstable atherosclerosis: clinical aspects." Am Heart J 138(5 Pt 2): S421-5.

(Fayad 2001) Z. A. Fayad and V. Fuster (2001). "Clinical imaging of the high-risk or vulnerable atherosclerotic plaque." Circ Res 89(4): 305-16.

(Feld 1996) S. Feld, M. Ganim, E. S. Carell, O. Kjellgren, R. L. Kirkeeide, W. K. Vaughn, R. Kelly, A. I. McGhie, N. Kramer, D. Loyd, H. V. Anderson, G. Schroth and R. W. Smalling (1996). "Comparison of angioscopy, intravascular ultrasound imaging and quantitative coronary angiography in predicting clinical outcome after coronary intervention in high risk patients." J Am Coll Cardiol 28(1): 97-105.

(Finet 2004) G. Finet, J. Ohayon and G. Rioufol (2004). "Biomechanical interaction between cap thickness, lipid core composition and blood pressure in vulnerable coronary plaque: impact on stability or instability." Coron Artery Dis 15(1): 13-20.

(Friedrich 1994) G. J. Friedrich, N. Y. Moes, V. A. Muhlberger, C. Gabl, G. Mikuz, D. Hausmann, P. J. Fitzgerald and P. G. Yock (1994). "Detection of intralesional calcium by intracoronary ultrasound depends on the histologic pattern." Am Heart J 128(3): 435-41.

(Frink 1994) R. J. Frink (1994). "Chronic ulcerated plaques: new insights into the pathogenesis of acute coronary disease." J Invasive Cardiol 6(5): 173-85.

(Fu 2000) D. Fu, S. F. Levinson, S. M. Gracewski and K. J. Parker (2000). "Non-invasive quantitative reconstruction of tissue elasticity using an iterative forward approach." Phys Med Biol 45(6): 1495-509.

(Fung 1981) Y. C. Fung (1981). Biomechanics: Mechanical properties of living tissue. New York, USA, Springer.

(Galis 1994) Z. S. Galis, G. K. Sukhova, M. W. Lark and P. Libby (1994). "Increased expression of matrix metalloproteinases and matrix degrading activity in vulnerable regions of human atherosclerotic plaques." J Clin Invest 94(6): 2493-503.

(Ge 1995) J. Ge, M. Haude, G. Gorge, F. Liu and R. Erbel (1995). "Silent healing of spontaneous plaque disruption demonstrated by intracoronary ultrasound." Eur Heart J 16(8): 1149-51.

(Ge 1999) J. Ge, F. Chirillo, J. Schwedtmann, G. Gorge, M. Haude, D. Baumgart, V. Shah, C. von Birgelen, S. Sack, H. Boudoulas and R. Erbel (1999). "Screening of ruptured plaques in patients with coronary artery disease by intravascular ultrasound." Heart 81(6): 621-7.

(Geng 1997) Y. J. Geng, L. E. Henderson, E. B. Levesque, M. Muszynski and P. Libby (1997). "Fas is expressed in human atherosclerotic intima and promotes apoptosis

of cytokine-primed human vascular smooth muscle cells." Arterioscler Thromb Vasc Biol 17(10): 2200-8.

(Giroud 1992) D. Giroud, J. M. Li, P. Urban, B. Meier and W. Rutishauer (1992). "Relation of the site of acute myocardial infarction to the most severe coronary arterial stenosis at prior angiography." Am J Cardiol 69(8): 729-32.

(Glagov 1987) S. Glagov, E. Weisenberg, C. K. Zarins, R. Stankunavicius and G. J. Kolettis (1987). "Compensatory enlargement of human atherosclerotic coronary arteries." N Engl J Med 316(22): 1371-5.

(Goldstein 2000) J. A. Goldstein, D. Demetriou, C. L. Grines, M. Pica, M. Shoukfeh and W. W. O'Neill (2000). "Multiple complex coronary plaques in patients with acute myocardial infarction." N Engl J Med 343(13): 915-22.

(Goldstein 2002) J. A. Goldstein (2002). "Multifocal coronary plaque instability." Prog Cardiovasc Dis 44(6): 449-54.

(Gow 1979) B. S. Gow and C. D. Hadfield (1979). "The elasticity of canine and human coronary arteries with reference to postmortem changes." Circ Res 45(5): 588-594.

(Gronholdt 1998) M. L. Gronholdt, B. G. Nordestgaard, B. M. Wiebe, J. E. Wilhjelm and H. Sillesen (1998). "Echo-lucency of computerized ultrasound images of carotid atherosclerotic plaques are associated with increased levels of triglyceride-rich lipoproteins as well as increased plaque lipid content." Circulation 97(1): 34-40.

(Gronholdt 2001) M. L. Gronholdt, B. G. Nordestgaard, T. V. Schroeder, S. Vorstrup and H. Sillesen (2001). "Ultrasonic echolucent carotid plaques predict future strokes." Circulation 104(1): 68-73.

(Haft 1988) J. I. Haft, B. J. Haik, J. E. Goldstein and N. E. Brodyn (1988). "Development of significant coronary artery lesions in areas of minimal disease. A common mechanism for coronary disease progression." Chest 94(4): 731-6.

(Hamers 2001) R. Hamers, N. Bruining, M. Knook, M. Sabate and J. R. T. C. Roelandt (2001). "A novel approach to quantitative analysis of intravascular ultrasound images." Computers in Cardiology: 589-592.

(Hanlon 2000) E. B. Hanlon, R. Manoharan, T. W. Koo, K. E. Shafer, J. T. Motz, M. Fitzmaurice, J. R. Kramer, I. Itzkan, R. R. Dasari and M. S. Feld (2000). "Prospects for in vivo Raman spectroscopy." Phys Med Biol 45(2): R1-59.

(Hatsukami 2000) T. S. Hatsukami, R. Ross, N. L. Polissar and C. Yuan (2000). "Visualization of fibrous cap thickness and rupture in human atherosclerotic carotid plaque in vivo with high-resolution magnetic resonance imaging." Circulation 102(9): 959-64.

(Hayashi 1997) K. Hayashi and Y. Imai (1997). "Tensile property of atheromatous plaque and an analysis of stress in atherosclerotic wall." J Biomech 30(6): 573-579.

(Hayes 1996) C. E. Hayes, C. M. Mathis and C. Yuan (1996). "Surface coil phased arrays for high-resolution imaging of the carotid arteries." J Magn Reson Imaging 6(1): 109-12.

(Hiro 1996) T. Hiro, C. Y. Leung, R. J. Russo, H. Karimi, A. R. Farvid and J. M. Tobis (1996). "Variability of a three-layered appearance in intravascular ultrasound coronary images: a comparison of morphometric measurements with four intravascular ultrasound systems." Am J Card Imaging 10(4): 219-27.

(Holzapfel 1998) G. A. Holzapfel and H. W. Weizsacker (1998). "Biomechanical behavior of the arterial wall and its numerical characterization." Comput Biol Med 28(4): 377-92.

(Honda 2004) O. Honda, S. Sugiyama, K. Kugiyama, H. Fukushima, S. Nakamura, S. Koide, S. Kojima, N. Hirai, H. Kawano, H. Soejima, T. Sakamoto, M. Yoshimura and H. Ogawa (2004). "Echolucent carotid plaques predict future coronary events in patients with coronary artery disease." J Am Coll Cardiol 43(7): 1177-84.

(Hoye 2004) A. Hoye, P. A. Lemos, C. A. Arampatzis, F. Saia, K. Tanabe, M. Degertekin, J. Daemen, P. C. Smits, E. McFadden, S. H. Hofma, G. Sianos, P. de Feyter, W. J. Giessen, R. T. van Domburg and P. W. Serruys (2004). "Effectiveness of sirolimus-Eluting stent implantation for coronary narrowings <50% in diameter." Am J Cardiol 94(1): 112-4.

(Huang 1991) D. Huang, E. A. Swanson, C. P. Lin, J. S. Schuman, W. G. Stinson, W. Chang, M. R. Hee, T. Flotte, K. Gregory, C. A. Puliafito and et al. (1991). "Optical coherence tomography." Science 254(5035): 1178-81.

(Huang 2001) H. Huang, R. Virmani, H. Younis, A. P. Burke, R. D. Kamm and R. T. Lee (2001). "The impact of calcification on the biomechanical stability of atherosclerotic plaques." Circulation 103(8): 1051-6.

(Jang 2002) I. K. Jang, B. E. Bouma, D. H. Kang, S. J. Park, S. W. Park, K. B. Seung, K. B. Choi, M. Shishkov, K. Schlendorf, E. Pomerantsev, S. L. Houser, H. T. Aretz and G. J. Tearney (2002). "Visualization of coronary atherosclerotic plaques in patients using optical coherence tomography: comparison with intravascular ultrasound." J Am Coll Cardiol 39(4): 604-9.

(Jeremias 1997) A. Jeremias, J. Ge and R. Erbel (1997). "New insight into plaque healing after plaque rupture with subsequent thrombus formation detected by intravascular ultrasound." Heart 77(3): 293.

(Jeremias 1999) A. Jeremias, M. L. Kolz, T. S. Ikonen, J. F. Gummert, A. Oshima, M. Hayase, Y. Honda, N. Komiyama, G. J. Berry, R. E. Morris, P. G. Yock and P. J. Fitzgerald (1999). "Feasibility of in vivo intravascular ultrasound tissue characterization in the detection of early vascular transplant rejection." Circulation 100(21): 2127-30.

(Kallel 1996) F. Kallel and M. Bertrand (1996). "Tissue elasticity reconstruction using linear perturbation method." IEEE Trans Med Imaging 15(3): 299-313.

(Kanai 2003) H. Kanai, H. Hasegawa, M. Ichiki, F. Tezuka and Y. Koiwa (2003). "Elasticity imaging of atheroma with transcutaneous ultrasound: preliminary study." Circulation 107(24): 3018-21.

(Kerensky 2002) R. A. Kerensky, M. Wade, P. Deedwania, W. E. Boden and C. J. Pepine (2002). "Revisiting the culprit lesion in non-Q-wave myocardial infarction. Results from the VANQWISH trial angiographic core laboratory." J Am Coll Cardiol 39(9): 1456-63.

(Kim 2001) W. Y. Kim, P. G. Danias, M. Stuber, S. D. Flamm, S. Plein, E. Nagel, S. E. Langerak, O. M. Weber, E. M. Pedersen, M. Schmidt, R. M. Botnar and W. J. Manning (2001). "Coronary magnetic resonance angiography for the detection of coronary stenoses." N Engl J Med 345(26): 1863-9.

(Kim 2004) K. Kim, W. F. Weitzel, J. M. Rubin, H. Xie, X. Chen and M. O'Donnell (2004). "Vascular intramural strain imaging using arterial pressure equalization." Ultrasound Med Biol 30(6): 761-71.

(Kinlay 2001) S. Kinlay (2001). "What has intravascular ultrasound taught us about plaque biology?" Curr Atheroscler Rep 3(3): 260-6.

(Kobayashi 2003) S. Kobayashi, N. Inoue, Y. Ohashi, M. Terashima, K. Matsui, T. Mori, H. Fujita, K. Awano, K. Kobayashi, H. Azumi, J. Ejiri, K. Hirata, S. Kawashima, Y. Hayashi, H. Yokozaki, H. Itoh and M. Yokoyama (2003). "Interaction of oxidative stress and inflammatory response in coronary plaque instability: important role of C-reactive protein." Arterioscler Thromb Vasc Biol 23(8): 1398-404.

(Kolodgie 2001) F. D. Kolodgie, A. P. Burke, A. Farb, H. K. Gold, J. Yuan, J. Narula, A. V. Finn and R. Virmani (2001). "The thin-cap fibroatheroma: a type of vulnerable plaque: the major precursor lesion to acute coronary syndromes." Curr Opin Cardiol 16(5): 285-92.

(Kolodgie 2003) F. D. Kolodgie, H. K. Gold, A. P. Burke, D. R. Fowler, H. S. Kruth, D. K. Weber, A. Farb, L. J. Guerrero, M. Hayase, R. Kutys, J. Narula, A. V. Finn and R. Virmani (2003). "Intraplaque hemorrhage and progression of coronary atheroma." N Engl J Med 349(24): 2316-25.

(Kolodgie 2004) F. D. Kolodgie, R. Virmani, A. P. Burke, A. Farb, D. K. Weber, R. Kutys, A. V. Finn and H. K. Gold (2004). "Pathologic assessment of the vulnerable human coronary plaque." Heart 90(12): 1385-91.

(Komiyama 2000) N. Komiyama, G. J. Berry, M. L. Kolz, A. Oshima, J. A. Metz, P. Preuss, A. F. Brisken, M. Pauliina Moore, P. G. Yock and P. J. Fitzgerald (2000). "Tissue characterization of atherosclerotic plaques by intravascular ultrasound radiofrequency signal analysis: an in vitro study of human coronary arteries." Am Heart J 140(4): 565-74.

(Konofagou 1998) E. Konofagou and J. Ophir (1998). "A new elastographic method for estimation and imaging of lateral displacements, lateral strains, corrected axial strains and Poisson's ratios in tissues." Ultrasound Med Biol 24(8): 1183-99.

(Krams 2003) R. Krams, D. Segers, B. M. Gourabi, W. Maat, C. Cheng, C. van Pelt, L. C. van Damme, P. de Feyter, T. van der Steen, C. L. de Korte and P. W. Serruys (2003). "Inflammation and atherosclerosis: mechanisms underlying vulnerable plaque." J Interv Cardiol 16(2): 107-13.

(Kullo 1998) I. J. Kullo, W. D. Edwards and R. S. Schwartz (1998). "Vulnerable plaque: pathobiology and clinical implications." Ann Intern Med 129(12): 1050-60.

(Kwan 2003) D. Kwan, A. Dries, T. Burton, G. Bhandari, D. Young, R. Green, K. Ouriel and R. K. Greenberg (2003). "Thrombus characterization with intravascular ultrasound: potential to predict successful thrombolysis." J Endovasc Ther 10(1): 90-8.

(Lally 2004) C. Lally, A. J. Reid and P. J. Prendergast (2004). "Elastic behavior of porcine coronary artery tissue under uniaxial and equibiaxial tension." Ann Biomed Eng 32(10): 1355-64.

(Landini 1986) L. Landini, R. Sarnelli, E. Picano and M. Salvadori (1986). "Evaluation of frequency dependence of backscatter coefficient in normal and atherosclerotic aortic walls." Ultrasound Med Biol 12(5): 397-401.

(Lanza 1996) G. M. Lanza, K. D. Wallace, M. J. Scott, W. P. Cacheris, D. R. Abendschein, D. H. Christy, A. M. Sharkey, J. G. Miller, P. J. Gaffney and S. A. Wickline (1996). "A novel site-targeted ultrasonic contrast agent with broad biomedical application." Circulation 94(12): 3334-40.

(Lee 1991) R. T. Lee, A. J. Grodzinsky, E. H. Frank, R. D. Kamm and F. J. Schoen (1991). "Structure-dependent dynamic mechanical behavior of fibrous caps from human atherosclerotic plaques." Circulation 83(5): 1764-70.

(Lee 1992) R. T. Lee, S. G. Richardson, H. M. Loree, A. J. Grodzinsky, S. A. Gharib, F. J. Schoen and N. Pandian (1992). "Prediction of mechanical properties of human

atherosclerotic tissue by high-frequency intravascular ultrasound imaging. An in vitro study." Arterioscler Thromb 12(1): 1-5.

(Lee 1993) R. T. Lee, H. M. Loree, G. C. Cheng, E. H. Lieberman, N. Jaramillo and F. J. Schoen (1993). "Computational structural analysis based on intravascular ultrasound imaging before in vitro angioplasty: prediction of plaque fracture locations." Journal of American College of Cardiology 21: 777-782.

(Lee 1994) R. T. Lee, H. M. Loree and M. C. Fishbein (1994). "High stress regions in saphenous vein bypass graft atherosclerotic lesions." J Am Coll Cardiol 24(7): 1639-44.

(Lee 1996) R. T. Lee, F. J. Schoen, H. M. Loree, M. W. Lark and P. Libby (1996). "Circumferential stress and matrix metalloproteinase 1 in human coronary atherosclerosis. Implications for plaque rupture." Arterioscler Thromb Vasc Biol 16(8): 1070-1073.

(Lendon 1991) C. L. Lendon, M. J. Davies, G. V. Born and P. D. Richardson (1991). "Atherosclerotic plaque caps are locally weakened when macrophages density is increased." Atherosclerosis 87(1): 87-90.

(Lendon 1993) C. L. Lendon, M. J. Davies, P. D. Richardson and G. V. Born (1993). "Testing of small connective tissue specimens for the determination of the mechanical behaviour of atherosclerotic plaques." J Biomed Eng 15(1): 27-33.

(Libby 1995) P. Libby (1995). "Molecular bases of the acute coronary syndromes." Circulation 91(11): 2844-50.

(Libby 2001) P. Libby (2001). "Current concepts of the pathogenesis of the acute coronary syndromes." Circulation 104(3): 365-72.

(Libby 2002a) P. Libby, P. M. Ridker and A. Maseri (2002). "Inflammation and atherosclerosis." Circulation 105(9): 1135-43.

(Libby 2002b) P. Libby (2002). "Inflammation in atherosclerosis." Nature 420(6917): 868-74.

(Little 1988) W. C. Little, M. Constantinescu, R. J. Applegate, M. A. Kutcher, M. T. Burrows, F. R. Kahl and W. P. Santamore (1988). "Can coronary angiography predict the site of a subsequent myocardial infarction in patients with mild-to-moderate coronary artery disease?" Circulation 78(5 Pt 1): 1157-66.

(Liuzzo 1994) G. Liuzzo, L. M. Biasucci, J. R. Gallimore, R. L. Grillo, A. G. Rebuzzi, M. B. Pepys and A. Maseri (1994). "The prognostic value of C-reactive protein and serum amyloid a protein in severe unstable angina." N Engl J Med 331(7): 417-24.

(Lombardo 2004) A. Lombardo, L. M. Biasucci, G. A. Lanza, S. Coli, P. Silvestri, D. Cianflone, G. Liuzzo, F. Burzotta, F. Crea and A. Maseri (2004). "Inflammation as a possible link between coronary and carotid plaque instability." Circulation 109(25): 3158-63.

(Loree 1992) H. M. Loree, R. D. Kamm, R. G. Stringfellow and R. T. Lee (1992). "Effects of fibrous cap thickness on peak circumferential stress in model atherosclerotic vessels." Circ Res 71(4): 850-8.

(Loree 1994a) H. M. Loree, B. J. Tobias, L. J. Gibson, R. D. Kamm, D. M. Small and R. T. Lee (1994). "Mechanical properties of model atherosclerotic lesion lipid pools." Arterioscler Thromb 14(2): 230-4.

(Loree 1994b) H. M. Loree, A. J. Grodzinsky, S. Y. Park, L. J. Gibson and R. T. Lee (1994). "Static circumferential tangential modulus of human atherosclerotic tissue." J Biomech 27(2): 195-204.

(Losordo 1994) D. W. Losordo, K. Rosenfield, J. Kaufman, A. Pieczek and J. M. Isner (1994). "Focal compensatory enlargement of human arteries in response to progressive atherosclerosis. In vivo documentation using intravascular ultrasound." Circulation 89(6): 2570-7.

(Lu 2003) X. Lu, J. Yang, J. B. Zhao, H. Gregersen and G. S. Kassab (2003). "Shear modulus of porcine coronary artery: contributions of media and adventitia." Am J Physiol Heart Circ Physiol 285(5): H1966-75.

(Lupotti 2003) F. A. Lupotti, J. J. Mai, C. Pellot-Barakat and M. F. Insana (2003). "Vascular elasticity from regional displacement estimates." Proceedings of the 2003 IEEE International Ultrasonics Symposium: 1895-1898.

(MacNeill 2003) B. D. MacNeill, H. C. Lowe, M. Takano, V. Fuster and I. K. Jang (2003). "Intravascular modalities for detection of vulnerable plaque: current status." Arterioscler Thromb Vasc Biol 23(8): 1333-42.

(Malek 1999) A. M. Malek, S. L. Alper and S. Izumo (1999). "Hemodynamic shear stress and its role in atherosclerosis." Jama 282(21): 2035-42.

(Mann 1996) J. M. Mann and M. J. Davies (1996). "Vulnerable plaque. Relation of characteristics to degree of stenosis in human coronary arteries." Circulation 94(5): 928-31.

(Mann 1999) J. Mann and M. J. Davies (1999). "Mechanisms of progression in native coronary artery disease: role of healed plaque disruption." Heart 82(3): 265-8.

(Maseri 2003) A. Maseri and V. Fuster (2003). "Is there a vulnerable plaque?" Circulation 107(16): 2068-71.

(Mathiesen 2001) E. B. Mathiesen, K. H. Bonaa and O. Joakimsen (2001). "Echolucent plaques are associated with high risk of ischemic cerebrovascular events in carotid stenosis: the tromso study." Circulation 103(17): 2171-5.

(Matsumoto 2002) T. Matsumoto, H. Abe, T. Ohashi, Y. Kato and M. Sato (2002). "Local elastic modulus of atherosclerotic lesions of rabbit thoracic aortas measured by pipette aspiration method." Physiol Meas 23(4): 635-48.

(McBane 2000) R. D. McBane, 2nd, M. A. Ford, K. Karnicki, M. Stewart and W. G. Owen (2000). "Fibrinogen, fibrin and crosslinking in aging arterial thrombi." Thromb Haemost 84(1): 83-7.

(Meier 1995) B. Meier and S. Ramamurthy (1995). "Plaque sealing by coronary angioplasty." Cathet Cardiovasc Diagn 36(4): 295-7.

(Meier 1997) B. Meier (1997). "Plaque sealing or plumbing for coronary artery stenoses?" Circulation 96(6): 2094-5.

(Mercado 2003) N. Mercado, W. Maier, E. Boersma, C. Bucher, V. de Valk, W. W. O'Neill, B. J. Gersh, B. Meier, P. W. Serruys and W. Wijns (2003). "Clinical and angiographic outcome of patients with mild coronary lesions treated with balloon angioplasty or coronary stenting. Implications for mechanical plaque sealing." Eur Heart J 24(6): 541-51.

(Miga 2003) M. I. Miga (2003). "A new approach to elastography using mutual information and finite elements." Phys Med Biol 48(4): 467-80.

(Mintz 2001) G. S. Mintz, S. E. Nissen, W. D. Anderson, S. R. Bailey, R. Erbel, P. J. Fitzgerald, F. J. Pinto, K. Rosenfield, R. J. Siegel, E. M. Tuzcu and P. G. Yock (2001). "American College of Cardiology Clinical Expert Consensus Document on Standards for Acquisition, Measurement and Reporting of Intravascular Ultrasound Studies (IVUS). A report of the American College of Cardiology Task Force on Clinical Expert Consensus Documents." J Am Coll Cardiol 37(5): 1478-92.

(Mizuno 1992) K. Mizuno, K. Satomura, A. Miyamoto, K. Arakawa, T. Shibuya, T. Arai, A. Kurita, H. Nakamura and J. A. Ambrose (1992). "Angioscopic evaluation of coronary-artery thrombi in acute coronary syndromes." N Engl J Med 326(5): 287-91.

(Mollet 2004) N. R. Mollet, F. Cademartiri, K. Nieman, F. Saia, P. A. Lemos, E. P. McFadden, P. M. Pattynama, P. W. Serruys, G. P. Krestin and P. J. de Feyter (2004). "Multislice spiral computed tomography coronary angiography in patients with stable angina pectoris." J Am Coll Cardiol 43(12): 2265-70.

(Moore 1998) M. P. Moore, T. Spencer, D. M. Salter, P. P. Kearney, T. R. Shaw, I. R. Starkey, P. J. Fitzgerald, R. Erbel, A. Lange, N. W. McDicken, G. R. Sutherland

and K. A. Fox (1998). "Characterisation of coronary atherosclerotic morphology by spectral analysis of radiofrequency signal: in vitro intravascular ultrasound study with histological and radiological validation." Heart 79(5): 459-67.

(Moreno 2002) P. R. Moreno, R. A. Lodder, K. R. Purushothaman, W. E. Charash, W. N. O'Connor and J. E. Muller (2002). "Detection of lipid pool, thin fibrous cap, and inflammatory cells in human aortic atherosclerotic plaques by near-infrared spectroscopy." Circulation 105(8): 923-7.

(Moreno 2003) P. R. Moreno and J. E. Muller (2003). "Detection of high-risk atherosclerotic coronary plaques by intravascular spectroscopy." J Interv Cardiol 16(3): 243-52.

(Morrison 2000) L. J. Morrison, P. R. Verbeek, A. C. McDonald, B. V. Sawadsky and D. J. Cook (2000). "Mortality and prehospital thrombolysis for acute myocardial infarction: A meta-analysis." Jama 283(20): 2686-92.

(Moulton 1995) M. J. Moulton, L. L. Creswell, R. L. Actis, K. W. Myers, M. W. Vannier, B. A. Szabo and M. K. Pasque (1995). "An inverse approach to determining myocardial material properties." J Biomech 28(8): 935-948.

(Mozersky 1972) D. J. Mozersky, D. S. Sumner, D. E. Hokanson and D. E. Strandness (1972). "Transcutaneous measurement of the elastic properties of the humen femoral artery." Circulation 46: 948-955.

(Muller 1994) J. E. Muller, G. S. Abela, R. W. Nesto and G. H. Tofler (1994). "Triggers, acute risk factors and vulnerable plaques: the lexicon of a new frontier." J Am Coll Cardiol 23(3): 809-13.

(Naghavi 2001) M. Naghavi, M. Madjid, M. R. Khan, R. M. Mohammadi, J. T. Willerson and S. W. Casscells (2001). "New developments in the detection of vulnerable plaque." Curr Atheroscler Rep 3(2): 125-35.

(Naghavi 2003a) M. Naghavi, M. Madjid, K. Gul, M. S. Siadaty, S. Litovsky, J. T. Willerson and S. W. Casscells (2003). "Thermography basket catheter: in vivo measurement of the temperature of atherosclerotic plaques for detection of vulnerable plaques." Catheter Cardiovasc Interv 59(1): 52-9.

(Naghavi 2003b) M. Naghavi, P. Libby, E. Falk, S. W. Casscells, S. Litovsky, J. Rumberger, J. J. Badimon, C. Stefanadis, P. Moreno, G. Pasterkamp, Z. Fayad, P. H. Stone, S. Waxman, P. Raggi, M. Madjid, A. Zarrabi, A. Burke, C. Yuan, P. J. Fitzgerald, D. S. Siscovick, C. L. de Korte, M. Aikawa, K. E. Airaksinen, G. Assmann, C. R. Becker, J. H. Chesebro, A. Farb, Z. S. Galis, C. Jackson, I. K. Jang, W. Koenig, R. A. Lodder, K. March, J. Demirovic, M. Navab, S. G. Priori, M. D. Rekhter, R. Bahr, S. M. Grundy, R. Mehran, A. Colombo, E. Boerwinkle, C. Ballantyne, W. Insull, Jr., R. S. Schwartz, R. Vogel, P. W. Serruys, G. K. Hansson,

D. P. Faxon, S. Kaul, H. Drexler, P. Greenland, J. E. Muller, R. Virmani, P. M. Ridker, D. P. Zipes, P. K. Shah and J. T. Willerson (2003). "From vulnerable plaque to vulnerable patient: a call for new definitions and risk assessment strategies: Part II." Circulation 108(15): 1772-8.

(Naghavi 2003c) M. Naghavi, P. Libby, E. Falk, S. W. Casscells, S. Litovsky, J. Rumberger, J. J. Badimon, C. Stefanadis, P. Moreno, G. Pasterkamp, Z. Fayad, P. H. Stone, S. Waxman, P. Raggi, M. Madjid, A. Zarrabi, A. Burke, C. Yuan, P. J. Fitzgerald, D. S. Siscovick, C. L. de Korte, M. Aikawa, K. E. Juhani Airaksinen, G. Assmann, C. R. Becker, J. H. Chesebro, A. Farb, Z. S. Galis, C. Jackson, I. K. Jang, W. Koenig, R. A. Lodder, K. March, J. Demirovic, M. Navab, S. G. Priori, M. D. Rekhter, R. Bahr, S. M. Grundy, R. Mehran, A. Colombo, E. Boerwinkle, C. Ballantyne, W. Insull, Jr., R. S. Schwartz, R. Vogel, P. W. Serruys, G. K. Hansson, D. P. Faxon, S. Kaul, H. Drexler, P. Greenland, J. E. Muller, R. Virmani, P. M. Ridker, D. P. Zipes, P. K. Shah and J. T. Willerson (2003). "From vulnerable plaque to vulnerable patient: a call for new definitions and risk assessment strategies: Part I." Circulation 108(14): 1664-72.

(Nair 2001) A. Nair, B. D. Kuban, N. Obuchowski and D. G. Vince (2001). "Assessing spectral algorithms to predict atherosclerotic plaque composition with normalized and raw intravascular ultrasound data." Ultrasound Med Biol 27(10): 1319-31.

(Nair 2002) A. Nair, B. D. Kuban, E. M. Tuzcu, P. Schoenhagen, S. E. Nissen and D. G. Vince (2002). "Coronary plaque classification with intravascular ultrasound radiofrequency data analysis." Circulation 106(17): 2200-6.

(Nieman 2002) K. Nieman, F. Cademartiri, P. A. Lemos, R. Raaijmakers, P. M. Pattynama and P. J. de Feyter (2002). "Reliable noninvasive coronary angiography with fast submillimeter multislice spiral computed tomography." Circulation 106(16): 2051-4.

(Nieman 2003) K. Nieman, A. van der Lugt, P. M. Pattynama and P. J. de Feyter (2003). "Noninvasive visualization of atherosclerotic plaque with electron beam and multislice spiral computed tomography." J Interv Cardiol 16(2): 123-8.

(Nijmeijer 2001) R. Nijmeijer, W. K. Lagrand, C. A. Visser, C. J. Meijer, H. W. Niessen and C. E. Hack (2001). "CRP, a major culprit in complement-mediated tissue damage in acute myocardial infarction?" Int Immunopharmacol 1(3): 403-14.

(Nishimura 1990) R. A. Nishimura, W. D. Edwards, C. A. Warnes, G. S. Reeder, D. R. Holmes, Jr., A. J. Tajik and P. G. Yock (1990). "Intravascular ultrasound imaging: in vitro validation and pathologic correlation." J Am Coll Cardiol 16(1): 145-54.

(Nissen 1991) S. E. Nissen, J. C. Gurley, C. L. Grines, D. C. Booth, R. McClure, M. Berk, C. Fischer and A. N. DeMaria (1991). "Intravascular ultrasound assessment

of lumen size and wall morphology in normal subjects and patients with coronary artery disease." Circulation 84(3): 1087-99.

(Nissen 2001) S. E. Nissen and P. Yock (2001). "Intravascular ultrasound: novel pathophysiological insights and current clinical applications." Circulation 103(4): 604-16.

(Nissen 2003) S. E. Nissen, T. Tsunoda, E. M. Tuzcu, P. Schoenhagen, C. J. Cooper, M. Yasin, G. M. Eaton, M. A. Lauer, W. S. Sheldon, C. L. Grines, S. Halpern, T. Crowe, J. C. Blankenship and R. Kerensky (2003). "Effect of recombinant ApoA-I Milano on coronary atherosclerosis in patients with acute coronary syndromes: a randomized controlled trial." Jama 290(17): 2292-300.

(Nissen 2004) S. E. Nissen, E. M. Tuzcu, P. Schoenhagen, B. G. Brown, P. Ganz, R. A. Vogel, T. Crowe, G. Howard, C. J. Cooper, B. Brodie, C. L. Grines and A. N. DeMaria (2004). "Effect of intensive compared with moderate lipid-lowering therapy on progression of coronary atherosclerosis: a randomized controlled trial." Jama 291(9): 1071-80.

(Nissen 2005) S. E. Nissen, E. M. Tuzcu, P. Schoenhagen, T. Crowe, W. J. Sasiela, J. Tsai, J. Orazem, R. D. Magorien, C. O'Shaughnessy and P. Ganz (2005). "Statin therapy, LDL cholesterol, C-reactive protein, and coronary artery disease." N Engl J Med 352(1): 29-38.

(Nobuyoshi 1991) M. Nobuyoshi, M. Tanaka, H. Nosaka, T. Kimura, H. Yokoi, N. Hamasaki, K. Kim, T. Shindo and K. Kimura (1991). "Progression of coronary atherosclerosis: is coronary spasm related to progression?" J Am Coll Cardiol 18(4): 904-10.

(Ohayon 2001) J. Ohayon, P. Teppaz, G. Finet and G. Rioufol (2001). "In-vivo prediction of human coronary plaque rupture location using intravascular ultrasound and the finite element method." Coron Artery Dis 12(8): 655-663.

(Ojio 2000) S. Ojio, H. Takatsu, T. Tanaka, K. Ueno, K. Yokoya, T. Matsubara, T. Suzuki, S. Watanabe, N. Morita, M. Kawasaki, T. Nagano, I. Nishio, K. Sakai, K. Nishigaki, G. Takemura, T. Noda, S. Minatoguchi and H. Fujiwara (2000). "Considerable time from the onset of plaque rupture and/or thrombi until the onset of acute myocardial infarction in humans: coronary angiographic findings within 1 week before the onset of infarction." Circulation 102(17): 2063-9.

(Okimoto 2002) T. Okimoto, M. Imazu, Y. Hayashi, H. Fujiwara, H. Ueda and N. Kohno (2002). "Atherosclerotic plaque characterization by quantitative analysis using intravascular ultrasound: correlation with histological and immunohistochemical findings." Circ J 66(2): 173-7.

(Oldgren 2003) J. Oldgren, L. Wallentin, L. Grip, R. Linder, B. L. Norgaard and A. Siegbahn (2003). "Myocardial damage, inflammation and thrombin inhibition in unstable coronary artery disease." Eur Heart J 24(1): 86-93.

(Ophir 1991) J. Ophir, I. Cespedes, H. Ponnekanti, Y. Yazdi and X. Li (1991). "Elastography: a quantitative method for imaging the elasticity of biological tissues." Ultrason Imaging 13(2): 111-34.

(Ophir 1996) J. Ophir, E. I. Céspedes, B. Garra, H. Ponnekanti, Y. Huang and N. Maklad (1996). "Elastography: ultrasonic imaging of tissue strain and elastic modulus in vivo." Eur J Ultrasound 3: 49-70.

(Pasterkamp 1998) G. Pasterkamp, A. H. Schoneveld, A. C. van der Wal, C. C. Haudenschild, R. J. Clarijs, A. E. Becker, B. Hillen and C. Borst (1998). "Relation of arterial geometry to luminal narrowing and histologic markers for plaque vulnerability: the remodeling paradox." J Am Coll Cardiol 32(3): 655-62.

(Pasterkamp 2000) G. Pasterkamp, E. Falk, H. Woutman and C. Borst (2000). "Techniques characterizing the coronary atherosclerotic plaque: influence on clinical decision making?" J Am Coll Cardiol 36(1): 13-21.

(Pearson 2003) T. A. Pearson, G. A. Mensah, R. W. Alexander, J. L. Anderson, R. O. Cannon, 3rd, M. Criqui, Y. Y. Fadl, S. P. Fortmann, Y. Hong, G. L. Myers, N. Rifai, S. C. Smith, Jr., K. Taubert, R. P. Tracy and F. Vinicor (2003). "Markers of inflammation and cardiovascular disease: application to clinical and public health practice: A statement for healthcare professionals from the Centers for Disease Control and Prevention and the American Heart Association." Circulation 107(3): 499-511.

(Perrey 2003) C. Perrey, G. Braeker, W. Bojara, M. Lindstaedt, S. Holt and H. Ermert (2003). "Strain imaging with intravascular ultrasound array scanners: validation with phantom experiments." Biomed Tech (Berl) 48(5): 135-40.

(Plewes 2000) D. B. Plewes, J. Bishop, A. Samani and J. Sciarretta (2000). "Visualization and quantification of breast cancer biomechanical properties with magnetic resonance elastography." Phys Med Biol 45(6): 1591-610.

(Polak 1998) J. F. Polak, L. Shemanski, D. H. O'Leary, D. Lefkowitz, T. R. Price, P. J. Savage, W. E. Brant and C. Reid (1998). "Hypoechoic plaque at US of the carotid artery: an independent risk factor for incident stroke in adults aged 65 years or older. Cardiovascular Health Study." Radiology 208(3): 649-54.

(Popper 2002) K. Popper (2002). In: The logic of scientific discovery, Routledge Classics 2002: 23.

(Potkin 1990) B. N. Potkin, A. L. Bartorelli, J. M. Gessert, R. F. Neville, Y. Almagor, W. C. Roberts and M. B. Leon (1990). "Coronary artery imaging with intravascular high-frequency ultrasound." Circulation 81(5): 1575-85.

(Prati 2001) F. Prati, E. Arbustini, A. Labellarte, B. Dal Bello, L. Sommariva, M. T. Mallus, A. Pagano and A. Boccanelli (2001). "Correlation between high frequency intravascular ultrasound and histomorphology in human coronary arteries." Heart 85(5): 567-70.

(Raghavan 1994) K. R. Raghavan and A. E. Yagle (1994). "Forward and inverse problems in elasticity imaging of soft tissues." Transactions on Nuclear Science 41(4): 1639-1648.

(Ramo 1997) M. P. Ramo, T. Spencer, P. P. Kearney, S. T. Shaw, I. R. Starkey, W. N. McDicken and K. A. Fox (1997). "Characterisation of red and white thrombus by intravascular ultrasound using radiofrequency and videodensitometric data-based texture analysis." Ultrasound Med Biol 23(8): 1195-9.

(Rasheed 1995) Q. Rasheed, P. J. Dhawale, J. Anderson and J. M. Hodgson (1995). "Intracoronary ultrasound-defined plaque composition: computer-aided plaque characterization and correlation with histologic samples obtained during directional coronary atherectomy." Am Heart J 129(4): 631-7.

(Reiber 1994) J. H. C. Reiber and P. M. Van Der Zwet (1994). Accuracy and precision of quantitative digital coronary arteriography; observer-, as well as short- and medium-term variabilities. In: Quantitative coronary angiography in clinical practice. P. W. Serruys, D. P. Foley and P. J. de Feyter. Dordrecht, Kluwer Academic Publishers: 7-26.

(Reilly 2003) M. P. Reilly, M. L. Wolfe, A. R. Localio and D. J. Rader (2003). "C-reactive protein and coronary artery calcification: The Study of Inherited Risk of Coronary Atherosclerosis (SIRCA)." Arterioscler Thromb Vasc Biol 23(10): 1851-6.

(Richardson 1989) P. D. Richardson, M. J. Davies and G. V. R. Born (1989). "Influence of plaque configuration and stress distribution on fissuring of coronary atherosclerotic plaques." The Lancet 2: 941-944.

(Ridker 1998a) P. M. Ridker, N. Rifai, M. A. Pfeffer, F. M. Sacks, L. A. Moye, S. Goldman, G. C. Flaker and E. Braunwald (1998). "Inflammation, pravastatin, and the risk of coronary events after myocardial infarction in patients with average cholesterol levels. Cholesterol and Recurrent Events (CARE) Investigators." Circulation 98(9): 839-44.

(Ridker 1998b) P. M. Ridker, C. H. Hennekens, B. Roitman-Johnson, M. J. Stampfer and J. Allen (1998). "Plasma concentration of soluble intercellular adhesion mol-

ecule 1 and risks of future myocardial infarction in apparently healthy men." Lancet 351(9096): 88-92.

(Ridker 2002) P. M. Ridker, N. Rifai, L. Rose, J. E. Buring and N. R. Cook (2002). "Comparison of C-reactive protein and low-density lipoprotein cholesterol levels in the prediction of first cardiovascular events." N Engl J Med 347(20): 1557-65.

(Ridker 2003) P. M. Ridker (2003). "Clinical application of C-reactive protein for cardiovascular disease detection and prevention." Circulation 107(3): 363-9.

(Rioufol 2002) G. Rioufol, G. Finet, I. Ginon, X. Andre-Fouet, R. Rossi, E. Vialle, E. Desjoyaux, G. Convert, J. F. Huret and A. Tabib (2002). "Multiple atherosclerotic plaque rupture in acute coronary syndrome: a three-vessel intravascular ultrasound study." Circulation 106(7): 804-8.

(Rioufol 2004) G. Rioufol, M. Gilard, G. Finet, I. Ginon, J. Boschat and X. Andre-Fouet (2004). "Evolution of spontaneous atherosclerotic plaque rupture with medical therapy: long-term follow-up with intravascular ultrasound." Circulation 110(18): 2875-80.

(Romson 1980) J. L. Romson, D. W. Haack and B. R. Lucchesi (1980). "Electrical induction of coronary artery thrombosis in the ambulatory canine: a model for in vivo evaluation of anti-thrombotic agents." Thromb Res 17(6): 841-53.

(Ross 1999a) R. Ross (1999). "Atherosclerosis is an inflammatory disease." Am Heart J 138(5 Pt 2): S419-20.

(Ross 1999b) R. Ross (1999). "Atherosclerosis--an inflammatory disease." N Engl J Med 340(2): 115-26.

(Rothkrantz-Kos 2002) S. Rothkrantz-Kos, M. P. Schmitz, O. Bekers, P. P. Menheere and M. P. van Dieijen-Visser (2002). "High-sensitivity C-reactive protein methods examined." Clin Chem 48(2): 359-62.

(Ryan 1997) L. K. Ryan and F. S. Foster (1997). "Ultrasonic measurement of differential displacement and strain in a vascular model." Ultrason Imaging 19: 19-38.

(SA de Winter 2003) I. H. SA de Winter, R Hamers, PJ de Feyter, PW Serruys, JRTC Roelandt, N Bruining (2003). "Computer assisted three-dimensional plaque characterization in ultracoronary ultrasound studies." Computers in Cardiology 30: 73-76.

(Sabetai 2000) M. M. Sabetai, T. J. Tegos, A. N. Nicolaides, S. Dhanjil, G. J. Pare and J. M. Stevens (2000). "Reproducibility of computer-quantified carotid plaque echogenicity: can we overcome the subjectivity?" Stroke 31(9): 2189-96.

(Saijo 2004) Y. Saijo, A. Tanaka, N. Owada, Y. Akino and S. Nitta (2004). "Tissue velocity imaging of coronary artery by rotating-type intravascular ultrasound." Ultrasonics 42(1-9): 753-7.

(Salunke 1997) N. V. Salunke and L. D. Topoleski (1997). "Biomechanics of atherosclerotic plaque." Crit Rev Biomed Eng 25(3): 243-285.

(Samani 2001) A. Samani, J. Bishop and D. B. Plewes (2001). "A constrained modulus reconstruction technique for breast cancer assessment." IEEE Trans Med Imaging 20(9): 877-85.

(Sarvazyan 1998) A. Sarvazyan (1998). "Mechanical imaging: a new technology for medical diagnostics." Int J Med Inf 49(2): 195-216.

(Schaar 2002) J. A. Schaar, C. L. de Korte, F. Mastik and A. F. W. van der Steen (2002). "Effect of temperature increase and freezing on intravascular elastography." Ultrasonics 40(1-8): 879-81.

(Schaar 2003a) J. A. Schaar, C. L. De Korte, F. Mastik, C. Strijder, G. Pasterkamp, E. Boersma, P. W. Serruys and A. F. W. Van Der Steen (2003). "Characterizing vulnerable plaque features with intravascular elastography." Circulation 108(21): 2636-41.

(Schaar 2003b) J. A. Schaar, F. Mastik, E. Regar, C. L. De Korte, A. F. W. van der Steen and P. W. Serruys (2003). "Reproducibility of three-dimensional palpography." Eur Heart J(suppl.): 2203.

(Schaar 2004a) J. A. Schaar, E. Regar, F. Mastik, E. P. McFadden, F. Saia, C. Disco, C. L. de Korte, P. J. de Feyter, A. F. van der Steen and P. W. Serruys (2004). "Incidence of high-strain patterns in human coronary arteries: assessment with three-dimensional intravascular palpography and correlation with clinical presentation." Circulation 109(22): 2716-9.

(Schaar 2004b) J. A. Schaar, J. E. Muller, E. Falk, R. Virmani, V. Fuster, P. W. Serruys, A. Colombo, C. Stefanadis, S. Ward Casscells, P. R. Moreno, A. Maseri and A. F. van der Steen (2004). "Terminology for high-risk and vulnerable coronary artery plaques. Report of a meeting on the vulnerable plaque, June 17 and 18, 2003, Santorini, Greece." Eur Heart J 25(12): 1077-82.

(Schaar 2005) J. A. Schaar, C. L. d. Korte, F. Mastik, L. C. A. v. Damme, R. Krams, P. W. Serruys and A. F. W. v. d. Steen (2005). "Three-Dimensional Palpography of Human Coronary Arteries." Herz 30(2): 125-133.

(Schartl 2001) M. Schartl, W. Bocksch, D. H. Koschyk, W. Voelker, K. R. Karsch, J. Kreuzer, D. Hausmann, S. Beckmann and M. Gross (2001). "Use of intravascular ultrasound to compare effects of different strategies of lipid-lowering therapy on

plaque volume and composition in patients with coronary artery disease." Circulation 104(4): 387-92.

(Schmermund 1999) A. Schmermund, A. E. Denktas, J. A. Rumberger, T. F. Christian, P. F. Sheedy, 2nd, K. R. Bailey and R. S. Schwartz (1999). "Independent and incremental value of coronary artery calcium for predicting the extent of angiographic coronary artery disease: comparison with cardiac risk factors and radionuclide perfusion imaging." J Am Coll Cardiol 34(3): 777-86.

(Schmermund 2001) A. Schmermund and R. Erbel (2001). "Unstable coronary plaque and its relation to coronary calcium." Circulation 104(14): 1682-7.

(Schoenhagen 2001) P. Schoenhagen, K. M. Ziada, D. G. Vince, S. E. Nissen and E. M. Tuzcu (2001). "Arterial remodeling and coronary artery disease: the concept of "dilated" versus "obstructive" coronary atherosclerosis." J Am Coll Cardiol 38(2): 297-306.

(Schoenhagen 2003) P. Schoenhagen, E. M. Tuzcu, A. E. Stillman, D. J. Moliterno, S. S. Halliburton, S. A. Kuzmiak, J. M. Kasper, W. A. Magyar, M. L. Lieber, S. E. Nissen and R. D. White (2003). "Non-invasive assessment of plaque morphology and remodeling in mildly stenotic coronary segments: comparison of 16-slice computed tomography and intravascular ultrasound." Coron Artery Dis 14(6): 459-62.

(Schroeder 2001) S. Schroeder, A. F. Kopp, A. Baumbach, C. Meisner, A. Kuettner, C. Georg, B. Ohnesorge, C. Herdeg, C. D. Claussen and K. R. Karsch (2001). "Noninvasive detection and evaluation of atherosclerotic coronary plaques with multislice computed tomography." J Am Coll Cardiol 37(5): 1430-5.

(Sechtem 1993) U. Sechtem, G. Arnold, T. Keweloh, C. Casper and J. M. Curtius (1993). "[In vitro diagnosis of coronary plaque morphology with intravascular ultrasound: comparison with histopathologic findings]." Z Kardiol 82(10): 618-27.

(Serruys 1996) P. W. Serruys, H. Emanuelsson, W. van der Giessen, A. C. Lunn, F. Kiemeney, C. Macaya, W. Rutsch, G. Heyndrickx, H. Suryapranata, V. Legrand, J. J. Goy, P. Materne, H. Bonnier, M. C. Morice, J. Fajadet, J. Belardi, A. Colombo, E. Garcia, P. Ruygrok, P. de Jaegere and M. A. Morel (1996). "Heparin-coated Palmaz-Schatz stents in human coronary arteries. Early outcome of the Benestent-II Pilot Study." Circulation 93(3): 412-22.

(Seshiah 2002) P. N. Seshiah, D. J. Kereiakes, S. S. Vasudevan, N. Lopes, B. Y. Su, N. A. Flavahan and P. J. Goldschmidt-Clermont (2002). "Activated monocytes induce smooth muscle cell death: role of macrophage colony-stimulating factor and cell contact." Circulation 105(2): 174-80.

(Shapo 1996) B. M. Shapo, J. R. Crowe, A. R. Skovoroda, M. Eberle, N. A. Cohn and M. O'Donnell (1996). "Displacement and strain imaging of coronary arteries with intraluminal ultrasound." IEEE Trans Ultrason Ferroelectr Freq Control 43(2): 234-246.

(Sherman 1986) C. T. Sherman, F. Litvack, W. Grundfest, M. Lee, A. Hickey, A. Chaux, R. Kass, C. Blanche, J. Matloff, L. Morgenstern and et al. (1986). "Coronary angioscopy in patients with unstable angina pectoris." N Engl J Med 315(15): 913-9.

(Skovoroda 1995) A. R. Skovoroda, S. Y. Emelianov and M. O'Donnell (1995). "Tissue elasticity reconstruction based on ultrasonic displacement and strain images." IEEE Trans Ultrason Ferroelectr Freq Control 42(4): 747-765.

(Slager 2000) C. J. Slager, J. J. Wentzel, J. C. Schuurbiers, J. A. Oomen, J. Kloet, R. Krams, C. von Birgelen, W. J. van der Giessen, P. W. Serruys and P. J. de Feyter (2000). "True 3-dimensional reconstruction of coronary arteries in patients by fusion of angiography and IVUS (ANGUS) and its quantitative validation." Circulation 102(5): 511-6.

(Sosnovik 2002) D. E. Sosnovik, J. E. Muller, S. Kathiresan and T. J. Brady (2002). "Non-invasive imaging of plaque vulnerability: an important tool for the assessment of agents to stabilise atherosclerotic plaques." Expert Opin Investig Drugs 11(5): 693-704.

(Sotoudeh 2002) M. Sotoudeh, Y. S. Li, N. Yajima, C. C. Chang, T. C. Tsou, Y. Wang, S. Usami, A. Ratcliffe, S. Chien and J. Y. Shyy (2002). "Induction of apoptosis in vascular smooth muscle cells by mechanical stretch." Am J Physiol Heart Circ Physiol 282(5): H1709-16.

(Soualmi 1997) L. Soualmi, M. Bertrand, R. Mongrain and J. C. Tardif (1997). Forward and inverse problems in endovascular elastography. In: Acoustical Imaging. S. Lees and L. A. Ferrari. New York, USA, Plenum. 23: 203-209.

(Spencer 1997) T. Spencer, M. P. Ramo, D. M. Salter, T. Anderson, P. P. Kearney, G. R. Sutherland, K. A. Fox and W. N. McDicken (1997). "Characterisation of atherosclerotic plaque by spectral analysis of intravascular ultrasound: an in vitro methodology." Ultrasound Med Biol 23(2): 191-203.

(Stefanadis 1999) C. Stefanadis, L. Diamantopoulos, C. Vlachopoulos, E. Tsiamis, J. Dernellis, K. Toutouzas, E. Stefanadi and P. Toutouzas (1999). "Thermal heterogeneity within human atherosclerotic coronary arteries detected in vivo: A new method of detection by application of a special thermography catheter." Circulation 99(15): 1965-71.

(Stefanadis 2001) C. Stefanadis, K. Toutouzas, E. Tsiamis, C. Stratos, M. Vavuranakis, I. Kallikazaros, D. Panagiotakos and P. Toutouzas (2001). "Increased local temperature in human coronary atherosclerotic plaques: an independent predictor of clinical outcome in patients undergoing a percutaneous coronary intervention." J Am Coll Cardiol 37(5): 1277-83.

(Stefanadis 2003) C. Stefanadis, K. Toutouzas, M. Vavuranakis, E. Tsiamis, S. Vaina and P. Toutouzas (2003). "New balloon-thermography catheter for in vivo temperature measurements in human coronary atherosclerotic plaques: a novel approach for thermography?" Catheter Cardiovasc Interv 58(3): 344-50.

(Sumi 1995) C. Sumi, A. Suzuki and K. Nakayama (1995). "Estimation of shear modulus distribution in soft tissue from strain distribution." IEEE Trans Biomed Eng 42(2): 193-202.

(Sumi 2000) C. Sumi, K. Nakayama and M. Kubota (2000). "An effective ultrasonic strain measurement-based shear modulus reconstruction technique for superficial tissues--demonstration on in vitro pork ribs and in vivo human breast tissues." Phys Med Biol 45(6): 1511-20.

(Takano 2001) M. Takano, K. Mizuno, K. Okamatsu, S. Yokoyama, T. Ohba and S. Sakai (2001). "Mechanical and structural characteristics of vulnerable plaques: analysis by coronary angioscopy and intravascular ultrasound." J Am Coll Cardiol 38(1): 99-104.

(Talhami 1994) H. E. Talhami, L. S. Wilson and M. L. Neale (1994). "Spectral tissue strain: a new technique for imaging tissue strain using intravascular ultrasound." Ultrasound Med Biol 20(8): 759-772.

(Thury 2001) A. Thury, J. J. Wentzel, J. C. Schuurbiers, J. M. Ligthart, R. Krams, P. J. de Feyter, P. W. Serruys and C. J. Slager (2001). "Prominent role of tensile stress in propagation of a dissection after coronary stenting: computational fluid dynamic analysis on true 3d-reconstructed segment." Circulation 104(11): E53-4.

(Toussaint 1995) J. F. Toussaint, J. F. Southern, V. Fuster and H. L. Kantor (1995). "T2-weighted contrast for NMR characterization of human atherosclerosis." Arterioscler Thromb Vasc Biol 15(10): 1533-42.

(Toussaint 1996) J. F. Toussaint, G. M. LaMuraglia, J. F. Southern, V. Fuster and H. L. Kantor (1996). "Magnetic resonance images lipid, fibrous, calcified, hemorrhagic, and thrombotic components of human atherosclerosis in vivo." Circulation 94(5): 932-8.

(Uchida 1995) Y. Uchida, F. Nakamura, T. Tomaru, T. Morita, T. Oshima, T. Sasaki, S. Morizuki and J. Hirose (1995). "Prediction of acute coronary syndromes by per-

cutaneous coronary angioscopy in patients with stable angina." Am Heart J 130(2): 195-203.

(Vallabhajosula 1997) S. Vallabhajosula and V. Fuster (1997). "Atherosclerosis: imaging techniques and the evolving role of nuclear medicine." J Nucl Med 38(11): 1788-96.

(van De Poll 2001) S. W. van De Poll, T. J. Romer, O. L. Volger, D. J. Delsing, T. C. Bakker Schut, H. M. Princen, L. M. Havekes, J. W. Jukema, A. van Der Laarse and G. J. Puppels (2001). "Raman spectroscopic evaluation of the effects of diet and lipid-lowering therapy on atherosclerotic plaque development in mice." Arterioscler Thromb Vasc Biol 21(10): 1630-5.

(van De Poll 2002) S. W. E. van De Poll, J. T. Motz and J. R. Kramer (2002). Prospects of Laser Spectroscopy to detect vulnerable plaque. In: Cardiovascular plaque rupture. D. L. Brown. New York, Dekker.

(van der Steen 1998) A. F. W. van der Steen, C. L. de Korte, E. I. Céspedes. Intravascular ultrasound elastography. Ultraschall Med 19: 196-201

(van der Steen 2003) A. F. W. van der Steen, C. L. de Korte, F. Mastik and J. A. Schaar (2003) "Three dimensional tissue hardness imaging" World patent WO03/ 017845 A1

(van der Wal 1994) A. C. van der Wal, A. E. Becker, C. M. van der Loos and P. K. Das (1994). "Site of intimal rupture or erosion of thrombosed coronary atherosclerotic plaques is characterized by an inflammatory process irrespective of the dominant plaque morphology." Circulation 89(1): 36-44.

(Van Houten 1999) E. E. Van Houten, K. D. Paulsen, M. I. Miga, F. E. Kennedy and J. B. Weaver (1999). "An overlapping subzone technique for MR-based elastic property reconstruction." Magn Reson Med 42(4): 779-86.

(Van Mieghem 2005) C. A. G. Van Mieghem, N. Bruining, J. A. Schaar, E. P. McFadden, N. Mollet, F. Cademartiri, F. Mastik, J. M. R. Ligthart, G. A. Rodriguez Granillo, M. Valgimigli, G. Sianos, W. J. van der Giessen, B. Backx, M. A. M. Morel, G. A. Van Es, J. D. Sawyer, J. Kaplow, A. Zalewski, A. F. W. van der Steen, P. de Feyter and P. W. Serruys (2005). "Rationale and methods of the integrated biomarker and imaging study (IBIS): combining invasive and non-invasive imaging with biomarkers to detect subclinical atherosclerosis and assess coronary lesion biology." Int J Cardivasc Imag (in press).

(Varnava 2002) A. M. Varnava, P. G. Mills and M. J. Davies (2002). "Relationship between coronary artery remodeling and plaque vulnerability." Circulation 105(8): 939-43.

(Veress 1998) A. I. Veress, J. F. Cornhill, E. E. Herderick and J. D. Thomas (1998). "Age-related development of atherosclerotic plaque stress: a population- based finite-element analysis." Coron Artery Dis 9(1): 13-19.

(Veress 2000) A. I. Veress, D. G. Vince, P. M. Anderson, J. F. Cornhill, E. E. Herderick, J. D. Klingensmith, B. D. Kuban, N. L. Greenberg and J. D. Thomas (2000). "Vascular mechanics of the coronary artery." Z Kardiol 89(Suppl 2): 92-100.

(Veress 2002) A. I. Veress, J. A. Weiss, G. T. Gullberg, D. G. Vince and R. D. Rabbitt (2002). "Strain measurement in coronary arteries using intravascular ultrasound and deformable images." J Biomech Eng 124(6): 734-41.

(Verheye 2002) S. Verheye, G. R. De Meyer, G. Van Langenhove, M. W. Knaapen and M. M. Kockx (2002). "In vivo temperature heterogeneity of atherosclerotic plaques is determined by plaque composition." Circulation 105(13): 1596-601.

(Virmani 2000) R. Virmani, F. D. Kolodgie, A. P. Burke, A. Farb and S. M. Schwartz (2000). "Lessons from sudden coronary death: a comprehensive morphological classification scheme for atherosclerotic lesions." Arterioscler Thromb Vasc Biol 20(5): 1262-75.

(Virmani 2001) R. Virmani, A. P. Burke and A. Farb (2001). "Sudden cardiac death." Cardiovasc Pathol 10(5): 211-8.

(Virmani 2002) R. Virmani, A. P. Burke, A. Farb and F. D. Kolodgie (2002). "Pathology of the unstable plaque." Prog Cardiovasc Dis 44(5): 349-56.

(Virmani 2003) R. Virmani, A. P. Burke, F. D. Kolodgie and A. Farb (2003). "Pathology of the thin-cap fibroatheroma: a type of vulnerable plaque." J Interv Cardiol 16(3): 267-72.

(Vogt 1993) A. Vogt, R. von Essen, U. Tebbe, W. Feuerer, K. F. Appel and K. L. Neuhaus (1993). "Impact of early perfusion status of the infarct-related artery on short-term mortality after thrombolysis for acute myocardial infarction: retrospective analysis of four German multicenter studies." J Am Coll Cardiol 21(6): 1391-5.

(von Birgelen 1997) C. von Birgelen, E. A. de Vrey, G. S. Mintz, A. Nicosia, N. Bruining, W. Li, C. J. Slager, J. R. Roelandt, P. W. Serruys and P. J. de Feyter (1997). "ECG-gated three-dimensional intravascular ultrasound: feasibility and reproducibility of the automated analysis of coronary lumen and atherosclerotic plaque dimensions in humans." Circulation 96(9): 2944-52.

(von Birgelen 2001) C. von Birgelen, W. Klinkhart, G. S. Mintz, A. Papatheodorou, J. Herrmann, D. Baumgart, M. Haude, H. Wieneke, J. Ge and R. Erbel (2001). "Plaque distribution and vascular remodeling of ruptured and nonruptured coro-

nary plaques in the same vessel: an intravascular ultrasound study in vivo." J Am Coll Cardiol 37(7): 1864-70.

(von Birgelen 2003) C. von Birgelen, M. Hartmann, G. S. Mintz, D. Baumgart, A. Schmermund and R. Erbel (2003). "Relation between progression and regression of atherosclerotic left main coronary artery disease and serum cholesterol levels as assessed with serial long-term (> or =12 months) follow-up intravascular ultrasound." Circulation 108(22): 2757-62.

(Von Birgelen 2004) C. Von Birgelen, M. Hartmann, G. S. Mintz, D. Bose, H. Eggebrecht, M. Gossl, T. Neumann, D. Baumgart, H. Wieneke, A. Schmermund, M. Haude and R. Erbel (2004). "Spectrum of remodeling behavior observed with serial long-term (>/=12 months) follow-up intravascular ultrasound studies in left main coronary arteries." Am J Cardiol 93(9): 1107-13.

(Vorp 1995) D. A. Vorp, K. R. Rajagopal, P. J. Smolinski and H. S. Borovetz (1995). "Identification of elastic properties of homogeneous, orthotropic vascular segments in distension." J Biomech 28(5): 501-12.

(Wada 1997) T. Wada, K. Fujishiro, T. Fukumoto and S. Yamazaki (1997). "Relationship between ultrasound assessment of arterial wall properties and blood pressure." Angiology 48(10): 893-900.

(Wan 2001) M. Wan, Y. Li, J. Li, Y. Cui and X. Zhou (2001). "Strain imaging and elasticity reconstruction of arteries based on intravascular ultrasound video images." IEEE Trans Biomed Eng 48(1): 116-20.

(Wang 2002) J. Wang, Y. J. Geng, B. Guo, T. Klima, B. N. Lal, J. T. Willerson and W. Casscells (2002). "Near-infrared spectroscopic characterization of human advanced atherosclerotic plaques." J Am Coll Cardiol 39(8): 1305-13.

(Wang 2004) J. C. Wang, S. L. Normand, L. Mauri and R. E. Kuntz (2004). "Coronary Artery Spatial Distribution of Acute Myocardial Infarction Occlusions." Circulation.

(Ward 2000) M. R. Ward, G. Pasterkamp, A. C. Yeung and C. Borst (2000). "Arterial remodeling. Mechanisms and clinical implications." Circulation 102(10): 1186-91.

(Weiss 2001) C. R. Weiss, A. E. Arai, M. N. Bui, K. O. Agyeman, M. A. Waclawiw, R. S. Balaban and R. O. Cannon, 3rd (2001). "Arterial wall MRI characteristics are associated with elevated serum markers of inflammation in humans." J Magn Reson Imaging 14(6): 698-704.

(Weizsacker 1988) H. W. Weizsacker and J. G. Pinto (1988). "Isotropy and anisotropy of the arterial wall." J Biomech 21(6): 477-487.

(Wellman 1999) P. S. Wellman and R. D. Howe (1999). "Extracting features from tactile maps." MICCAI: 1133-42.

(Wickline 1994) S. A. Wickline, J. G. Miller, D. Recchia, A. M. Sharkey, S. L. Bridal and D. H. Christy (1994). "Beyond intravascular imaging: Quantitative ultrasonic tissue characterization of vascular pathology." IEEE Ultrasonics Symposium.

(Wilson 1994) L. S. Wilson, M. L. Neale, H. E. Talhami and M. Appleberg (1994). "Preliminary results from attenuation-slope mapping of plaque using intravascular ultrasound." Ultrasound Med Biol 20(6): 529-42.

(Yamada 1970) H. Yamada and F. Evans (1970). Strenght of biological materials. Baltimore, USA, The Williams & Wilkins Company.

(Yamagishi 2000) M. Yamagishi, M. Terashima, K. Awano, M. Kijima, S. Nakatani, S. Daikoku, K. Ito, Y. Yasumura and K. Miyatake (2000). "Morphology of vulnerable coronary plaque: insights from follow-up of patients examined by intravascular ultrasound before an acute coronary syndrome." J Am Coll Cardiol 35(1): 106-11.

(Yuan 1998) C. Yuan, K. W. Beach, L. H. Smith, Jr. and T. S. Hatsukami (1998). "Measurement of atherosclerotic carotid plaque size in vivo using high resolution magnetic resonance imaging." Circulation 98(24): 2666-71.

(Yuan 2001) C. Yuan, L. M. Mitsumori, K. W. Beach and K. R. Maravilla (2001). "Carotid atherosclerotic plaque: noninvasive MR characterization and identification of vulnerable lesions." Radiology 221(2): 285-99.

(Zhu 2003) Y. Zhu, T. J. Hall and J. Jiang (2003). "A finite-element approach for Young's modulus reconstruction." IEEE Trans Med Imaging 22(7): 890-901.

Part VIII
Publications
Curriculum Vitae
Acknowledgement

Chapter 19

Publications

Peer reviewed papers

Schaar JA, de Korte CL, Mastik F, van Damme LCA, Krams R, Serruys PW, van der Steen AFW. Three-Dimensional Palpography of Human Coronary Arteries. Herz (2005) 30, 125-133

Baldewsing RA, Schaar JA, Mastik F, Oomens CW, van der Steen AF. Assessment of vulnerable plaque composition by matching the deformation of a parametric plaque model to measured plaque deformation. IEEE Trans Med Imaging. 2005; 4: 514-28.

Regar E, Schaar JA, Mont E, Virmani R, Serruys PW. Optical coherence tomography. Cardiovasc Radiat Med 2003; 4: 198-204.

Baldewsing RA, de Korte CL, Schaar JA, Mastik F, van der Steen AFW. A finite element model for performing intravascular ultrasound elastography of human atherosclerotic coronary arteries. Ultrasound Med Biol. 2004; 30: 803-13.

Schaar JA, Muller JE, Falk E, Virmani R, Fuster V, Serruys PW, Colombo A, Stefanadis C, Casscells SW, Moreno PR, Maseri A, van der Steen AFW. Terminology for high-risk and vulnerable coronary artery plaques. Eur Heart J. 2004; 25: 1077-82.

Schaar JA, Regar E, Mastik F, McFadden EP, Saia F, Disco C, de Korte CL, de Feyter PJ, van der Steen AFW, Serruys PW. Incidence of High-Strain Patterns in Human Coronary Arteries. Assessment With Three-Dimensional Intravascular Palpography and Correlation With Clinical Presentation. Circulation 2004; 109: 2716-2719

Schaar JA, de Feyter P, van der Steen AFW, Serruys PW. Plaques vulnérables: detection en sale de cathéterisme. Abstract Cardiologie 2004; 390: 20-24

Brusseau E, de Korte CL, Mastik F, Schaar JA, van der Steen AFW. Fully automatic luminal contour segmentation in intracoronary ultrasound imaging - a statistical approach. IEEE Trans Med Imaging. 2004; 23: 554-66

Baldewsing RA, de Korte CL, Schaar JA, Mastik F, van der Steen AF. Finite element modeling and intravascular ultrasound elastography of vulnerable plaques: parameter variation. Ultrasonics 2004; 42: 723-9

Baldwesing RA, de Korte CL, Schaar JA, Mastik F, van der Steen AFW. A Finite Element Model for performing Intravascular Ultrasound Elastography of Human Atherosclerotic Coronary Arteries. Ultrasound in Medicine and Biology 2004; 30: in press

Regar E, Schaar JA, Mont E, Virmani R; Serruys PW. Optical Coherence Tomography. Cardiovasc Rad Med. 2004; 4: 198-204

Schaar JA, de Korte CL, Mastik F, Strijder C, Pasterkamp G, Boersma E, Serruys PW, van der Steen AF. Characterizing vulnerable plaque features with intravascular elastography. Circulation. 2003; 108: 2636-41

Schaar JA, de Korte CL, Mastik F, Baldewsing R, Regar E, de Feyter PJ, Slager CJ, van der Steen AFW, Serruys PW. Intravascular palpography for high-risk vulnerable plaque assessment. Herz. 2003; 28: 488-95

Arampatzis CA, Ligthart JM, Schaar JA, Nieman K, Serruys PW, de Feyter PJ.Images in cardiovascular medicine. Detection of a vulnerable coronary plaque: a treatment dilemma. Circulation. 2003; 108: e34-5

de Korte CL, Schaar JA, Mastik F, Serruys PW, van der Steen AFW. Intravascular elastography: from bench to bedside. J Interv Cardiol 2003; 16: 253-9

de Feyter PJ, Serruys PW, Nieman K, Mollet N, Cademartiri F, van Geuns RJ, Slager C, van der Steen AFW, Krams R, Schaar JA, Wielopolski P, Pattynama PMT, Arampatzis, van der Lught A, Regar E, Lighthart J, Smits P. Imaging of coronary atherosclerosis and identification of vulnerable plaque. Netherlands Heart Journal 2003; 11: 347-358

Bartel T, Vanheiden H, Schaar J, Mertzkirch W, Erbel R. Biomechanical modeling of hemodynamic factors determining bulging of ventricular aneurysms. Ann Thorac Surg 2002; 74: 1581-7

Carlier SG, de Korte CL, Brusseau E, Schaar JA, Serruys PW, van der Steen AFW. Imaging of atherosclerosis. Elastography. J Cardiovasc Risk 2002; 9: 237-45

de Korte CL, Sierevogel M, Mastik F, Strijder Ch, Schaar JA, Velema E, Pasterkamp G, Serruys PW, Van der Steen AFW. Identification of Atherosclerotic Plaque Components With Intravascular Ultrasound Elastography In Vivo. Circulation 2002; 105: 1627

Schaar JA, de Korte CL, Mastik F, A.F.W. van der Steen. Effect of temperature and freezing on intravascular elastograms. Ultrasonics 2002; 40: 879-81

Schaar J. Multimedia presentations, Deutsches Ärzteblatt B-2352, 96, 45, 1999

Oldenburg O, Eggebrecht H, Gutersohn A, Schaar J, Brauck K, Haude M, Erbel R, Baumgart D. Myocardial lactate release after intracoronary verapamil application in humans: acute effects of intracoronary verapamil on systemic and coronary hemodynamics, myocardial metabolism, and norepinephrine levels. Cardiovasc Drugs Ther 15: 55 - 61, 2001

Bruch C, Schmermund A, Marin D, Katz M, Bartel T, Schaar J, Erbel R. Tei-index in patients with mild-to-moderate congestive heart failure. Eur Heart J 21: 1888-95, 2000

Bruch C, Schmermund A, Bartel T, Schaar J, Erbel R. Tissue doppler imaging: A new technique for assessment of pseudonormalization of the mitral inflow pattern. Echocardiography 17: 539-46, 2000

Oldenburg O, Baumgart D, Schaar J, Eggebrecht H, Caspari G, Haude M, Erbel R, Anti-ischemic effect of verapamil within the scope of interventional recanalization. Herz 24:581-6, 1999

Bruch C, Schmermund A, Bartel T, Schaar J, Erbel R, Tissue Doppler imaging (TDI) for on-line detection of regional early diastolic ventricular asynchrony in patients with coronary artery disease. Int J Card Imaging 15; 379-90, 1999

Bruch C, Marin D, Kuntz S, Schmermund A, Bartel T, Schaar J, Erbel R. Analysis of mitral annulus excursion with tissue Doppler echocardiography (tissue Doppler echocardiography = TDE). Noninvasive assessment of left ventricular, diastolic dysfunction. Z Kardiol 88;353-62, 1999

Bruch C, Schmermund A, Marin D, Kuntz S, Bartel T, Schaar J, Erbel R, M-mode analysis of mitral annulus motion for detection

of pseudonormalization of the mitral inflow pattern. Am J Cardiol 15; 84: 692-71999

Bruch C, Bartel T, Schmermund A, Schaar J, Erbel R. Asynchrony of Ventricular Contraction and Relaxation - On-Line Assessment in the Clinical Setting. Herz 23; 506-15, 1998

Bartel T, Müller S, Möhlenkamp S, Bruch C, Schaar J, Erbel R, Improved Structure Identification Using Tissue Doppler Echocardiography. Herz 23; 499-505, 1998

Bruch C, Baumgart D, Görge G, Pink R, Schaar J, Schönfelder B, Markgraf G, Olivier L, Drochner D, Kabatnik M, Erbel R, Aortic rupture after blunt chest trauma. Rapid diagnosis using transesophageal echocardiography when radiographic and computed tomographic findings are unclear. Dtsch Med Wochenschr 27; 244-249; 1998

Schramm L, Heidbreder E, Lopau K, Schaar J, Zimmermann J, Harlos J, Teschner M, Ling H, Heidland A Influence of nitric oxide on renal function in toxic acute renal failure in the rat. Miner Electrolyte Metab 22; 168-77, 1996

Schramm L, Heidbreder E, Schaar J, Lopau K, Zimmermann J, Gotz R, Ling H, Heidland A Toxic acute renal failure in the rat: effects of diltiazem and urodilatin on renal function. Nephron 68; 454-61, 1994

Schramm L, Heidbreder E, Lopau K, Schaar J, De Cicco D, Gotz R, Heidland A, Toxic acute renal failure in the rat: effects of L-arginine and N-methyl-L-arginine on renal function. Nephrol Dial Transplant 9, Suppl 4; 88-93, 1994

Schramm L, Lopau K, Schaar J, Götz R, Heidbreder E. Effects of diltiazem and urodilatin on renal function in toxic acute renal failure in the rat. Renal failure 15, No. 5, 705, 1993

Patent

A. F. W. van der Steen, C. L. de Korte, F. Mastik and J. A. Schaar (2003) "Three dimensional tissue hardness imaging" World patent WO03/ 017845 A1

Proceedings

Baldewsing RA, Schaar JA, Mastik F, Oomens CWJ, Van der Steen AFW. IVUS modulography of vulnerable plaques using a parametric finite element model; validation on a phantom and human coronary artery. Proceedings of the Second International Conference on the Ultrasonic measurement and Imaging of tissue elasticity 2003, Texas, USA, page 75

van der Steen AFW, de Korte CL, Schaar JA, Mastik F, Baldewsing RA, Serruys PW. 3D intrasvascular ultrasound palpography for vulnerable plaque detection. Proceedings of the 2004 IEEE International Symposium on Biomedical Imaging.

de Korte CL, Mastik F, Schaar JA, van der Steen AFW. 3 D Intravascular Palpography: From Phantoms to in vivo Applications. 2002 IEEE Ultrasonics Symposium Proceedings. Munich, Germany

Brusseau E, de Korte CL, Mastik F, Schaar JA, van der Steen AFW. Fully Automated Endoluminal Contour Detection in Intracoronary Ultrasound Images: A Preprocessing for Intravascular Elastography 2002 IEEE Ultrasonics Symposium Proceedings. Munich, Germany

R.A. Baldewsing, C.L. de Korte, F. Mastik, J.A. Schaar, and A.F.W. van der Steen Comparison of Finite Elements Model Elastograms and IVUS Elastograms Acquired from Phantoms and Arteries. 2002 IEEE Ultrasonics Symposium Proceedings. Munich, Germany

Book chapters

Schaar JA, Regar E, Saia F, Arampatzis CA, Hoye A, Mastik F, Krams R, Sjager CJ, Gijsen FJ, Wentzel JJ, de Feyter PG, van der Steen AFW, Serruys PW. Diagnosing the Vulnerable Plaque in the cardiac catheterization laboratory. In Waksman R, Serruys PW (Eds): Handbook of the vulnerable plaque. London: Martin Dunitz Publishers.

Regar E, Schaar JA, Mont E, Virmani R, Serruys PW: OCT - optical coherence tomography. In Waksman R, Serruys PW (Eds): Handbook of the vulnerable plaque. London: Martin Dunitz Publishers.

de Korte CL, Schaar JA, Mastik F, Serruys PW, van der Steen AFW. Intravascular elastography: from idea to technique. In Waksman R, Serruys PW (Eds): Handbook of the vulnerable plaque. London: Martin Dunitz Publishers.

de Korte CL, Mastik F, Schaar JA, Serruys PW, van der Steen AFW. Intravascular Elastography: From Idea to Clinical Tool. In Saijo Y, van der Steen AFW (Eds): Vascular Ultrasound. 2003 Springer ISBN 4-431-70328-4

Schaar JA, van der Steen AFW, Arampatzis CA, Kram R, Slager CJ, ten Have AG, van der Poll SW, Gijsen FJ, Wentzel JJ, de Feyter PJ, Serruys PW. Diagnosis of Vulnerable Plaque in the Cardiac Catheterization Laboratory. In Saijo Y, van der Steen AFW (Eds): Vascular Ultrasound. 2003 Springer ISBN 4-431-70328-4

Schaar JA, Regar E, Arampatzis CA, van der Ven ARA, Slager CJ, Gijsen FJ, Wentzel JJ, de Feyter PJ, van der Steen AFW, Serruys PW. Diagnosis of Vulnerable Plaque in the Cardiac Catheterization Laboratory. In Khachigian LM (Ed): High-Risk Atherosclerotic Plaques: Mechanisms, Imaging, Models, and Therapy. 2005 CRC Press ISBN 0-8493-3028-9

Regar E, Schaar JA, Saia F, Lemos PA, van der Giessen W, Magnin PA, Serruys PW. New intracoronary diagnostic methods. In Marco J, Serruys PW, Biamino G, Fajadet J, de Feyter P, Morice MC (Eds): The Paris course on revascularization. Paris: Europa edition. 2003. ISBN 2-913628-12-5

Regar E, Schaar JA, Wilensky RL, Mc Fadden E, van der Giessen W, de Feyter P, Serruys PW: Invasive Detection, Quantification and Monitoring of Plaque Vulnerability: Methods and Implications for Upcoming Clinical Trials. In Marco J, Serruys PW, Biamino G, Fajadet J, de Feyter P, Morice MC (Eds): The Paris course on revascularization. Paris: Europa edition 2004. ISBN 2-913628-16-8

Baldewsing RA, Schaar JA, de Korte CL, Mastik F, Serruys PW, van der Steen AFW. Intravascular Ultrasound Elastography: A Clinician's Tool for Assessing Vulnerability and Material Composi-

tion of Plaques.In Suri, Chun, Wilson and Laxminarayan (Eds): Plaque Characterization Using Multimodality imaging: Pixel to Molecular, Publisher: IOS press, The Netherlands 2005

Regar E, Lee CH, Schaar JA, Lemos PA, Serruys PW: New devices in interventional cardiology and atherosclerotic disease. In Tonkin A (Ed): Atherosclerosis and Heart Disease. London: Martin Dunitz Publishers 2005.

Schaar J, Erbel R, Compendium of cardiology, HOS Multimedica, http:\\www.multimedica.de

Schaar J, Erbel R, Valvular heart disease, in: Hombach V, Handbook of Cardiovascular Disease. Schattauer, Ulm, 2002 in press

Oral presentations:

Schaar JA. Vulnerable Plaque Detection. Keynote lecture of the 5th International Conference on New Trends in Cardiology. April 8 - 10, 2005, Thessaloniki, Greece

Schaar JA. Epidemiology of Heart Failure. The AG Edwards Meeting, New York, USA, March 3, 2005

Schaar JA. Palpography and the Vulnerable Plaque. February 18 - 19, 2005. Kitzbuehl, Austria

Schaar JA. Summary of the Taormina VP -2 Meeting. Athens Interventional Cardiovascular Therapeutics VI. April 8-9, 2004, Athens, Greece.

Schaar JA, Serruys PW. The IBIS Trial. Athens Interventional Cardiovascular Therapeutics VI. April 8-9, 2004, Athens, Greece.

Schaar JA, Mastik F, de Korte CL, Pasterkamp G, Baldewsing R, Regar E, Slager C, Krams R, de Feyter P, Serruys PW, van der Steen AFW. Palpography for Vulnerable Plaque Detection. ICIN Projectdag 06.10.2004. Utrecht. The Netherlands.

Schaar JA, van der Steen AFW. Featured lecture: The evolution of adjunctive catheter-based coronary imaging: Next generation IVUS and futuristic alternatives. TCT 2004, September 30, 2004. Washington DC, USA.

Schaar JA, van der Steen AFW. Palpography: Technique, Description, Case Examples and Clinical Developement Plans. TCT 2004, October 1st, 2004. Washington DC, USA.

Schaar JA, Mastik F, de Korte CL, Pasterkamp G, Baldewsing R, Regar E, Slager C, Krams R, de Feyter P, Serruys PW, van der Steen AFW. Palpography. The 2nd Vulnerable Plaque Meeting, June 7-8, 2004. Taormina, Italy

Schaar JA, Mastik F, Regar E, McFadden E, van der Steen AFW, de Feyter PJ, Serruys PW. CRP levels and vulnerable plaque detection with three-dimensional intravascular palpography. Eur Heart J 2004 suppl 209.

Baldewsing RA, Schaar JA, Mastik F, Oomens CWJ, van der Steen AFW. Young's Modulus Reconstruction for Assessing Vulnerable Atherosclerotic Plaque Composition In Vivo. 2004 IEEE International Ultrasonics Ferroelectrics and Frequency Control 50th Anniversary Conference, August 24-27, 2004, Montreal, Canada

Schaar JA, de Feyter PJ, van der Steen AFW, Serruys PW. Invasive Plaque Imaging. New Frontiers in Cardiology. Munich May 20-21, 2004

Schaar JA, Regar E, Saia F, de Korte CL, Mastik F, van der Steen AF, Serruys PW. Incidence of vulnerable plaque in humans: Assessment with 3D intravascular palpography. J Am Coll Cardiol 2004; 43 (Suppl A): 307A

Schaar JA. Assessment of drug eluting stents with IVUS. The AG Edwards Meeting, New York, USA, March 3, 2004

Schaar JA. Palpography. 1st International Vulnerable Plaque Meeting. June 17 - 18th, 2005, Santorini, Greece

Gijsen FJH, Wentzel JJ, Schuurbiers JCH, Schaar JA, Mastik F, de Korte CL, van der Steen AFW, Serruys PW, Slager CJ. 2003 Shear Stress and wall strain distribution in human coronary arteries in-vivo.Summer Bioengineering Conference, June 25-29, Sonesta Beach Resort in Key Biscayne, Florida

van der Steen AFW, Schaar JA, Mastik F, de Korte CL, Baldewsing RA, Serruys PW. EBR 2003 March 27, Intravascular ultrasound palpography for vulnerable plaque detection. Hôpital Européen Georges Pompidou, Paris

Baldewsing RA, Schaar JA, Mastik F, Oomens CWJ, van der Steen AFW. IVUS modulography of vulnerable plaques using a parametric finite element model; validation on a phantom and human coronary artery. Proceedings of the Second International Conference on the Ultrasonic measurement and Imaging of Tissue Elasticity 2003, Texas, USA, page 75.

van der Steen AFW, Schaar JA, Mastik F, de Korte CL, Baldewsing RA, Serruys PW. Intrasvascular ultrasound palpography for vulnerable plaque detection. International Workshop Endocoronary Biomechanics and Restenosis 2003, Paris, France

Schaar JA, Regar E, Mastik F, van der Steen AFW, Serruys PW. Forward looking optical coherence tomography: a potential tool to visualize the total chronic occlusion. Eur Heart J 2003 suppl Abstract: 2556

de Korte CL, Carlier SG, Mastik F, Schaar JA, Serruys PW, van der Steen AFW. Detection of plaque composition with intracoronary elastography as validated with directional atherectomy. Eur Heart J 2002 suppl. 1963

Schaar JA, de Korte CL, Mastik F, van der Steen AFW, Serruys PWS. Vulnerable plaque detection. Cardiology Seminars at the University South Alabama. March 15, 2002

Schaar JA, de Korte CL, Mastik F, Strijder C, Pasterkamp G, van der Steen AFW. Vulnerable Plaque Detection with Intravascular Elastography: A Sensitivity and Specificity Study. Circulation 104, Suppl 2176, 2001

Schaar JA, de Korte CL, Mastik F, van der Steen AFW, Serruys PWS. Elastic properties of coronary artery stenosis. The pressure area relation is dependent on stenosis type. Eur Heart J 22, Suppl. Sep, 3242, 2001

Schaar J, Oldenburg O, Caspari G, Gutersohn A, Sack S, Erbel R. A New Treatment of Pulmonary Hypertension: Simultaneous pulsatile Inhalation of Nitric Oxide and Iloprost. JACC Suppl A, 826-1, 2001

Schaar J, Oldenburg O, Gutersohn A, Baumgart D, Erbel R. A new steerable angioscopy catheter for diagnosis of pulmonary embolism. Eur Heart J 21, Suppl August/September, 1330, 2000

Schaar J, Gutersohn A, Heinzel F, Oldenburg O, Neurohr K, Erbel R, Sack S. Inhaled nitric oxide in patients with pulmonary hypertension leads to an upregulation of tumor necrosis factor alpha and atrial natriuretic peptide. Eur Heart J 21, Suppl August/September, 3255, 2000

Schaar J, Kopp S, Oldenburg O, Gutersohn A, Erbel R. Cholesterol self-management: a new way lowering cholesterol levels. Eur Heart J 21, Suppl August/September, 3309, 2000

Schaar J, Oldenburg O, Kopp S, Brehm D. Cholesterinselbstmessung: Eine Möglichkeit erhöhte Cholesterinwerte dauerhaft zu senken. Z Kardiol 89, Suppl 5, 1913, 2000

Schaar J, Oldenburg O, Erbel R. Diagnostik der pulmonalen Hypertonie. Fortbildungsveranstaltung der Ruhruniversität Bergmannsheil.

Schaar J, G. Görge, J. Ge, O. Oldenburg, M.H. Raus, D. Baumgart, R. Erbel. Percutaneous Intravascular Ultrasound-Guided Fenestration of Dissection Membranes in Patients With Aortic Dissection and Abdominal Ischemia. Abstract: 880-4, ACC, New Orleans, 1999

Schaar J, Oldenburg O, Baumgart D, Erbel R. Angioscopic diagnosis of lung embolism. 4th Congress of Angioscopy, Jena, 1999

Schaar J, Görge G, Oldenburg O, Raus MH, Baumgart D, Ge J, Erbel R. IVUS guided percutaneous transluminal fenestration (PTF) of aortic dissection. 28th meeting of the German Society of Thoracic Surgery, Dresden, 1999

Oldenburg O, Eggebrecht H, Gutersohn A, Schaar J, Brauck K, Baumgart D. Eine selektive Blockade a2- adrenerger Rezeptoren bei stenosierender KHK führt zur Steigerung des koronaren Blutflusses ohne Anstieg der Noradrenalinkonzentration im koronarvenösen Plasma. Z Kardiol 89, Supp 5, 1063, 2000

Oldenburg O, Gutersohn A, Schaar J, Eggebrecht H, Brauck K, Baumgart D. Die Verapamil-induzierte koronare Blutflusssteigerung geht über den anti-adrenergen Effekt auf koronare a2- Rezeptoren hinaus. Z Kardiol 89, Supp 5, 1143, 2000

Gutersohn A, Schaar J, Naber C. Der GNB3 C825T Polymorphismus ist mit der endothelialen Dysfunktion assoziiert. Z Kardiol 89, Supp 5, 1151, 2000

Erbel R, Schaar J, Eggebrecht H, Buck TH, Bartel TH, Management of acute aortic dissection, follow-up after surgery. Paris 1999

Erbel R, Schaar J. Morphologische Untersuchung der Lungenstrombahn mit einem steuerbaren Katheter: Kombination von Angiographie, Angioskopie und IVUS. Ingoldstadt 1999

Erbel R, Schaar J, Oldenburg O, Ge J, Baumgart D. Percutaneous, intravascular ultrasound-guided transluminale fenestration (PTF) of dissection membranes in patients with aortic dissection and abdominal ischemia. TCT Washington September 1999

Bartel T, Müller S, Nesser HJ, Mölenkamp S, Schaar J, Verbesserte Strukturidentifizierung mittels Gewebe-Doppler-Echokardiographie: Experimentelle und klinische Klassifizierung, Z Kardiol 88, Supp 1, 89; 1999

Görge G, Schaar J, Schaaf H, Erbel R. Angioscopy as a tool of evaluating the lung circulation with a steerable cartheter. 3th Congress of Angioscopy, Jena, 1998

Görge G, Ge J, Schaar J, Erbel R. An alternative to surgery: percutaneous, intravascular ultrasound guided fenestration of dissection membrane in patients with aortic dissection and ischemic syndroms. XXth Congress of the ESC, Vienna, 2586, 1998

Erbel R, Schaar J. Transesophageal echocardiography for the diagnosis of diseases of the aorta (intramural hematoma, aortic dissection): comparison with CT and MRI. Davos 1998

Poster presentations

Schaar JA, Mastik F, van Deel E, Slager C, Serruys PW, Duncker DJ, van der Steen AFW. The Thrombus Becomes Stiffer In the First 3 Hours: In Vivo Assessment with Palpography. J Am Coll Cardiol 2005; 44 (suppl A): 123A

Schaar JA, de Feyter P, McFadden E, Zalewski A, Mastik F, Backx B, van der Steen AFW, Serruys PW. Palpography in the IBIS Trial: The Assessment of Mechanical Properties of Coronary Atheroma in 85 Patients. Circulation 110, Suppl 1803, 2004

Serruys PW, de Feyter PJ, Bruining N, Schaar JA, Mollet NRA, Van Mieghem C, Backx B, Zalewski A. IBIS: multimodality imaging of non-culprit coronary lesions. Eur Heart J. 2004 suppl. 2852.

Schaar JA, Mastik F, van Deel ED, Slager C, Serruys PW, Duncker DJ, van der Steen AFW. The thrombus becomes stiffer in the first 3 hours: in vivo assessment with palpography. Eur Heart J. 2004 Suppl. 593

Schaar JA, Mastik F, Baldewsing RA, de Korte CL, Krams R, Intravascular Palpography: A new method to diagnose vulnerable plaque. Hartstichting 2004

Schaar JA, Regar E, Mastik F, van der Steen AF, Serruys PW: Forward looking optical coherence tomography: A potential tool to visualize the total chronic occlusion. J Am Coll Cardiol 2004; 43 (Suppl A): 35A

Baldewsing RA, de Korte CL, Schaar JA, Mastik F, van der Steen AFW. Finite element modelling and intravascular ultrasound elastography of phantoms and coronary arteries: parameter variation. Ultrasonics International 2003, Granada, Spain

Schaar JA, Regar E, Mastik F, Saia F, de Korte F, de Feyter PJ, van der Steen AFW, Serruys PW. Incidence of vulnerable plaques in humans: assessment with intravascular palpography. Eur Heart J 2003 suppl. P2210

Schaar JA, Mastik F, Regar E, de Korte CL, van der Steen AFW, Serruys PW. Reproducibility of three-dimensional palpography. Eur Heart J 2003 suppl. P2203

Schaar JA, de Korte CL, Mastik F, Strijder C, Pasterkamp G, Baldewsing RA, P.W. Serruys, A.F.W. van der Steen. Intravascular elastography detects the weak vulnerable plaque. Eur Heart J 2002 suppl. P482

Regar E, Schaar J, van der Giessen W, van der Steen A, Serruys PW. Real-time, in-vivo optical coherence tomography of human coronary arteries using a dedicated imaging wire. Am J Cardiol 2002; 90 (6A): TCT332 Suppl. S

Schaar JA, de Korte CL, Mastik F, Strijder C, Pasterkamp G, Serruys PW, van der Steen AFW. Vulnerable Plaque Characterization With Intravascular Elastography. JACC 39, Suppl A, 1054-20, 2002

Schaar JA, Mastik F, de Korte CL, Doyley MM, Carlier S, Bom N, Serruys PW, van der Steen AFW. Three-dimensional palpography: a new tool for detection of vulnerable plaque, a feasibility and reproducibility in vitro. Eur Heart J 22, Suppl. Sep, P2784, 2001

Schaar JA, de Korte CL, Mastik F, A.F.W. van der Steen. Effect of temperature and freezing on intravascular elastograms. Eur Heart J 22, Suppl. Sep, P2781, 2001

Schaar J, Oldenburg O, Gutersohn A, Erbel R, Schaar S. Cholesterol Self Management: a New Way for Better Cholesterol Control. JACC 37, Suppl A, 1161-175, 2001

Schaar J. Combined inhalation of nitric oxide and aerosolised iloprost in patients with pulmonary hypertension leads to successful reduction of pulmonary resistance. Z Kardiol 90, Suppl 2, 252, 2001

Schaar J, Gutersohn A, Oldenburg O, Heinzel F, Schmermund A, Sack S, Erbel R. Combined inhalation of nitric oxide and aerosolised iloprost in patients with pulmonary hypertension leads to successful reduction of pulmonary resistance. Eur Heart J 21, Suppl Aug/Sep, P1711, 2000

Schaar J, Oldenburg O, Hunold P, Kopp S, Brehm D, Erbel R. Improvement of Cholesterol Levels by a Structured and Standardized Cholesterol Physiology and Diet Education Program. JACC 35, Suppl A, 1159, 2000

Schaar J, Oldenburg O, Heinzel F, Gutersohn A, Baumgart D, Erbel R. Inhaled nitric oxide in patients with pulmonary hypertension leads to an upregulation of tumor necrosis factor alpha and atrial natriuretic peptide. Intensivmed 37, P 21, 2000

Schaar J, Gutersohn A, Heinzel F, Oldenburg O, Neurohr K, Sack S, Erbel R. Akute-Phase-Proteine nach Behandlung einer Aortendissektion. Intensivmed 37, P69, 2000

Schaar J, Gutersohn A, Heinzel F, Oldenburg O, Schmermund A, Bartel T, Sack S, Erbel R. Simultaneous pulsatile inhalation of nitric oxide and aerosolized iloprost (SPINI) in patients with Pulmonary Hypertension leads to successful reduction of pulmonary resistance: an in vivo study. Intensivmed 37, P18, 2000

Schaar J, Oldenburg O, Gutersohn A, Görge G, Heinzel F, Baumgart D, Erbel R. Ein neuer steuerbarer Angioskopie Katheter zur Diagnose von Lungenembolien. Intensivmed 37, P12, 2000

Schaar J, Oldenburg O, Gutersohn A, Heinzel F, Zimmermann U, Sack S, Baumgart D, Erbel R. Inhaled nitric oxide in patients with pulmonary hypertension leads to an upregulation of tumor necrosis factor alpha and atrial natriuretic peptide. Basic Res Cardiol 94, 220, 1999

Schaar J, Oldenburg O, Gutersohn A, Raus M, Koch L, Baumgart D. Eine neue Methode zur Untersuchung koronarer Physiologie: Gleichzeitige Messung und Aufnahme von relativer koronarer Flußreserve und intrakoronarem Druck. Z Kardiol, Suppl. 2, 61, 1999

Schaar J, Oldenburg O, Gutersohn A, Heinzel F, Zimmermann U, Sack S, Baumgart D, Erbel R. Inhalatives Stickstoffmonoxid führt bei Patienten mit pulmonaler Hypertonie zu einem Anstieg von ANP und TNFa. Z Kardiol 88, Suppl. 2, 96, 1999

Schaar J, Oldenburg O, Hunold P, Kopp S, Baumgart D, Erbel R. Ein strukturiertes Schulungsprogramm zur cholesterinsenkenden Diät und Physiologie der Fette führt bei Patienten mit koronarer Herzerkrankung zu signifikanter Reduktion von Cholesterin- und LDL-Spiegeln innerhalb von sechs Monaten. Z Kardiol, Suppl. 2, 304, 1999

Schaar J, Oldenburg O, Görge G, Raus MH, Baumgart D, Erbel R. IVUS guided percutaneous transluminal fenestration (PTF) with a Brockenbrough Needle in aortic dissection Typ III. 65. Congress of the German Society of Cardiology, Z Kardiol 88, Suppl 1, 1024, S. 239, 1999

Schaar J, Oldenburg O, Haude M, Baumgart D, Erbel R. Increased Coronary Constriction bay a1-Adrenergic Stimulation in Arteriosclerotic Coronary Arteries Compared to Normal Coronary Arteries. Cardiovascular Drugs and Therapy, Abstract 103, Volume 13, Number 1, 1999

Oldenburg O, Eggebrecht H, Herrmann J, Schaar J, Brauck K, Baumgart D. Unabhängigkeit von koronarer Flussgeschwindigkeitsreserve und epikardialer Endothelfunktion bei Patienten mit Syndrom X. Z Kardiol 89, Suppl. 6, 238, 2000

Oldenburg O, Eggebrecht H, Schaar J, Gutersohn A, Naber C, Baumgart D. Gestörte Sympatikusaktivität bei Patienten mit Syndrom X. Z Kardiol 89, Suppl. 6, 385, 2000

Oldenburg O, Baumgart D, Schaar J, Eggebrecht H, Gutersohn A, Brauck K, Haude M, Erbel R. Selective intracoronary alpha-2-blockade in patients with coronary artery disease leads to an increase in coronary blood flow without augmentation of coronary sinus norepinephrine levels. Eur Heart J 21, Suppl August/ September, P2806, 2000

Gutersohn A, Schaar J, Sack S, Erbel R. Increased Interleukine by pulsative Nitric Oxide Insufilation in Patients with Pulmonary Hypertension. JACC Suppl A, 1025-186, 2001

Gutersohn A, Schaar J, Heinzel F, Sack S. Induktion von Interleukine 6 durch pulsative Stickstoff (NO) Inhalation bei Patienten mit pulmonaler Hypertonie. Intensivmed 37, P20, 2000

Mitchell A, Wenzel RR, Loock J, Schaar J, Schmermund A, Schäfers RF, Kribben A. Das Phäochromozytom als seltene Ursache einer akuten Herzinsuffizienz. Intensivmed 37, P86, 2000

Oldenburg O, Baumgart D, Schaar J, Brauck K, Eggebrecht H, Gutersohn A, Erbel R. Unexplained myocardial lactate production as an acute result after intracoronary calcium-antagonist application in patients with syndrome X. Eur Heart J 20, Suppl August/ September, 3470, 1999

Baumgart D, Oldenburg O, Schaar J, Gutersohn A, Brauck K, Eggebrecht H, Haude M, Erbel R. Lactate production following intracoronary verapamil application: unexplained findings in patients with syndrome X. Basic Res Cardiol 94, 165, 1999

Oldenburg O, Baumgart D, Schaar J, Gutersohn A, Eggebrecht H, Brauck K, Haude M, Erbel R. Comparable vasodilatory effects on coronary of verapamil and yohimbine on coronary microcirculation. Basic Res Cardiol 94, 168, 1999

Oldenburg O, Baumgart D, Gutersohn A, , Eggebrecht H, Schaar J, Brauck K, Haude M, Erbel R. Detection of microcirculatory disorders in patients with coronary artery disease: Superiority of the acetylcholine test compared to the Cold Pressor Test. Basic Res Cardiol 94, 162, 1999

Oldenburg O, Gutersohn A, Eggebrecht H, Schaar J, Brauck K. Induktion myokardialer Ischämien durch a2-adrenerge Stimulation bei Patienten mit typischer Angina Pectoris. Z Kardiol 88, Suppl. 2, 125, 1999

Oldenburg O, Schaar J, Baumgart D, Erbel R. Superiority of Acetylcholine Test compared to the Cold Pressor Test in the Dedection of Microvascular Disease in Patients with Syndrom X. Cardiovascular Drugs and Therapy, Abstract 104, Volume 13, Number 1, 1999

Oldenburg O, Kribben A, Schaar J, Baumgart D, Philipp T, Erbel R. Ambulatory Norepinephrine Infusion as a New Therapeutic Option in the Treatment of Refractory Autonomic Orthostatic Hypotension. Cardiovascular Drugs and Therapy, Abstract 241, Volume 13, Number 1, 1999

Oldenburg O, Eggebrecht H, Schaar J, Gutersohn A, Brauck K, Baumgart D. Vergleichbare vasodilatatorische Effekte von Verapamil und Yohimbin in der koronaren Mikrozirkulation. Z Kardiol 88 Suppl 2, 63, 1999

Oldenburg O, Schaar J, Brauck K, Gutersohn A, Baumgart D. Überlegenheit der Acetylcholin-Provokation gegenüber dem Cold Pressor Test in der Diagnose von koronaren Mikrozirkulationsstörungen bei Syndrom X. Z Kardiol 88, Supp 1, 370, S. 41, 1999

Oldenburg O, Kribben A, Schaar J, Baumgart D, Philipp T, Erbel R. Neue Behandlungsoption bei therapierefraktärer autonomer orthostatischer Hypotonie durch eine ambulante Noradrenalininfusion. Z Kardiol 88, Supp 1, 997, 1999

Raus M, Schaar J, Chung H, Ge J, Erbel R. Using the 3COM palmpilot personal digital assistant for bed-site acquisition and analysis of patient risk factors. Abstract: D1550, XXth Congress of the ESC Vienna, 1998

Görge G, Schaar J, Schaaf H, Ge J, Erbel R. New steerable, combined intravascular ultrasound, angioscopy, and Doppler catheter for visually guided diagnosis and interventions in the pulmonary circulation Abstract: P1770, XXth Congress of the ESC Vienna, 1998

Görge G, Schaar J, Erbel R. Steuer- und einschwemmbarer, kombinierter Angioskopie und intravasaler Ultraschallkatheter zum

Einsatz in den Pulmonalarterien. Z Kardiol 88, Suppl 1, 1111, 1998

Gutersohn A, Schaar J, Heinzel F, Herrmann J, Sack S, Erbel R. Upregulation of interleukine 6 by Nitric oxide insufflation in patients with pulmonary hypertension. Basic Res Cardiol 94, 239, 1999

Gutersohn A, Schaar J, Heinzel F, Sack S. Induktion von Interleukine 6 durch pulsative Stickstoff (NO) Inhalation bei Patienten mit pulmonaler Hypertonie. Z Kardiol 88, Suppl 2, 97 1999

Chapter 20
Curriculum Vitae

Johannes Antonius Schaar was born on May 03, 1967 in Griesbach im Rottal, Bavaria. He grew up in Pfarrkirchen, Germany where he attended grammar school and went later to the humanistic St. Michaels-Gymnasium in Metten. After studying medicine in St. Louis, USA and New York, USA, he earned his M.D. at the Julius-Maximilians-University Wuerzburg, Germany with cum laude. After a character forming internship in Aschaffenburg, Germany he worked at the University Essen, Germany under the mentorship of Prof. Raimund Erbel as research fellow. In September 2000, he started at the Biomedical Engineering of Thorax centre, Erasmus University Rotterdam, The Netherlands, headed by Prof. Antonius FW van der Steen, in close cooperation with the intervention cardiology of the Thorax centre, headed by Professor Dr. Patrick.W. Serruys His main interest was to develop palpography for clinical applications. He participated in several projects like NHS 2001-B191, ICIN 32 and the 2000 NWO PIONIER award, all aiming at vulnerable plaque detection. He has been awarded several research grants from organizations such as the German Heart Foundation and the Dutch Heart Foundation. He is co-organizer of the annual vulnerable plaque meetings (VPM) Currently the Erasmus MC Rotterdam, The Netherlands, employs him as cardiologist in training, which is planned to be finalized in 2007.

Chapter 21
Acknowledgement

Niemand maakt zijn eigen kind alleen

As I came to Rotterdam I knew that I would meet a conglomeration of the finest cardiologists in the world. I planned to stay for a year, than go back with a couple of papers, a new line in my CV and a bucket full of experience. Somewhere in the back of my brain I was even dreaming to get a PhD, but I considered this as a dream since I had only money for one year out of a grant of the German Heart Foundation.

I knew from the beginning that I would like the Thoraxcenter. What made me so optimistic were meetings that I had several months before my arrival. I met a couple of seniors: the first was colorblind (like me), the second had no time, the third was incredible funny and the last discussed with me the life of Jimmy Hendrix and the music of AC/DC. I was impressed. I have to admit that coming from Germany I was surprised to see that professional people, like these leading cardiologists can be relaxed and humble, without losing their aura of professionalism. After all these meetings I was scheduled to meet with the boss. Prof. Serruys was sitting in a very small room together with his secretary and started to ask in English with a light French accent looking over his glasses: "What you want to do?"

I was not sure. At a meeting in Vienna I saw a poster, which described a new method, which can measure vessel elasticity. The poster was optically so prominent that it was hard to overlook. I did not understand a word, of what was written there, but I liked the pictures.

I started to tell the professor something about elasticity. He nodded and left the office. I had time to enjoy the flavour of the room. It was so packed with files, papers and somewhere in between the secretary. The professor came back and said: "You have to contact Klaas Bom! He has his office on the 23rd floor. I'll call him." He

took the phone and started in Dutch to talk about me. I understood nothing, but I got another appointment.

Leaving the office I asked myself: Who is Klaas Bom? And where is the 23rd floor?

It turned out that Prof. Bom was one of the gentlest people, I have ever met. After the usual hello, he looked at me and said: "you need a coffee", stood up and served me a coffee. Again I was surprised and again we were talking about a lot of things, but nothing about research. After a while he introduced me to Chris de Korte and I got an introduction into elastography. I had no idea what he was talking about, this was all far to complicated for me, but I had the feeling that the story made a lot of sense. He gave me his PhD book and I left, not without recognizing a black guy, who was sitting with headphones in front of a computer, programming and shaking his head to whatever music. Later I learned that in this lab the first intracardiac echo probe, the first handheld echo, the linear array, the first TEE, the micromotor based IVUS, and many other things had been developed.

Back in Germany I started to write a grant (about elastography) with the support of Prof. Raimund Erbel, submitted the grant and forgot about it.

Six month later I received a letter saying I could go to Rotterdam for a year. I was not happy at all. My wife was pregnant and we just moved into a new apartment. After long discussions we decided that a year is not that long and I could leave.

I left in September 2000, Maximilian was meanwhile born and I was looking forward to an adventure, from which I had no idea what to expect and what to get.

I learned so much in the last years. I started with a one-year grant and am now in training to be a cardiologist. Such a development is only possible in the environment of the Thoraxcenter. I would compare this center with a huge salt-water aquarium. Somebody cares for refreshing the water, enough food, some oxygen, but the swimming has to be done alone. In an aquarium like this the fauna can be extremely colorful: sharks, snakes, old experienced whales

and very intelligent dolphins, some have found biotopes in the cold deep and some are behaving like they got a job in SeaWorld. The beauty of the variety is unbelievable.

Three components make the Thoraxcenter so unique:

First the clinic, second the 23rd floor and third Cardialysis. I have the pleasure to be involved in all three of them. It is an honour to thank a couple of people in these institutions for the support and the chances they gave me.

The 23rd floor is in the hands of Prof. Anton van der Steen. Ton, I learned from you so much that I could fill a couple of pages. We met first in Paris at an Elastography meeting at the EuroPCR. The conversation lasted about 10 minutes and I walked away with the feeling that communication with you will be easy, funny and productive. You took care that on my arrival I had a shelter (I never will forget the time in the home hotel), a working space and a project. I had to learn that engineers work quite different than cardiologists. Contemplation is more important than un-reflected excitement. I learned that experiments need time independent from the next deadline and that science needs good planning. Rutherford had once stated that science could be either based on physical models or on the desire to collect stamps. Empirical research has it's beauty, but model based research is hard to beat. We had long discussions about science, cooperation with clinicians, industry, patents and contracts. I learned a big part of diplomacy from you and how important it is to de-mystify situations, which have caused trouble or may cause trouble in the future. Your way is the way of patience, firmness and balance. You motivate people in a very positive way, never by building up fear and concerns. We share the same taste for music, which is very important. In general I guess somebody, who likes Tom Waits cannot be a bad human being.

Ton put me in the beginning in the hands of Chris de Korte. Chris, you took care that I got a good start. You've been a great mentor. With your ability to slice problems into slices so thin that they don't exist anymore or are rather easy to solve, you gave me confidence enough to survive demands, I learned from you that limitations of a technique can only be solved by developing a good strategy, not by creating fears. I will never forget the moment in Stockholm as

you went with me to a session in which an opinion leader explained rhetorically firm how vulnerable plaque detection had to work. I was after his talk not sure, if we are working in the right direction. You explained me point by point the physical background of all the proposed visions and my nervousness was healed. We had great times sharing hotels at meetings discussing life, faith, family and many other things more.

Very quickly I came in contact with Frits Mastik. This thesis is partly dedicated to him. We were most of the time the last ones leaving the lab. Your critical view on methods, techniques and experiments was of so much importance to the success of palpography that the technique would not be here without you. You joined me in most of the experiments, we fought ourselves through countless live cases and we enjoyed together the curiosity of some situations we had to face on the road. You are one of the brightest people I have ever met and one of the most humble. Your helpfulness is legendary in the lab. Your clear principles, which are the basis of your behaviour, are influenced by deep humanistic believe. Your knowledge about almost everything makes you a most distinguished discussion partner. Thank you standing next to me at the time of the defense.

There are many people more in this lab, who take care that things stay enjoyable: Mieke, thanx for your help preparing the thesis; Riekje, the mother of the lab; Frans, the silent organizer; Charles Lancee, the only genius I have ever met; Rob Krams, the most loyal basic researcher in the building. Wim and Leo, thanx for making technical problems a breeze; Jan, thanx for fixing almost everything, which has to do with current. Marvin Doyley, thanx for learning palpography how to walk. Radj, for taking care that the rights of the minorities are taken care of and thanx for explaining me in your very own style what math is all about. The hemodynamic group with Cees Slager as boss. Cees you are such a brilliant thinker, with such a stronghold view on certain things, that I always enjoy discussing whatever with you, doesn't matter, if we talk about your boss the Jewish carpenter, science or whatever else. Jolanda, you are a source of help, an independent thinker and well aware of your tremendous capabilities. You stayed humble, great. Frank, as I said before: somebody who likes Tom Waits cannot be a bad guy. I admire your taste regarding pants and shoes.

On the other side of the hall we got so much help from Dirk Duncker from experimental cardiology. Thank you Dirk for the support and thank you Elza for spending the days with us and taking care that the pigs are doing well.

Let's move from the ivory tower of the lazy and arrogant engineers on the 23rd floor downstairs to the cath lab. A technique like palpography had sooner or later to be proven to be able to withstand the pressure of real life. There is no better place for this than the cath lab of the Thoraxcenter. This is based on the attentiveness and courage of Patrick Serruys. Patrick, so many things were written about you in other books like this one. I have to thank you for all the chances you have given me: Including me in the organizing team of the vulnerable plaque meeting is only one of them. It is so much fun to work on this project and you lead me from a distance towards that we get every year a meeting organized, which is better than the one before. Writing articles with you on a Sunday afternoon is an experience I never will forget. I remember the day, when we wrote an essay about vulnerable plaque detection. You had 38.9 degrees Celsius fever sitting on your sofa at home and discussing with me this paper. Even with the fever in your head you were sharp, rhetorically unbeatable and full of ideas. Regarding palpography it has to be said that without your patience and fortitude we would not be, where we are today. At meetings people ask me often about the secret behind your success. My answer is always: he just works hard. If anyone thinks from himself he is working hard, I recommend following you for a week or two. In these weeks one would see half of the planet, be in 2-3 advisory boards, treating a couple of patients in the cath lab, giving key note lectures at conferences and finishing some articles. One day I would like to understand, from where you get this energy, which deserves so much respect.

Behind every strong man stands a strong women, is a saying in Germany. No, I am not talking about your wonderful wife, Patrick. I am talking about Anja.

Thank you Anja for squeezing me so often in the agenda of Patrick, which is always full. I admire how you still can organize this man, who I would declare as not organize-able. Your sometimes-grum-

bling way of communicating is often misjudged, but you treat everybody the same and behind the rough surfaces sits a heart of gold.

The second man in the cath lab, which has taken care that palpography is going to be a success is Pim de Feyter. What a man! Silent, humble, sharp, with a great sense of humour. Pim, your mind stood independent, which I admire very much. You treat your fellows with respect and warmth. You are the perfect role model for fellows, who fall after a while into the ego trap, since you are still a gentleman over all this years even after times, when it became a bit stormy outside.

Palpography needed over the years also support from the group of people, who will use it in the future in other cath labs. No, I am not talking about cardiologists. I am talking about the technicians. Two have contributed a lot: Emile, who likes everything fancy and eccentric, and Jurgen. Jurgen is a real IVUS animal. His interpretations of IVUS recordings are full of great intuition. Thank you for your help in the different clinical projects taking care that the quality of the recordings is not going down. There is also Miss OCT Evelyn Regar. Thanx Evelyn for recording most of the clinical cases. You have a wonderful pragmatic way dealing with science.

The third entity, which contributes to the success story of the Thoraxcenter is undeniable Cardialysis. Regarding Palpography we got the chance “to play core lab” in the IBIS I trial. We started as the highly experimental technique and ended as the primary endpoint of two multicenter trials. This would be not possible without the help of a couple of people. Let's start with Gerrit-Anne van Es. You are very open accepting crazy scientists in your environment and you opened resources for us. You have a great feeling in dealing with people from different backgrounds and you stay professional in the most difficult situations. As I said before: Someone who likes Tom Waits cannot be a bad guy.

Michael Koenders, my favorite secretary of finance. We had a bad start in our relationship, but this has improved towards a friendship. Organizing with you the vulnerable plaque meeting is pure fun. Going with you to meetings is always a great mixture of professionalism and entertainment. Thank you for all the support and energy you have given to me.

Marie-angele, the most charming of the women in Cardialysis. You are involved in so many projects that I wonder how you keep track. Your communication skills are of indispensable value to everybody. Thank you for helping the core lab for palpography grow.
This brings us to the hidden expert on palpography: Ravindra Pavar. Ravindra, we know that palpography is in good hands when you work on it. I admired your skills in learning how to analyze palpograms and your way of dealing with Frits and me.

I know I have not mentioned everybody in this list. I tried to concentrate on the Thoraxcenter and I limited myself to people, who joined forces for palpography. My work would not have been possible without the continuous support of all co-workers at the 23rd floor, the cathlab and Cardialysis. I have to ask for forgiveness of everybody that I left unmentioned.

Outside the Thorax center I owe gratitude to the global vulnerable plaque fighting force that is gathering every year on a sunny Island in the Mediterranean to discuss life in general and vulcanoes and vulnerable plaques in particular. These discussions have been an important source of inspiration, but on top of that have directly resulted in two chapters in this thesis.

I want to acknowledge the institutes that contributed in a financial manner to the work described in this thesis. The Dutch Heart Foundation (NHS), der German Heart Foundation (DHS), The Dutch Technology foundation (STW), The Netherlands Organization for Scientific Research (NWO), the Interuniversity Cardiology Institute of the Netherlands (ICIN), the Royal Academy of Arts an Sciences (KNAW) and the recent contributions of the industries that take care of utilization: Glaxo Smith Kline and Volcano corporation. Furthermore I have to acknowledge that the work in this book is built on a long lasting framework of cooperation e.g. through the ICIN (thank you Manja) in particular with the experimental cardiology in Utrecht (thank you Gerard), the Laser Center of the AMC in Amsterdam (thank you Ton), the cardiology department in Leiden, the biomechanical engineering department of the TU Eindhoven and the seismic and acoustics group of applied physiscs of the TU Delft.

Finally, there is one person, who deserves most of the acknowledgements: My wife. Stephanie gave me support and love over the last years. She is the base of my life. You take care that Maximilian and Sophia are getting a valuable character. You never complained, but you've been always critical. Behind every strong man is a strong woman. The first has still to be proven, the second not. Thank you!